



National Library  
of Canada

Bibliothèque nationale  
du Canada

Canadian Theses Service

Service des thèses canadiennes

Ottawa, Canada  
K1A 0N4

## NOTICE

The quality of this microform is heavily dependent upon the quality of the original thesis submitted for microfilming. Every effort has been made to ensure the highest quality of reproduction possible.

If pages are missing, contact the university which granted the degree.

Some pages may have indistinct print especially if the original pages were typed with a poor typewriter ribbon or if the university sent us an inferior photocopy.

Reproduction in full or in part of this microform is governed by the Canadian Copyright Act, R.S.C. 1970, c. C-30, and subsequent amendments.

## AVIS

La qualité de cette microforme dépend grandement de la qualité de la thèse soumise au microfilmage. Nous avons tout fait pour assurer une qualité supérieure de reproduction.

S'il manque des pages, veuillez communiquer avec l'université qui a conféré le grade.

La qualité d'impression de certaines pages peut laisser à désirer, surtout si les pages originales ont été dactylographiées à l'aide d'un ruban usé ou si l'université nous a fait parvenir une photocopie de qualité inférieure.

La reproduction, même partielle, de cette microforme est soumise à la Loi canadienne sur le droit d'auteur, SRC 1970, c. C-30, et ses amendements subséquents.

UNIVERSITY OF ALBERTA

STUDY OF IONIZED CALCIUM AND MAGNESIUM MEASUREMENTS  
BY ION EXCHANGE/ATOMIC ABSORPTION

by

AMITHA KUMUDINI HEWAVITHARANA (C)

A THESIS

SUBMITTED TO THE FACULTY OF GRADUATE STUDIES AND  
RESEARCH IN PARTIAL FULFILLMENT OF THE REQUIREMENTS  
FOR THE DEGREE OF DOCTOR OF PHILOSOPHY

DEPARTMENT OF CHEMISTRY

EDMONTON, ALBERTA

FALL 1991



National Library  
of Canada

Bibliothèque nationale  
du Canada

Canadian Theses Service    Service des thèses canadiennes

Ottawa, Canada  
K1A 0N4

The author has granted an irrevocable non-exclusive licence allowing the National Library of Canada to reproduce, loan, distribute or sell copies of his/her thesis by any means and in any form or format, making this thesis available to interested persons.

The author retains ownership of the copyright in his/her thesis. Neither the thesis nor substantial extracts from it may be printed or otherwise reproduced without his/her permission.

L'auteur a accordé une licence irrévocable et non exclusive permettant à la Bibliothèque nationale du Canada de reproduire, prêter, distribuer ou vendre des copies de sa thèse de quelque manière et sous quelque forme que ce soit pour mettre des exemplaires de cette thèse à la disposition des personnes intéressées.

L'auteur conserve la propriété du droit d'auteur qui protège sa thèse. Ni la thèse ni des extraits substantiels de celle-ci ne doivent être imprimés ou autrement reproduits sans son autorisation.

ISBN 0-315-69938-8

Canada

UNIVERSITY OF ALBERTA  
RELEASE FORM

NAME OF AUTHOR: AMITHA KUMUDINI HEWAVITHARANA

TITLE OF THESIS: STUDY OF IONIZED CALCIUM AND  
MAGNESIUM MEASUREMENTS BY ION  
EXCHANGE/ATOMIC ABSORPTION

DEGREE: PH.D.

YEAR THIS DEGREE GRANTED: 1991

Permission is hereby granted to the University of Alberta library to reproduce single copies of this thesis and to lend or sell such copies for private, scholarly or scientific research purposes only.

The author reserves all other publication and other rights in association with the copyright in the thesis, and except as hereinbefore provided neither the thesis nor any substantial portion thereof may be printed or otherwise reproduced in any material form whatever without the author's prior written permission.



B-31, 2/4, Senpathi mawatha

Maligawatta

Colombo 10

Sri Lanka

Date: 23<sup>rd</sup> Sept. 1991

UNIVERSITY OF ALBERTA  
FACULTY OF GRADUATE STUDIES AND RESEARCH

The undersigned certify that they have read, and recommend to the faculty of graduate studies and research for acceptance, a thesis entitled **STUDY OF IONIZED CALCIUM AND MAGNESIUM MEASUREMENTS BY ION EXCHANGE/ATOMIC ABSORPTION** submitted by **AMITHA KUMUDINI HEWAVITHARANA** in partial fulfillment of the requirements for the degree of **DOCTOR OF PHILOSOPHY**.

B. Kratochvil  
B. Kratochvil, Supervisor

F. F. Cantwell  
F. F. Cantwell

James A. Plambeck  
J.A. Plambeck

J. C. Vederas  
J. C. Vederas

P. Sporns  
P. Sporns

R. S. Reid  
R. S. Reid, External Examiner

Date: 12<sup>th</sup> Sept 1991

*To my parents and husband*

*In memory of my first born*

## ABSTRACT

A quantitative ion exchange flow-through column equilibration method with atomic absorption detection is described for the measurement of millimolar levels of free (ionized) calcium and magnesium in ligand-containing solutions. Practical applications include analyzing biological fluids, such as urine, to aid in the diagnosis of kidney stone diseases. To obtain the necessary "trace ion" conditions for practical use, the concentration of electrolyte in the samples and standards must be high enough that the fraction of exchange sites occupied by calcium or magnesium on the strongly acidic sulphonic acid ion exchange resin is very small.

With 0.75M sodium nitrate as electrolyte, useful calibration curves up to 200 ppm are obtained. The method is selective for free over bound calcium in the presence of citrate and phosphate, although raising the electrolyte concentration of samples to 0.75M perturbs the original equilibria and raises free calcium levels. To minimise this perturbation, the possibility of replacing sodium with organic cations with high affinities for the resin is investigated. Normal alkylammonium ions give the best performance while quaternary ammonium ions are not satisfactory. Octylammonium as electrolyte cation gives a straight line calibration plot up to 200 ppm calcium, at concentrations as low as 0.07M, and is insensitive to the variations in pH and salt

concentration typically found in urine. The selectivity of the system for free calcium is poor; several possible reasons for this behaviour are discussed.

Washing the resin after sample equilibration is found to perturb the ion exchange equilibria. The flow system is modified to minimise this effect. Since magnesium is found to interfere with free calcium measurements, a method is developed for the simultaneous determination of both free calcium and magnesium. This involves measurement of resin-sorbed calcium and magnesium from solutions containing sodium and potassium at urine-like concentrations followed by multiple regression. The procedure gives good selectivity for both free metals in the presence of citrate, phosphate and sulphate, and is applied to the simultaneous determination in standard urine SRM 2670 from NIST.

The method is also applied successfully to the determination of both free metals in ligand-containing solutions at micro molar levels.



## **ACKNOWLEDGEMENTS**

The author is grateful to Dr. B. Kratochvil for his guidance and kind encouragement throughout the course of this research and in the preparation of this thesis.

Sincere thanks are due to Dr. F. F. Cantwell for his constructive advice, which was always provided when needed.

Thanks are also extended to Dr. A. R. Fernando for assisting with column construction and to Mr. A. Chan for providing calcium ion selective electrodes.

## TABLE OF CONTENTS

CHAPTER	PAGE
1. INTRODUCTION .....	1
1.1 Calcium ion speciation in biological fluids .....	2
1.2 Ion selective electrode potentiometry for the analysis of free calcium .....	3
1.3 Use of indicator dyes for the analysis of free calcium .....	6
1.4 Importance of magnesium in kidney stone formation .....	11
1.5 Review of methods for the determination of free magnesium .....	13
1.6 Importance of evaluating both free calcium and free magnesium in body fluids .....	16
1.7 Research objectives .....	17
2. THEORY OF FREE METAL SPECIATION BASED ON ION EXCHANGE .....	21
2.1 Ion exchange equilibria under trace conditions .....	21
2.2 Ion exchange equilibria under non-trace conditions .....	24
2.3 Flow-through column equilibration method .....	26
3. DESCRIPTION OF ION EXCHANGE/ATOMIC ABSORPTION SYSTEM FOR IONIC CALCIUM DETERMINATION .....	27
3.1 Introduction .....	27
3.2 Apparatus .....	28

3.3	Cleaning of equipment . . . . .	33
3.4	Resin conditioning . . . . .	33
3.5	Column construction . . . . .	34
3.6	Instrumental conditions . . . . .	36
3.7	Calculation of free metal concentrations from theory . . . . .	36
3.8	Procedure for free metal determination . . . . .	38
4.	<b>DETERMINATION OF FREE CALCIUM IN THE PRESENCE OF SODIUM UNDER TRACE CONDITIONS . . . . .</b>	<b>42</b>
4.1	Introduction . . . . .	42
4.2	Experimental . . . . .	43
4.2.1	Apparatus . . . . .	43
4.2.2	Chemicals and solutions . . . . .	44
4.3	Investigation of the negative Y intercept of the calibration curves in earlier work . . . . .	45
4.4	Selectivity of the method for free over bound calcium . . . . .	50
4.5	Determination of free calcium in urine . . . . .	61
4.6	Use of conductance to estimate the urine ionic strength . . . . .	63
4.7	Conclusions . . . . .	64
5.	<b>USE OF ORGANIC SALTS AS THE ELECTROLYTE IN THE DETERMINATION OF FREE CALCIUM BY ION EXCHANGE . . . . .</b>	<b>68</b>
5.1	Introduction . . . . .	68

5.2	Experimental	69
5.2.1	Apparatus	69
5.2.2	Chemicals and solutions	71
5.3	Selection of the optimum organic cation for use in obtaining trace conditions	72
5.4	Determination of free $\text{Ca}^{2+}$ in the presence of octylammonium ion under trace conditions	83
5.4.1	Effect of sodium on octylammonium system	83
5.4.2	Test of column trace conditions with octylammonium	86
5.4.3	Peak tailing problem	86
5.4.4	Effect of pH	89
5.4.5	Calibration curve with buffered standards	91
5.4.6	Selectivity of the method for free over bound calcium	95
5.4.7	Investigation of the reason for the high experimental free $\text{Ca}^{2+}$ value	97
5.5	Conclusions	127
6.	<b>INVESTIGATION OF THE EFFECT OF RESIN CROSS- LINKING AND WASH CYCLE ON ION EXCHANGE EQUILIBRIUM</b>	130
6.1	Introduction	130

6.2	Experimental	131
6.3	Study of 2% cross-linked resin	132
6.3.1	Tetraethylammonium bromide as electrolyte	132
6.3.2	Study of the sorption of a series of tetraalkyl ammonium ions	135
6.3.3	Use of Na <sup>+</sup> and K <sup>+</sup> as electrolyte	138
6.4	Perturbation of the ion exchange equilibrium during the wash cycle	141
6.4.1	Using an air purge cycle between the load and the wash cycle	146
6.4.2	Removal of the column from the system between the air purge and wash cycles	146
6.4.3	Modification of flow system	147
6.5	Conclusions	148
7.	<b>MEASUREMENT OF FREE CALCIUM UNDER NON-TRACE CONDITIONS</b>	152
7.1	Introduction	152
7.2	Experimental	154
7.3	Use of KNO <sub>3</sub> as electrolyte	154
7.4	Use of Na <sup>+</sup> and K <sup>+</sup> salts as electrolytes	157
7.5	Determination of minimum number of sets of standards required	163

7.6	Using one set of $\text{Na}^+/\text{K}^+$ concentrations in the $\text{Ca}^{2+}$ standards .....	165
7.7	Conclusions .....	171
8.	<b>DETERMINATION OF BOTH FREE CALCIUM AND FREE MAGNESIUM IN URINE</b> .....	172
8.1	Introduction .....	172
8.2	Experimental .....	173
8.3	$\text{Mg}^{2+}$ interference with measurement of free $\text{Ca}^{2+}$ .....	177
8.4	Simultaneous determination of free $\text{Ca}^{2+}$ and free $\text{Mg}^{2+}$ in a single solution .....	185
8.4.1	Determination of free $\text{Mg}^{2+}$ .....	186
8.4.2	Determination of free $\text{Ca}^{2+}$ and free $\text{Mg}^{2+}$ .....	189
8.5	Determination of free $\text{Ca}^{2+}$ and free $\text{Mg}^{2+}$ at low concentrations under trace conditions .....	216
8.6	Conclusions and suggestions for future work .....	221
	<b>BIBLIOGRAPHY</b> .....	228
	<b>APPENDIX</b> .....	241

## LIST OF TABLES

TABLE	PAGE
1.1 Ionic equilibria present in a typical urine that can affect the species distribution of calcium and magnesium . . . . .	18
3.1 Instrumental parameters for the atomic absorption spectrophotometric determination of calcium and magnesium . . . . .	37
4.1 A listing of the stability constants used in the calculation of free calcium in the presence of citrate and sodium nitrate. . . . .	59
4.2 A listing of the stability constants used in the calculation of free calcium in the presence of phosphate and sodium nitrate. . . . .	60
4.3 Results of the determination of free and total calcium in the urine of seven normal individuals. . . . .	62
4.4 Comparison of methods for the adjustment of urinary ionic strength to 0.75. . . . .	65
5.1 Comparison of the average experimental free $\text{Ca}^{2+}$ values obtained with 0.07M octylammonium nitrate and variable total citrate levels with the calculated values. . . . .	98

5.2	Comparison of free $\text{Ca}^{2+}$ concentrations obtained for a solution of 100 ppm calcium in 0.07M octylammonium nitrate and 5mM citrate, by the ion exchange method (IEX), the colorimetric method (TMMA) and theoretical calculation. . . . .	110
5.3	Variation in effluent citrate level with method of collection and pH in the case of octylammonium nitrate as the electrolyte. . . . .	120
5.4	Variation of effluent citrate level with method of collection, solution citrate level and pH in the case of sodium nitrate as the electrolyte. . . . .	121
7.1	A listing of the stability constants used in the calculation of free calcium in the presence of citrate and potassium nitrate. . . . .	155
7.2	Calculated free $\text{Ca}^{2+}$ concentrations for a solution containing 100 ppm total calcium and 5mM total citrate. $\text{Na}^+$ and $\text{K}^+$ concentrations and pH were varied to represent typical variations in urine. . . . .	162
7.3	Variation in 100 ppm $\text{Ca}^{2+}$ signal with ionic strength and $\text{Na}^+/\text{K}^+$ ratio. . . . .	168
8.1	Certified values of constituent elements in SRM 2670 (freeze dried urine). . . . .	178



8.2	The F-test and t-test results for the calibration curve in terms of calcium peak areas. . . . .	194
8.3	The F-test and t-test results for the calibration curve in terms of magnesium peak areas. . . . .	195
8.4	A listing of the stability constants used in the calculation of free $\text{Ca}^{2+}$ and free $\text{Mg}^{2+}$ concentrations in the presence of citrate. . . . .	197
8.5	A listing of the stability constants used in the calculation of free $\text{Ca}^{2+}$ and free $\text{Mg}^{2+}$ in the presence of phosphate. . . . .	198
8.6	A listing of the stability constants used in the calculation of free $\text{Ca}^{2+}$ and free $\text{Mg}^{2+}$ in the presence of sulphate. . . . .	199

## LIST OF FIGURES

FIGURE	PAGE
3.1 Flow system 1 for ion exchange equilibration . . . . .	29
3.2 Flow system 2 for ion exchange equilibration . . . . .	30
3.3 A cross-section diagram of the column . . . . .	35
4.1 Calibration curves for calcium standards in 0.75M sodium nitrate in terms of peak areas and absorbance of collected peaks . . . . .	46
4.2 Calibration curve for calcium standards in 0.75M sodium nitrate in terms of absorbance of collected peaks in a constant volume, using PE 4000. . . . .	49
4.3 Variation of free $\text{Ca}^{2+}$ fraction with the total citrate level in 0.75M $\text{NaNO}_3$ . . . . .	55
4.4 Variation of free $\text{Ca}^{2+}$ fraction with the total phosphate level in 0.75M $\text{NaNO}_3$ . . . . .	56
5.1 Variation of peak area for 50 ppm $\text{Ca}^{2+}$ in 0.1M alkylammonium nitrate solution with the number of carbon atoms in the alkyl chain. . . . .	75
5.2 Variation of peak area for 50 ppm $\text{Ca}^{2+}$ with the concentration of octylammonium nitrate. . . . .	76
5.3 Variation of peak area for 50 ppm $\text{Ca}^{2+}$ with the concentration of hexylammonium nitrate. . . . .	77

5.4	Variation of peak area for 50 ppm $\text{Ca}^{2+}$ in 0.07M octylammonium nitrate with the concentration of $\text{NaNO}_3$ . . . . .	85
5.5	Calibration curve for standard calcium solutions in 0.07M octylammonium nitrate. . . . .	87
5.6	Variation of peak area for 75 ppm $\text{Ca}^{2+}$ in 0.07M octylammonium nitrate with the pH. . . . .	90
5.7	Variation of peak area for 75 ppm $\text{Ca}^{2+}$ in 0.07M octylammonium nitrate with the concentration of the buffer, PIPES. . . . .	93
5.8	Variation of peak area for 125 ppm $\text{Ca}^{2+}$ in 0.07M octylammonium nitrate with the concentration of the buffer, PIPES. . . . .	94
5.9	Calibration curve for standard $\text{Ca}^{2+}$ solutions in 0.07M octylammonium nitrate, buffered at pH 6.4 with 0.01M PIPES. . . . .	96
5.10	Conductometric titration of 0.02M sodium citrate with 0.07M octylammonium nitrate. . . . .	101
5.11	Absorption spectra of a solution of 0.01M nickel nitrate and 0.01M sodium citrate. . . . .	105
5.12	Absorption spectra of a solution of 0.01M nickel nitrate, 0.01M sodium citrate and 0.01M octylammonium nitrate. . . . .	106

5.13	A plot of the absorbance ratio 480 nm/550 nm vs. the concentration of $\text{Ca}^{2+}$ in 0.07M octylammonium, as measured by the colorimetric method using TMMA. . . . .	109
5.14	Calibration curve for standard citrate solutions as obtained by the colorimetric method using iron(III) chloride. . . . .	114
5.15	Absorption spectra of the 0.2M KCl reference solution and the 75 $\mu\text{M}$ citrate in 0.2M KCl solution. . . . .	115
5.16	Difference spectra for 50 $\mu\text{M}$ and 75 $\mu\text{M}$ citrate solutions with iron(III) chloride. . . . .	116
6.1	Calibration curve for standard $\text{Ca}^{2+}$ solutions in 1M tetraethylammonium bromide. . . . .	134
6.2	Calibration curves for standard $\text{Ca}^{2+}$ solutions in 0.3M $\text{KNO}_3$ , using 8% crosslinked resin and 2% crosslinked resin. . . . .	140
6.3	Calibration curves for standard $\text{Ca}^{2+}$ solutions in 0.75M $\text{NaNO}_3$ , using 8% crosslinked resin and 2% crosslinked resin. . . . .	142
6.4	Calibration curves for standard $\text{Ca}^{2+}$ solutions in 0.3M and 0.5M $\text{KNO}_3$ . . . . .	144

6.5	Variation of free $\text{Ca}^{2+}$ concentration with total citrate level in solution at pH 6-7, in 0.35M $\text{NaNO}_3$ and 0.15M $\text{KNO}_3$ as a comparison of flow systems. . . . .	149
7.1	Calibration curve for standard $\text{Ca}^{2+}$ solutions in 0.35M $\text{NaNO}_3$ and 0.15M $\text{KNO}_3$ . . . . .	159
7.2	Variation of free $\text{Ca}^{2+}$ concentration with total citrate level in solution at pH 6-7 in 0.35M $\text{NaNO}_3$ and 0.15M $\text{KNO}_3$ as a comparison of ion exchange and colorimetric methods. . . . .	160
7.3	Calibration curves for standard $\text{Ca}^{2+}$ solutions in 0.15M $\text{KNO}_3$ and in 0.05M $\text{KNO}_3$ and 0.1M $\text{NaNO}_3$ . . . . .	170
8.1	Peak area for a 100 ppm $\text{Ca}^{2+}$ signal as a function of $\text{Mg}^{2+}$ concentration at ionic strengths of 0.1 and 0.3. . . . .	180
8.2	Peak area for a 100 ppm $\text{Ca}^{2+}$ signal as a function of $\text{Mg}^{2+}$ concentration; at 0.1 ionic strength using a column containing 0.08 mg resin, and at 0.3 ionic strength using a column containing 0.2 mg resin. . . . .	182
8.3	Calibration curve for a set of standard $\text{Mg}^{2+}$ solutions in 0.1M $\text{NaNO}_3$ and 0.05M $\text{KNO}_3$ . . . . .	188
8.4	Variation of free $\text{Mg}^{2+}$ fraction with total citrate level, in the pH range 4.1 to 4.6 and 6.2 to 6.6. . . . .	190

8.5	3-axis calibration curves for standard $\text{Ca}^{2+}$ and $\text{Mg}^{2+}$ solutions in 0.114M $\text{NaNO}_3$ plus 0.038M $\text{KNO}_3$ . . . . .	192
8.6	Variation of free $\text{Ca}^{2+}$ and free $\text{Mg}^{2+}$ fractions with total citrate level, at pH range 4.3 to 5.5. . . . .	201
8.7	Variation of free $\text{Ca}^{2+}$ and free $\text{Mg}^{2+}$ fractions with total citrate level, at pH range 6 to 6.8 . . . . .	202
8.8	Variation of free $\text{Ca}^{2+}$ and free $\text{Mg}^{2+}$ fractions with total phosphate level, at pH range 5.5 to 6.5. . . . .	203
8.9	Variation of free $\text{Ca}^{2+}$ and free $\text{Mg}^{2+}$ fractions with total sulphate level, at pH range 6 to 6.4. . . . .	204
8.10	Variation of free $\text{Ca}^{2+}$ and free $\text{Mg}^{2+}$ fractions, in a solution of 3 mM citrate, 0.02M phosphate and 0.02M sulphate, with the pH. . . . .	205
8.11	Variation of the absorbance ratio (480 nm/550 nm) for 100 ppm $\text{Ca}^{2+}$ as a function of $\text{KNO}_3$ concentration. . . . .	211
8.12	Estimated variation of spectrophotometrically determined free $\text{Ca}^{2+}$ signal for a 100 ppm $\text{Ca}^{2+}$ solution as a function of the ionic strength. . . . .	212
8.13	Loading curves for $2.5 \times 10^{-5}\text{M}$ $\text{Ca}^{2+}$ and $\text{Mg}^{2+}$ solutions in 0.1M $\text{KNO}_3$ . . . . .	218
8.14	Calibration curves for standard $\text{Ca}^{2+}$ and $\text{Mg}^{2+}$ solutions in 0.1M $\text{KNO}_3$ . . . . .	219

8.15	Variation of free $\text{Ca}^{2+}$ and free $\text{Mg}^{2+}$ concentrations with total citrate level, at pH range 6 to 7. . . . .	222
8.16	Variation of free $\text{Ca}^{2+}$ and free $\text{Mg}^{2+}$ concentrations with total phosphate level at pH 7. . . . .	223
A.1	Scheme of COMICS method. . . . .	242
A.2	Data input for COMICS. . . . .	245
A.3	COMICS output #1. . . . .	248
A.4	COMICS output #2. . . . .	250

## CHAPTER 1

### INTRODUCTION

Speciation is defined as the determination of one or more specific forms of an element or compound present in a system. Knowledge about the speciation of metals is of critical importance in medicine, in the environment and in toxicology. Research during the last few decades shows that knowledge of the total metal concentration alone is inadequate to allow conclusions regarding a system.<sup>1-12</sup> An increased awareness of the importance of speciation has led to the development of analytical techniques that do not give just "how much" of a metal is present, but rather give "how much of a particular form or forms" of the metal is present.

The species of interest may be either kinetically inert or labile. Speciation of kinetically inert species can be accomplished relatively easily by using standard separation techniques such as solvent extraction, chromatography and ion-exchange.

Selecting or developing a method for the speciation of kinetically labile metal species is a much more delicate matter because the method must not perturb the positions of metal equilibria in the system. Any form of sample pretreatment, or interaction of the analytical probe with the sample, can



perturb the equilibria of a system. Therefore an ideal method requires no sample pretreatment and does not perturb the position of equilibria during the measurement step. This thesis will focus on the speciation of calcium and magnesium in biological fluids, especially on measurement of the free, or hydrated, forms of metals, and will discuss how the above target is achieved for these speciation measurements.

### 1.1 Calcium ion speciation in biological fluids

The importance of calcium in biological systems has been the subject of many books<sup>13-17</sup> and numerous publications<sup>18-22</sup>. It is well established that ionized, or free, calcium (hydrated calcium ion,  $\text{Ca}^{2+}$ ) is the most physiologically active form of calcium<sup>10-12,23-27</sup>.

In biological fluids, calcium exists as both free ions and as bound forms. Calcium binds to a variety of complexing ligands such as citrate, phosphate, sulphate and oxalate<sup>28,29</sup>, and also to proteins<sup>30</sup>. Knowledge of the ionized, or free, calcium concentration in urine<sup>14,31-33</sup> and in serum<sup>34,35</sup> is an important tool in the diagnosis of urinary tract or kidney stone diseases. The largest group of urinary stones occurring in humans is composed mainly of calcium oxalate, and to some extent of calcium phosphate<sup>31,36-37</sup>. If the concentrations of calcium, oxalate and phosphate ions are such that the solubility product of either of these salts is exceeded, precipitation and deposition of the salt occurs, causing stone formation<sup>14</sup>. Clearly, the determination of calcium ion concentrations in

urine and blood is useful for diagnostic purposes. Statistics show that analysis for the ionic or free calcium concentration is ordered by physicians ten times more often than the total calcium concentration<sup>27</sup>.

Essentially all the calcium complexes in biological fluids fall in the kinetically labile category. Therefore, a method to determine ionized calcium should take this into account. This thesis will emphasise the study of the determination of ionized calcium in urine. Methods currently available for this purpose include the use of a calcium ion selective electrode and spectrophotometry with indicator dyes. In addition, computer programs<sup>38-41</sup> have also been used to estimate the free calcium in urine. The programs require the determination of all metals and complexing ligands in the system using instruments such as the autoanalyser<sup>42</sup>. Finally, ion-exchange has been used for speciation in other biological fluids<sup>43-45</sup>, but not in urine. Each of these methods is discussed in the following sections.

## 1.2 Ion selective electrode potentiometry for the analysis of free calcium

The calcium ion selective electrode has been greatly improved since 1967, when the first design was published by Ross<sup>46</sup>. The original concept was to measure the potential across a porous plastic membrane saturated with an organic solvent containing an organo phosphate ligand that selectively bound calcium ions. If the calcium ion concentration was held constant on one side of the membrane, the potential varied with the concentration on the other side

according to Nernst equation. After 1978 a neutral carrier type calcium ligand was developed that has been found superior to the organo phosphates<sup>27</sup>. To simplify routine analyses newer instruments are often automated, require only about 100 micro-litres of sample, and measure potassium, sodium, pH and calcium simultaneously. Examples include the Baker Instruments Model Analyte +2, and the Sentech Model ChemPro-1000<sup>27</sup>.

To measure the free calcium concentration of a sample using a calcium ion selective electrode, the standards must be very similar to the sample. Due to sample variations in the pH and ionic strength of urine, hospitals frequently perform free calcium measurements on blood, where sample to sample variation is small. Therefore the calcium ion selective electrode most commonly found today has been developed to eliminate problems which are specifically associated with measurements in blood rather than in urine. Orion SS-20<sup>47,48</sup>, Orion 98-20<sup>49,50</sup>, Orion 99-20<sup>51,48</sup> (Orion Research U. S.), NOVA-2<sup>28</sup> (NOVA Biomedical U. S.) and Radiometer model ICA 1<sup>52</sup> (Radiometer A/S Denmark) are some of the models often used to analyze free calcium in blood.

Although calcium selective electrode potentiometry is frequently used to measure free calcium in blood, questions about freedom from interference and reliability are still asked. The Orion 99-20 electrode is sometimes used with a dialysis membrane attached in front of the electrode to avoid protein poisoning<sup>53</sup>. The Orion SS-20, NOVA-2 and ICA 1A electrodes are reported to be significantly affected by proteins<sup>54,55</sup>, but the ICA 1B is not affected<sup>54</sup>.

Another study<sup>56</sup> claims that the effect of protein interference on ICA 1 is not significant.

As mentioned earlier, present-day calcium selective electrodes were not specifically developed for urine and therefore specific interference studies or evaluation of the reliability of the calcium values obtained have not been done for urine to the same extent as they have for blood. In spite of this, several studies have used the calcium selective electrode to measure free calcium in urine. Early Orion models required the addition of known amounts of KCl and CaCl<sub>2</sub> to urine in order to prevent irreversible inactivation of the electrode<sup>57,58,59</sup>. The measured calcium value was then corrected for the added salts. Also, early Radiometer models (such as the 2112 model) required the use of a dialysis membrane in order to prevent electrode poisoning and loss of Nernstian response of the electrode when used for urine<sup>33</sup>. A study done using an Orion 92-32 shows that the interference caused by high concentrations of urea in urine is not significant at urine-like ionic strengths<sup>60</sup>. Another serious problem in measuring the free calcium in urine is the matching of standards to each sample in terms of sodium, potassium, magnesium and pH<sup>57,61</sup>. To avoid matching in terms of ionic strength, the activity of free calcium rather than the concentration is often measured<sup>61,62</sup>. As mentioned in section 1.1, the solubility product of calcium oxalate or calcium phosphate determines the stone forming tendency of urine. Since the solubility product is defined in terms of activity rather than the concentration, the determination of the activity of calcium ions

may be justified<sup>62</sup>. The calcium electrodes used for urine in these studies were the Orion SS-20<sup>63</sup> and ICA 1<sup>62</sup>. A comparative study showed that the urine free calcium values measured with an ion selective electrode correlate well with calculated values (correlation coefficient = 0.94)<sup>39</sup>.

Since little work has been done on the use of calcium selective electrodes for urine, the reliability of electrode-determined calcium values is not clear. Some calcium electrodes are found to be pH sensitive and are not able to measure free calcium when the sample pH is below 5.3<sup>35,39</sup>. The Orion SS-20 on the other hand was found to be insensitive to pH within the range of 4 to 8.5<sup>47</sup>. In a private communication, the manufacturer revealed that the CIBA CORNING model 634 Ca<sup>2+</sup>/pH analyzer, which is presently used in hospitals for the analysis of free calcium in blood, is detrimentally affected by both the ammonia levels in urine, and pH values lower than 5 (pH of urine can vary between 4 and 7). The effect of pH on many other electrodes has either not been studied or is not mentioned. Routine use and automation of the calcium selective electrode for the analysis of free calcium in urine thus requires a great deal of further work.

### 1.3 Use of indicator dyes for the analysis of free calcium

The concept here is to measure the amount of calcium that is bound to the indicator which is usually a weak calcium binding ligand. Since the ligand is a weak one, it binds only a very small fraction of the ionized Ca<sup>2+</sup>, so that

the sample equilibria are perturbed to a negligible extent. The amount of  $\text{Ca}^{2+}$ -indicator complex is colorimetrically determined using Beer's law and it is proportional to the amount of free  $\text{Ca}^{2+}$  in the sample. Several calcium binding dyes can be used to colorimetrically determine free calcium concentrations. Arsenazo III was evaluated for the determination of free calcium in the presence of several proteins<sup>64</sup>. But in the presence of ligands such as EGTA, the stoichiometry of  $\text{Ca}^{2+}$ -Arsenazo complex changes with pH<sup>65</sup>. This is attributed to the competition between  $\text{Ca}^{2+}$ -EGTA and  $\text{Ca}^{2+}$ -Arsenazo complexes. While Arsenazo III is difficult to obtain in pure form, procedures for its purification are available<sup>66</sup>. Due to the above mentioned problems, however, this indicator is not appropriate for the measurement of free calcium in biological fluids.

The fluorescent indicator Aequorin has also been used to measure free calcium<sup>20,67-70</sup>. This indicator is isolated from jelly fish. Since it is difficult to obtain and is unstable on storage, it is not commonly used.

Murexide and tetramethylmurexide (TMMA) are the most commonly used calcium indicators for the determination of free calcium in biological fluids. Murexide was first used in 1951<sup>71</sup>. It was found to be selective for free calcium in the presence of citrate<sup>72</sup> and was used to analyze free calcium in urine<sup>73</sup>. Problems associated with murexide, such as its pH dependence and interferences from sodium and protein, led to the use of TMMA, which is pH insensitive within the range 4-9<sup>74</sup> and suffers less from interference by protein

and sodium. Since the first use of TMMA in 1962<sup>75</sup>, it has been widely used for the determination of free calcium in urine<sup>76-79</sup> and plasma<sup>79-81</sup>. This indicator is commercially available.

Since proteins still interfere with calcium measurements by TMMA, it cannot be used for whole blood. Therefore it is employed mainly for plasma ultrafiltrates. The wavelength of maximum absorbance of TMMA is at 550 nm and that of the  $\text{Ca}^{2+}$ -TMMA complex is at 480 nm. Therefore, the absorbance ratio 480/550 is often plotted against calcium concentration for the preparation of calibration plots. This method is preferred to single wavelength measurements at 480 nm for the following reasons.

1. The two wavelength method gives a straight line calibration plot.
2. The absorbance ratio is insensitive to the small volume differences produced by the addition of indicator solution. (It was found that the absorbance ratio is constant for significantly different amounts of indicator added to the same volume of sample<sup>82</sup>.) Also, dilution artifacts can be eliminated by taking the absorbance difference at two wavelengths, at which wavelengths the molar absorptivities of the indicator are equal<sup>83</sup>.
3. Although the stability of the  $\text{Ca}^{2+}$ -TMMA complex is such that the colour fades with time, and therefore individual absorbances change, it has been shown that the absorbance ratio is not significantly affected over a period as long as three days<sup>82</sup>.

With this method, and with use of a thermostat and strict control of wavelength, very reproducible results were obtained<sup>74</sup>. The stability constants for calcium with each of the ligands citrate, phosphate, sulphate and lactate were determined using TMMA. The values observed agreed with the reported literature values. A semi automated system is available to make routine analysis of urine and plasma more convenient<sup>79</sup>.

The TMMA colorimetric method using two wavelengths claims to give reliable values for free calcium concentrations for the following reasons.

1. The added volume of indicator can be made small relative to the sample volume so that dilution of the sample volume is negligible. Thus changes in sample ionic strength are not significant enough to cause perturbation of equilibria in sample solutions.
2. Since the  $\text{Ca}^{2+}$ -TMMA (1:1) complex is very weak, TMMA complexes with less than one percent of the calcium ions in the sample, causing minimal perturbation of calcium equilibria in the sample.
3. No corrections are required for the differences in sample and standard pH, because the indicator response is insensitive to pH variations over the physiological pH range of 4 to 8.

Interference by proteins prevents use of the method with blood, although plasma ultrafiltrate may be analysed. When applied to urine, proteins are not usually a problem but the inherent color of urine is. To overcome this problem, urine blanks were used for referencing<sup>77</sup> or decolorizing charcoal was



used to adsorb the compounds causing interference by absorption at the wavelength of analysis<sup>79</sup>. In addition, since the indicator response is both sodium and ionic strength dependent, it imposes difficulties in the analysis because both samples and standards require matching in terms of sodium and ionic strength. Some workers overcame this problem by applying a correction factor taken from empirically derived tables according to the sodium-calcium ratio and the ionic strength of the urine sample<sup>76</sup>. Others used calibration curves in terms of activity of calcium rather than concentration<sup>82</sup>. This enabled use of a single set of standards for a large number of urine samples. But even with this approach the concentration of sodium in each sample had to be accurately measured to correct for the sodium interference. In order to convert activities to concentration, the ionic strength of each sample was measured and activity coefficients were calculated. Comparison studies show that the free calcium concentrations in urine measured using TMMA correlate highly, (correlation coefficient = 0.98) with calculated values<sup>39</sup>, and that the mean values of free calcium obtained for 17 serum samples using an Orion 98-20 electrode and TMMA agreed well<sup>84</sup>.

In the case of the TMMA colorimetric method, the addition of indicator slightly perturbs the equilibria in the sample, whereas for ion-selective electrodes and, as described later, for the column equilibration method, there is no such perturbation. Also, being a colorimetric method, the TMMA procedure is not ideally suited to use in a coloured fluid such as urine. The

TMMA method is also not very convenient to use for the routine analysis of free calcium in urine because of its dependence on ionic strength and the sodium concentration of the sample.

#### 1.4 Importance of magnesium in kidney stone formation

The biological importance of magnesium is well known and well established<sup>85-87</sup>. In biological systems, magnesium exists as either free ions or as complexes bound to ligands such as citrate, phosphate, sulphate and oxalate. As with calcium, ionized or free magnesium is the most physiologically active form in biological systems<sup>85,88-91</sup>. Unlike calcium, methods for determining free magnesium are not well developed, and not many studies have been done on the use of free magnesium measurements in clinical diagnosis. Knowledge of the free magnesium concentration in blood can be an important tool in assessing the magnesium treatment of patients with cardio-vascular and neuro-muscular disorders<sup>90</sup>. Although free magnesium in urine has not been studied as extensively as has free calcium, there is some evidence that it may be important. Kidney stones of the type  $\text{Mg-NH}_4\text{-PO}_4$  have been reported<sup>14</sup>, and so knowledge of the free magnesium concentration can be useful in the diagnosis of and treatment for such stones. Also, experimental evidence shows that increased magnesium concentrations decrease the incidence of calcium stone formation<sup>85</sup>. According to the suggested mechanism, magnesium ties up oxalate as magnesium oxalate, which has a higher solubility than calcium

oxalate<sup>92</sup> ( $K_{sp}$  of  $9 \cdot 10^{-5}$  vs.  $2 \cdot 10^{-9}$ ). The urinary excretion of calcium and magnesium is positively correlated, that is, values of urinary calcium tend to parallel those of urinary magnesium. The ratio of urinary magnesium to urinary calcium has been used as an index of stone forming potential and low values have been reported to be associated with an increased frequency of stones<sup>93-95</sup>. Magnesium, administered as magnesium salts, reduced the incidence of urinary stone formation in rats<sup>96</sup>. Magnesium treatment has also significantly reduced the formation of new stones in stone forming patients<sup>97</sup>. Magnesium deficiency can cause a drift of calcium out of bone<sup>98</sup>, which again agrees with the solubility mechanism described above.

All of the above calcium-magnesium studies were performed using measurements of total metal concentrations. This is likely due to the lack of appropriate methods for free magnesium analysis. If the above mentioned mechanism for the reduction of calcium stone formation by increased magnesium is correct, ionic magnesium should be responsible for this mechanism rather than total magnesium, because it is the ionized magnesium which competes with ionized calcium to tie up oxalate. Therefore it is of interest to compare free magnesium levels in stone-forming patients with those in the normal population.

### 1.5 Review of methods for the determination of free magnesium

The methods available for measuring free magnesium in biological fluids are not as widespread or as well developed as those for free calcium.

Magnesium ion selective electrode and the spectrophotometric methods using Mg binding dyes are the two major areas of development.

#### Mg ion selective electrodes

Magnesium ion-selective electrodes are still in the developmental stage. The major problem associated with them is calcium interference<sup>99</sup>. In addition, some models show poor selectivity in the presence of sodium and potassium<sup>100</sup>. One recently developed model<sup>101,102</sup> gave less calcium interference but was sensitive to pH and can only be used for buffered solutions of relatively high pH (8 to 9). Another newly available model can operate at physiological pH values, but still shows significant interference from calcium<sup>90</sup>. This model has been employed to measure free magnesium in serum, using standards with the same amount of calcium as is present in the sample in the unbound form. The calcium in the sample is measured using a calcium ion-selective electrode. To overcome interference by other metal ions, a chemometric approach<sup>91</sup> has been proposed which involves the simultaneous determination of sodium, potassium, calcium and magnesium using standards containing all 4 metal ions, and treating the data with partial least squares (PLS) analysis. Clearly, at present

no magnesium selective electrode can reliably measure free magnesium in urine.

### Spectrophotometry

Colorimetric indicators available for free magnesium include mainly calmagite, Eriochrome Black T, Eriochrome Blue SE and azo dyes. Most other magnesium indicators show insufficient selectivity in the presence of calcium within physiological pH values<sup>103</sup>. Calmagite is not suitable for kinetically labile systems because masking agents are required to prevent other metals from interfering<sup>104</sup>. Eriochrome Black T has high selectivity to magnesium over calcium but is sensitive to ionic strength and proteins<sup>88</sup>. Also it is useful only within the pH range 7.3 - 8, which does not include physiological pH values<sup>105</sup>. Eriochrome Blue SE is sensitive to both calcium and magnesium but calcium gives a different absorption spectrum from magnesium. Therefore, by choosing two wavelengths it is possible to measure free magnesium without calcium interference<sup>106</sup>. Unfortunately, this indicator is also pH sensitive within the physiological pH range and is likely subject to interference from other metals. Several other azo dyes were synthesized and evaluated for free magnesium analysis<sup>10</sup>, but were either calcium or pH sensitive. Therefore none of these colorimetric methods is suitable for the determination of free magnesium in blood or urine.

### Other methods

Phosphorus-31 nmr was used to determine intracellular free magnesium by measuring the magnesium dependent shift of ATP<sup>108-110</sup>. Fluorinated chelators which can be studied by <sup>19</sup>F nmr were also used for the analysis of intracellular free magnesium<sup>109,111,112</sup>. The pK<sub>a</sub> values of these chelators are around 5, so that they are suitable for intracellular free magnesium analysis at pH 7. All of these chelators are sensitive to calcium to a certain extent, but the levels of calcium relative to magnesium in cells are such that the calcium interference can easily be ignored<sup>112</sup>. Considering the typical calcium and magnesium levels and the typical pH range associated with urine, clearly these chelators are not appropriate for free magnesium determination in urine.

Recently, a fluorescent indicator FURAPTRA, or mag-fura-2, was developed by modification of one of the above chelators<sup>113</sup> and used for the determination of intracellular free magnesium<sup>114-116</sup>. Again, the pK<sub>a</sub> of the indicator and its sensitivity to calcium make it unsuitable for urinary free magnesium determinations.

An ion exchange method was developed over twenty years ago for the determination of free magnesium in urine with a low capacity ion exchange resin<sup>89</sup>. However, this study did not demonstrate that the method is selective for free magnesium in the presence of other metal ions and in the presence of complexing ligands in urine. Therefore the values reported may not represent only free Mg<sup>2+</sup>. Standards containing levels of sodium, potassium and calcium

typical for the urine samples were used for the determination of free  $Mg^{2+}$  in the real samples. Since the sample to sample variation of these metals in urine is often large, the reliability of free magnesium concentrations determined by this method is questionable.

#### 1.6 Importance of evaluating both free calcium and free magnesium in body fluids

As described in section 1.4, knowledge of both free calcium and free magnesium values can be highly useful in the diagnosis of stone diseases. Magnesium and calcium are intimately tied together in their biological functions and abnormality in the level of either one has a marked effect on the metabolism of the other<sup>98</sup>. Since the physiologically active form for both the metals is the free, or ionized form, information about the combination of free magnesium and free calcium in a body fluid might be useful in the pathogenesis of other disorders as well. For example, neonatal tetany has been correlated with decreased ionic calcium levels, but owing to the lack of convenient methods to analyze magnesium its correlation to ionic magnesium is rarely considered<sup>117</sup>. It is possible therefore, that given a convenient and reliable method for the determination of free magnesium, correlation of both free magnesium and free calcium concentrations to biological malfunctions will be as frequent as that of the present general practise of considering only free calcium.

### 1.7 Research objectives

It is clear that knowledge of free calcium and free magnesium concentrations can aid in assessing the stone forming tendency of a urine. A number of studies show that the free calcium concentration in urine is correlated to the incidence of stone formation. As discussed in the previous section related studies of free magnesium are rare due to the lack of reliable analytical methods.

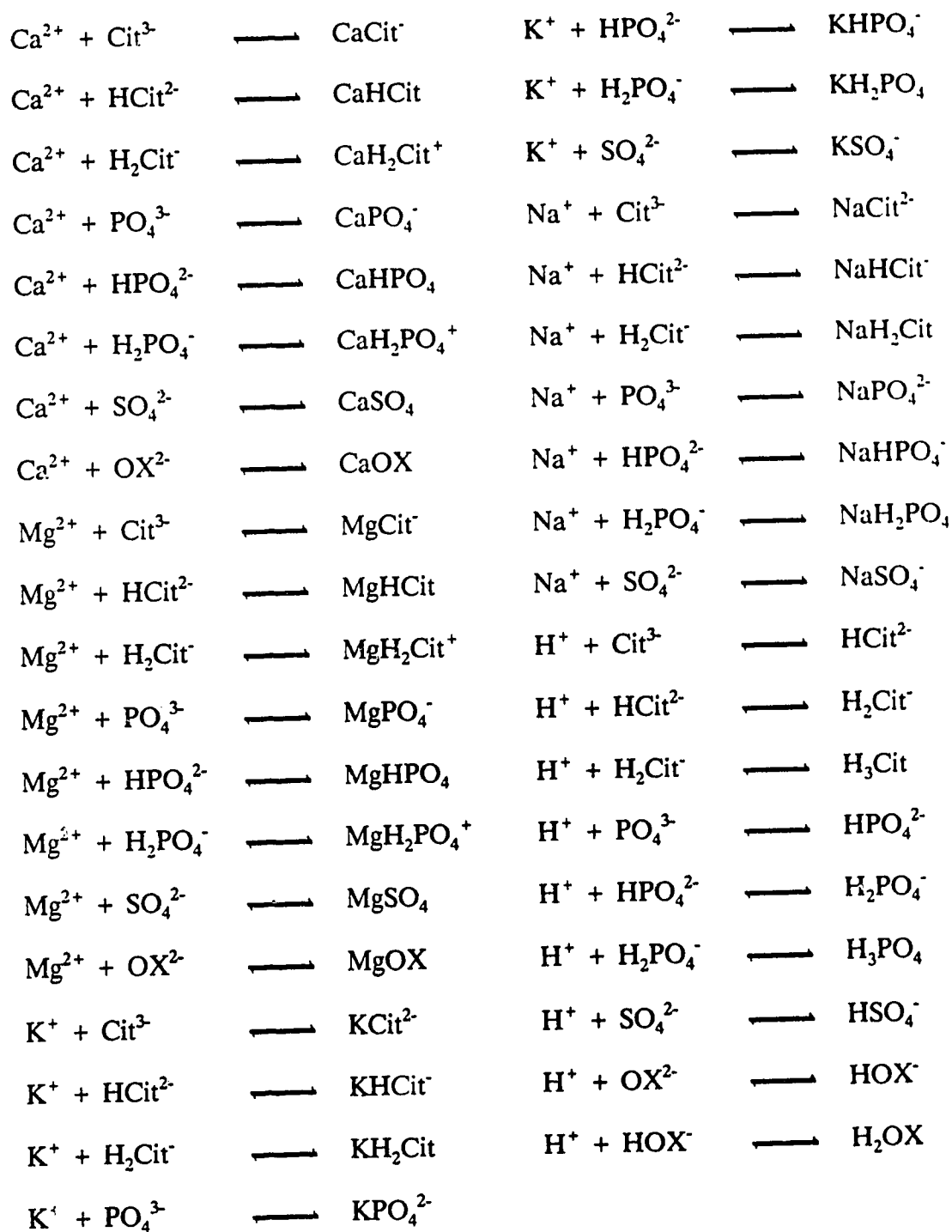
For calcium and magnesium urine is a kinetically labile system which involves a large number of interconnected equilibria. A list of the major equilibria that are considered in the present study is given in table 1.1.

The objective of the present study is therefore, to determine the concentrations of free calcium and magnesium ions present in equilibrium with all other constituents, without perturbing any of these equilibria. Several of the sample pretreatment practices commonly used in quantitative analysis can perturb a system of this type. Owing to the kinetically labile nature of the system, an ideal method of analysis for this system should not:

1. Involve dilution of the sample, because this changes the ionic strength of the system. A change in the ionic strength results in a change in all the activity coefficients involved and in all the conditional stability constants, resulting in a shift of all equilibria. In addition, dilution of a ligand concentration changes the concentrations of each species of that ligand which then alters the free metal ion concentrations.



**Table 1.1:** Ionic equilibria present in a typical urine that can affect the species distribution of  $\text{Ca}^{2+}$  and  $\text{Mg}^{2+}$  (Cit = citrate, OX = oxalate)



2. Change the pH of the system, because this will alter all the equilibria which involve  $H^+$  or  $OH^-$ . Since all the ligand equilibria in table 1 are pH sensitive, they will be altered, resulting in changes in the existing free metal concentrations.
3. Involve the addition of a substance to the system as a step of the measurement procedure. Ionic substances will at least cause a change in the ionic strength, and may cause a shift in equilibria involving free calcium or magnesium. Non ionic compounds may affect ion solvation, cause dilution or shift equilibria.

From a medical point of view, what is needed is an "in-vivo" concentration of metal ions rather than an "in-vitro" concentration. Therefore an ideal method of analysis will provide the closest possible value to the actual free metal concentration present in the body fluid in place. If any one of the above requirements is not met, what is measured is not the concentration of the metal that normally exists in equilibrium, but the concentration of the metal that exists in equilibrium after the changes imposed by the method on the system.

This thesis will present results of a study of an ion-exchange column equilibration technique for the determination of free calcium and free magnesium in solutions containing ligand-bound metal species. The work was aimed particularly at the measurement of these free species in urine. The first and major part will concentrate on the analysis of free calcium, and the second

part on the simultaneous analysis of free calcium and free magnesium. In addition, the measurement of free calcium and free magnesium at trace levels, some 100 times lower than those found in typical body fluids, will be described.

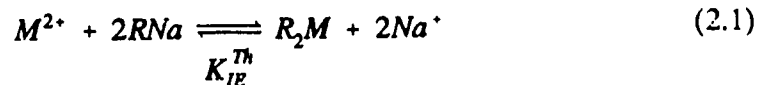
## CHAPTER 2

### THEORY OF FREE METAL SPECIATION BASED ON ION EXCHANGE

Ion exchange is used for metal speciation in two ways. The batch method has been the commonly used technique in the past<sup>118-123</sup>. The more recently developed column equilibration method<sup>124-126</sup> is especially suited for metal speciation in kinetically labile systems and is the method used in the present study. Therefore the theoretical treatment described in this chapter is specific to the column equilibration method.

#### 2.1 Ion exchange equilibria under trace conditions

Consider a solution containing the metal ion of interest,  $M^{2+}$ , and a relatively high concentration of an electrolyte (eg.,  $NaNO_3$ ). If this solution is equilibrated with a strong acid type cation exchange resin (eg., DOWEX 50W-X8), the following equilibrium will occur,



where R represents the exchange sites in the resin and  $K_{IE}^{Th}$  is the thermodynamic ion exchange equilibrium constant for the metal ion distributed between the solution and the resin phases and is defined as:

$$K_{IE}^{Th} = \frac{a_{R_2M} \cdot a_{Na^+}^2}{a_{M^{2+}} \cdot a_{RNa}^2} \quad (2.2)$$

The same equation can also be written in terms of species concentrations, [i], and activity coefficients,  $\gamma_i$ , instead of activities,  $a_i$ :

$$K_{IE}^{Th} = \frac{[R_2M][Na^+]^2}{[M^{2+}][RNa]^2} \cdot \frac{\gamma_{R_2M} \cdot \gamma_{Na^+}^2}{\gamma_{M^{2+}} \cdot \gamma_{RNa}^2} \quad (2.3)$$

where  $\gamma_{R_2M}$  and  $\gamma_{RNa}$  are the respective activity coefficients of  $R_2M$  and  $RNa$  in the resin phase.

The standard solutions for calibration are usually made with a constant amount of electrolyte and varying amounts of metal ion. If the concentrations of metal ion in these solutions are negligibly small relative to the concentration

of electrolyte, that is if the solutions are "swamped" with the electrolyte, it is safe to assume that the ionic strengths of all these solutions are the same. Since the ionic strength is a constant, the activity coefficients are constant for this set of solutions. Therefore, as shown below by rearranging equation (2.3),  $K_{IE}$ , the concentration ion exchange equilibrium constant, becomes a true constant for this set of solutions.

$$K_{IE} = K_{IE}^{Th} \cdot \frac{\gamma_{M^{2+}} \cdot \gamma_{RNa}^2}{\gamma_{R_2M} \cdot \gamma_{Na^+}^2} = \frac{[R_2M][Na^+]^2}{[M^{2+}][RNa]^2} \quad (2.4)$$

If the affinities of the metal ion and the electrolyte for the resin are such that the metal ions sorb only on a very small fraction (<1%) of the exchange sites, i.e.  $R_2M \ll RNa$ , the entity  $RNa$  also becomes a constant for this set of solutions. When the metal ion has a higher affinity to the resin than the electrolyte cation, this condition is achieved by making the solution electrolyte concentration much higher than the metal ion concentration. Thus in the case of divalent metal ions, swamping the solutions with high concentration of electrolyte not only makes  $K_{IE}$  a true constant but also fulfils the condition  $R_2M \ll RNa$ . This is called the trace ion exchange condition<sup>127,128</sup>. Since the entity  $RNa$  is a constant at trace conditions and the solutions are made with a constant amount of electrolyte, the ratio  $[RNa]/[Na^+]$  becomes a constant for this system. Therefore upon rearranging

equation 2.4, the following equation can be obtained in which the distribution coefficient of the free metal ion between the solution and resin phase,  $\lambda_o$ , is a constant for all the standards.

$$\frac{[R_2M]}{[M^{2+}]} = K_{IE} \cdot \frac{[RNa]^2}{[Na^+]^2} = \lambda_o \quad (2.5)$$

In other words, at trace conditions, the concentration of metal ion sorbed is directly proportional to the free metal ion concentration of the solution, therefore a straight line calibration curve is obtainable. If the electrolyte concentration of the sample is brought to the same level as standards, this calibration curve can be used to determine the free metal concentration of the sample.

## 2.2 Ion exchange equilibria under non-trace conditions

Consider the same set of standards described in section 2.1, but under conditions where the concentration of sodium is still much higher than the metal ion concentration, yet not sufficiently high to completely ignore the effect of the metal ion of interest. In this case, the ionic strength of the system is not a constant. If the concentration of sodium is high enough, as with the levels found in urine and blood, to make the ionic strength of all solutions roughly constant, one can still assume  $K_{IE}$  to be a true constant for this system.

However at this level of sodium the trace condition, i.e.  $R_2M \ll RNa$ , is not achieved. Therefore equation 2.5 for such a system takes the form:

$$[R_2M] = constant \cdot [M^{2+}] \cdot [RNa]^2 \quad (2.6)$$

where

$$constant = \frac{K_{IE}}{[Na^+]^2} \quad (2.7)$$

However,

$$2R_2M + RNa = C \quad (2.8)$$

where  $C$  is the exchange capacity of the column, which is a constant.

Due to the capacity constraint, amount of  $RNa$  decreases with increasing amount of  $R_2M$ . This decrease in  $RNa$  counteracts the increase in  $R_2M$  due to the increase in  $[M^{2+}]$ . Therefore, the calibration curve in this case is not a straight line, unlike in the case of trace ion exchange conditions.

In either case it is assumed that only the free metal ion is sorbed onto the resin. Since any cationic species is likely to undergo ion exchange, this assumption is not likely to be met. However, the contribution to errors by such sorptions depends on the concentration of such species and their distribution coefficient relative to the metal ion of interest. Whenever this assumption



could be brought into question in this study, it was tested. In all cases, with the concentrations and charges of metal ion complexes at the solution pH values used in this study, no significant deviations from the assumption were found.

### 2.3 Flow-through column equilibration method

This method involves passing a test solution through a very small amount of strong cation exchange resin until the total analyte concentration in the effluent becomes equal to that in the test solution. Thus the resin in the column is brought to equilibrium with the unperturbed test solution. Once equilibrium has been achieved, therefore, no additional analyte species in any form is taken up by the resin. Any further passage of solution through the column will not change the concentration of the analyte in either phase.

A wash cycle follows this equilibration step, where water is passed through the column in order to remove the solution in the fittings and between resin particles. Although this step is necessary to isolate the resin-sorbed analyte, there is a potential perturbation of equilibrium due to this step of the procedure. This is considered in detail later in this thesis.

The wash cycle is followed by an elution step in which the resin-sorbed analyte is eluted and detected. A plot of analyte concentration in the resin vs. that in solution gives the calibration plot.

## CHAPTER 3

### DESCRIPTION OF ION EXCHANGE/ATOMIC ABSORPTION SYSTEM FOR IONIC CALCIUM DETERMINATION

#### 3.1 Introduction

An ideal method for measuring individual species of a metal ion in a solution containing kinetically labile metal complexes will introduce little or no perturbation to the existing equilibria. The ion exchange column equilibration method allows the resin to be in equilibrium with fresh unperturbed test solution at complete breakthrough. This way, at the complete breakthrough stage, the test solution in contact with the resin does not lose any of its constituents to the resin, therefore leaving the existing equilibria completely undisturbed.

A semi-automated system was developed in the initial work on the column equilibration method<sup>124</sup>. This involved one six-way rotary valve and 4 slider valves in order to direct the solution flow through various pathways required by the method, depending on the valve positions. The system was coupled to a flame atomic absorption spectrophotometer followed by an integrator to measure the area of the eluted peak. Later, a fully automated

system was developed<sup>129</sup>, in which 8 solenoid valves were controlled by a microcomputer in order to direct the flow in various ways. Also, the data acquisition and data processing necessary to produce peak areas and peak heights was done by the same microcomputer.

Several changes to the valve system described above were made during the present study in order to make the system more efficient and in order to obtain more reliable results. The final version of the present study is semi-automated, and can be fully automated using a similar approach to the previously mentioned automated system.

The apparatus, the method for cleaning the equipment, resin conditioning and column construction, instrument parameters, procedures of experimental determination and theoretical calculation of free metal, all of which are described in this chapter, are common to all subsequent chapters, unless otherwise stated.

### 3.2 Apparatus

The instrument setups used are shown schematically in figures 3.1 and 3.2. The setup in figure 3.1 (flow system 1) was used in the first part of this study while the remainder of the study was done using the improved version in figure 3.2 (flow system 2). In terms of the physical set up, the only significant difference between figures 3.1 and 3.2 is the addition of one more valve. But there is a crucial difference in terms of the operation as described in section

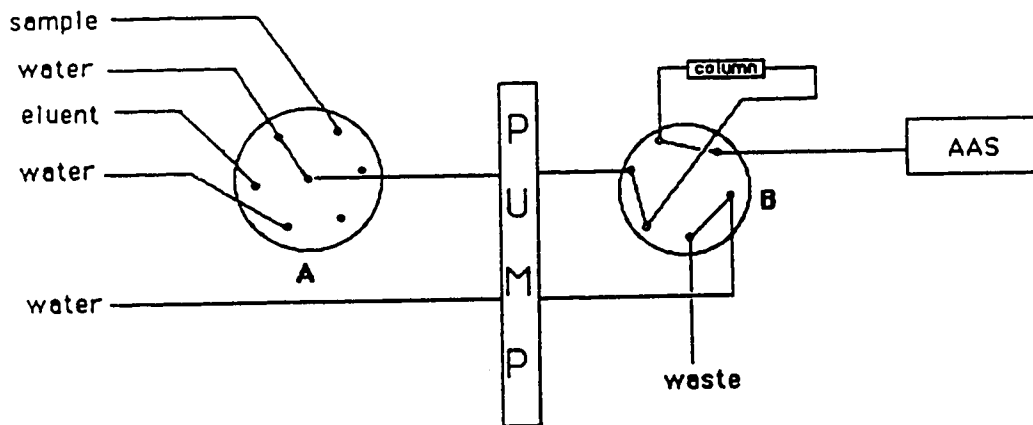
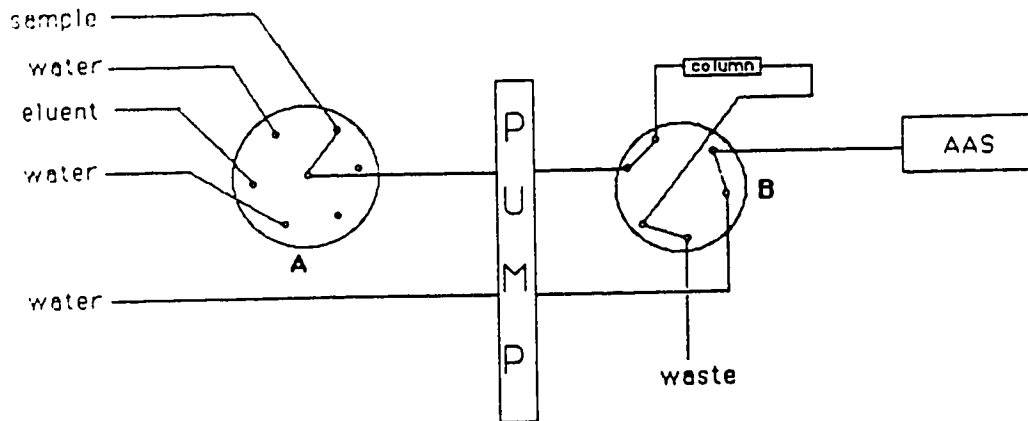


**Figure 3.1:** Flow system 1 for ion exchange equilibration. A and B represent a six-port rotary valve and a rotary sample-injection valve respectively.

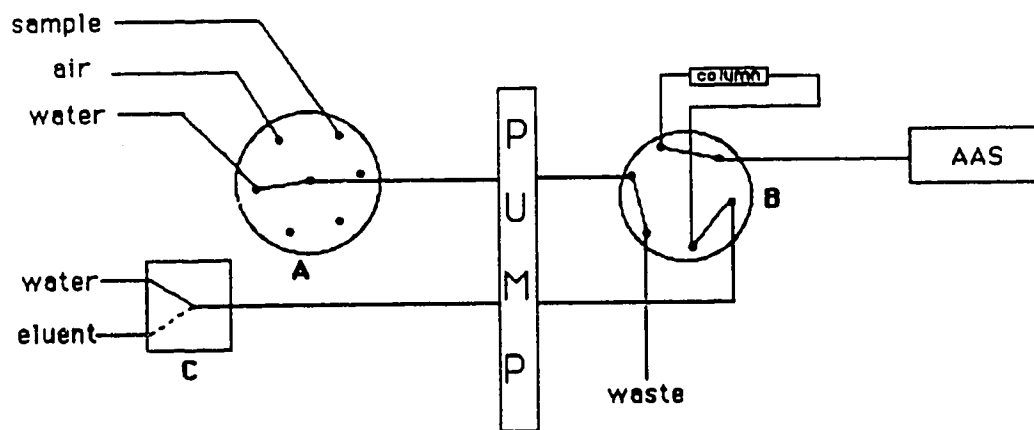
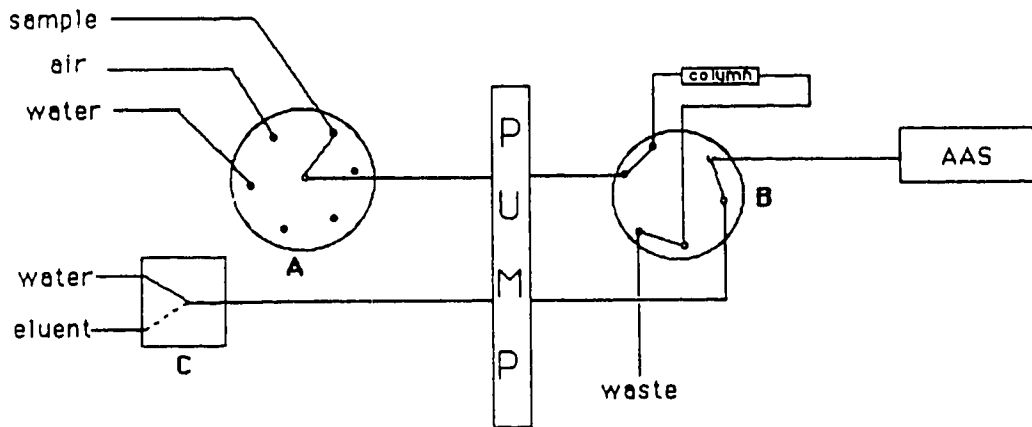


**Figure 3.2:** Flow system 2 for ion exchange equilibration. A and B represent a six-port rotary valve and a rotary sample-injection valve respectively. C is a three-way slider valve.

3.8 and in terms of the reliability of the results obtained as described in a later chapter.

The variable speed peristaltic pump (Minipuls 2, Gilson, Villiers-le-Bel, France) was fitted with two 0.081-inch i.d. clear standard PVC tubes (Technicon Corp.). One pumped water (figure 3.1) or was fitted to a 3-way valve (valve C in figure 3.2) to allow choice between water or eluent (2M HNO<sub>3</sub>). The second line was connected to a type 50 Teflon 6-way rotary valve, A, (Rheodyne Inc.) which pumped water, sample, air (figure 3.2) or eluent depending on the position of the valve A. The type 50 Teflon 4-way rotary valve (or rotary sample-injection valve), B, (Rheodyne Inc.) in figure 3.1 is used to maintain a continuous supply of water to the flame of the atomic absorption instrument while directing the sample through the column during the column equilibration step, or to direct the eluent flow through the column to the flame while diverting the supply of water to waste in the elution step. In figure 3.2, valve B directed either one of the lines through the column depending on the position. When the flow from valve A is directed through the column, the effluent is diverted to waste while supplying a continuous flow of water to the flame from valve C. When the flow from valve C is directed through the column, the effluent is diverted to the flame while the flow from valve A is diverted to waste. All tubing used in the system was 0.5-mm i.d. Teflon (Mandel Scientific Company Ltd.) except the pump tubing and the column. In order to connect the pump tubing with the rest of the tubes,

Polypropylene Tefzel tube connectors (Mandel Scientific Company Ltd., stock # 20051) were used. The valves and the column are connected to the tubing by means of Polypropylene couplings (stock # 20052, Mandel Scientific Company Ltd.). To make the ends of the tubing compatible with the valve outlets and the column outlets, the end of each piece of tubing was fitted with a Polypropylene tube end fitting (Mandel Scientific Company Ltd.), and a stainless steel washer. The tube ends were flared using a Chromatronix model FT-1 flaring apparatus. The Polypropylene couplings fitted over the tube end fittings and the flared end. Details of column construction are given in sections 3.4 and 3.5.

The metal concentration of the column effluent was monitored with a Perkin Elmer flame atomic absorption spectrophotometer (AAS) model 4000 equipped with a Perkin Elmer Ca only or Ca-Mg hollow cathode lamp. A stripchart recorder model 7101BM (Hewlett Packard Corp.) was used to trace the analog signal. The pH and potentiometric measurements were made with a Fisher model 520 digital pH/ion meter and Fisher glass calomel electrodes calibrated with Fisher standard buffers at pH 4 and 7. A Hewlett Packard model HP 8451A diode array spectrophotometer was used for spectrophotometric studies. A 1650A impedance bridge (General Radio Co. MA) in combination with a Phillips PR 9510 cell was used for conductivity measurements (the reciprocal of the resistance measured by this instrument was taken as the conductance). A Barnstead NANOpure water system was

used to purify water for the preparation of solutions. The sources of chemicals and their purity are described in subsequent chapters as appropriate.

### 3.3 Cleaning of Equipment

All glassware used in the experiments was first cleaned by washing with liquid detergent and thoroughly rinsing with tap water. This was followed by soaking overnight in 30% (v/v)  $\text{HNO}_3$  and then rinsing thoroughly with distilled-deionized water. The flow system and the column were cleaned by pumping 2M  $\text{HNO}_3$  and then rinsed by pumping nano-pure water.

### 3.4 Resin Conditioning

The columns were prepared with analytical grade 200-400 mesh Dowex 50W-X8 cation exchange resin (J. T. Baker Chemical Co.). One of the columns was made with 200-400 mesh DOWEX 50X2-400 cation exchange resin (Aldrich Chemical Co.). The ion exchange capacity was 5.1 milli-equivalents per gram of dry resin in both cases.

The conditioning of the Dowex 50W-X8 resin is given elsewhere<sup>127</sup>. The DOWEX 50X2-400 resin was ground in a clean, dry agate mortar and pestle until most of the material passed a 200 mesh sieve. Then the fines were removed by sieving again with a 325 mesh sieve followed by repeated decanting of the suspension of resin in water. Next, the resin was placed on glass wool in a glass column and washed with water, then with 1M NaOH, followed again by



water. Then it was washed with 1M HCl, followed by water. Next, the column was flushed with 0.2M sodium citrate in order to remove any metal ions present in the resin as impurity by means of complexation. This was followed by washing with water, 1M NaOH, water, 1M HCl and again water. Finally the resin was washed with methanol, followed by a water wash and dried by air at room temperature<sup>130</sup>. Both resins were stored in glass bottles.

### 3.5 Column construction

The column design was similar to that described in the literature<sup>124</sup>. About 5 cm. of Teflon tube, 1.5 mm i.d. (Mandel Scientific Co.), was used to make the column. This length of tubing is necessary to accommodate the two end fittings. Approximately 2 mm long cylindrical glass frits (1.5 mm diameter) were made by drilling cores from a sintered glass plate of 50  $\mu$ M nominal pore size. One of these glass frits was gently pressed into the Teflon tube and placed about 2 cm. from the tube end. This can be facilitated either by using a pair of forceps to widen the end of the tube or by very gentle heating of the tube in order to accommodate the frit. The column was weighed at this point and from the other end the desired amount of the dry resin was introduced using a fine spatula. The column was reweighed and the weight of added resin was estimated by the difference in weights. Then another glass frit was pressed from the other end of the tube, so that the resin was very loosely held between the two frits. Some extra space allowed for swelling of the resin. Since the two

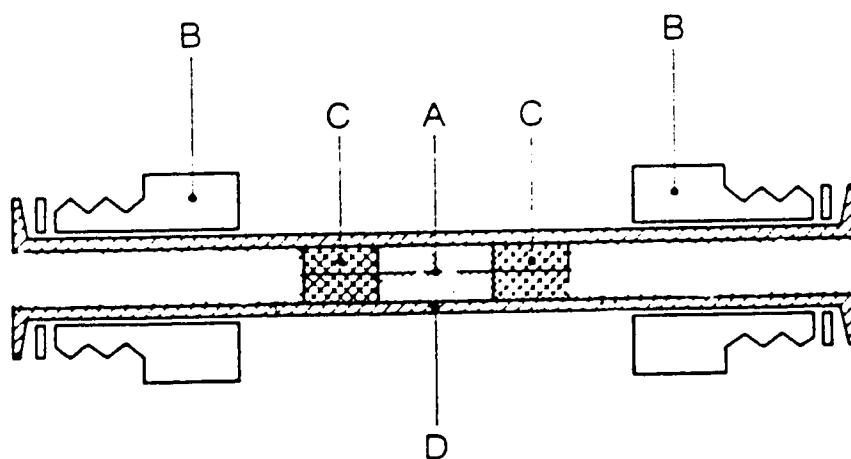


**Figure 3.3:** A cross-section diagram of the column. A, resin bed sandwiched between 2 glass frits C; B, end fittings with stainless steel washers; D, Teflon column body.

glass frits are of almost the same diameter as the tube, and since the pore diameter of the glass frits is smaller than the resin particle size, the resin cannot escape from the column. One end of the tube was then flared and a stainless steel washer, two connectors and another washer were fitted, after which the other end of the tube was flared. Figure 3.3 shows a cross section of a column constructed following this method.

### 3.6 Instrumental conditions

The peristaltic pump was set at 650 in order to maintain a flow rate of about 5 mL/min. The pump setting was changed in order to reduce the flow rate when columns with larger amounts of resin were used. The atomic absorption spectrophotometer conditions for monitoring the calcium and magnesium signals are listed in Table 3.1.

### 3.7 Calculation of free metal concentrations from theory

The calculation of theoretical free metal concentrations in all solutions containing ligands was based on simultaneous calculations of multiple equilibria<sup>131-133</sup>. A slightly modified version of the computer program COMICS<sup>134</sup> on the University of Alberta Amdahl system was used for these calculations. The modification is an additional subroutine which provides the fraction of each form of the metal of interest in tabular form. A detailed description of the algorithm, input procedure and output format is given in the

Table 3.1: Instrumental parameters for the atomic absorption spectrophotometric determination of calcium and magnesium.

---

Lamp current, mA	5 (Ca lamp) 15 (Ca-Mg lamp)
Wavelength, nm	422.7 (Ca) 285.2 (Mg)
Spectral slit width, Å	7
Aspiration rate, mL/min	8
Mode	Absorbance
Signal	Peak area
Integration time,sec	35-60
Acetylene pressure, psig	12
Air pressure, psig	40

---

appendix. In all free metal calculations, the complexation of metals with  $\text{OH}^-$  and  $\text{NO}_3^-$  were ignored because of the very low formation constants associated with these complexation reactions under the conditions used in all experiments. Unless otherwise stated, all corrections to the formation constants for the required ionic strength were carried out using activity coefficients calculated from the Davies equation<sup>135</sup>.

Whenever possible the stability constants were taken from "Critical Stability Constants"<sup>136</sup> which provides uncertainties in the constants if measurements had been made by more than one group. To assess the uncertainty in the calculated values, the COMICS program was run for several systems using constants equal to the average value plus and minus the reported uncertainty. The calculated values for free calcium or magnesium changed by only about one percent, a negligible value under the conditions used.

### 3.8 Procedure for free metal determination

#### a. Flow system 1 (figure 3.1)

The test solution was selected by valve A and pumped through the column via valve B to waste while the water line pumped water to the flame via valve B. This is called the loading cycle and is shown in the first diagram of figure 3.1. The period required to attain complete breakthrough during the loading cycle was determined by studying column equilibration or loading curves as described in later chapters. After loading the column for the

required time, the column was back washed by selecting water with valve A and turning valve B to its second position. This is called the wash position (second diagram of figure 3.1), during which the interstitial test solution is flushed to the flame while the flow of the water line is pumped to waste via valve B. After this wash is completed (no signal in the detector), the elution cycle is carried out, during which the valve settings and flow path are similar to the wash cycle except for valve A, which selects eluent (2M HNO<sub>3</sub>) instead of water. Finally, another wash cycle is performed using the second water inlet to valve A before introducing the next solution. During the elution cycle, the AAS is set to measure the peak area within a specified time selected to include the entire peak.

The function of this setup is the same as the earlier semi-automated system except that in this case only 2 valves and 2 pump lines are used rather than 5 valves and 3 pump lines. This is a much simpler system and is easier to operate when slider valves are replaced by rotary valves. When compared with the automated system which uses 8 valves, this setup is simpler and has the additional feature that the flame is supplied with a continuous flow of water during the loading cycle so that the flame never runs dry.

#### b. Flow system 2 (figure 3.2)

In the second system, an additional 3-way valve, C, was added and the position of the waste line and one of the column lines of valve B were

exchanged. Only 3 ports of the 6-way valve A are used and the 3-way valve served to select between water and eluent.

The test solution was selected by valve A and pumped through the column to waste via valve B. During this load cycle, valve C is used to select water and pump it through valve B to the flame. This process is shown in the first diagram of figure 3.2. The load cycle was followed by an air purge cycle during which air is selected by valve A and pumped through the tubing and the column for 1 minute. The valve positions are the same as the loading cycle except that valve A selects air. Then the column was back washed by the water line from valve C by changing valve B to its next position. Valve A is turned so that water flows through the tubing, flushing the remaining test solution in the tubes to the waste. During this wash cycle, which is much shorter than with flow system 1, any interstitial solution left after the blow cycle is flushed to the flame. This wash cycle is shown in the second diagram of the figure 3.2. This was followed by elution and detection as in the case of flow system 1. During the elution, the valve settings are similar to the wash cycle except that valve C selects eluent instead of water. The column is washed with water before the introduction of the next solution by changing the position of valve B to the first position, and at the same time valve C is switched to direct water to the flame.

One advantage of this system over the previous flow systems is that during the backwash of the column, the flow of sample into the flame is minimal due to the preceding air purge cycle. This minimises any undesirable

effects on the flame and nebulizer due to the introduction of very high levels of salt or organic matter from samples.

The major advantage of this system over the earlier systems is that it reduces perturbation of the ion-exchange equilibrium established during the equilibration or load cycle. With this flow system the equilibrated column does not encounter a momentarily low electrolyte concentration as the initial solution is diluted by the first portion of wash water, with corresponding changes in calcium or magnesium ion levels in the column. The results obtained are more reliable than with the earlier systems, wherein a severe perturbation of the ion exchange equilibria occurred during the wash cycle that immediately followed the load cycle. This modified flow system and the crucial differences it made in the results obtained are discussed in detail in chapter 6.



## CHAPTER 4

### DETERMINATION OF FREE CALCIUM IN THE PRESENCE OF SODIUM UNDER TRACE CONDITIONS

#### 4.1 Introduction

A previous study<sup>128</sup> on the analysis of free calcium in urine focused on working under trace conditions, using  $\text{NaNO}_3$  as the electrolyte. With 0.75M  $\text{NaNO}_3$  the system, though not completely under trace conditions, provided a usable calibration curve. The effects on the measured free  $\text{Ca}^{2+}$  levels of  $\text{Mg}^{2+}$  and urea, possible interfering substances, were found to be negligible at concentrations normally expected in urine. The selectivity of the method for free calcium in the presence of citrate and phosphate, major calcium complexing ligands in urine, was also studied.

Several problems were associated with the method at this stage. They included:

1. The calibration curves had a negative Y intercept, the reason for which was unknown.
2. The selectivity studies showed poor agreement between calculated and experimental free calcium values.

3. To make the  $\text{Na}^+$  plus  $\text{K}^+$  concentration in the sample 0.75 M, estimates of  $\text{Na}^+$  and  $\text{K}^+$  already present in the sample are required. (As a first approximation  $\text{Na}^+$  and  $\text{K}^+$  levels were summed to produce an estimate of the  $\text{Na}^+$  concentration in the sample). This estimation was carried out using flame emission spectroscopy, a procedure which, though satisfactory, is time consuming. To reduce decomposition, therefore, urine samples had to be refrigerated until the  $\text{Na}^+$  and  $\text{K}^+$  analyses could be done. Refrigeration causes precipitation of some substances in urine, a process that could possibly perturb the existing equilibria in the samples.

The work described in this chapter discusses a study of these problems with the method.

## 4.2 Experimental

### 4.2.1 Apparatus

The instrumental setup in this work was the same as in the previous study<sup>128</sup>, which in turn is similar in function to the flow system 1 described in chapter 3. The atomic absorption spectrophotometer used with the previous set up was a Perkin Elmer model 290B which was interfaced with an IBM PC for data acquisition and processing. The instrument was used in the flame emission mode to determine sodium and potassium in the samples. The column contained 4.8 mg of Dowex 50W-X8 resin and was conditioned as described in chapter 3. A flow rate of 4.8 mL/min was used throughout.

#### 4.2.2 Chemicals and solutions

$\text{CaCO}_3$  (J. T. Baker Chemicals Co.),  $\text{NaNO}_3$ ,  $\text{NaOH}$  (British Drug House) and  $\text{HNO}_3$  (Fisher Scientific Co.) were used as received for the work described in this chapter. Stock calcium solution (1000 ppm) was prepared by dissolving  $\text{CaCO}_3$  in an appropriate amount of concentrated nitric acid followed by dilution with deionized water. Stock  $\text{NaNO}_3$  (2M) was prepared by dissolving 169.98 g of salt in water to a volume of 1 L. Standards were prepared by mixing appropriate amounts of these 2 stock solutions with water. The pH of each solution was adjusted by adding a small amount of  $\text{NaOH}$  or  $\text{HNO}_3$ , as required, before final dilution to 100 mL.

Urine samples, obtained from 7 healthy volunteers were tested for free calcium with the minimum possible delay so that refrigeration could be avoided. The concentrations of sodium and potassium in each sample were determined after dilution by a factor of 400. Standards for these analyses contained 0 to 10 ppm of sodium or potassium. Sodium standards contained 2000 ppm potassium and potassium standards contained 1000 ppm sodium as ionization suppressor. An appropriate amount of sodium or potassium was added to 0.25 mL of sample before dilution to 100 mL in order to match the suppressor concentration with that of the standards. Total calcium levels of the samples were also measured by direct aspiration of the samples into the spectrometer in the atomic absorption mode, after 50-fold dilution with water. Standards used in this analysis contained 0 to 8 ppm calcium.

#### 4.3 Investigation of the negative Y intercept of the calibration curves in earlier work

A systematic investigation was done to determine the cause of the negative intercept in the calibration plots for ionic calcium, and of the increase in size of the intercept with increasing concentration of  $\text{NaNO}_3$  in the standards. Several different possibilities were to be considered, although the reason became clear after the third possibility was thoroughly tested.

##### 1. Erroneous response of the detector:-

A new calibration curve was constructed using more standards, especially at lower concentrations, than in the previous study<sup>128</sup>, in order to confirm the presence of a negative intercept at 0.75M  $\text{NaNO}_3$ . A plot of the resulting curve is shown in figure 4.1. Also plotted on the same axes are the absorbances for the 3 lowest concentration standards: these were obtained by direct aspiration of the solutions into the flame of the atomic absorption spectrophotometer. The samples eluted from the column clearly show the presence of a negative intercept while the samples aspirated directly into the flame give a line which goes through the origin. The second graph shows that the performance of the atomic absorption spectrophotometer is normal.

##### 2. Possible interference of $\text{NaNO}_3$ with the calcium signal:

One of the differences in the 2 plots in figure 4.1 is that the amount of calcium received by the flame is much lower in the case of the sample peaks eluted from the column compared to direct aspiration. Therefore if  $\text{Na}^+$

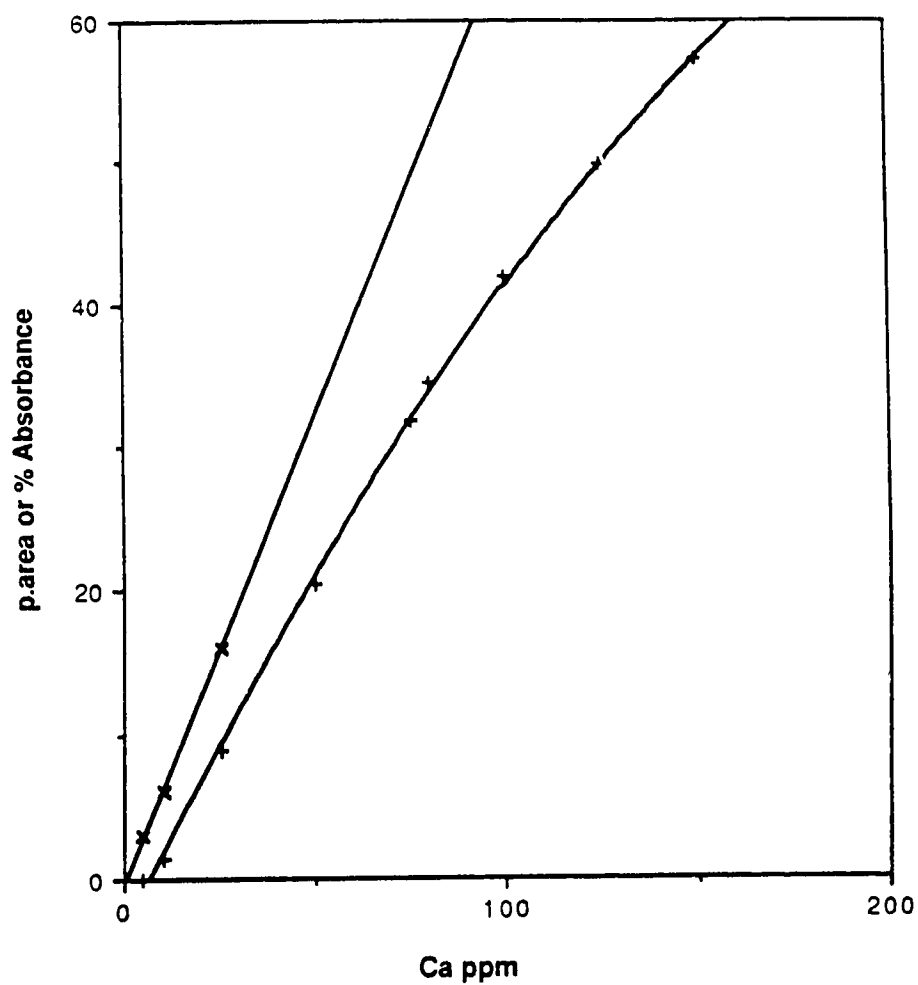


**Figure 4.1:** Calibration curves for calcium standards in 0.75M sodium nitrate; in terms of +, peak areas and x, absorbances of collected peaks in a constant volume. The AAS (PE 290B) sensitivity was changed for the two curves.

interfered with the calcium signal, even slightly, the effect would be significant because of the very high  $\text{Na}^+/\text{Ca}^{2+}$  ratio in the samples. There are two possible ways by which  $\text{NaNO}_3$  might be postulated to negatively interfere with the calcium signal:

- A. If sodium in the flame emits light at 422.7 nm, the absorption maximum of calcium, it could reduce the absorption signal of calcium. But the major emission lines of sodium occur at 589 nm and at 330 nm and there are not even weak emission lines around 422.7 nm. Also, when the absorbance of pure water was set to 30% and 0.75M  $\text{NaNO}_3$  was aspirated into the flame, the absorbance did not change. If sodium emits at this wavelength, the absorbance should have been less than 30%.
- B. Since  $\text{NaNO}_3$  is a salt, it can increase the viscosity of the solution, especially at high concentrations. A change in viscosity can affect the flow rate through the narrow tubing used to aspirate sample solutions into the flame, which in turn affects the AAS signal. But when the aspiration rates for water and for 0.75M  $\text{NaNO}_3$  were measured, no difference was observed between the two solutions.

Therefore interference of  $\text{NaNO}_3$  with the calcium signal can be eliminated from consideration as a possible cause for the negative intercept.

### 3. Software problem in the calculation of the peak area by the computer:-

Since the detector performance was shown to be normal, the signal received by the computer could be considered to be without error. Therefore

the next possible source of error investigated was the computer algorithm used for calculation of the area of the eluted calcium peak. A error in this algorithm could cause a systematic downward shift in the peak areas to create a negative intercept. It was decided that the best way to check this was to repeat the experiment using a different software package for the calculation. The Perkin Elmer model 4000 has a built in software package to calculate peak areas, but the software has very low limits on absorbance values and integration times. Therefore the peak areas obtained from a column containing 4.8 mg of resin were too large to measure with the PE 4000, and it was not possible to obtain a plot of peak area vs.  $[Ca^{2+}]$  with this instrument using the standard column. Therefore a calibration curve was obtained in a different way. Instead of eluting the calcium solutions directly into the flame, they were collected, diluted to an appropriate level and the signals obtained by direct aspiration of the diluted peaks into the flame. A calibration curve obtained in this way, shown in figure 4.2, can be seen to have a zero intercept. This result did not conclusively prove that the problem with the previous system was in the software, but the experiment did provide an important piece of information. That is, the negative intercept is not related to the resin or the column as previously suspected<sup>128</sup>.

It will be shown later in chapter 6 that use of a smaller quantity of resin in the column gave concentrations of calcium small enough to allow direct collection of integrated peaks by the software in the Perkin Elmer instrument,

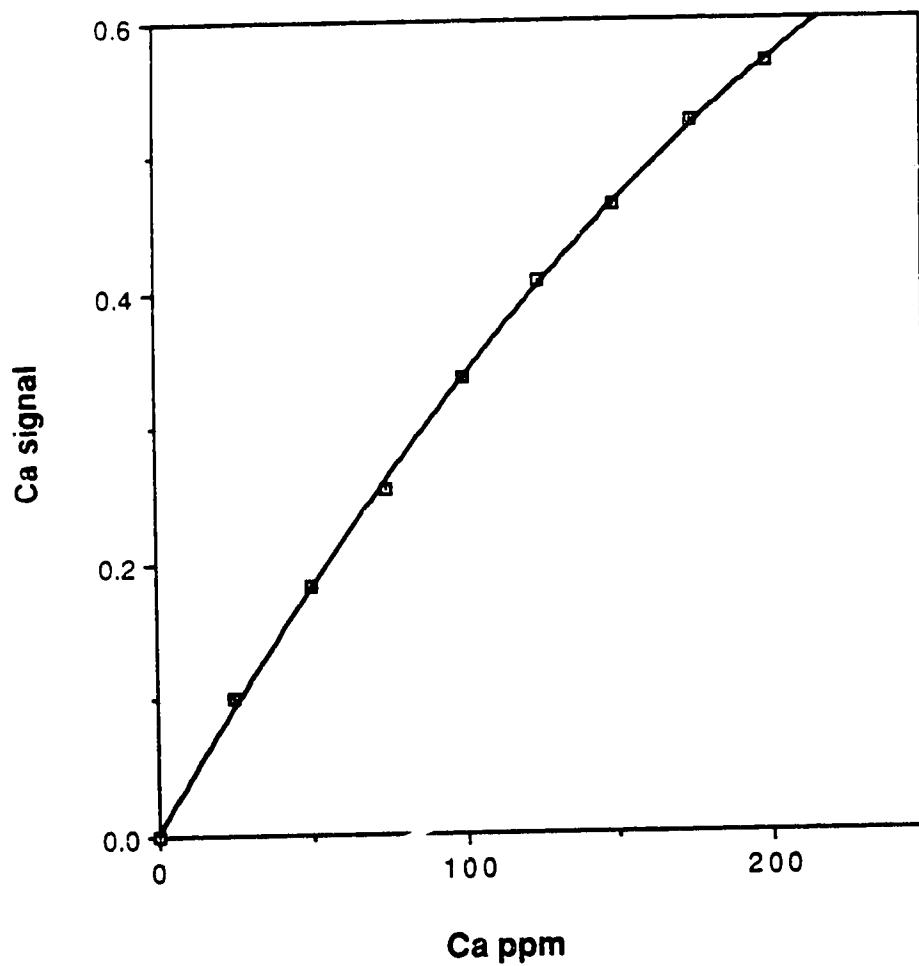


**Figure 4.2:** Calibration curve for calcium standards in 0.75M sodium nitrate in terms of absorbance of collected peaks in a constant volume. The AAS used here was PE 4000.



and that plots of calibration solutions run using this column also give zero intercepts (figure 6.3).

In addition to the calibration curve shown in chapter 6, and the one obtained using the procedure described here, still another observation confirms that the cause of the negative intercept was a software problem. When peak areas obtained with the PE 4000 and the PE 290B in previous system<sup>128</sup> were compared for the same solutions, it was found that although the larger peaks were in good agreement, the smaller peaks were not. For smaller peaks the previous system gave smaller peak area values compared to the PE 4000. Therefore the software in the previous system underestimate the size of the peaks. This effect is more pronounced for small peaks than for larger ones.

When the electrolyte concentration in the standards is increased, the calcium signal decreases. That means the signals become more prone to the software problem at high concentrations of electrolytes. This is consistent with the observation in the previous study, that the negative intercept increases with increasing electrolyte concentration<sup>128</sup>. Clearly, the peak area calculation in the previous system is responsible for the negative Y intercept.

#### 4.4 Selectivity of the method for free over bound calcium

In the previous study, selectivity of the ion exchange method for free calcium was evaluated in the presence of citrate and phosphate, the two major calcium binding ligands in urine<sup>128</sup>. The evaluation was done by comparison of

experimental values obtained by the ion exchange procedure with values calculated for free calcium from equilibrium constants for the calcium-ligand complexes. The agreement obtained for each ligand was not satisfactory. The reason given for this discrepancy was the difference in ionic strength between the experiments and the data used in the calculations. The calculations were based on reported stability constants<sup>136,137</sup> which are often measured at 0.1 or lower ionic strength. The experiments were performed at 0.75 ionic strength. Therefore direct comparison of calculated and experimental values was not possible.

Although the stability constants are not measured at high ionic strengths, they can be estimated for high ionic strengths using a theoretical adjustment. If activity coefficients for the required ionic strengths are available, the stability constants can be estimated for any given ionic strength as shown below (in this case stability constants for ionic strength 0.75 are calculated from data measured at 0.1 ionic strength):

The thermodynamic stability constant  $K^0$  for the formation of the metal complex ML can be written as follows:

$$K^0 = \frac{[ML]}{[M][L]} \cdot \frac{\gamma_{ML}}{\gamma_M \cdot \gamma_L} \quad (4.1)$$

where  $[i]$  = concentration of species  $i$  and  $\gamma_i$  = activity coefficient of the species.

If the conditional stability constant for an ionic strength of 0.1 is denoted as  $K_{0.1}$ , using the activity coefficients for ionic strength of 0.1, the following equation can be written:

$$K^0 = K'_{0.1} \cdot \left( \frac{\gamma_{ML}}{\gamma_M \cdot \gamma_L} \right)_{0.1} \quad (4.2)$$

A similar equation can be written for the ionic strength of 0.75. Since  $K_0$  is a true constant, the following can be written:

$$K'_{0.1} \cdot \left( \frac{\gamma_{ML}}{\gamma_M \cdot \gamma_L} \right)_{0.1} = K'_{0.75} \cdot \left( \frac{\gamma_{ML}}{\gamma_M \cdot \gamma_L} \right)_{0.75} \quad (4.3)$$

Equation 4.3, or its logarithmic form, can be used to convert stability constants from one ionic strength to another, given that the activity coefficients for both ionic strengths are known.

In an ideal solution, in which the solute concentration is extremely low, the concentration equals activity, thus the activity coefficient is unity. When the concentration of the solute increases (i.e. increasing ionic strength), the activity, due to the increase in solute interactions, and therefore the activity coefficient, drops. However, beyond a certain point the activity coefficient rises with increasing ionic strength. Therefore a plot of activity coefficient vs. ionic strength shows a minimum. The rising portion of the plot is explained in terms

of changes in the dielectric constant of the solvent, changes in the activity of the solvent, and changes in the number of free solvent molecules or ion association as described below.

The Debye Hückel approach<sup>131,138</sup> explains only the first part of an activity coefficient - ionic strength plot based on electrostatic interactions. This approach can be used only for ionic strengths below 0.1. The Hückel approach<sup>139,140</sup> explains the second part of the curve in terms of changes in the solvent dielectric constant that occur when the solute concentration increases. This approach is applicable for ionic strengths up to 1, but only for 1:1 type salts. The ionic radii required for these calculations have been measured for a variety of ions<sup>141</sup>. The Hückel approach was not appropriate for calculating stability constants in the present study because of the restriction in the type of salt and because of the unavailability of the ionic radii for some ions.

The Stokes-Robinson approach<sup>140</sup> explains the second part of the above mentioned curve in terms of changes in solvent activity and changes in the amount of free solvent present. This equation is applicable for ionic strengths up to 4, and for 1:1 and 1:2 type salts. Unfortunately the Stokes-Robinson expression is not useful for the present system because of the lack of data on hydration numbers and ion sizes for the species involved. Moreover, this approach does not provide single ion activity coefficients, but rather values for salts. In the present study, since the solution consists of more than one salt, this approach cannot be used.

On the other hand, the Davies approach<sup>135,142</sup> explains the second part of the above mentioned curve in terms of ion association. This method is applicable to single ions, and ion sizes are not required for the calculation. However, it is valid with small error only up to an ionic strength of 0.2, and with about 2% error up to an ionic strength of 0.3<sup>135</sup>.

Given the above options, it was decided that the best approach to use with the present system was the Davies equation. Since activity coefficient ratios rather than activity coefficients are used in the stability constant estimations, the effects of errors in the activity coefficients on the calculated stability constants may not be serious. The form of the Davies equation used in the present study is:

$$-\log \gamma = Az^2 \left( \frac{\sqrt{\mu}}{1 + \sqrt{\mu}} - 0.3\mu \right) \quad (4.4)$$

where  $A = 0.511$  for aqueous solutions at 25°C,  $z =$  the charge of the ion, and  $\mu =$  the ionic strength.

The activity coefficients of uncharged species were considered to be unity<sup>131</sup>, since the ionic strength in the system under study was less than 1.

After all the stability constants were corrected for an ionic strength of 0.75, the free metal concentrations were recalculated by computer using the corrected stability constants. The results are plotted as solid lines in figures 4.3

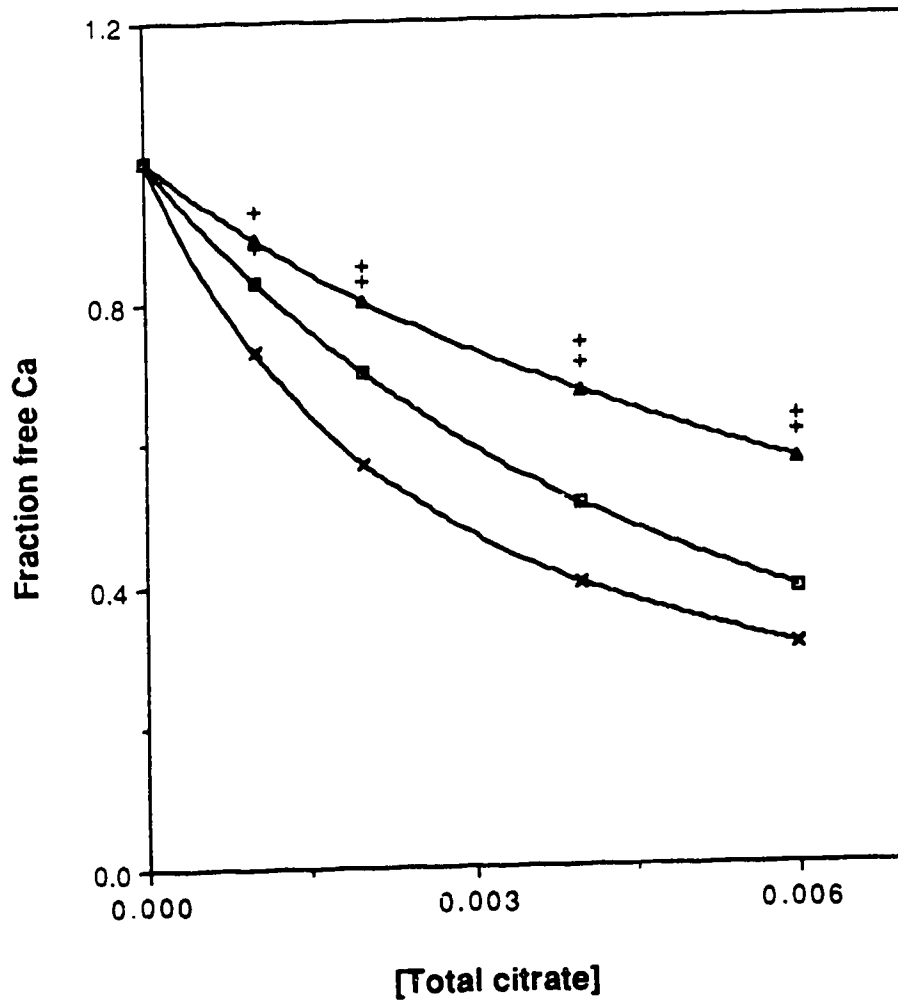


**Figure 4.3:** Variation of free  $\text{Ca}^{2+}$  fraction with total citrate level in 0.75M  $\text{NaNO}_3$ . +, experimental values. Calculated values at ionic strengths; x, 0.1,  $\square$ , 0.75,  $\triangle$ , 0.75 including Na-citrate complexation.

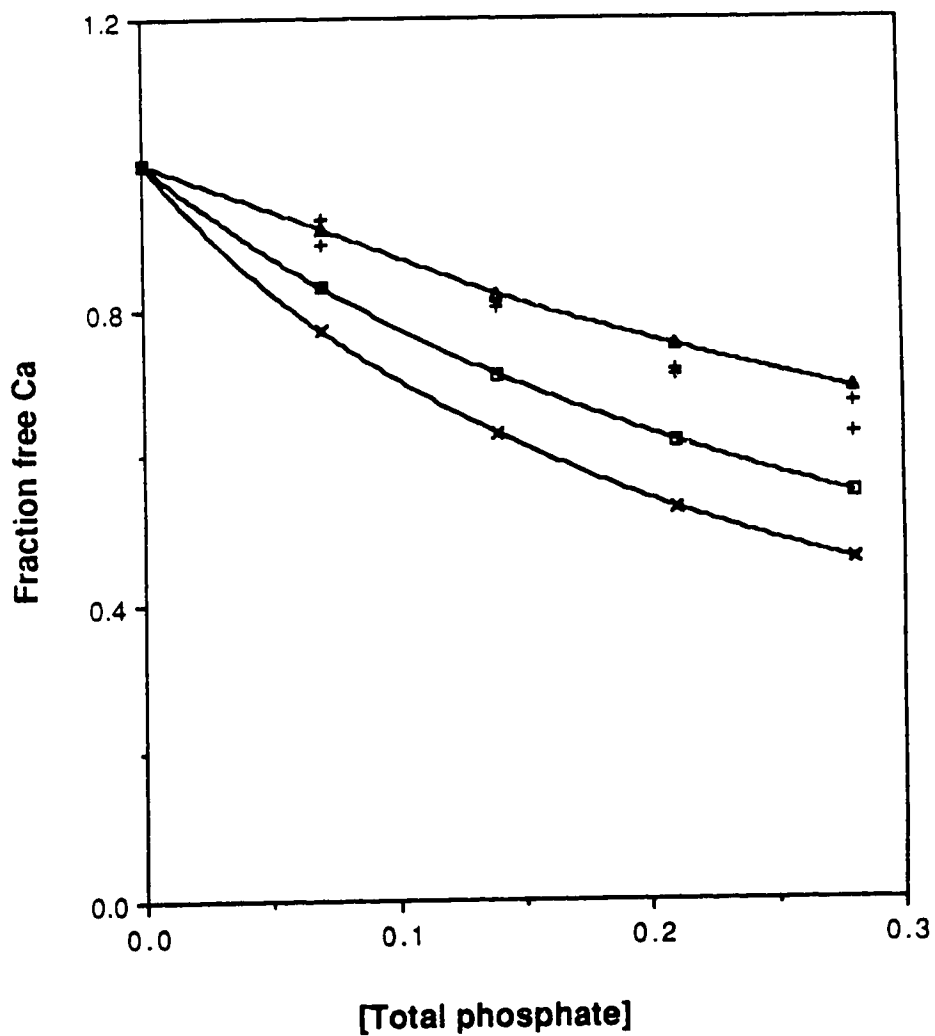


**Figure 4.4:** Variation of free  $\text{Ca}^{2+}$  fraction with total phosphate level in 0.75M  $\text{NaNO}_3$ . +, experimental values. Calculated values at ionic strengths; x, 0.1, □, 0.75, △, 0.75 including Na-phosphate complexation.

and 4.4. These plots show that the experimental and calculated values agree more closely with this correction. However, even after correction the agreement is still not as close as is desirable.

Another possible improvement to the calculation procedure is to consider whether all of the significant equilibria in the system have been taken into account. A list of all possible complexes was written and potentially significant reactions chosen from the list and incorporated into tables 4.1 and 4.2. Calculations show that below pH 10,  $\text{Ca}^{2+}$  does not complex with  $\text{OH}^-$ . Complexation of  $\text{Ca}^{2+}$  and  $\text{Na}^+$  with  $\text{NO}_3^-$  can be ignored, partly because of the very low stability constants and partly because of the fact that these complexes also occur in the standards used in the calibration plot as well as in the ligand-containing solutions. However, possible complexation of  $\text{Na}^+$  with the ligands cannot be ignored because the stability constants are significant and especially because of the very high  $\text{Na}^+/\text{Ca}^{2+}$  ratio in the solutions.

Although the stability constants for a large number of metal-citrate and metal-phosphate complexes are well known, those with the alkali metals are often ignored. The first estimation of the stability constant of  $\text{NaCit}^{2-}$  was done in 1961<sup>143</sup>. This study also suggested the existence of  $\text{NaHCit}^-$ . Later an independent study<sup>144</sup> measured the same constant and obtained the same value. A more recent study<sup>145</sup> evaluated the stability constants for both  $\text{NaCit}^{2-}$  and  $\text{NaHCit}^-$  and many other alkali metal-citrate complexes. Also, a correction was made<sup>146</sup> for the 3 acid dissociation constants of citric acid because  $\text{K}^+$ , which



complexes with citrate, was used as the electrolyte in the measurements of these constants. Similarly, stability constants for complex formation between alkali metal ions and phosphates have been measured<sup>147</sup>. Therefore, the free calcium concentrations were recalculated using all of the available Na-citrate and Na-phosphate stability constants; these results are also plotted in figures 4.3 and 4.4. Listings of all the stability constants considered in this calculation are given in tables 4.1 and 4.2.

Figures 4.3 and 4.4 show that when the improvements in the calculations described above are included, the calculated and observed values are in reasonable agreement. They also show that the added sodium ties up a significant fraction of the calcium binding ligands, allowing more calcium to exist in the free form. The reasons for the small differences that remain between the calculated and experimental values may be one or more of the following:

1. Imperfect correction by the Davies equation for use of stability constants measured at lower ionic strengths to calculate free calcium values at high ionic strengths.
2. In the case of citrate (L), the possible presence of a  $\text{NaH}_2\text{L}$  complex, which would also tie up citrate. A stability constant value for this species is not available. This species, if present but not included in the calculations, would cause calculated values of free calcium to be lower than is actually the case. For example, if one assumes a log stability constant of 0.7 for

Table 4.1: A listing of the stability constants used in the calculation of free calcium in the presence of citrate. (Charges of species are not shown for convenience and the triply charged citrate ion is shown as L).

---

<u>equilibrium</u>	<u>log K (<math>\mu</math>, temp.°C)</u>
CaL/Ca.L	4.68 (0, 25)
CaHL/Ca.HL	3.09 (0, 25)
CaH <sub>2</sub> L/Ca.H <sub>2</sub> L	1.10 (0, 25)
NaL/Na.L	0.70 (0.1, 25)
NaHL/Na.HL	0.10 (0.15, 37)
HL/H.L	6.396 (0, 25)
H <sub>2</sub> L/H.HL	4.761 (0, 25)
H <sub>3</sub> L/H.H <sub>2</sub> L	3.128 (0, 25)

---

Table 4.2: A listing of the stability constants used in the calculation of free calcium in the presence of phosphate. (Charges of species are not shown for convenience and triply charged phosphate ion is shown as L).

---

<u>equilibrium</u>	<u>log K (<math>\mu</math>, temp.°C)</u>
CaL/Ca.L	6.46 (0, 25)
Ca <sub>i</sub> HL/Ca.HL	2.68 (0, 25)
CaH <sub>2</sub> L/Ca.H <sub>2</sub> L	0.80 (0, 25)
NaL/Na.L	0.75 (0.15, 37)
NaHL/Na.HL	0.60 (0.2, 25)
NaH <sub>2</sub> L/Na.H <sub>2</sub> L	0.114 (0.3, 37)
HL/H.L	12.35 (0, 25)
H <sub>2</sub> L/H.HL	7.199 (0, 25)
H <sub>3</sub> L/H.H <sub>2</sub> L	2.148 (0, 25)

---

$\text{NaH}_2\text{L}$  in the calculations of the equilibria, the experimental values in figure 4.3 coincide with the calculated values.

3. In the case of phosphate (L), stability constant values in the literature for  $\text{NaL}$  and  $\text{NaH}_2\text{L}$  were measured only at  $37^\circ\text{C}$ <sup>147</sup>, whereas all other stability constants used in the calculations were measured at  $25^\circ\text{C}$ . The stability constant for  $\text{NaHL}$ , which has been measured at both temperatures, shows a slightly lower value for  $25^\circ\text{C}$  than for  $37^\circ\text{C}$ . The use of two stability constants measured at  $37^\circ\text{C}$  could cause calculated values of free calcium to be slightly higher than is actually the case.
4. The calculated values shown are for a pH of 5. Any deviation in experimental pH will cause a difference between calculated and observed free calcium values.

#### 4.5 Determination of free calcium in urine

To provide a preliminary test of the method, the free calcium levels in the urine of 7 normal individuals were determined as described in section 4.2. The results are shown in table 4.3.

Although the individual free calcium and total calcium values for the urine samples fall within a wide range, the percentage of free calcium falls within the relatively narrow range of 49 to 65%. This range is similar to that reported by other methods<sup>35,57</sup>.

Table 4.3: Results of the determination of free (n=2) and total (n=3) calcium in the urine of seven normal individuals. Uncertainties are  $\pm$  one standard deviation.

---

<u>(Ca)free ppm</u>	<u>(Ca)total ppm</u>	<u>%free Ca</u>
26, 32	55 $\pm$ 1	53
51, 52	80 $\pm$ 1	65
119, 126	240 $\pm$ 1	51
110, 111	180 $\pm$ 2	62
172, 176	320 $\pm$ 1	54
85, 90	180 $\pm$ 1	49
30, 32	50 $\pm$ 1	62

---

#### 4.6 Use of conductance to estimate the urine ionic strength

A correlation has been established between the electrical conductivity and the ionic strength of several media<sup>148,150</sup> including urine<sup>150</sup>. In these studies the concentrations of all the ions and the conductivities of a large number of samples were measured. Then the ionic strength for each sample was computed from the ion concentrations and the ionic strengths were plotted against conductivities. From such plots a general relationship between the ionic strength and the conductivity could be obtained for the sample of interest.

So far in this study,  $\text{Na}^+$  and  $\text{K}^+$  have been considered to be the only metal ions which contribute to the ionic strength of urine. Since the concentrations of other metal ions are very low compared to  $\text{Na}^+$  and  $\text{K}^+$ , this is a reasonable assumption.

The measurement of  $\text{Na}^+$  and  $\text{K}^+$  in each sample, as described above, is somewhat lengthy, and requires the refrigeration of samples until their ionic strengths can be adjusted for the free  $\text{Ca}^{2+}$  determination. The objective of the present study was to investigate the possibility of replacing the usual but slow flame photometric method with a conductivity method which is much faster. Therefore a comparison of the two methods was made to assess their performance in evaluating urinary ionic strength.

Three samples were used in this study. The levels of  $\text{Na}^+$  and  $\text{K}^+$  in each sample were measured by flame photometry, and the required amount of  $\text{NaNO}_3$  was added to an aliquot of each sample to bring the ionic strength up

to 0.75. Then the conductance of each of these aliquots was measured, and compared with the conductance of a solution of 0.75M  $\text{NaNO}_3$ . To a second aliquot of each sample, premeasured amounts of  $\text{NaNO}_3$  were added until the conductance of each aliquot equalled that of 0.75M  $\text{NaNO}_3$ . All the conductance measurements were done at 24°C. The results of this experiment are shown in table 4.4.

The results show that after the addition of  $\text{NaNO}_3$ , following flame photometry, the conductance of each sample was similar to that of 0.75M  $\text{NaNO}_3$ . Also, the amounts of  $\text{NaNO}_3$  added to bring the ionic strength to 0.75 were similar with both methods. This shows that the lengthy flame photometric procedure for ionic strength adjustment can be replaced with a much faster conductance measurement. Also, the results suggest that the sum  $[\text{Na}^+] + [\text{K}^+]$  gives a good estimate of urinary ionic strength. Although  $\text{H}^+$  has a very high conductivity, calculations show that, at the pH values of interest, the contribution of  $\text{H}^+$  to the urinary conductance is negligible.

#### 4.7 Conclusions

In summary, a useful calibration plot with zero intercept was obtained for the determination of ionic calcium in solution, valid up to a free calcium concentration of 200 ppm, the upper limit of urine free calcium. While the calibration is somewhat non-linear, it provides useful values up to 200 ppm.

**Table 4.4:** Comparison of two methods for the adjustment of urinary ionic strength to 0.75.  $C_o$  = original conductance ( $\Omega$ ),  $C_{f1}$  = final conductance following flame photometry ( $\Omega$ ),  $C_{f2}$  = final conductance following the conductivity method ( $\Omega$ )  $W_1$  = Weight of  $\text{NaNO}_3$  added according to the flame photometric method (g),  $W_2$  = Weight of  $\text{NaNO}_3$  added according to the conductivity method (g), ref = 0.75M  $\text{NaNO}_3$  solution.

<u>Sample#</u>	<u>pH</u>	<u><math>C_o</math></u>	<u><math>C_{f1}</math></u>	<u><math>C_{f2}</math></u>	<u><math>W_1</math></u>	<u><math>W_2</math></u>
1	5.8	0.0192	0.0846	0.0820	2.949	2.868
2	6.0	0.0174	0.0806	0.0816	2.778	2.772
3	5.4	0.0345	0.0820	0.0819	2.414	2.214
ref	4.2		0.0816	0.0816		



The initial adjustment for ionic strength can be done within a very short time using conductance measurements. In this way a more reliable value can be obtained for free calcium levels in urine since refrigeration of the sample can be avoided.

According to the results reported in section 4.4, the method appears to be highly selective for free over bound calcium. With phosphate (as L) present, the fraction of CaHL can be as high as 10% and the fraction of  $\text{CaH}_2\text{L}^+$  can be as high as 20%, at pH 5. Also, with citrate (as L) present, the fraction of CaHL can be as high as 12%. Although the ion exchange resin might be expected to sorb both cationic and neutral calcium-ligand complexes, as discussed in chapter 2, under the conditions studied such sorption processes appear to be negligible

In terms of selectivity therefore the method is very promising. The requirement to add salt in order to match sample and standard ionic strengths is still a problem however. Figures 4.3 and 4.4 indicate that the addition of  $\text{Na}^+$  can perturb existing equilibria by complexing with ligands and by raising the ionic strength. According to figures 4.3 and 4.4, the major perturbation occurs through complexation of sodium with ligands. Therefore, although the levels of free calcium measured in section 4.5 are within the reported range, they are expected to be higher than the actual free calcium levels in the samples. This is because the addition of  $\text{NaNO}_3$  to the samples raises the ionic strength and also causes  $\text{Ca}^{2+}$ -binding urinary ligands to be complexed by the

added  $\text{Na}^+$ . Both of these processes increase the original free calcium concentration in urine. Therefore the measured values do not represent the exact original free calcium concentrations, desired for diagnostic purposes; rather they yield the free calcium concentrations of the perturbed samples.

One way to reduce the high  $\text{Na}^+$  concentration required to maintain swamping electrolyte conditions is to replace  $\text{Na}^+$  with a cation having a stronger affinity for the resin. This would allow a lower concentration of that cation to be used, thereby reducing disruption of the original equilibrium present in the samples. Such an approach is discussed in the next chapter.

## CHAPTER 5

### USE OF ORGANIC SALTS AS THE ELECTROLYTE IN THE DETERMINATION OF FREE CALCIUM BY ION EXCHANGE

#### 5.1 Introduction

In chapter 4 it was shown that although the ion exchange column equilibration method is capable of selectively determining free calcium, the sample pretreatment required by this method (i.e. the addition of a high concentration of salt) changes the original free calcium concentration of the sample. An ideal method would not involve alternation, especially in kinetically labile systems such as urine. However, to achieve trace conditions and thereby to obtain a straight line calibration curve, the presence of a cation in sufficient amount to compete with  $\text{Ca}^{2+}$  for ion exchange sites on the resin is required. As described in chapter 2, trace conditions can be achieved either by using a relatively high concentration of a cation which has low affinity for the resin such as  $\text{Na}^+$ , or by using a relatively low concentration of a cation which has a high affinity for the resin. The work described in this chapter has taken the latter approach. An additional restriction which is imposed in choosing such cations is that they should not complex with the calcium binding ligands in

urine. This eliminates the possibility of using di- or tri-valent metal ions in spite of their high affinity for the resin because almost all complex with citrate<sup>136</sup>. Therefore the objective of the work described in this chapter is to explore the possibility of using organic cations which can have high affinity for the resin, and which will not complex with calcium binding ligands in urine. Even though these ions might complex to some degree with the ligands in the sample, if the amount required to achieve trace conditions is small, the change in free calcium caused by such complexations can be negligible. In this way the use of such cations might provide a more valid estimate of the free calcium concentration in urine.

## 5.2 Experimental

### 5.2.1 Apparatus

All the experiments in this chapter were carried out using flow system 1 (figure 3.1) and a Perkin Elmer model 4000 atomic absorption spectrophotometer. The linear range for calcium with this instrument was measured by direct aspiration using 0 to 40 ppm  $\text{Ca}^{2+}$  in 0.01M  $\text{NaNO}_3$  and in 2M  $\text{HNO}_3$ . This matrix composition was chosen in order to closely resemble the effluent which is eluted to the spectrometer from the column. The linear range obtained was 0 - 16 ppm calcium. Considering the linear range obtainable with the system, and the fact that the spectrometer has a 60-second limit on the integration time for peak areas, it was therefore estimated that a

5-fold reduction in the peak areas would be required in order to obtain reliable values for solutions containing up to 200 ppm  $\text{Ca}^{2+}$  in 0.75M  $\text{Na}^+$ . The best way to reduce peak areas was to use less resin in the column. Therefore a new column was constructed containing approximately 0.5 mg of dry resin, by the procedure described in chapter 3. The capacity of the column was estimated by equilibrating the column for 2 to 5 minutes with 1000 ppm  $\text{Ca}^{2+}$  as  $\text{Ca}(\text{NO}_3)_2$  followed by the elution and analysis of the sorbed calcium as outlined in the previous chapter. By dividing the number of equivalents of sorbed calcium by the resin capacity reported by the manufacturer, it is estimated that this column contained about 0.4 mg of resin. The flow rate used in all these experiments was 5 mL/min, which was obtained by setting the peristaltic pump speed control to 665.

A loading curve for 25 ppm  $\text{Ca}^{2+}$  in 0.75M  $\text{Na}^+$  was constructed for this column by equilibrating the column for different time periods followed by measurement of the peak areas. The peak area values obtained for time periods ranging from 15 seconds to 3 minutes were constant and equal, suggesting that the column equilibrates with  $\text{Ca}^{2+}$  solutions containing 0.75M  $\text{Na}^+$ , within 15 seconds. To allow for a reasonable margin of safety an equilibration time of 30 seconds was used for all solutions with this column.

### 5.2.2 Chemicals and solutions

10% tetramethylammonium hydroxide and 40% tetrabutylammonium hydroxide (J. T. Baker) were neutralized with appropriate amounts of  $\text{HNO}_3$  to obtain solutions of the nitrate salts of the ammonium ions.

n-Hexyltrimethylammonium bromide (Tokyo Kasei Inc.) was used as received. Since the pKa values of all the n-alkyl amines used (pentylamine, hexylamine, octylamine, dodecylamine (Aldrich) and heptylamine (Terrochem)) were around 10.5<sup>151</sup>, all the amines exist as the ammonium ions at pH values lower than 8. The amines were mixed with appropriate amounts of  $\text{HNO}_3$  to obtain a solution of around pH 5. A 0.1M stock PIPES (Sigma) solution was prepared first by adding NaOH to 0.01 moles of PIPES in about 20 mL of water until it dissolved, followed by addition of more NaOH to bring the pH to about 6.5 before diluting to 100 mL. Citric acid (Matheson Coleman and Bell),  $\text{NiCl}_2 \cdot 6\text{H}_2\text{O}$ ,  $\text{FeCl}_3$  (British Drug House) were used as received. A 5 mg portion of tetramethylmurexide ammonium salt (TMMA) (Sigma) was dissolved in 10 mL of water to make 0.05% TMMA working solution; it was stored in a dark bottle. When refrigerated, this solution was stable for more than 30 days.

### 5.3 Selection of the optimum organic cation for use in obtaining trace conditions

The organic ions considered in this study were alkyl ammonium cations. Initially, the primary criterion for selection of organic cations with the highest affinity to the resin was the hydration radius of the ion. According to the table by Kielland<sup>141</sup> the tetramethylammonium ion has the smallest radius of the quaternary ammonium ions. Therefore it would be expected to have the highest affinity to the resin used here. The complexing properties of this ion with citrate and phosphate have not been reported in the literature. However, nmr studies show<sup>152</sup> that it does not complex with the dicarboxylic anion, tartrate. Furthermore, tetramethylammonium salts have been used as electrolytes in the measurement of stability constants of other metal citrates<sup>136</sup>.

Considering these facts, it seemed safe to assume that the tetramethylammonium ion does not complex to a significant degree with citrate. Since data are not available, a parallel assumption was made regarding complexation with phosphates. A similar situation holds for many organic ammonium ions. Therefore, as a preliminary test, several organic ammonium salts were studied. The ammonium ion with the highest affinity to the resin was chosen by comparing the calcium peak areas obtained with each organic ammonium ion with those obtained with 0.75M Na<sup>+</sup>.

As a preliminary study to investigate the affinity of these ions for the resin, a moderate concentration, 0.3M, of ammonium ion was used as the

electrolyte. The peak areas for calcium (25 ppm) obtained with 0.3M tetramethylammonium and 0.3M tetraethylammonium were much larger than those obtained with 0.75M Na<sup>+</sup>. Also, the volume of solution required to be passed through the resin to achieve equilibration in both cases was much higher than that with Na<sup>+</sup>. This shows that the affinities of these ions are not high enough to provide trace conditions at a relatively low concentration.

Since affinity for the resin increases with the length of the alkyl chain of the quaternary ammonium ion<sup>130</sup>, the possibility of using 0.1M n-hexyltrimethylammonium bromide to obtain trace conditions was investigated. Equilibration of the column to 25 ppm calcium also required large volumes and gave large peaks as in the case of the other quaternary ammonium salts. However, 0.1M solutions of: pentyl and heptyl ammonium salts gave much smaller peak areas, indicating strong competition by these ions for calcium on the resin column, with very small volumes of equilibration. Therefore, a systematic study of the normal alkyl ammonium ions was done using pentyl, hexyl, heptyl, octyl and dodecyl ammonium nitrates.

For each system the resin column was equilibrated with 50 ppm Ca<sup>2+</sup> solutions 0.1M in alkyl ammonium ion, followed by elution of the Ca<sup>2+</sup> and measurement of the peak areas. The dodecylammonium ion was not included in this study because its very low solubility did not allow the concentration levels to be attained.



When the log of peak area was plotted against the number of carbon atoms in the alkyl chain of the ammonium ion (figure 5.1), a straight line relationship was obtained.

In earlier work using 0.75M Na<sup>+</sup> in the equilibration solution, plots of peak area vs. concentration of Ca<sup>2+</sup> (the calibration curve) were linear up to about 50 ppm, indicating that trace conditions are satisfied only up to 50 ppm. But to analyse urine, a calibration curve should include Ca<sup>2+</sup> concentrations up to about 200 ppm. This means that for a given free Ca<sup>2+</sup> concentration the peak area should be 4 times smaller than those obtained with 0.75M Na, otherwise trace condition requirements for the entire range of Ca<sup>2+</sup> concentrations are not likely to be met. The next step in this work was to determine which of the alkylammonium salts could satisfy this requirement.

According to the results shown in figure 5.1, one of the variables that can be used to optimize calcium determinations is the alkyl chain length of the alkylammonium ion. Another is the concentration of the ammonium ion. From this preliminary study the longer alkyl chains appeared to give results in the best range of the peak areas. Therefore, in the next experiment the dependence of the peak area of eluted Ca<sup>2+</sup> on the concentration of alkylammonium ion was studied using hexyl and octyl ammonium ions. The concentration of hexylammonium was varied from 0.1M to 0.3M while that of octylammonium was varied from 0.05M to 0.1M. Figures 5.2 and 5.3 show the results of this study. When the peak areas obtained in this study were

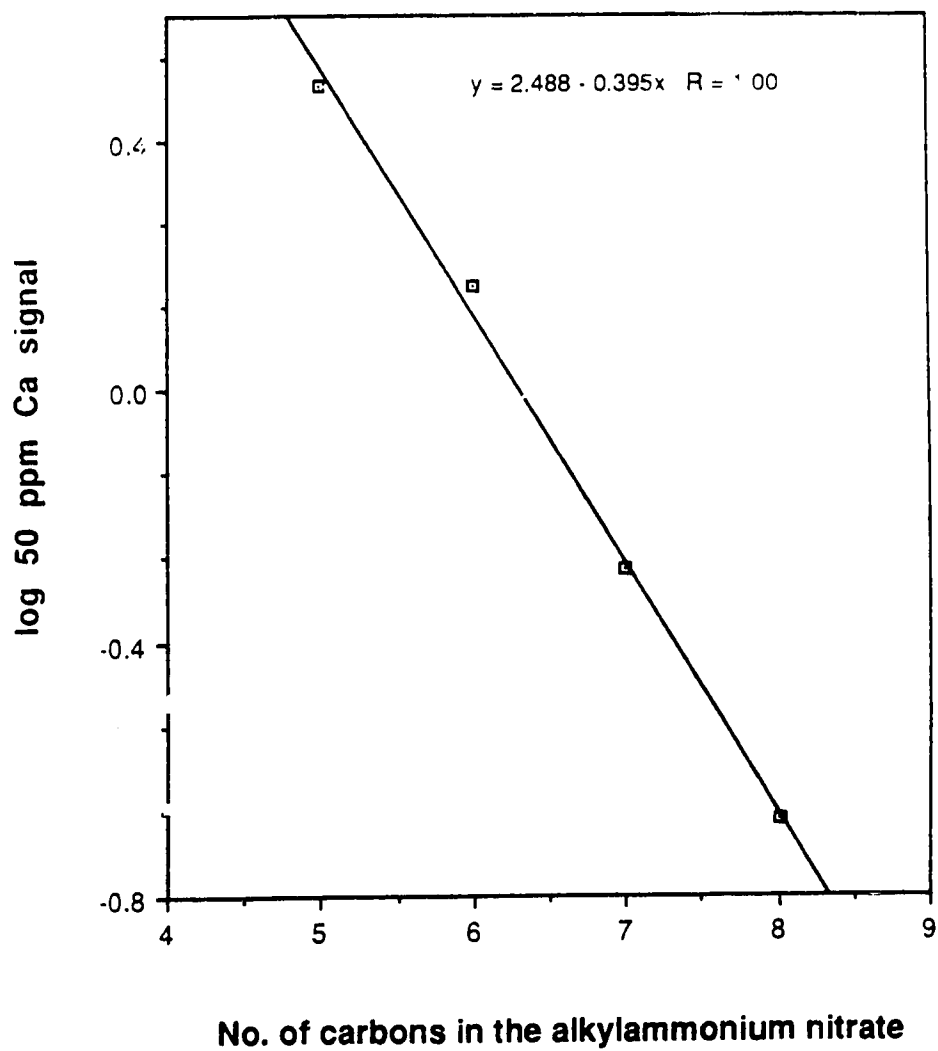


**Figure 5.1:** Variation of peak area for 50 ppm  $\text{Ca}^{2+}$  in 0.1M alkylammonium nitrate solution with the number of carbon atoms in the alkyl chain.

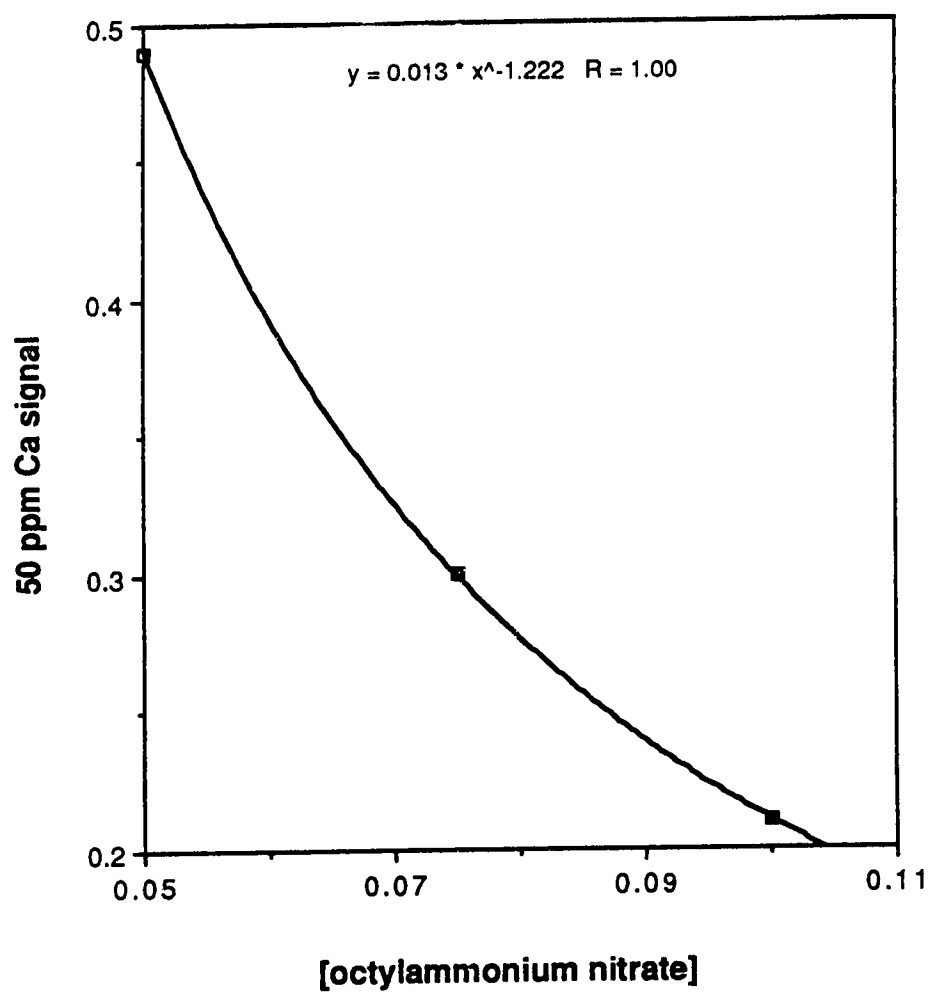


**Figure 5.2:** Variation of peak area for 50 ppm Ca<sup>2+</sup> with the concentration of octylammonium nitrate.

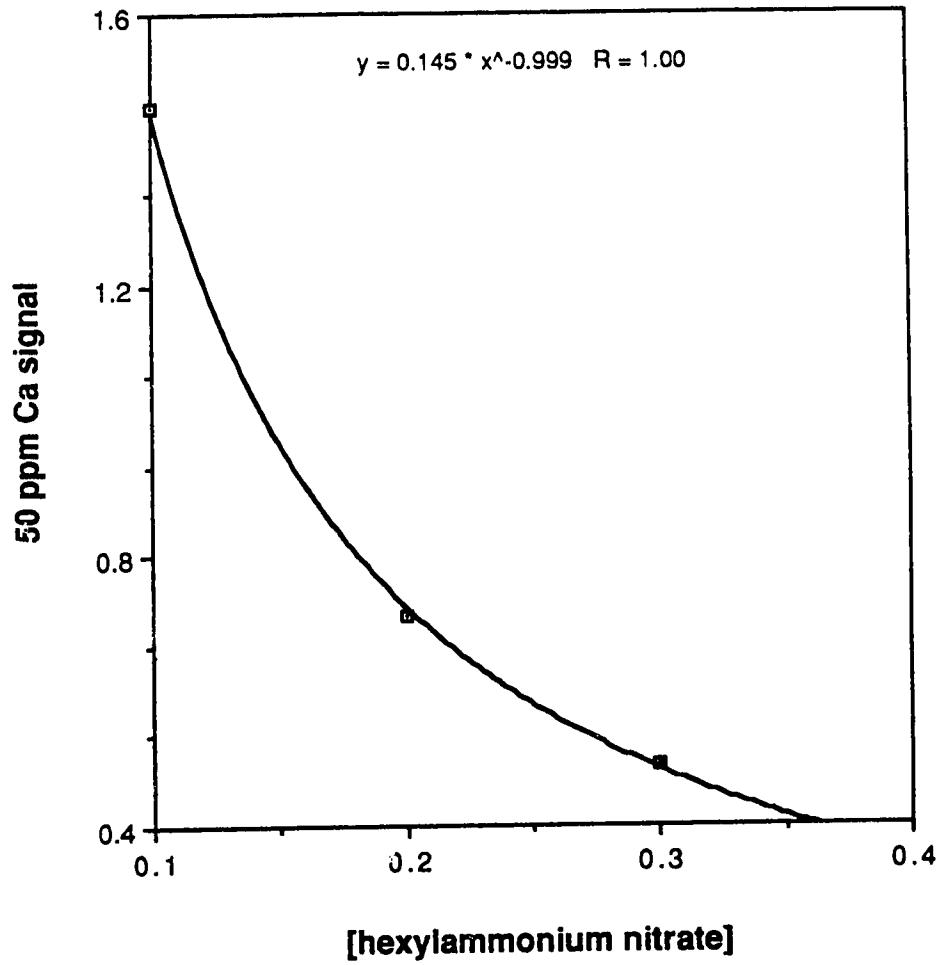


**Figure 5.3:** Variation of peak area for 50 ppm Ca<sup>2+</sup> with the concentration of hexylammonium nitrate.

compared with those obtained with 0.75M Na<sup>+</sup>, the use of 0.07M octylammonium nitrate as electrolyte seemed to be the best way to obtain a straight line calibration plot up to 200 ppm Ca<sup>2+</sup> because the peak areas obtained were four times smaller.

In contrast to the sorption of inorganic ions, the sorption of organic ions increases with increasing size of the ion<sup>130,154</sup> because Vanderwaal forces become more important than coulombic forces. Vanderwaal forces include dipole-dipole interactions, induced dipole interactions (or induction effect) and instantaneous dipole interactions (or London forces)<sup>155</sup>. Induced dipole interactions increase with increasing polarizability, which in turn is related to the number of atoms of the molecule that come into contact with the resin surface. Therefore the increase in sorption with increasing size of the organic ions can be explained in terms of the number of carbon atoms in the organic ion<sup>154</sup>. When two organic ions which have the same number of carbon atoms are compared, the structure of the ion matters. That is, a stronger sorption is achieved for the ion that has the larger number of carbon atoms which are capable of coming into contact with the resin<sup>154</sup>. London forces become stronger with increasing structural similarity between the solute and the resin. Therefore aromatic organic ions can be sorbed more strongly onto a divinylbenzene (DVB) resin matrix than aliphatic organic ions with the same number of carbon atoms.

When simultaneous sorption of organic and inorganic ions occurs, as is the case in the present study, both coulombic and Vanderwaal forces must be considered. Essentially, a competition between these two forces occurs in the process of sorption. When the resin has a high degree of cross linking, the smaller ion is preferably sorbed because of the restriction imposed by the cross linking on the size of the solute. That is, at high cross linking coulombic forces dominate, resulting in preferential sorption of the inorganic ion over the organic ion. At low cross linking, Vanderwaal forces become dominant, resulting in preferential sorption of the organic ion<sup>121,156,157</sup>. This kind of selectivity reversal also occurs with two inorganic ions of different size<sup>158</sup>. Depending on the relative strength of coulombic or Vanderwaal forces between a molecule and the resin, the percentage cross linking at which this reversal occurs varies. For example, aromatics which exert very strong Vanderwaal forces can be preferred over inorganic ions even at 9% cross linking, whereas for aliphatics this turning point occurs around 3% cross linking<sup>121</sup>. In the case of aliphatic quaternary ammonium ions, Na<sup>+</sup> is preferred to tetramethyl, tetraethyl, tetrapropyl and tetrabutyl ammonium ions at 8% cross linking<sup>159</sup>.

The facts described above explain the failure to obtain trace conditions with quaternary ammonium ions using 8% crosslinked DVB resin in the present study. Another important factor to consider when dealing with highly crosslinked resins is the variation in exchange capacity with different ions. The exchange capacity of a resin for an ion decreases with increasing cross-linking.

The exchange capacity of a resin also decreases with increasing size of the hydrated ion<sup>160,161</sup>. Therefore, the exchange capacity could be lower for the tetraalkylammonium ions compared to  $\text{Na}^+$ . This variation in the exchange capacity can also be a reason for the lower affinity of the quaternary ammonium ion to the resin observed in the present study.

According to the results obtained with this study, sorption of normal alkylammonium ions ( $\text{RNH}_3^+$ ) is quite different from that of quaternary ammonium ions ( $\text{R}_4\text{N}^+$ ). Even when two very similar ammonium ions are compared (hexylammonium and hexyltrimethylammonium, which differs from the former only in having 3 methyl groups around the N atom), the sorption of hexylammonium was much stronger than that of hexyltrimethylammonium. Although ion exchange studies of organic ions have largely focussed on quaternary ammoniums, very little has been done with normal alkylammoniums. This may partly be due to the non-availability of the alkylammoniums in solid form, unlike quaternary ammoniums. A comparison of the sorption of ammonium ions on the cation exchanger Zeolite (an aluminosilicate)<sup>162</sup> shows that sorption decreases in the following order:  $\text{NH}_3\text{Me}^+ > \text{NH}_2\text{Me}_2^+ > \text{NHMe}_3^+$ . This is attributed to size differences between the ions. The stronger sorption observed with hexylammonium, compared to hexyltrimethylammonium in the present study, is in accordance with this observation. According to our results, however, the reason could not be the size factor, because octylammonium showed a stronger sorption

compared to hexylammonium. The preference of normal alkylammonium to quaternary alkylammonium therefore could be due to forces such as H-bonding since the only difference between quaternary and normal alkylammonium seems to be the presence of H in the normal alkylammonium (i.e. H-bonding between O atoms on sulphonate groups of the resin and H atoms of the alkylammonium ion). The sorption series shown above can also be explained in terms of H-bonding because that order is the same as the order of the number of H atoms in the alkylammonium ion.

Among normal alkylammonium ions, the increasing strength of sorption with increasing size must then be due to induced dipole interactions (or inductive effect) as described earlier. Thus the distribution coefficient of a normal alkylammonium ion  $\text{RNH}_3^+$  increases with increasing number of carbon atoms in the alkyl chain. This has been quantitatively explained by the Martin equation<sup>163-166</sup>. According to the Martin equation, the energy of interaction of the solute molecule with the stationary phase is equal to the sum of the interaction energies of the individual groups that constitute the solute molecule.

The quantitative expression of the Martin equation is:

$$\log K_i = \log K_{\text{CH}_2} \cdot n + A \quad (5.1)$$

where  $K_i$  = distribution coefficient of the solute

$K_{\text{CH}_2}$  = distribution coefficient of the  $\text{CH}_2$  group



$n$  = number of carbon atoms (methylene groups) in the solute

$A$  = a constant for a given homologous series

The distribution coefficient,  $K$ , is defined as the ratio of the concentration of solute in the stationary phase to that in the mobile phase. In the present study, the concentration of alkylammonium ion in the mobile phase was constant, 0.1M, for all alkylammonium ions. The volume of the stationary phase is also a constant. Therefore,  $K$ , is proportional to the number of moles of alkylammonium ions sorbed on the stationary phase, which is represented by the peak areas. According to the Martin equation, a plot of  $\log$  (peak area) for the alkylammonium ions vs. the number of carbon atoms in the alkylammonium ions should be a straight line with increasing slope. Since in the present study the only other ion sorbed (calcium) was monitored, and because the total exchange capacity of the resin is a constant, the slope for calcium should be negative. The straight line plot with a negative slope obtained in figure 5.1 is therefore consistent with the Martin equation.

Since sorption increases with increasing size of the alkylammonium ion, octylammonium on this basis should be the best choice for obtaining trace conditions for  $\text{Ca}^{2+}$ . The concentration of octylammonium required to obtain trace conditions, 0.07M, is significantly lower than that for the other alkylammonium ions.

#### 5.4 Determination of free $\text{Ca}^{2+}$ in the presence of octylammonium ion under trace conditions

According to figure 5.2, in order to get peak areas which are 1/4 the size of those obtained with 0.75M Na, 0.07M octylammonium is required in the  $\text{Ca}^{2+}$  standards. Therefore equilibration solutions containing 0.07M octylammonium should give a straight line calibration plot up to a  $\text{Ca}^{2+}$  concentration of 200 ppm, in contrast to the 0.75M  $\text{Na}^+$  solutions used previously, which gave a straight line only up to 50 ppm. The critical micelle concentration (CMC) of octylammonium is 0.175M<sup>167</sup>. Therefore at 0.07M it will be available only as cations and micelle formation can be considered negligible. The  $\text{pK}_a$  of octylammonium is 10.65<sup>152</sup>, indicating the protonated form is present almost exclusively at pH values below about 7. The standards used in this study were always within the pH range of 4 to 7.

##### 5.4.1 Effect of sodium on octylammonium system

In order to analyse urinary free  $\text{Ca}^{2+}$  using the octylammonium system, a 0.07M concentration of the salt must be added to urine. Standards contain  $\text{Ca}^{2+}$  and 0.07M octylammonium. But samples also contain high concentrations of cations such as  $\text{Na}^+$  and  $\text{K}^+$  which can participate in the ion exchange process. This means standards must be matched in terms of  $\text{Na}^+$  and  $\text{K}^+$  in order to obtain reliable free  $\text{Ca}^{2+}$  values. Since the sorption of octylammonium is very strong, the sorption of  $\text{Na}^+$  and  $\text{K}^+$  could be negligible despite their

high concentrations. If this is true, standards might not require matching in terms of  $\text{Na}^+$  and  $\text{K}^+$  concentrations.

$\text{Na}^+$  is the major cation in urine; concentrations in normal individuals vary between 0.2 and 0.38M. The concentration of  $\text{K}^+$  can vary between 0.03 and 0.09M<sup>168</sup>. Assuming that  $\text{Na}^+$  and  $\text{K}^+$  sorb to a similar extent, the range of metal ion concentration can be considered as roughly 0.03 - 0.4M. In order to investigate the effect of  $\text{Na}^+$  and  $\text{K}^+$  in urine on the sorption of  $\text{Ca}^{2+}$  in the presence of octylammonium ion, the following experiment was done. To solutions which contained 50 ppm  $\text{Ca}^{2+}$  and 0.07M octylammonium, 0, 0.2M and 0.4M  $\text{NaNO}_3$  were added. A level of 50 ppm was chosen as the  $\text{Ca}^{2+}$  concentration since it is at the low end of typical urine  $\text{Ca}^{2+}$  levels. In this way the experiment would test the worst case effect of interference from  $\text{Na}^+$  and  $\text{K}^+$  on the measured free  $\text{Ca}^{2+}$  signal. The free  $\text{Ca}^{2+}$  signal of each of these solutions was measured and the results are shown in figure 5.4. The free  $\text{Ca}^{2+}$  signal at different  $\text{Na}^+$  concentrations does not appear to change significantly. Analysis of variance (ANOVA) confirms that there is no significant difference among free  $\text{Ca}^{2+}$  values obtained at different concentrations of  $\text{Na}^+$ , at the 95% confidence level. This means that there is no need to match the standards with the  $\text{Na}^+$  and  $\text{K}^+$  levels of individual samples. Since urine  $\text{Na}^+$  and  $\text{K}^+$  levels vary from sample to sample, preparation of a separate set of standards for each sample can therefore be avoided.

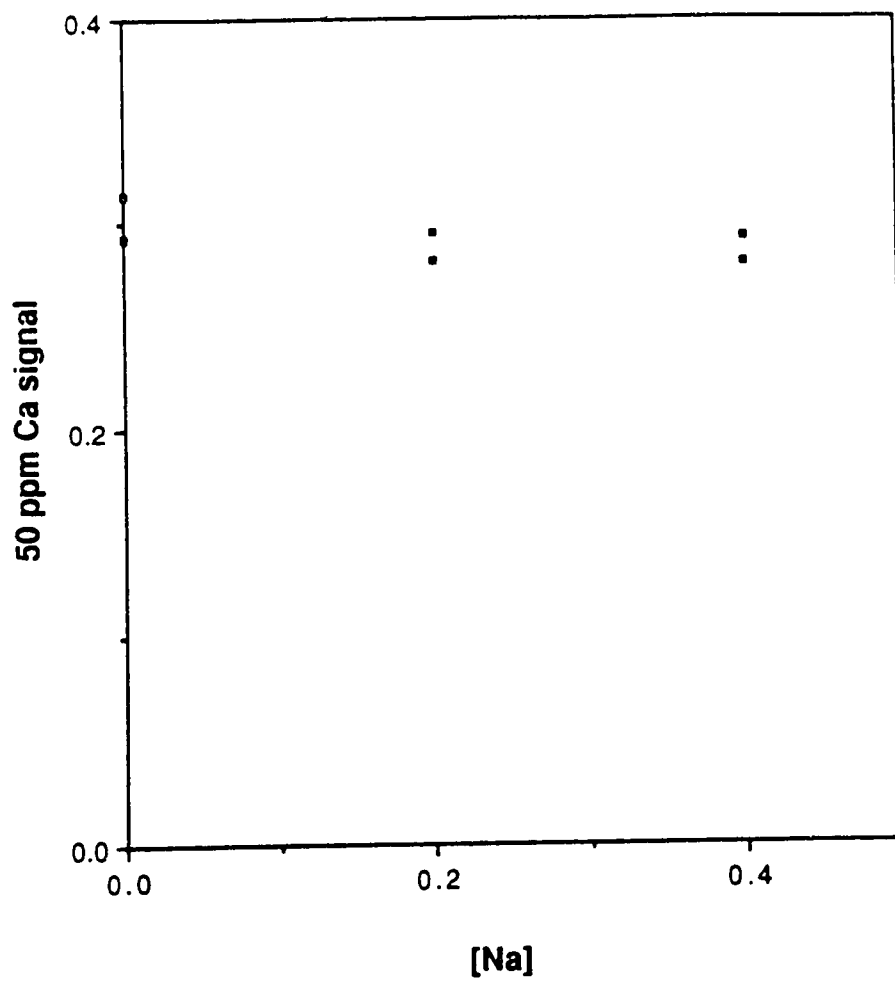


Figure 5.4: Variation of peak area for 50 ppm  $\text{Ca}^{2+}$  in 0.07M octylammonium nitrate with the concentration of  $\text{NaNO}_3$  in the solution.

#### 5.4.2 Test of column trace conditions with octylammonium

A 5-point calibration plot was therefore constructed over the range of 0 to 200 ppm  $\text{Ca}^{2+}$  using only 0.07M octylammonium nitrate in the standards. This plot (see figure 5.5) shows that trace conditions are satisfied up to 200 ppm  $\text{Ca}^{2+}$  using 0.07M octylammonium nitrate as the equilibrating solution electrolyte.

#### 5.4.3 Peak tailing problem

Throughout the study using normal alkylammoniums, a tailing problem was observed with the peaks. This problem became more severe with increasing size of the ammonium ion, so that octylammonium showed the worst peak shape. This means the tailing is related to sorption of the ammonium ion rather than that of  $\text{Ca}^{2+}$ .

Tailing results from abnormal sorption of some of the solute molecules compared to the majority of the solute molecules. This is a result of the existence on the resin of a small number of sites which are relatively inaccessible. In the present study there are two possible solutes which could sorb onto these sites, namely  $\text{Ca}^{2+}$  and alkylammonium. If some of the alkylammonium ions are sorbed onto these sites, tailing can result during elution. However, it can be observed only if the ammonium ion also absorbs at 422.7 nm, which is the calcium detection line. (The octylammonium absorption considered here is a broad band often shown by organic substances.) If this is

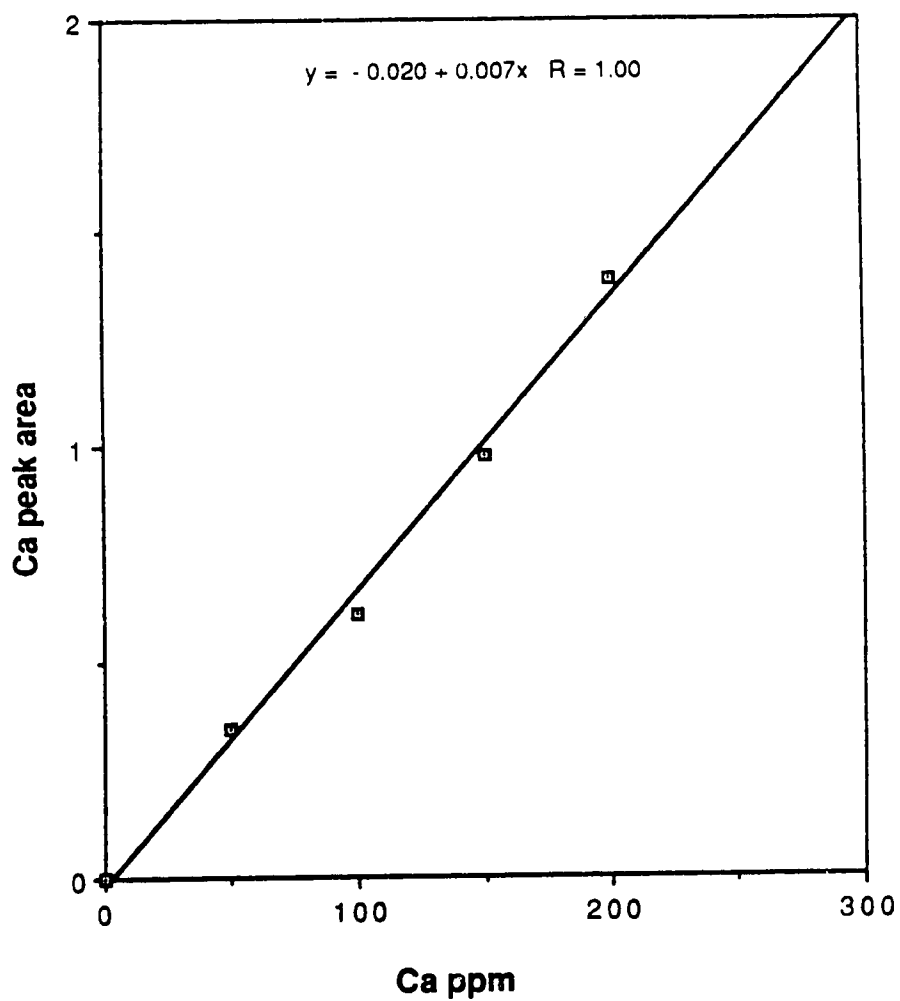


Figure 5.5: Calibration curve for standard  $\text{Ca}^{2+}$  solutions in 0.07M octylammonium nitrate.

the case, the tail is not due to  $\text{Ca}^{2+}$  but due to ammonium ions. The organic absorption can be subtracted by using a background correction option in the AAS. However, direct aspiration of 0.07M octylammonium showed no absorption at 422.7 nm, suggesting the tail is not directly caused by ammonium ion.

The tailing part of the peak must therefore be caused by  $\text{Ca}^{2+}$  ions which are eluted more slowly from the above described sites on the resin. The normal procedure employed to overcome peak tailing is to use an ion which can compete effectively with  $\text{Ca}^{2+}$  for such sites, and block them from  $\text{Ca}^{2+}$ . The ions present in the standards in this experiment are octylammonium and  $\text{H}^+$ .  $\text{H}^+$  is not a good competitor because its affinity for the resin is much less than that of  $\text{Ca}^{2+}$ . Also, at the pH value of about 5, used in the standards, the  $\text{H}^+$  concentration is extremely low causing virtually no sorption of  $\text{H}^+$  on to the resin. Although octylammonium is a good competitor for  $\text{Ca}^{2+}$ , it may be blocked from reaching the relatively inaccessible sites due to its large size.

Evidence to support this explanation can be found in the increase in tailing observed with increasing length of the alkyl chain of the alkylammonium as mentioned earlier. This means that when alkylammonium ions are used, masking of relatively inaccessible sites described above does occur, the extent of which is diminished with increasing size of the ammonium ion. In contrast, when  $\text{Na}^+$  was used in section 5.4.1, the peak shape showed negligible tailing. Although  $\text{Na}^+$  is not as effective a competitor ion as the alkylammonium ions

for exchange sites, due to the relatively high concentrations of  $\text{Na}^+$  used and due to its smaller size (hydration radius of  $\text{Na}^+ = 0.36\text{\AA}$  and  $\text{Ca}^{2+} = 0.41\text{\AA}$ ), it could reach most exchange sites and compete with  $\text{Ca}^{2+}$ .

One way to retain the advantages of use of the alkylammonium ions as electrolyte while reducing peak tailing is to have  $\text{Na}^+$  present in all standards and samples. As was shown in section 5.4.1, in the presence of 0.07M octylammonium ion, up to 0.4M  $\text{Na}^+$  can be present without significant effect upon the free  $\text{Ca}^{2+}$  signal. As will be shown later, the  $\text{Na}^+$  typically present in the buffer is sufficient to reduce tailing of  $\text{Ca}^{2+}$  elution significantly.

#### 5.4.4 Effect of pH

In addition to matching the samples and standards in terms of metal ions present, a matching in terms of pH is also required in order to obtain reliable free  $\text{Ca}^{2+}$  values for urine samples. Since urine pH typically varies from sample to sample over the range 5 - 7<sup>168</sup>, a set of standards is required for each sample in the analysis of free  $\text{Ca}^{2+}$ .

The extent of variation of the free  $\text{Ca}^{2+}$  value with pH was studied as follows. The pH of a solution of 75 ppm  $\text{Ca}^{2+}$  in 0.07M octylammonium nitrate was varied from 5.2 to 7.2, and free  $\text{Ca}^{2+}$  signals were measured. The results are shown in figure 5.6. Although there is some scatter in the data, ANOVA showed no significant difference among the free  $\text{Ca}^{2+}$  values obtained at different pH values, at the 95% confidence level.



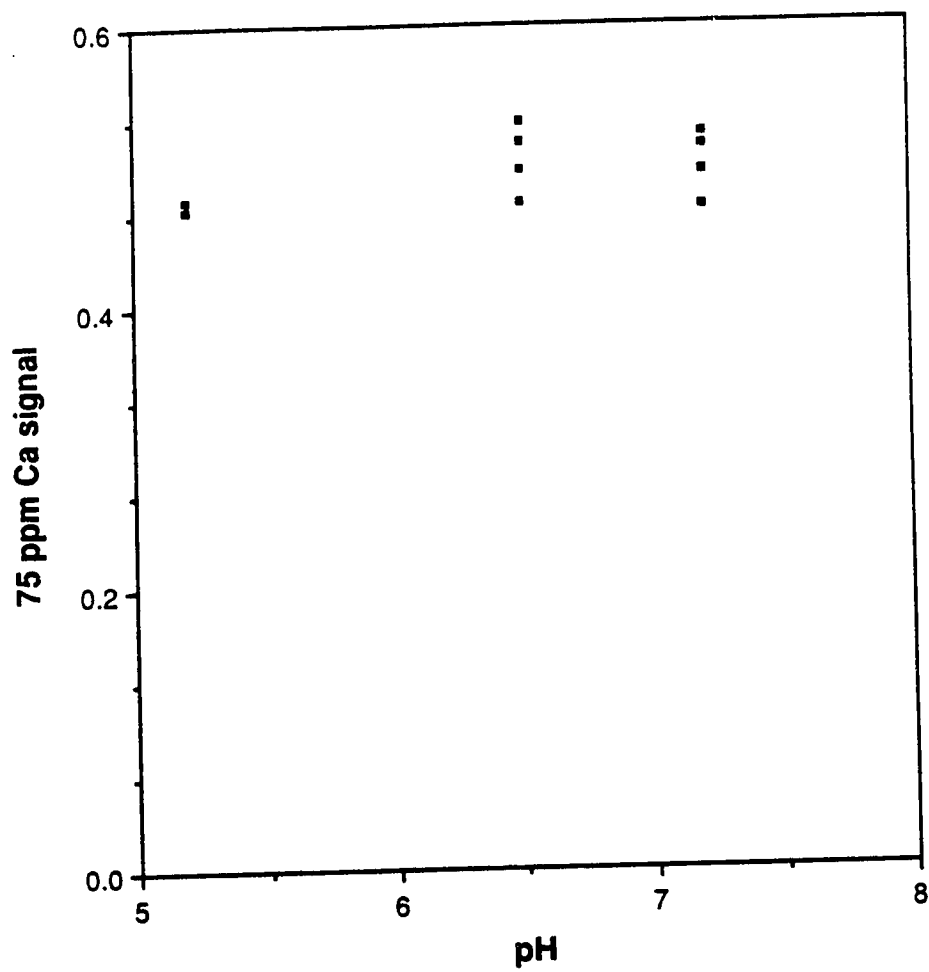


Figure 5.6: Variation of peak area for 75 ppm  $\text{Ca}^{2+}$  in 0.07M octylammonium nitrate with the pH.

This result is important because it shows that standards do not require matching with samples in terms of pH, so long as the sample pH falls within the range 5 to 7. Since the  $H^+$  concentration at these pH values is extremely low, and since  $H^+$  does not have a high affinity to the resin, the sorption of  $H^+$  is negligible. Moreover, octylamine is completely in the protonated form at all pH values below 7 and the ion exchanger sites do not take up protons at these pH values because the resin is a strongly acidic cation exchanger. Even over a wider pH range, such as 3 to 7, no difference is expected in the measured free  $Ca^{2+}$  signal.

#### 5.4.5 Calibration curve with buffered standards

From the results of section 5.4.4, one set of standards whose pH is within 5-7 should be sufficient to allow the determination of  $Ca^{2+}$  in urine samples with pH values in the normal range. Because of the inconvenience involved in adjusting the pH of standards using acid or base, the possibility of using a pH buffer was investigated. The criteria for selecting a buffer for this purpose were:

1. The buffer should be in the range of pH 5 to 7 (i.e. the conjugate acid-base pair should have a pKa of about 6).
2. The ions comprising the buffer solution should not complex with any of the species in the standards. Of major concern here is complexation between the buffer and calcium ions.

3. The buffer components should be water soluble and stable.

Several buffers were considered: KHPthalate-NaKPhthalate and NaMaleate- $\text{Na}_2$ Maleate each give the required buffer range, but both phthalate and maleate ions complex with calcium<sup>136</sup>. Other buffers have been designed especially for biological research over the pH range 6-8<sup>170</sup>. Among these, PIPES (Piperazine-N,N'-bis[2-ethanesulphonic acid]) appeared best suited for this work. The pKa of PIPES is 6.8, with a useful buffer range of 6.1 to 7.5.

Accordingly, the pH of a set of standards was adjusted by first adding the calculated amount of stock PIPES solution followed by addition of small amounts of 1M NaOH or  $\text{HNO}_3$  before final dilution, to provide a pH of 6.4 in each solution. The complexation of PIPES with  $\text{Ca}^{2+}$  and  $\text{Mg}^{2+}$  is reported to be negligible<sup>170</sup>. In order to check the extent of  $\text{Ca}^{2+}$ -PIPES complexation at the  $\text{Ca}^{2+}$  and PIPES levels used in the present study, the following experiment was carried out.

Two  $\text{Ca}^{2+}$  concentrations, 75 and 125 ppm, were prepared in 0.07M octylammonium nitrate. The pH of the solutions were adjusted using either  $\text{HNO}_3$  alone (no buffer) or using different amounts of buffer, to 6.4. The solutions were equilibrated with the resin column, then washed and eluted as before. The resulting peak areas were then measured and compared.

The results, shown in figures 5.7 and 5.8, indicate that the buffer has no significant effect on the measured free  $\text{Ca}^{2+}$  value, even at buffer concentrations as high as 0.1M. Also, ANOVA shows that there is no

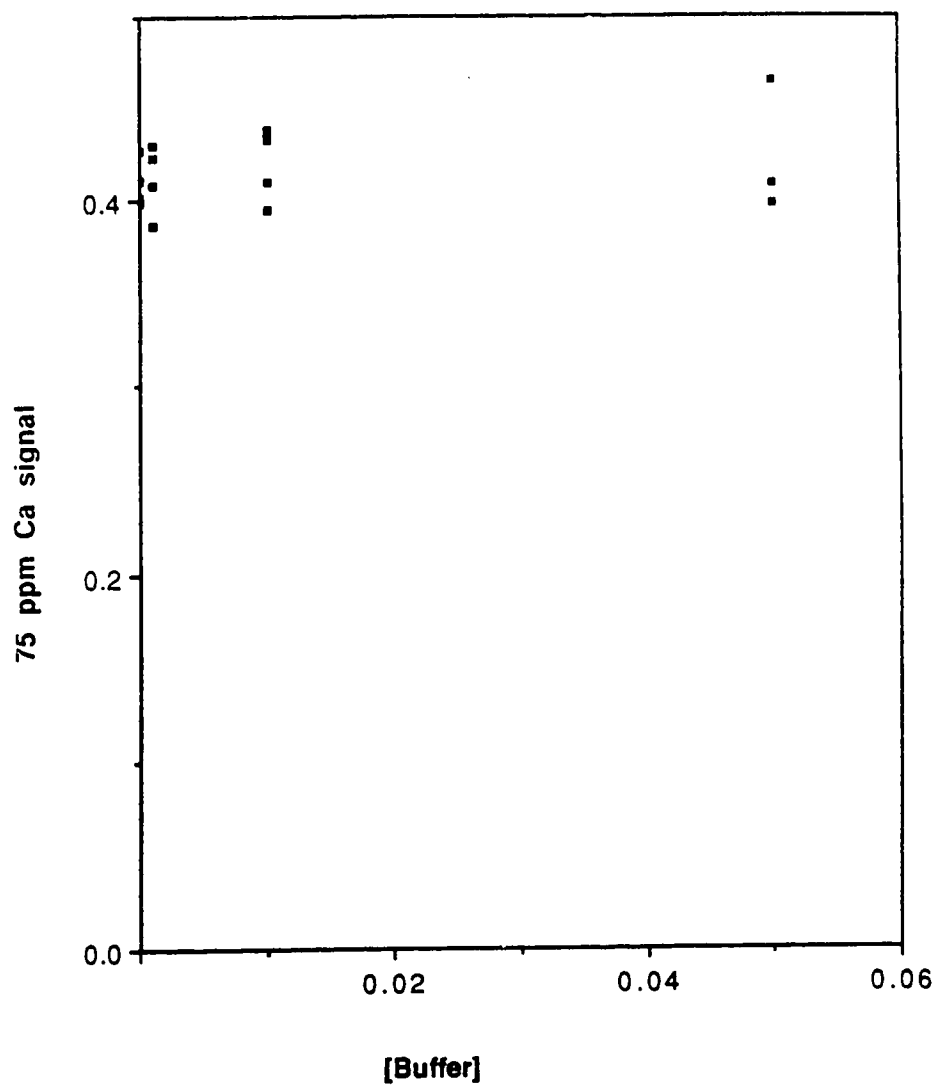


**Figure 5.7:** Variation of peak area for 75 ppm  $\text{Ca}^{2+}$  in 0.07M octylammonium nitrate with the total concentration of the buffer, PIPES.

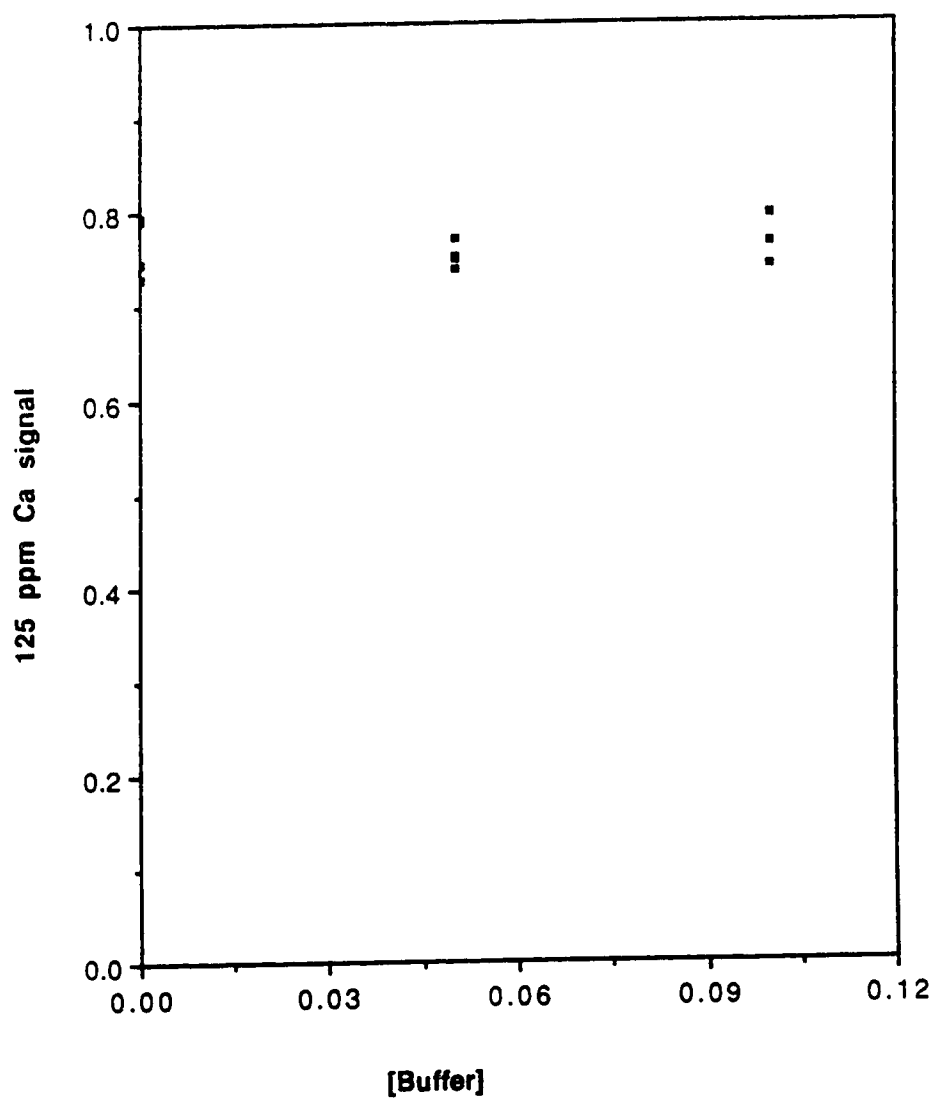


**Figure 5.8:** Variation of peak area for 125 ppm  $\text{Ca}^{2+}$  in 0.07M octylammonium nitrate with the concentration of the buffer, PIPES.

significant difference among the peak areas obtained at different buffer concentrations at the 95% confidence level.

Therefore PIPES may be considered suitable for the preparation of standards in the present study. An additional advantage of using a buffer in the standards is that the  $\text{Na}^+$  in the buffer also functions as a masking agent for the resin active sites and prevents peak tailing as described in section 5.4.3.

A calibration curve was then prepared over the range of 0 to 200 ppm  $\text{Ca}^{2+}$  in 0.07M octylammonium nitrate and in 0.01M PIPES adjusted to a pH of 6.4. The resultant plot, shown in figure 5.9, is linear up to a  $\text{Ca}^{2+}$  concentration of at least 200 ppm. This shows that trace conditions are satisfied over this range of  $\text{Ca}^{2+}$  concentrations.

#### 5.4.6 Selectivity of the method for free over bound calcium

So far the studies have shown that, with octylammonium nitrate as the electrolyte, determination of free  $\text{Ca}^{2+}$  can be done without interference from variable concentrations of major cations or variable pH values typically found in urine. Standards can be easily prepared using a non-interfering buffer. The next step therefore was to study the selectivity of the method for free  $\text{Ca}^{2+}$  in the presence of other calcium species formed by complexation between  $\text{Ca}^{2+}$  and major ligands found in urine. As mentioned in an earlier chapter, citrate is the major calcium binding ligand in urine. As a first test, citrate alone was studied over the typical range of concentrations reported<sup>168</sup> for in urine.

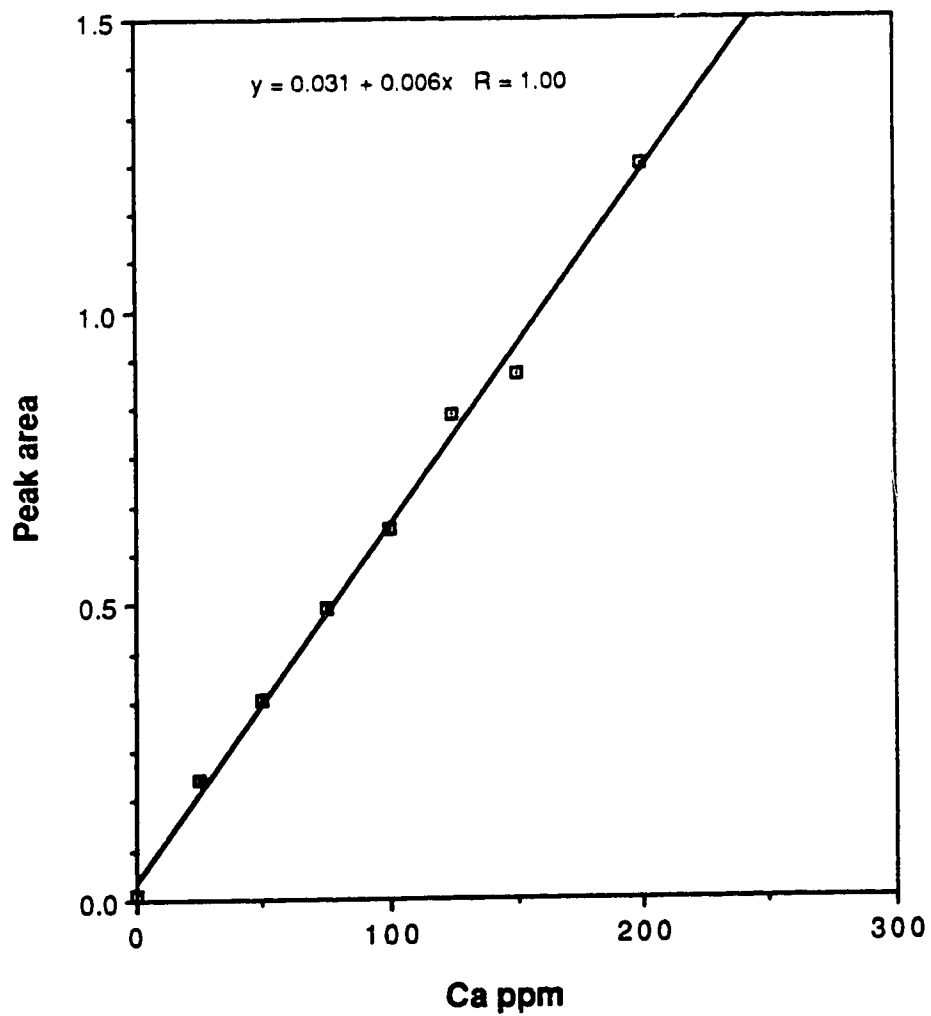


**Figure 5.9:** Calibration curve for standard  $\text{Ca}^{2+}$  solutions in 0.07M octylammonium nitrate. Solutions were buffered at pH 6.4 with 0.01M PIPES.

Variable amounts of citrate ranging from 0 to 0.04M were added to a 100 ppm  $\text{Ca}^{2+}$  solution in 0.07M octylammonium nitrate and 0.01M PIPES. Resin equilibration and elution were carried out and the resulting peak areas were measured and converted to free  $\text{Ca}^{2+}$  values in the usual way, using a calibration curve similar to figure 5.9. The expected free  $\text{Ca}^{2+}$  level for each solution was calculated using COMICS, taking into account complexation between  $\text{Ca}^{2+}$  and citrate. The experimental free  $\text{Ca}^{2+}$  levels were then compared with the calculated values in table 5.1.

The experimental free  $\text{Ca}^{2+}$  value decreases with increasing concentration of citrate, as expected. However, the extent of the decrease is much less than predicted. Clearly, the method does not selectively measure free  $\text{Ca}^{2+}$ . In order to check whether the presence of the PIPES buffer was responsible for this discrepancy, two of the above points were repeated without buffer, at pH values 5 and 6.4. In both cases discrepancies similar to those reported in table 5.1 resulted, indicating that the presence of buffer is not the reason for the differences in the experimental and calculated free  $\text{Ca}^{2+}$  values in table 5.1.

#### 5.4.7 Investigation of the reason for the high experimental free $\text{Ca}^{2+}$ value

Two main reasons can be suggested for the discrepancy between the experimental and the calculated free  $\text{Ca}^{2+}$  values shown in table 5.1.



Table 5.1: Comparison of the average experimental free Ca values (n=2) obtained with 0.07M octylammonium nitrate and variable total citrate levels at pH 6.4 (0.01M PIPES buffer), with calculated values based on complexation of  $\text{Ca}^{2+}$  by citrate.

---

<u>[Total citrate]</u>	<u>Fraction free Ca</u>	
	<u>experimental</u>	<u>calculated</u>
0.005	0.89	0.11
0.01	0.85	0.04
0.02	0.76	0.02
0.04	0.47	0.01

---

- I. In the presence of octylammonium ion  $\text{Ca}^{2+}$  does not complex with citrate to the same extent as it would otherwise. This results in a higher concentration of free  $\text{Ca}^{2+}$  than expected. According to this hypothesis, the method is still selective for free  $\text{Ca}^{2+}$  and it measures the correct free  $\text{Ca}^{2+}$  concentration in the solution. That is, the sample pretreatment step is responsible for the high experimental value. This possibility was studied in detail and is discussed later in this section.
- II. The resin does not selectively sorb free  $\text{Ca}^{2+}$  in the presence of other calcium species. That is, the method is not selective for free  $\text{Ca}^{2+}$  over bound calcium when octylammonium nitrate is used as the electrolyte. Such behaviour could also result in a higher than expected experimental free  $\text{Ca}^{2+}$  value. This possibility is also discussed in detail later in this section.

Ia. Conductivity studies

One possibility that could explain the observed results is the formation of ion pairs of appreciable stability between octylammonium ion and citrate. If ion pairing is occurring, the concentration of free  $\text{Ca}^{2+}$  would increase because that citrate ion paired with octylammonium is not available for complexation with  $\text{Ca}^{2+}$ . The possibility of ion pairing between octylammonium and alkylsulphonates has been investigated using conductance measurements<sup>166</sup>, but there have been no reports of ion pairing with citrate or similar anions. The

possibility of ion pairing between octylammonium and citrate was therefore tested in a manner similar to that outlined in reference 166.

Solutions of 0.02M trisodium citrate and 0.07M octylammonium nitrate, each adjusted to pH 7.8, were mixed in different proportions and the conductances of the mixtures were measured using the apparatus described in chapter 3. At this pH both the octylammonium and citrate ions are fully ionized. The conductance of each mixture was predicted, assuming no ion pair formation, using the weighted average of the conductances of the two pure solutions.

Since  $\text{Na}^+$  does not complex with  $\text{NO}_3^-$  to a significant extent<sup>137,171</sup>, the only cause for a difference in the conductance of the solutions from the calculated values should be ion pairing between octylammonium and citrate. If such ion pairing occurs, the experimental conductance of the mixtures should be lower than the predicted values based on the total absence of ion pairing. The results obtained are plotted in figure 5.10, where the solid line gives the calculated values and the points are from the experimental measurements of conductance.

The figure shows no significant differences between experimental and predicted values. The small differences observed can be attributed to uncertainties in reading the resistance values, the reciprocals of which were taken as conductance. The results therefore imply that no ion pairing occurs between octylammonium and citrate. In order to explain the discrepancy in the

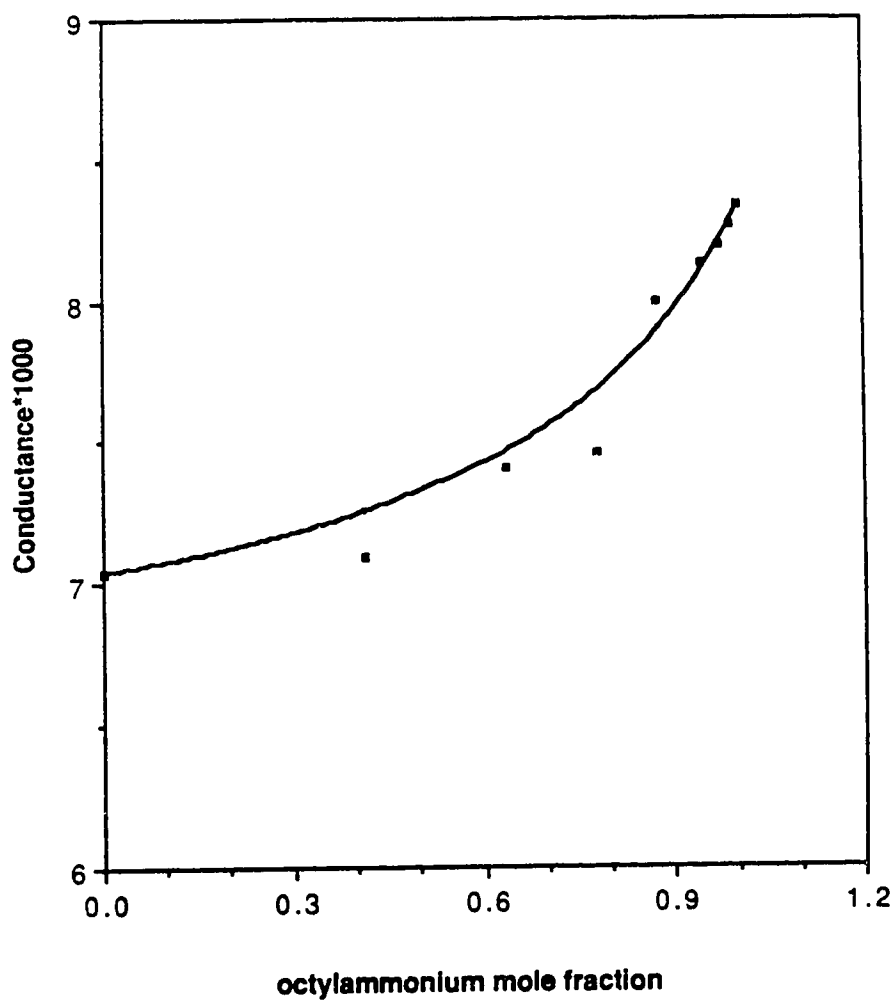


**Figure 5.10:** Conductometric titration of 0.02M sodium citrate with 0.07M octylammonium nitrate. ■, experimental conductances ( $\Omega$ ). Solid line shows the values calculated assuming that citrate does not complex with octylammonium.

experimental and calculated free  $\text{Ca}^{2+}$  values in table 5.1 in terms of such ion pairing, figure 5.10 would be required to show very significant differences between the predicted and experimental conductances. For instance, when  $\text{Ca}(\text{NO}_3)_2$  was used in place of octylammonium a definite drop in the conductance was observed, providing clear evidence of complexation between  $\text{Ca}^{2+}$  and citrate. Therefore this experiment shows that the discrepancy in free  $\text{Ca}^{2+}$  values in table 5.1 is not due to ion pairing between octylammonium and citrate.

Ib. Comparison with a  $\text{Ca}^{2+}$  ion selective electrode (ISE)

If hypothesis I is true, the solution free  $\text{Ca}^{2+}$  concentration should be higher than expected. A common technique used to determine free  $\text{Ca}^{2+}$  in solution is the ion selective electrode potentiometry. Two types of  $\text{Ca}^{2+}$  ISE's were used in this study. Both were made in this department according to a standard procedure<sup>172</sup>, and were tested for Nernstian response.

One was of the organophosphate or ion exchanger type using as ion carrier di[4-(2,2-dimethylhexyl)phenyl] phosphate. The other was of the neutral carrier type using the carrier ETH 1001, which is (-)-(R,R)-N,N'-bis[11-(ethoxycarbonyl)undecyl]-N,N',4,5-tetramethyl-3,6-dioxaoctanediamide<sup>173</sup>. In each case the membrane consisted of about 65% plasticizer, 33% PVC, 1% carrier and 1% potassium tetraphenyl borate. The internal reference was Ag/AgCl and a saturated calomel electrode was used as the reference electrode.

The calcium electrode potentials for 0, 50 and 100 ppm  $\text{Ca}^{2+}$  in 0.07M octylammonium were measured using each electrode. In each case all 3 solutions gave essentially the same reading.

This means that octylammonium itself is causing a high background signal which overwhelms the  $\text{Ca}^{2+}$  signal. Furthermore, the calcium electrode potential varied at constant calcium but varying octylammonium concentrations. Clearly both forms of the calcium electrode are sensitive to octylammonium, possibly owing to London dispersion interactions between the long alkyl chain of the octylammonium ion and the large organic entities present in the ion carriers of the electrode membranes.

Because of this octylammonium interference it is not possible to measure free  $\text{Ca}^{2+}$  concentrations in its presence. Therefore hypothesis I could not be investigated using a  $\text{Ca}^{2+}$  ISE.

Ic. Use of an indirect colorimetric method to investigate possible interference of octylammonium ions on the complexation of citrate and  $\text{Ca}^{2+}$  ions

Consider a metal ion which forms a colored citrate. If octylammonium also interacts with citrate, addition of octylammonium should change the color of this metal citrate solution. When this happens, the colorimetric signal of metal-citrate complex will be lower than normal. Since  $\text{Ca}^{2+}$  does not form a colored citrate, a different metal was used in this study, so that it is an indirect colorimetric method which could demonstrate the possible interference of

octylammonium with the complexing ability of citrate to metal ions.  $\text{Co}^{2+}$ ,  $\text{Ni}^{2+}$ ,  $\text{Mn}^{2+}$ ,  $\text{Fe}^{2+}$  and  $\text{Cu}^{2+}$  are metal ions which form colored citrate complexes.  $\text{Ni}^{2+}$  was the best choice since it had a reasonably high stability constant for the complexation with citrate and does not form interfering hydroxide complexes in the pH range of interest, 6 to 7.

The following 3 solutions were prepared and the pH was adjusted to within 6.3 to 6.5. The absorption spectra of the solutions were recorded as described below.

1. 0.01M  $\text{NiCl}_2 \cdot 6\text{H}_2\text{O}$
2. 0.01M  $\text{NiCl}_2 \cdot 6\text{H}_2\text{O}$  + 0.01M trisodium citrate
3. 0.01M  $\text{NiCl}_2 \cdot 6\text{H}_2\text{O}$  + 0.01M trisodium citrate + 0.01M octylammonium nitrate

Spectra for solutions #2 and #3 were taken using water as the reference and using solution #1 as the reference. These spectra are shown in figures 5.11 and 5.12.

Solutions of  $\text{NiCl}_2$  give an absorption maximum at 392 nm. When citrate is added, the absorption maximum shifts to 388 nm. Therefore when water is used as the reference the maximum absorption occurs at 392 nm, while with 0.01M  $\text{NiCl}_2$  as the reference it occurs at 388 nm. When the absorbance values at 392 nm and at 388 nm in figures 5.11 and 5.12 were compared, no significant difference was found between them. This implies that octylammonium does not interfere with the complexation between  $\text{Ni}^{2+}$  and citrate. The only

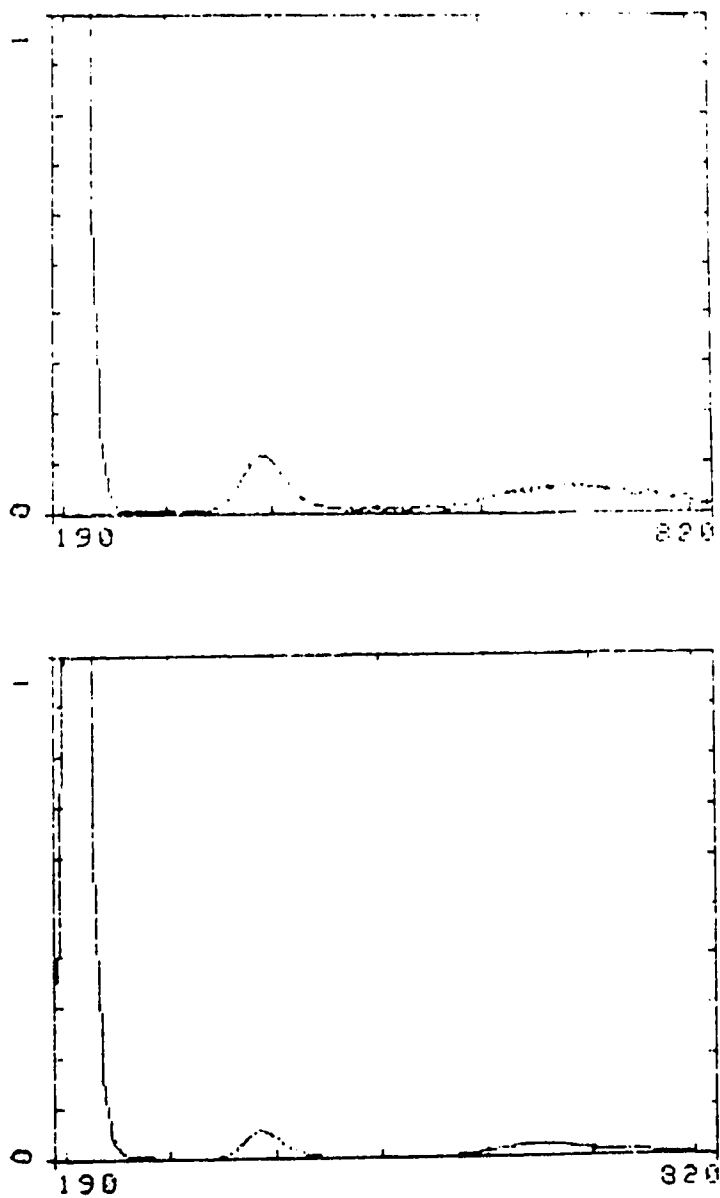


**Figure 5.11:** Absorption spectra of a solution of 0.01M nickel nitrate and 0.01M sodium citrate. top, referenced with water; bottom, referenced with 0.01M nickel nitrate.



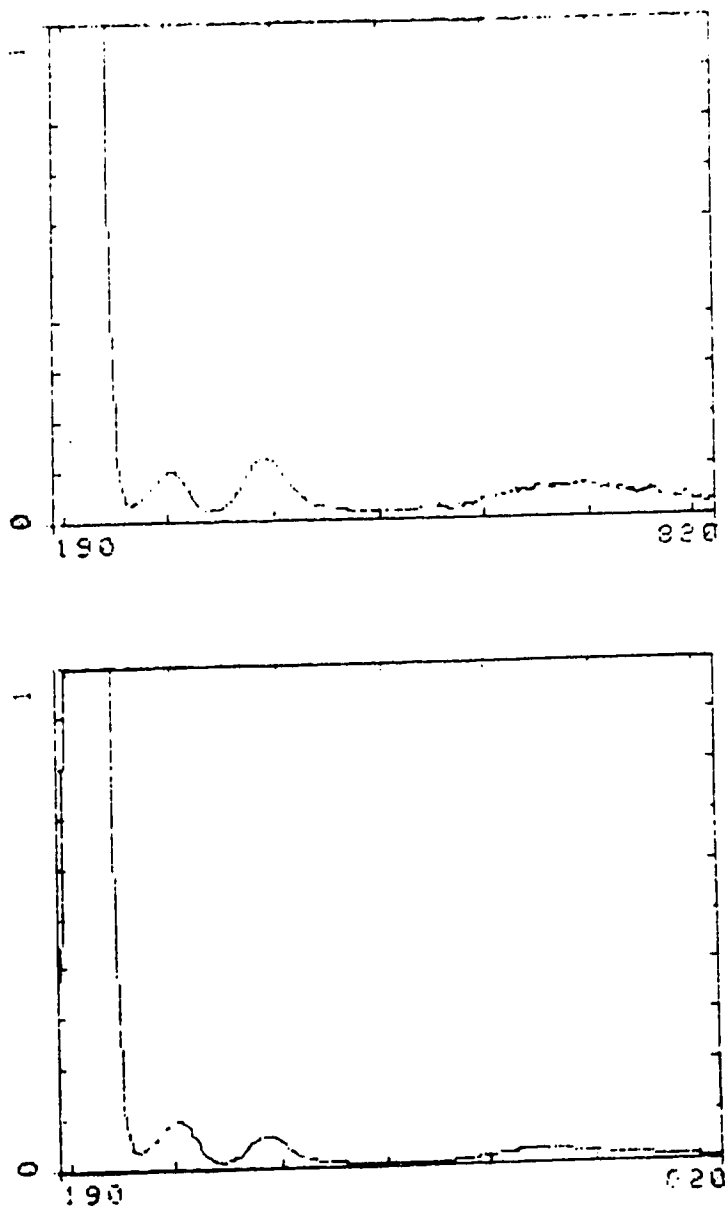


**Figure 5.12:** Absorption spectra of a solution of 0.01M nickel nitrate, 0.01M sodium citrate and 0.01M octylammonium nitrate. top, referenced with water; bottom, referenced with 0.01M nickel nitrate.

difference observed between the spectra in figures 5.11 and 5.12 was an additional peak at 304 nm. Spectra of octylammonium nitrate and sodium nitrate both showed an absorption maximum at 304 nm, confirming that this additional peak is caused by the nitrate ion.

The results of this experiment show that octylammonium ion does not interfere with the complexation between  $\text{Ni}^{2+}$  and citrate. It can be assumed that the same is likely to be true for the complexation between  $\text{Ca}^{2+}$  and citrate as well. Therefore this experiment suggests that free  $\text{Ca}^{2+}$  concentrations in solutions containing citrate are not changed by the addition of octylammonium nitrate.

Id. Use of a direct colorimetric method

As discussed in chapter 1, the 2 commonly used analytical techniques for the determination of solution free  $\text{Ca}^{2+}$  solutions are the  $\text{Ca}^{2+}$  ISE and the colorimetric method which uses tetramethylmurexide ammonium (TMMA). Since the  $\text{Ca}^{2+}$  ISE, as demonstrated in Ib, cannot be used in solutions containing octylammonium salts, the possibility of using the TMMA method was investigated. As discussed in chapter 1, the two-wavelength (480 and 550nm) method gives a straight line calibration plot and is pH insensitive over the pH range 4 to 8.

A set of  $\text{Ca}^{2+}$  standards were prepared over the range of 0 to 100 ppm  $\text{Ca}^{2+}$  in 0.07M octylammonium and the pH of each was adjusted to within 6.3 to 6.5. Since  $\text{Na}^+$  interferes with this method, citric acid was used in place of

tri sodium citrate. To a 100 ppm  $\text{Ca}^{2+}$  solution in 0.07M octylammonium nitrate was added sufficient citric acid to make the solution 5mM in citrate. Then the solution pH was raised, by adding 1-2 drops of octylamine, to a final pH of 5.8 and 7.9.

The free  $\text{Ca}^{2+}$  signals were measured at 480 nm and 550 nm, for each solution after the addition of 0.1 mL of 0.05% TMMA to 5 mL of the calcium solution. A calibration curve, constructed by plotting the absorbance ratio 480 nm/550 nm vs.  $\text{Ca}^{2+}$  concentration is shown in figure 5.13. From this plot, the free  $\text{Ca}^{2+}$  concentrations in the solutions containing citrate were evaluated.

The experiment was repeated using the ion-exchange equilibration method on the same solutions. The free  $\text{Ca}^{2+}$  concentration of each solution was also calculated using the COMICS computer program, taking into account the complexation between  $\text{Ca}^{2+}$  and citrate at pH values used in the experiment. Table 5.2 shows the results.

The difference between the colorimetric and the calculated values can be attributed to the uncertainties in the stability constants or possibly ion pairing between octylammonium and citrate. The free  $\text{Ca}^{2+}$  values from the colorimetric method and those from calculations, agree within the uncertainties of the methods. This implies that, there is no significant complexation between octylammonium and citrate in these solutions.

The experiments carried out in this section all suggest that the high free  $\text{Ca}^{2+}$  values obtained with the ion exchange method in tables 5.1 and 5.2, do

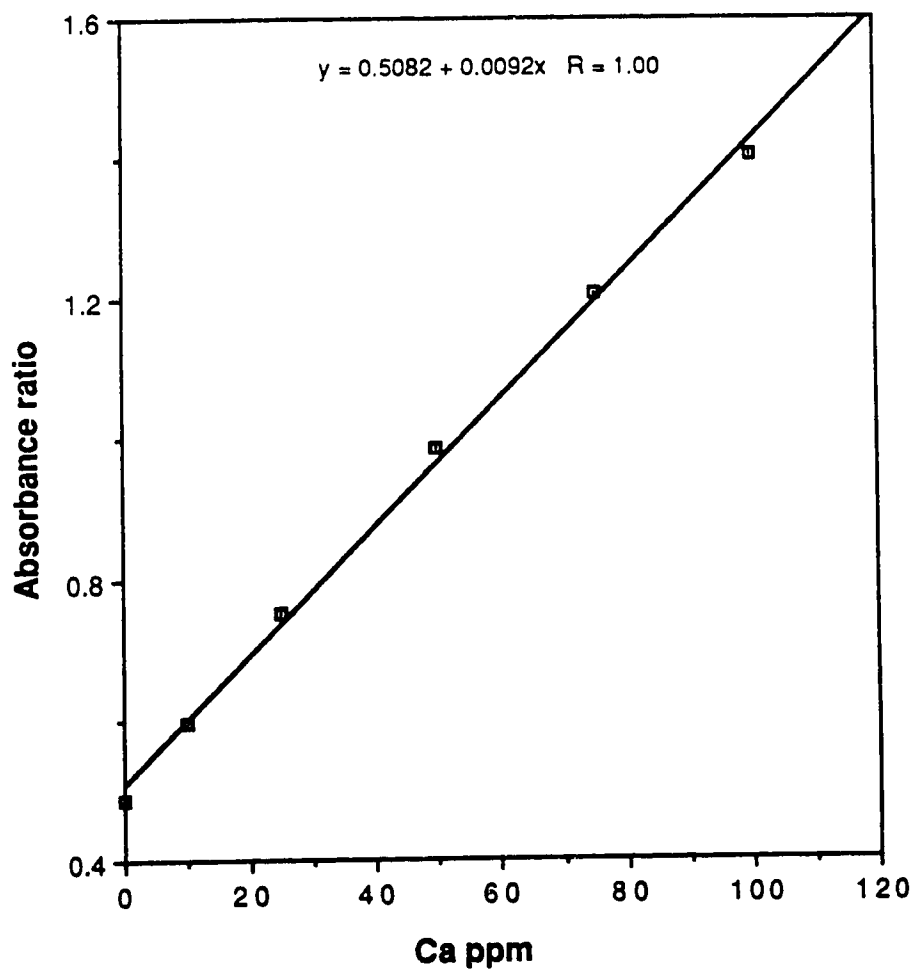


**Figure 5.13:** A plot of the absorbance ratio 480nm/550nm vs. the concentration of  $\text{Ca}^{2+}$  in 0.07M octylammonium, as measured by the colorimetric method using TMMA.

Table 5.2: Comparison of free  $\text{Ca}^{2+}$  concentrations (in ppm) obtained for a solution of 100 ppm calcium in 0.07M octylammonium nitrate and 5mM citrate, by (a) the ion exchange method (IEX), (b) the colorimetric method (TMMA) and (c) theoretical calculation.

<u>pH</u>	<u>IEX</u>	<u>TMMA</u>	<u>Calculation</u>
5.8	95	25	15
7.9	85	16	9

not fit hypothesis I. Another set of experiments were therefore carried out to explore hypothesis II.

#### IIa. Use of an organic solvent in the wash cycle

It is known that in addition to metal ions, positively charged and neutral metal ligand complexes can be sorbed on to cation exchange resins<sup>126</sup>. If this should happen in the present system the experimental value for ionized calcium would be higher than the actual value. Previous investigations of this phenomenon were based on the possible sorption of either positively charged or neutral complexes. For the ligand citrate in the present study, the pH was such that the concentrations of these species are negligible (Average fractions expected are:  $\text{CaH}_2\text{L}^+ = 0\%$ ,  $\text{CaHL} \sim 1\%$ ,  $\text{CaL}^- \sim 95\%$ ,  $\text{Ca}^{2+} \sim 5\%$ ). In fact, the  $\text{Ca}^{2+}$ -ligand species present in significant amount is a negatively charged ion, which by the ion exchange mechanism would be expected to be excluded from the resin<sup>130</sup>.

On the other hand, the octylammonium ion is a relatively large organic cation that sorbs readily on the resin. A sorbed layer of long alkyl tails could allow the interaction of solutes by mechanisms other than ion exchange. Thus it might be possible for negatively charged species to be sorbed on the organic alkyl film. Since in this scheme the negatively charged species are sorbed only as a result of relatively weak Vanderwaal forces, they should be able to be removed by flushing the resin with an organic solvent.

To test this hypothesis 95% methanol was used instead of water to wash the column, prior to the elution step. During washing no calcium signal was observed in the flame of the AA detector, but during elution a high free  $\text{Ca}^{2+}$  signal was observed as before. This means that either methanol is not capable of removing sorbed  $\text{Ca}^{2+}$ -ligand species, or no  $\text{Ca}^{2+}$ -ligand species are sorbed on the resin.

#### IIb. Analysis of the elution peak for citrate

If a negatively charged  $\text{Ca}^{2+}$ -citrate species is sorbed on to the resin, the peak/effluent must contain citrate. Therefore a method which can determine total citrate in a solution should be able to quantify the amount of  $\text{Ca}^{2+}$ -citrate species that was sorbed.

Both 0.07M octylammonium and 0.75M Na systems were included in this study. Since the  $\text{Na}^+$  system had been extensively studied earlier<sup>128</sup> as well as in the present work, the results from the two systems can be compared.

The method of citrate analysis used here was adapted from a short letter<sup>174</sup> and a related paper<sup>175</sup> in the literature. It is based on the photometric measurement of an iron(III)-citrate complex, which has an absorption maximum at 392 nm and a log stability constant of 11.5<sup>136</sup>. The solutions were maintained at pH 2 to avoid the formation of iron(III) hydroxide. Although a pH 2 HCl solution was used in the original work, in the present study a 0.2M KCl solution of pH 2 was used. The reason for this substitution will be discussed later. Computer calculations, using the COMICS program described

earlier, showed that in a system containing  $K^+$ , citrate, and  $Fe^{3+}$  at the concentrations employed here, at pH 2, virtually no K-citrate complex formation is observed up to a total  $[K^+]$  of 2M, and citrate is almost exclusively complexed by iron(III). The solutions for the spectral analysis were prepared by mixing 0.25 mL of 40 mM  $FeCl_3$  (pH 2) with 4.5 mL of a solution of citrate in 0.2M KCl (pH 2), followed by dilution of the solution to 5 mL with 0.2M KCl (pH 2). The reference solution was made in a similar manner, except that a solution of 0.2M KCl was used in place of the citrate in KCl solution.

The calibration curve obtained for citrate levels up to 75  $\mu$ M is shown in figure 5.14. The spectra obtained for the reference solution and for the citrate solution against an air reference are shown in figure 5.15, while the spectra obtained for the 50 and 75  $\mu$ M citrate solutions against the above mentioned reference solution (i.e. a difference spectra) are shown in figure 5.16. The absorbance at 392 nm was used for the calculation of concentrations from absorbance.

Since the effluent to be analysed contain octylammonium ion or  $Na^+$  and  $Ca^{2+}$  in the matrix, the effect of the expected concentrations of these ions on the amount of iron(III)-citrate (i.e. the citrate signal) was studied. For a solution of 100 ppm  $Ca^{2+}$  in 0.07M octylammonium nitrate, the expected level of calcium in the collected peak was about 50  $\mu$ M and that of octylammonium was about 2 mM. Addition of up to 250  $\mu$ M  $Ca^{2+}$  and up to 4 mM octylammonium caused no change in the citrate signal of a 50  $\mu$ M citrate



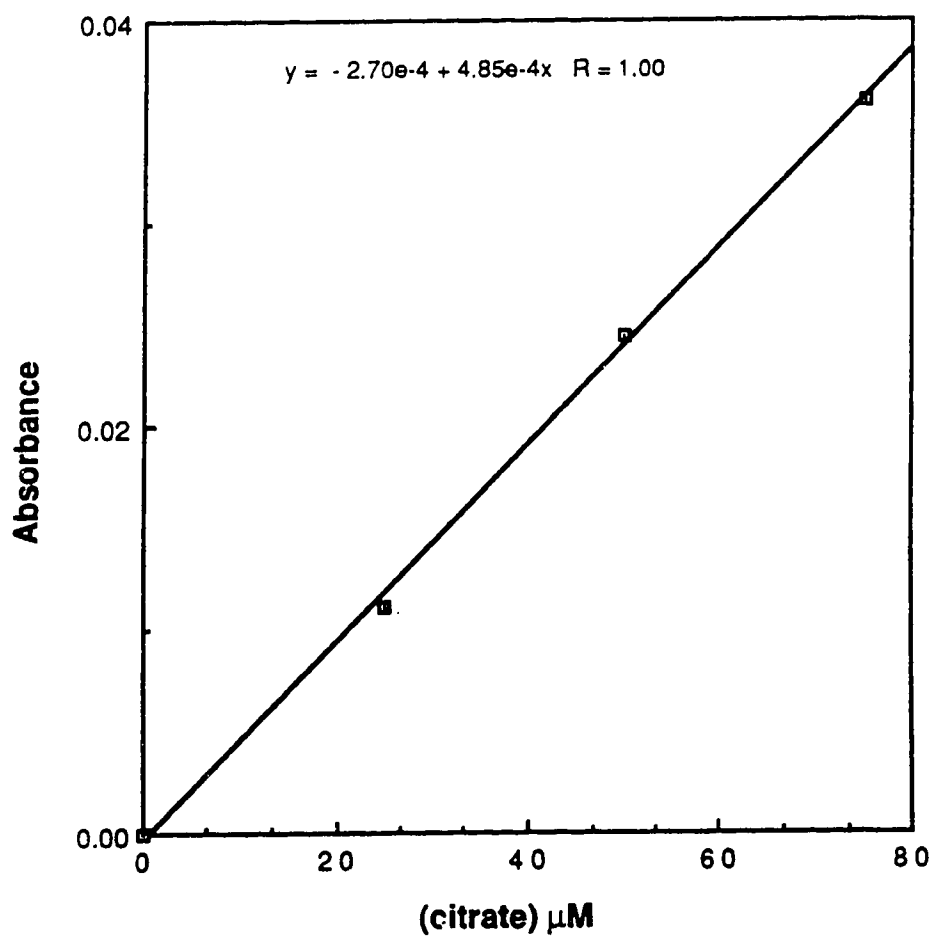


**Figure 5.14:** Calibration curve for standard citrate solutions as obtained by the colorimetric method using iron(III) chloride.

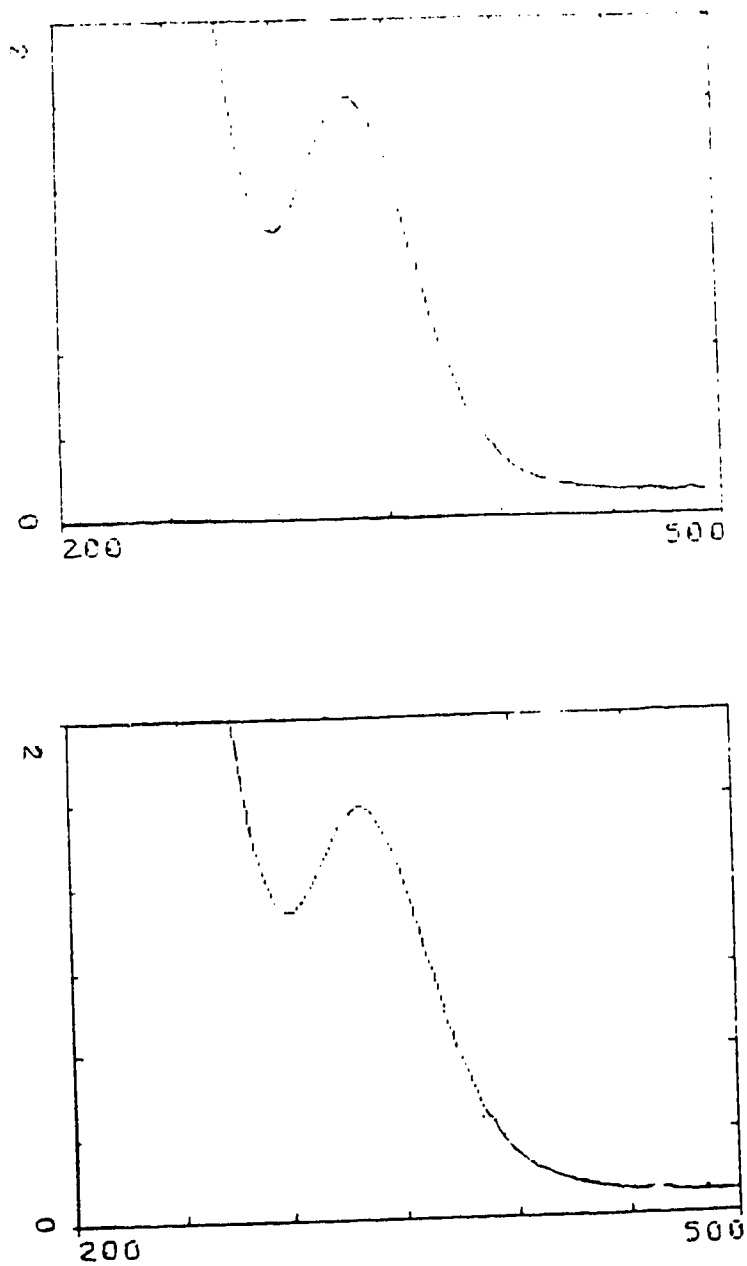


**Figure 5.15:** Absorption spectra of the 0.2M KCl reference solution (above) and the 75 $\mu$ M citrate in 0.2M KCl solution (below). Both spectra were air referenced and the same amount of iron(III) chloride was added to both solutions.

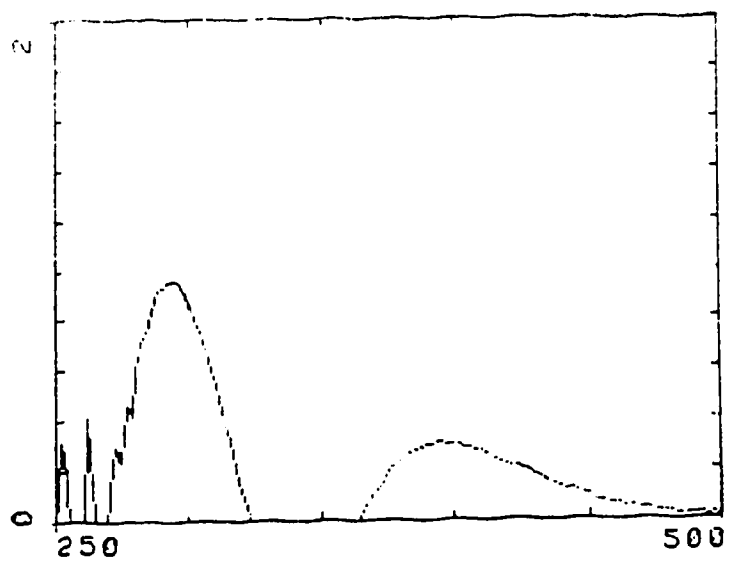
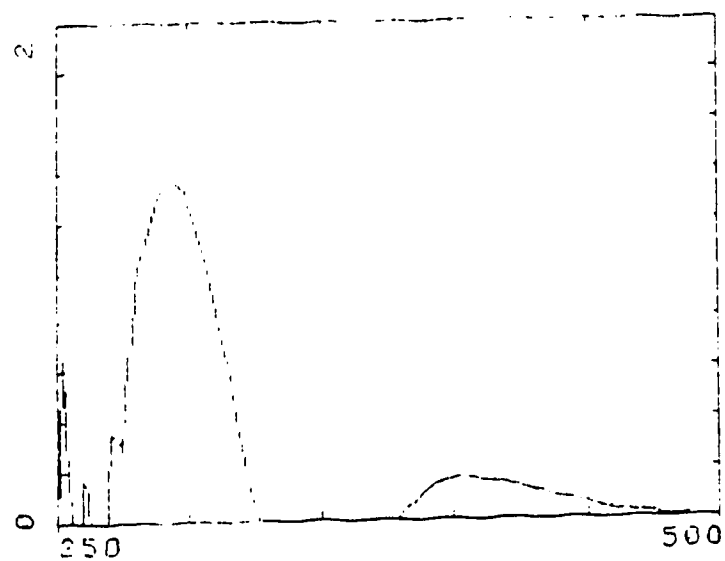


**Figure 5.16:** Difference spectra for 50 μM (above) and 75 μM (below) citrate solutions with iron(III) chloride. Both spectra were referenced with 0.2M KCl solution to which the same amount of indicator was added.

solution. A COMICS computer calculation of the equilibrium concentrations for this system showed no change in the amount of iron(III)-citrate present as a function of addition of  $\text{Ca}^{2+}$  even up to  $450 \mu\text{M}$ . Also, similar calculations show no effect by  $\text{Na}^+$ , even up to concentrations of 1M, on the amount of iron(III)-citrate formed in a  $50 \mu\text{M}$  citrate solution. These observations confirm the ability of the method to analyse peak/effluent citrate levels in both octylammonium and sodium systems.

Although 2M  $\text{HNO}_3$  was used as the eluent in all the other experiments, in this study a different eluent is required because the effluent pH is required to be 2 for the citrate analysis. 0.2M KCl showed similar performance as an eluent in terms of peak area, though not in elution volume. Thus, where the elution volume for 2M  $\text{HNO}_3$  was 5 mL, for 0.2M KCl an elution volume of 25 mL was needed to ensure complete elution. From earlier experimental results, a resin weight of about 10 mg was estimated to be high enough to ensure a citrate concentration of the peak within the range of 25 to  $50 \mu\text{M}$  in 25 mL effluent volume. Therefore, a column containing about 12 mg of resin was constructed by the procedure described in chapter 3. The solution flow rate was also lowered from the normal 5 mL/min to 3 mL/min to compensate for the larger amount of resin used in the column.

Solutions of 100 ppm calcium in 0.07M octylammonium ion or in 0.75M  $\text{Na}^+$ , with and without citrate, were passed through the column to equilibrium. Then the column was washed or centrifuged, eluted with 0.2M KCl of pH 2

and the effluent was collected. The citrate concentration of the effluent was determined as described below:

1. All the solutions were measured relative to the reference solution mentioned earlier.
2. The absorbances of the effluents obtained using with-ligand solutions ( $A_L$ ) and without-ligand solutions ( $A$ ), were measured at 392 nm.
3. The absorbance due to citrate is equal to  $A_L - A$ . (to account for any matrix effects in the collected peak). This absorbance value was converted to citrate concentration using the calibration curve shown in figure 5.14, and is denoted as  $(\text{citrate})_e$ , the experimental citrate level.

The predicted citrate level of the eluted peaks was estimated based on the difference in the experimental and calculated free  $\text{Ca}^{2+}$  levels, as explained below:

1. The concentration of calcium in each peak was measured by atomic absorption at 422.7 nm. From this concentration and the volume of solution collected, the total mols of calcium sorbed by the resin was calculated.
2. With the assumption that the difference in the observed and the calculated ionized  $\text{Ca}^{2+}$  fractions is caused by the sorption of a  $\text{Ca}^{2+}$ -citrate species, the effluent citrate level was estimated as follows (all quantities are in mols):

Measured amount of free  $\text{Ca}^{2+}$  sorbed from with-ligand solution =  $(\text{Ca})_L$

Measured amount of free  $\text{Ca}^{2+}$  sorbed from without-ligand solution =  $(\text{Ca})$

If the calculated fraction of free  $\text{Ca}^{2+}$  in the solution (based on equilibrium calculations using known stability constants) is denoted as  $f$ , then the predicted amount of free  $\text{Ca}^{2+}$  sorbed from with-ligand solution =  $f \times (\text{Ca}) = (\text{Ca})'_L$

As mentioned above, if the difference in the calculated and experimental free  $\text{Ca}^{2+}$  levels is due to the sorption of  $\text{Ca}^{2+}$ -citrate species, then the predicted  $\text{Ca}^{2+}$ -citrate level =  $(\text{Ca})_L - (\text{Ca})'_L = (\text{Ca-cit})_p$

Since  $\text{Ca}^{2+}$  forms only a 1:1 complex with citrate,

$$(\text{citrate})_p = (\text{Ca-cit})_p$$

Therefore, the predicted effluent citrate level =  $(\text{citrate})_p = (\text{Ca})_L - (\text{Ca}) \times f$

The results obtained for measurements made on a 100 ppm  $\text{Ca}^{2+}$  solution in 0.07M octylammonium ion are summarised in table 5.3, and those for a 100 ppm  $\text{Ca}^{2+}$  solution in 0.75M  $\text{Na}^+$  are summarised in table 5.4.

The no-wash procedure was used because there is a possibility of sorbed  $\text{Ca}^{2+}$ -citrate being dissociated and citrate being washed off during wash cycle. In the no-wash procedure, the column was centrifuged, instead of washing, in order to remove the interstitial solution. With the octylammonium system the experiment was repeated at 2 different pH values and with the  $\text{Na}^+$  system, lower pH values and a higher solution citrate level was used in the second set of experiments in order to form more  $\text{Ca}^{2+}$ -citrate species in solution.

When the peaks which contained almost no citrate were spiked with known amounts of citrate, the spiked amounts were recovered, showing that the method can detect citrate in this matrix. Also, when the same experiment was

Table 5.3: Variation in effluent citrate level with method of collection and pH. Electrolyte is 0.07M octylammonium nitrate. Symbols are the same as in the text except quantities are given in concentrations:  $\text{Ca}^{2+}$  in ppm and citrate in  $\mu\text{M}$ .  $(\text{cit})_s$  refers to citrate concentration (in mM) in the solution with which the column was equilibrated.  $(\text{cit})_e$  values are average of two runs with one standard deviation.

<u>Method</u>	<u><math>(\text{cit})_s</math> mM</u>	<u>pH</u>	<u><math>(\text{Ca})_L</math> ppm</u>	<u><math>(\text{Ca})'_L</math> ppm</u>	<u><math>(\text{cit})_e</math> <math>\mu\text{M}</math></u>	<u><math>(\text{cit})_p</math> <math>\mu\text{M}</math></u>
wash	5	6.5	100	11	$3 \pm 2$	47
no-wash	5	6.5	100	11	$2 \pm 1$	47
no-wash	5	4.8	100	34	$4 \pm 2$	28

Table 5.4: Variation of peak citrate level with method of collection, solution citrate level and pH. Electrolyte is 0.75M sodium nitrate. Symbols are the same as in the text except quantities are given in concentrations:  $\text{Ca}^{2+}$  in ppm and citrate in  $\mu\text{M}$ .  $(\text{cit})_s$  refers to citrate concentration (in mM) in the solution with which the column was equilibrated.  $(\text{cit})_e$  values are average of two runs with one standard deviation.

<u>Method</u>	<u><math>(\text{cit})_s</math></u> <u>mM</u>	<u>pH</u>	<u><math>(\text{Ca})_L</math></u> <u>ppm</u>	<u><math>(\text{Ca})'_L</math></u> <u>ppm</u>	<u><math>(\text{cit})_e</math></u> <u><math>\mu\text{M}</math></u>	<u><math>(\text{cit})_p</math></u> <u><math>\mu\text{M}</math></u>
no-wash	5	4.9	68	55	$4 \pm 1$	6
no-wash	5	4.2	89	78	$9 \pm 2$	9
no-wash	50	3.9	58	36	$16 \pm 3$	10
wash	50	3.9	76	36	$4 \pm 2$	46



carried out on peaks eluted with 2M HNO<sub>3</sub> (after adjusting the pH to 2 with KOH to a final K<sup>+</sup> concentration of about 0.3M), similar results were obtained. Therefore the possibility that citrate is not eluted when 0.2M KCl is used as the eluent can be eliminated.

Since the method for citrate used here depends on measurement of differences in absorbance between sample and reference, both of which absorb strongly at 392 nm (see the spectra for these two solutions in figure 5.15), the absorbance value is very much subject to errors (in measuring volumes, volume of FeCl<sub>3</sub> in particular). Therefore, the precision of this method is such that the presence of citrate cannot be proven for solution citrate levels of 8 μM or less. Furthermore, if only 10 μL of an equilibrated 5 mM solution of citrate were to remain as interstitial solution in the column when the no-wash procedure was used, it would produce an effluent citrate level of 2 μM. Therefore in the case of an initial 5 mM citrate solution, if the citrate level in the effluent were less than 10 μM, the presence of citrate in the peak could not be confirmed. The amounts of citrate found (Table 5.4) using the no-wash procedure with 50 mM citrate equilibration solution could therefore be due to the presence of as little as 10 μL of equilibration solution which remained in the column after centrifugation. As a result, the practical detection limit for citrate in this case is of the order of 20 μM in the effluent.

The results shown in table 5.3 indicate that the citrate levels found in the octylammonium ion system are well below the detection limit of 10 μM (for

initial equilibration solution of 5 mM citrate). This certainly suggests that there is no significant sorption of  $\text{Ca}^{2+}$ -citrate species on the column.

With 0.75M sodium nitrate the observed values were on average slightly higher than expected (Table 5.4). Taking into account the detection limits discussed above, however, even at these levels the presence of citrate cannot be proven, and a definite conclusion cannot be reached as to whether  $\text{Ca}^{2+}$ -citrate species are sorbed on the resin under these conditions. Thus the difference in the calculated and experimental free calcium levels cannot be definitely assigned to sorption of  $\text{Ca}^{2+}$ -citrate species.

The data obtained on the  $\text{Na}^+$  and octylammonium ion systems do allow a definite conclusion to be made about the sorption of negatively charged  $\text{Ca}^{2+}$ -citrate species on the resin. With  $\text{Na}^+$  only cation exchange occurs, causing the negatively charged  $\text{CaL}^-$  species to be excluded. Since the experimentally measured sorbed citrate levels obtained with octylammonium ion are lower yet than those obtained with  $\text{Na}^+$ , the evidence is even stronger against sorption of negatively charged species in the octylammonium ion system.

According to the results obtained in this section, therefore, the reason for the discrepancy between the calculated and experimental free  $\text{Ca}^{2+}$  values in table 5.1 is not the sorption of  $\text{Ca}^{2+}$ -citrate species by the resin. As shown earlier in section I, the reason is not the interaction between octylammonium

and citrate. Therefore both major hypotheses suggested at the beginning of this section have been rejected.

There is no known literature published about ion-pairing of octylammonium with citrate in solution. According to the results in section I, such interaction was not detected in this study. In ion-pair reversed phase chromatography, however, octylammonium has been used as an ion pair reagent in methanol-water mixtures<sup>176</sup> as well as in aqueous media<sup>177</sup>. Reference 176 suggests the presence of interactions between octylammonium and citrate when citrate was used as a competing ion in the eluent. Reference 177 used octylammonium as an ion-pair reagent to achieve retention and separation of a variety of carboxylic acids. In order to achieve retention on a reversed phase column, octylammonium should be able to ion pair with the carboxylic acids either in the mobile phase or in the stationary phase. Moreover, these separations were carried out in completely aqueous media and it was observed that increasing the alkyl chain length of the ion pairing ammonium ion from hexyl to octyl dramatically increased the retention of carboxylic acids, showing the stronger ion-pairing ability of longer chain alkylammonium ions.

Since citric acid is a carboxylic acid, an ion pairing similar to that in reference 177 could conceivably occur. The only substantial difference between the experiments described in reference 177 and the present work is that in reference 177 the stationary phase was a reversed phase, while in the present

study it is an ion exchange resin. Unlike inorganic ions, however, normal alkylammonium ions may sorb on ion exchange resins through Vanderwaal forces. Their behaviour on the resin was also found to obey the Martin equation, in a way similar to that reported in reference 177, and shown in figure 5.1. Therefore the retention of alkylammonium ions on a sulphonate resin resembles their behaviour on a reversed phase, thereby allowing retention studies on reversed phase columns to be related to the ion exchange resin results obtained in the present study. According to reference 177, in order to achieve retention, ion pairing between carboxylic acid and octylammonium ion must occur, even though the medium is aqueous, either in the solution phase or in the stationary phase. On the other hand, according to reference 166, octylammonium ion functions as an ion pair reagent for the retention of sulphonates even though conductivity studies showed no ion pairing between octylammonium ion and sulphonates in a mixed water-methanol medium. The retention therefore is attributed to a "dynamic ion-exchange" which essentially means an "ion-pairing" between octylammonium and sulphonate in the stationary phase. In the present study, although ion pairing between octylammonium and citrate was not detected in solution, it could occur in the resin phase, just as in reference 166. If this happens, the amount of free  $\text{Ca}^{2+}$  will increase in the stationary phase as it would in a solution. This would result in the sorption of a higher amount of free  $\text{Ca}^{2+}$  than expected.

Further support for this explanation can be found in the following calculation. If one assumes a log stability constant of 3.7 for the ion pairing reaction between octylammonium and citrate in the calculations of the equilibria, all four of the experimental free  $\text{Ca}^{2+}$  values in table 5.1 agree with the calculated values. This suggests that the reason for the discrepancy between experimental and calculated free  $\text{Ca}^{2+}$  values in table 5.1 may be some kind of interaction between octylammonium and citrate rather than sorption of  $\text{Ca}^{2+}$ -citrate species on the resin. Since section I showed no evidence of ion pairing or complexation in the solution, a reasonable explanation is the occurrence of ion pairing in the stationary phase. However, even according to this mechanism the effluent must contain citrate. Although not sorbed as  $\text{Ca}^{2+}$ -citrate, citrate is present in the resin, according to this mechanism, as octylammonium-citrate. Therefore, even this mechanism is not supported by the experimental evidences obtained so far.

Further investigations of an explanation would likely be highly time consuming, especially considering the different ideas proposed concerning the mechanism of retention in ion-pair chromatography<sup>166,178</sup>. Additional experimental observations would be required in order to gain insight into the retention mechanism of calcium in the presence of octylammonium ions. In relation to the objectives of this project, as outlined in chapter 1, it can be concluded that octylammonium or other alkylammoniums are not suitable

electrolyte ions to use in the pretreatment step of the ion-exchange column equilibration method for the analysis of free  $\text{Ca}^{2+}$ .

### 5.5 Conclusions

Unlike inorganic cations, organic cations sorb on resin used in this study as a result of Vanderwaal forces. Normal alkylammonium cations ( $\text{RNH}_3^+$ ) show a high affinity for the resin relative to  $\text{Na}^+$  and quaternary ammonium ( $\text{R}_4\text{N}^+$ ) ions. The sorption of normal alkylammonium ions follows the Martin equation, and the extent of sorption can be varied by changing the length of the alkyl chain as well as the concentration of the alkylammonium ion in the solution in contact with the resin. With 0.07M octylammonium nitrate, trace conditions for the sorption of  $\text{Ca}^{2+}$  were achieved for calcium ion levels up to 200 ppm. Interferences from sodium ions and from pH variations, on the  $\text{Ca}^{2+}$  signal were found to be negligible when octylammonium nitrate was used as the electrolyte. Although  $\text{Ca}^{2+}$  peaks obtained with octylammonium nitrate showed tailing, this problem could be overcome either by using a pH buffer containing  $\text{Na}^+$ , or by simply adding a small amount of  $\text{NaNO}_3$  to the standards.

The selectivity of the method for free over bound calcium was poor with octylammonium nitrate as the electrolyte. Two hypotheses were proposed for this lack of selectivity. The first was ion pairing between octylammonium and citrate in solution, and the second was sorption of  $\text{Ca}^{2+}$ -ligand species on the

resin. Both were rejected on the basis of a series of experiments. On the other hand, it was observed that the experimental results obtained for free  $\text{Ca}^{2+}$  agreed with the calculated values when a log stability constant of 3.7 was used for the ion-pair association constant of octylammonium citrate in the calculation of solution equilibria. This suggests that the cause of the problem is related to an interaction between octylammonium and citrate rather than non-selective sorption of calcium species on the resin. Since such an interaction was not evident in the solution phase, the possibility of such interactions occurring in the resin phase was suggested. However, this suggestion is not in agreement with the experimental evidence obtained so far. Further investigation of the retention mechanism could not be carried out without additional experimental observations.

In summary, the use of organic ions as the electrolyte was investigated as means of obtaining trace conditions for  $\text{Ca}^{2+}$  concentrations up to 200 ppm in samples, without significantly perturbing existing equilibria. Quaternary ammonium ions did not show promise in preliminary experiments. The reason for this may have been the high degree of cross linking used in this study. Therefore a detailed study was carried out on the use of normal alkylammonium nitrate salts. Octylammonium nitrate was not satisfactory as an electrolyte for the determination of free  $\text{Ca}^{2+}$  by the ion exchange column equilibration method.

However, a quaternary ammonium salt might possibly be used to obtain trace conditions if the resin cross linking were lowered to allow less steric hindrance to sorbing ammonium ions. This possibility is explored in the next chapter. In addition, from table 5.4 it can be seen that  $\text{Ca}^{2+}$  peak areas when  $\text{Na}^+$  is used as the electrolyte are higher in the washed column than when no washing was used. This difference is also investigated in the next chapter.



## CHAPTER 6

### INVESTIGATION OF THE EFFECT OF RESIN CROSS-LINKING AND WASH CYCLE ON ION EXCHANGE EQUILIBRIUM

#### 6.1 Introduction

As discussed in earlier chapters, to achieve trace conditions for the measurement of free  $\text{Ca}^{2+}$  concentrations up to 200 ppm with minimum perturbation to sample equilibria, the presence of either a small amount of non complexing electrolyte which has a high affinity to the resin, or a high concentration of electrolyte with a smaller affinity, is required. Since metal ions that do not complex with sample ligands to a significant extent required too high concentrations to satisfy this requirement, an alternative was to use organic cations which do not have a record of complexation with sample ligands. Unlike metal ions, the sorption of organic ions increases with the size of the ion<sup>130,154</sup>, and is governed primarily by Vanderwaal interactions. However, due to size constraints, highly cross-linked resins prefer small metal ions to large organic cations<sup>121,159-161</sup>. For low cross-link resins the sorption of organic ions is preferred to that of metal ions<sup>121,156,157</sup>.

The ion exchange studies done to this point in the present study employed an 8% cross-link resin. With this resin, as shown in the previous chapter, quaternary ammonium ions showed no promise as competing cations for  $\text{Ca}^{2+}$  to obtain trace conditions. Therefore, in this chapter studies involving a 2% cross-link resin are discussed.

Ion exchange column equilibration using cation exchange resins for trace metal ion determinations has been extensively studied and a flow system for this study has been worked out in the literature<sup>124-128</sup> and earlier in this thesis. Therefore the flow system and the procedure used to this point in the present study was unchanged from that used previously. However, column equilibration studies of magnesium by Persaud showed<sup>179</sup> that the wash cycle perturbs the equilibrium established between the resin and the solution under study. A similar perturbation was observed in this research and is evident in table 5.4. Therefore ways to minimize or eliminate this perturbation were studied and are discussed in this chapter. As a result the flow system was modified and improved.

## 6.2 Experimental

A new column containing about 0.4 mg of 2% DOWEX 50X2-400 resin was constructed and conditioned as described in chapter 3. The flow rate used for all experiments was 5 mL/min and the time of equilibration was 30

seconds. Flow system 1 in chapter 3 was used for all the experiments unless otherwise stated.

The quaternary ammonium salts were in bromide form (Eastman Chemicals) and were used as received. All other chemicals were the same as those used in previous chapters.

### 6.3 Study of 2% cross-linked resin

#### 6.3.1 Tetraethyl ammonium bromide ( $\text{Et}_4\text{N}^+\text{Br}^-$ ) as electrolyte

Among the alkyl ammonium salts studied, the tetraethylammonium ion is reported to form the weakest complexes with citrate<sup>145</sup>. Therefore the addition of this ion to urine should alter free  $\text{Ca}^{2+}$  levels the least. The size of this ion is similar to that of  $\text{Ca}^{2+}$  and the column capacity for it on 2% cross linked resin is 100%<sup>130</sup>. That is, all resin exchange sites are accessible to  $\text{Et}_4\text{N}^+$  for this resin.

In order to evaluate the performance of the tetraethyl ammonium ion as the electrolyte in obtaining trace conditions,  $\text{Ca}^{2+}$  peak areas obtained with varying concentrations of this ion were compared with those obtained with 0.75M  $\text{Na}^+$ . The pH of the solutions varied between 4 and 5. Since both  $\text{Na}^+$  and tetraethylammonium ion are completely ionized at all pH values, pH variations were not of major concern.

The 2% cross-linked resin equilibrated more rapidly (30 seconds) with tetraethylammonium ion than the 8% cross-linked resin, and yielded smaller

peak areas. To obtain a  $\text{Ca}^{2+}$  peak area similar in size to that obtained with 0.75M  $\text{Na}^+$ , a tetraethylammonium concentration of 1M was required. This shows that although tetraethyl ammonium shows a better performance with low cross-link resin, its performance as an electrolyte in achieving trace conditions is inferior to  $\text{Na}^+$ . However, since the extent of complexation of tetraethyl ammonium with citrate is lower than that of  $\text{Na}^+$ , higher concentrations of this ion will cause a smaller perturbation of the sample equilibria. Therefore standards were prepared, with 1M tetraethyl ammonium, up to a  $\text{Ca}^{2+}$  concentration of 100 ppm.

The calibration curve obtained is shown in figure 6.1 (the positive intercept is a result of slight absorbance by tetraethyl ammonium at 422.7 nm). A solution of 100 ppm  $\text{Ca}^{2+}$  in 5 mM citrate was then prepared with 1M tetraethylammonium at pH 6.7. The  $\text{Ca}^{2+}$  peak area from this solution was measured and the concentration of free  $\text{Ca}^{2+}$  was estimated using the above calibration curve. A value of 51 to 52 ppm was obtained. For comparison, the expected free  $\text{Ca}^{2+}$  concentration for this solution was calculated considering the complexation between  $\text{Ca}^{2+}$  and citrate. The stability constants were corrected for solution ionic strength using the Davies equation as discussed in chapter 4. A free  $\text{Ca}^{2+}$  concentration of 12 ppm was calculated.

The difference in the above values may be due to errors introduced in correcting the stability constants for high ionic strength and to possible complexation between tetraethylammonium and citrate. Even if the stability

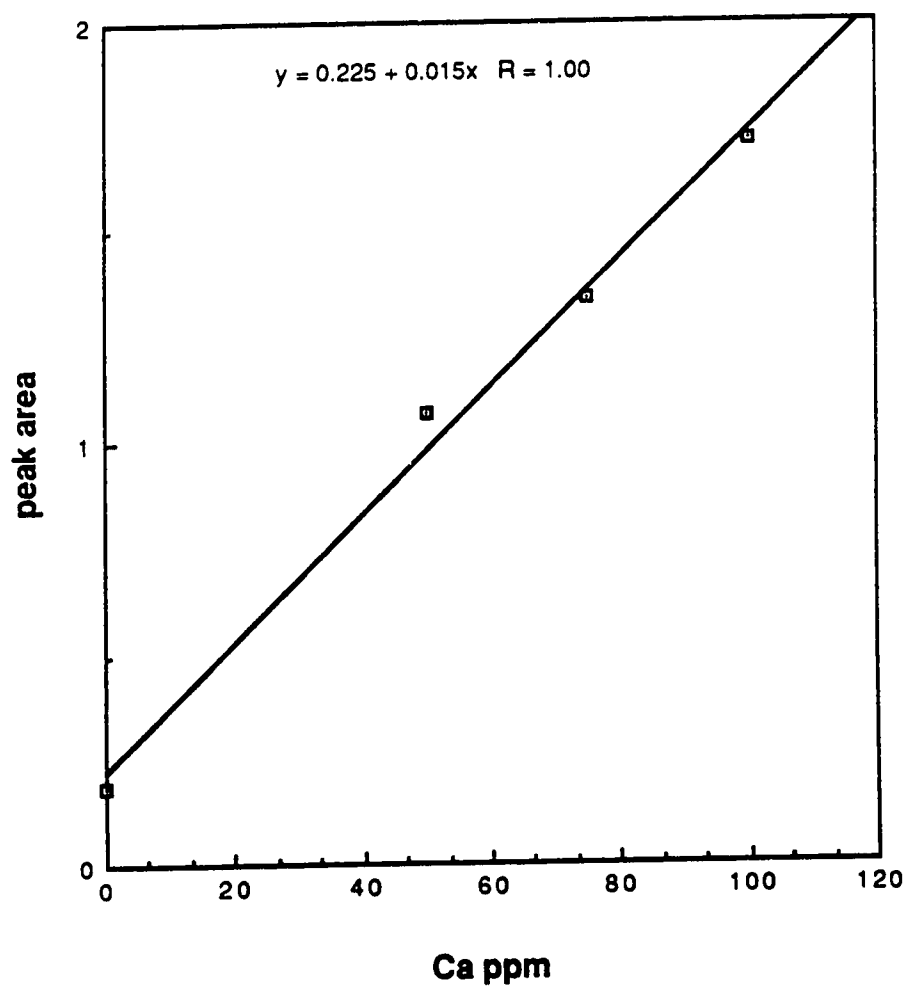


Figure 6.1: Calibration curve for standard  $\text{Ca}^{2+}$  solutions in 1M tetraethylammonium bromide.

constant of this complexation is very small, the free  $\text{Ca}^{2+}$  concentration would likely be altered to a considerable extent by the very high concentration of tetraethylammonium.

This preliminary experiment shows that tetraethylammonium is not a suitable electrolyte to be used as the electrolyte in the analysis of free  $\text{Ca}^{2+}$  by the column equilibration method under trace conditions.

### 6.3.2 Study of the sorption of a series of tetraalkylammonium ions

As shown in the previous section, when a large amount of  $\text{Et}_4\text{NBr}$  is added to the sample, the concentration of free  $\text{Ca}^{2+}$  is altered due to ionic strength and complexing effects. A cation with a higher affinity to the resin that is able to provide trace conditions at low concentration should give minimal perturbation of the sample. To extend the above work on  $\text{Et}_4\text{NBr}$ , a series of tetraalkylammonium bromides were studied using 2% cross-linked resin. These included the tetramethyl-, tetraethyl-, tetrabutyl- and hexyltrimethyl-ammonium bromides. For this study 100 ppm  $\text{Ca}^{2+}$  solutions were prepared in 0.5M solutions of each tetraalkylammonium salt. Also, 0.5M solutions of each tetraalkylammonium salt were prepared as blanks since they showed a slight absorbance at 422.7 nm. The resin column was equilibrated with each solution as before, and  $\text{Ca}^{2+}$  peak areas for each were obtained. Blank peak areas were subtracted where required. For comparison purposes, 100 ppm  $\text{Ca}^{2+}$  solutions in 0.5M and 0.75M  $\text{NaNO}_3$  were also used in this

study. The average peak areas from 3 runs, obtained for each of the above solutions, are shown below with the standard deviations.

0.5M tetramethylammonium	$1.58 \pm 0.06$
0.5M tetraethylammonium	$1.37 \pm 0.04$
0.5M tetrabutylammonium	$1.57 \pm 0.04$
0.5M hexyltrimethylammonium	$0.94 \pm 0.03$
0.5M Na <sup>+</sup>	$0.97 \pm 0.04$
0.75M Na <sup>+</sup>	$0.55 \pm 0.05$

These results show that the performance of hexyltrimethylammonium is the best among the quaternary ammonium ions studied, and that it gives results similar to Na<sup>+</sup>. However, in order to obtain a performance similar to that of 0.75M Na<sup>+</sup>, a concentration higher than 0.5M is required even with hexyltrimethylammonium. As discussed in the previous section, ionic strength and complexation complications restrict the use of high concentrations of electrolytes because of the resultant sample perturbation. Therefore, this experiment clearly shows that even with low cross-linked resins, none of the quaternary ammonium ions are suitable as the electrolyte used to obtain trace conditions.

As discussed in chapter 5, the coulombic and Vanderwaal forces are both important in the sorption of ions on the ion exchange resin. At a low degree of cross linking, Vanderwaal forces dominate and the sorption of large organic ions is preferred to that of metal ions<sup>121,156,157</sup>. However, the results

obtained in the present study show that metal ions are preferentially sorbed. The only difference between the present study and previous studies<sup>121,156,157</sup> is that the ionic strength used in this study was 0.5 rather than 0.1. This suggests that the high ionic strength suppresses the domination of Vanderwaal forces. The additional ionic character created on the resin by the high ionic strength may have been the reason for the domination of coulombic forces in the process of sorption. Therefore at high ionic strengths such as that used in the present study, the transition from domination of Vanderwaal forces to coulombic forces for quaternary ammoniums may be occurring at 2% or lower cross linking rather than at 3% cross linking as reported previously<sup>121</sup>.

According to the results shown above, the extent of sorption of all 3 tetraalkylammonium ions is similar. In fact at the 95% confidence level the peak areas obtained showed no significant difference in an ANOVA test. This again is a deviation from previous studies where the sorption of organic ions showed an increase with increasing size<sup>130,154</sup>. As discussed above, Vanderwaal forces are not dominant under the experimental conditions used in our study. Therefore sorption occurs due to a combination of effects. The sorption of the largest ion, hexyltrimethylammonium, should show the highest contribution of Vanderwaal forces. Therefore it showed the strongest sorption among the other organic ions resulting in the lowest  $\text{Ca}^{2+}$  peak area. Compared to hexyltrimethylammonium, the other 3 ammonium ions do not differ much in terms of size, so that the increase in the contribution of Vanderwaal force with



increasing size may not be very significant. Moreover, with the coulombic force contribution, the sorption must decrease with increasing size. Therefore a combination of these effects could make the extent of sorption of all 3 ammonium ions more or less the same.

### 6.3.3 Use of Na<sup>+</sup> and K<sup>+</sup> as electrolyte

Section 6.3.2 shows that even with 2% cross linking Na<sup>+</sup> shows a higher affinity for the resin than any of the other ions studied. Also, since the selectivity of a resin increases with the degree of cross linking<sup>130</sup>, the difference in the affinities of Ca<sup>2+</sup> and Na<sup>+</sup> for a 2% cross link resin should be lower than that for an 8% cross link resin. As a result, with 2% cross link resin, a smaller concentration of Na<sup>+</sup> may be able to provide trace conditions for the sorption of Ca<sup>2+</sup> up to 200 ppm. Therefore the objective of this part of the study was to investigate the possibility of using lower concentration of Na<sup>+</sup> or K<sup>+</sup> as the electrolyte to obtain trace conditions. K<sup>+</sup> was expected to be a better choice for two reasons.

1. Since its hydration radius is smaller than that of Na<sup>+</sup> it should have a higher affinity to the resin<sup>133</sup>. Therefore trace conditions should be feasible at lower concentrations.
2. The extent of complexation with citrate is lower for K<sup>+</sup><sup>136</sup> compared to Na<sup>+</sup>, so it should cause a smaller perturbation of the sample equilibria.

As a preliminary study, the peak areas obtained for solutions of 100 ppm  $\text{Ca}^{2+}$  in 0.5M  $\text{K}^+$  and 0.5M  $\text{Na}^+$  were compared. The average peak areas obtained for 3 runs each, and the standard deviations were  $0.77 \pm 0.01$  for  $\text{NaNO}_3$  and  $0.49 \pm 0.02$  for  $\text{KNO}_3$ .

These results confirm the first reason given above. In order to find the minimum concentration of  $\text{K}^+$  required to obtain trace conditions, a calibration curve was constructed for  $\text{Ca}^{2+}$  concentrations up to 200 ppm with the concentration of  $\text{K}^+$  set at 0.3M as an initial estimate. The pH values of the solutions were held within the range 4 to 5. For comparison purposes another calibration curve was constructed using a column of about 0.5 mg of 8% cross link resin with the same solutions. To compensate for the difference between the 2 columns in terms of exchange capacity, the peak areas obtained with the smaller column (with 2% cross link resin) were multiplied by 1.4, which was the ratio of column capacities, and another curve was constructed. All 3 curves are shown in figure 6.2.

According to figure 6.2, the linearity of the calibration curves does not change very much with the change in cross linking. Moreover the 8% cross-linked resin shows a higher slope even after compensating for the lower exchange capacity of the column with 2% cross linked resin. This is expected since selectivity increases with the degree of cross linking, as mentioned before. However, in terms of obtaining trace conditions (i.e. obtaining a linear calibration curve), 2% cross link resin is no better than 8% cross link resin.

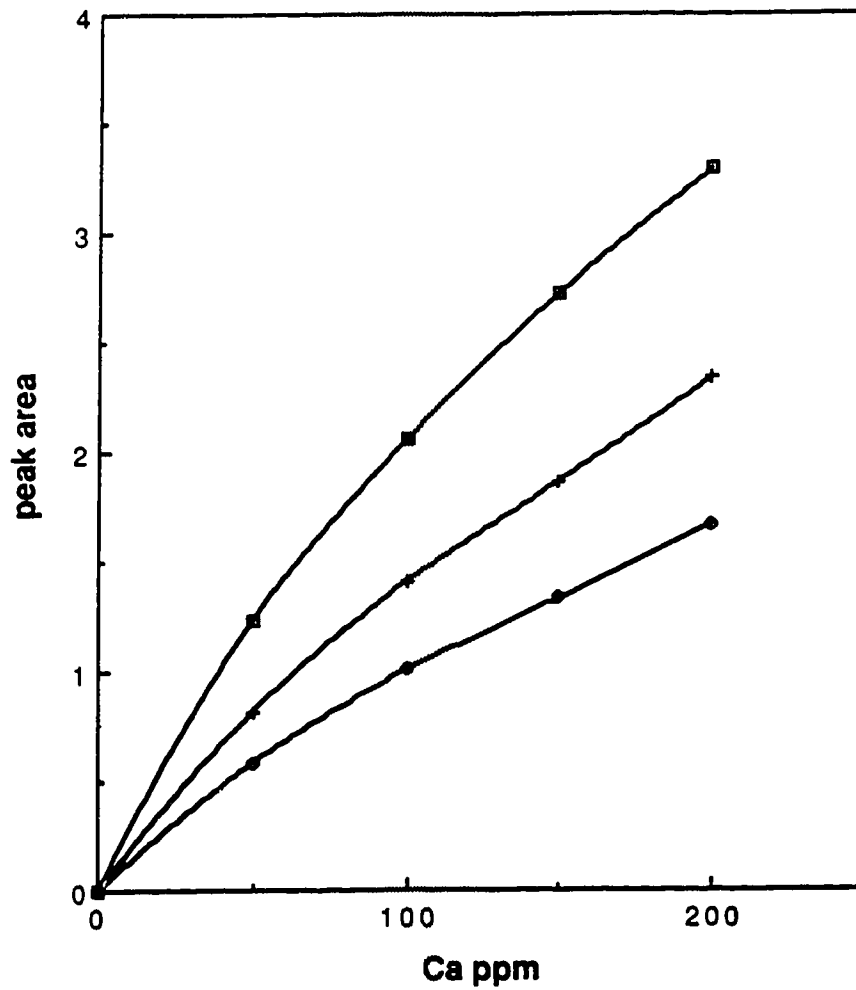


**Figure 6.2:** Calibration curves for standard  $\text{Ca}^{2+}$  solutions in 0.3M  $\text{KNO}_3$ ;  $\square$ , using 8% and  $\blacklozenge$ , 2% crosslinked resins. Curve  $+$  was constructed by the multiplication of curve  $\blacklozenge$  by the column capacity ratio.

A similar experiment was carried out using 0.75M Na<sup>+</sup> instead of 0.3M K<sup>+</sup> in order to determine whether the performance of 0.75M Na<sup>+</sup> as the electrolyte to obtain trace conditions varies between the 2% cross linking and the 8% cross linking resin used in the experiments in chapter 4. The results, shown in figure 6.3, are similar to those obtained for 0.3M K<sup>+</sup>.

Therefore, in relative terms the use of an 8% cross link resin is more profitable since it gives higher sensitivity. The linearity of calibration curves is similar for both degrees of crosslinking.

Even with low concentrations of electrolytes, for example 0.3M K<sup>+</sup>, calibration curves obtained do not reach a plateau or a saturation up to a Ca<sup>2+</sup> concentration of 200 ppm. Therefore calibration curves obtained with lower electrolyte concentrations are as useful as those obtained at high electrolyte concentrations for the determination of free Ca<sup>2+</sup> up to 200 ppm.

#### 6.4 Perturbation of the ion exchange equilibrium during the wash cycle

As mentioned in section 6.1 a significant variation in peak area was observed as a function of the specific technique used to measure peak areas for measurements on Ca<sup>2+</sup> solutions containing 0.75M Na<sup>+</sup>. Since such variations were not detected with 0.07M octylammonium ion solutions, the variation may be related to the ionic strength of the solution.

According to the theory of ion exchange, as discussed in chapter 2, the distribution coefficient of Ca<sup>2+</sup>,  $\lambda_{Ca}$ , is inversely proportional to the electrolyte

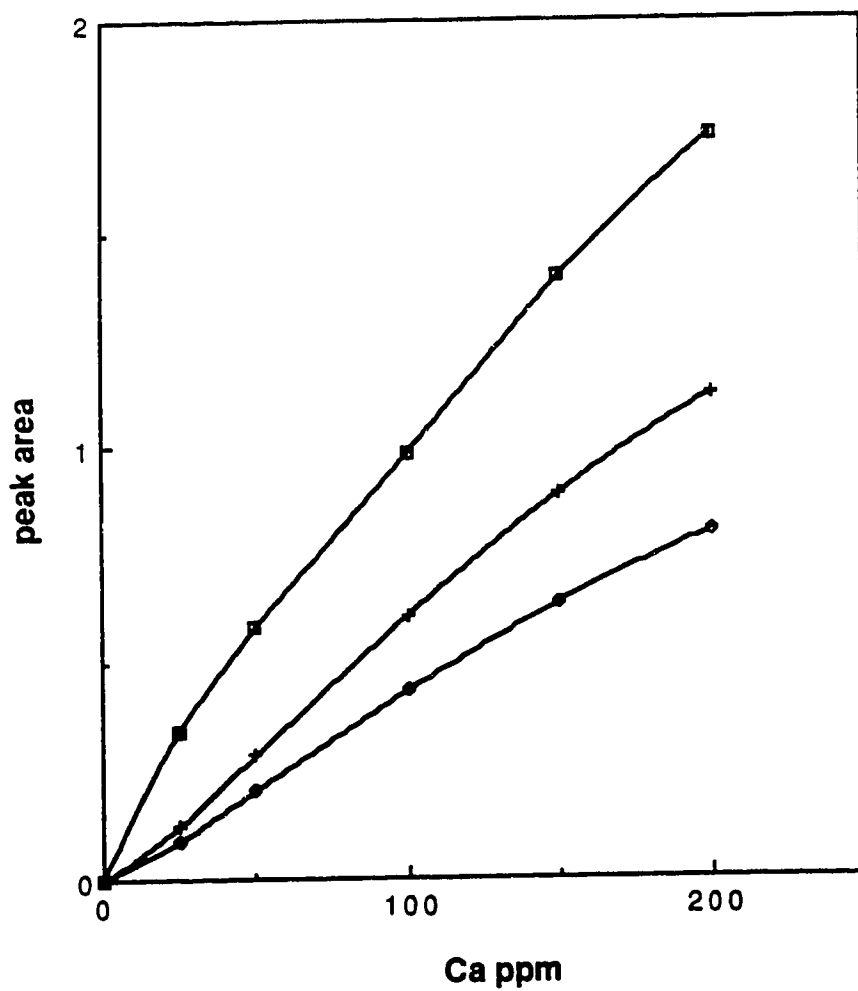


**Figure 6.3:** Calibration curves for standard  $\text{Ca}^{2+}$  solutions in 0.75M  $\text{NaNO}_3$ ; □, using 8% and ◆, 2% crosslinked resins. Curve + was constructed by the multiplication of curve ◆ by the column capacity ratio.

cation concentration in solution (equation 2.5). Therefore  $\text{Ca}^{2+}$  peak areas will increase with decreasing electrolyte cation concentration in solution. In order to confirm this phenomenon in the systems under study in this work, calibration curves were constructed for  $\text{Ca}^{2+}$  concentrations up to 100 ppm using two different concentrations of  $\text{K}^+$  in solution, 0.3M and 0.5M. Figure 6.4 shows the results.

Individual peak areas, thus the slope of the calibration curves, decrease with increasing electrolyte concentration in solution. Another important feature of this figure is the significant effect on the linearity of the curves with the concentration of electrolyte in the solution. This is in contrast to the effect of the degree of cross linking, which was shown in section 6.3 to have no effect on the linearity of the calibration curve.

In flow system 1 (figure 3.1), during the loading/equilibration cycle sample solution is passed through the column to the waste. Then valve A is rotated so that the sample solution is replaced by water. Before the sample solution/water interface reaches the column, mixing of the solution and water occurs. Mixing is enhanced during passage of the interface through the peristaltic pump. Therefore the first few millilitres of water that reach the column are a diluted version of the original solution. At high concentrations of electrolyte in solution, the column sorbs little  $\text{Ca}^{2+}$  during the loading cycle. When the resin, however, encounters a diluted solution of the electrolyte in the interface, more  $\text{Ca}^{2+}$  may be sorbed owing to the lower concentration of

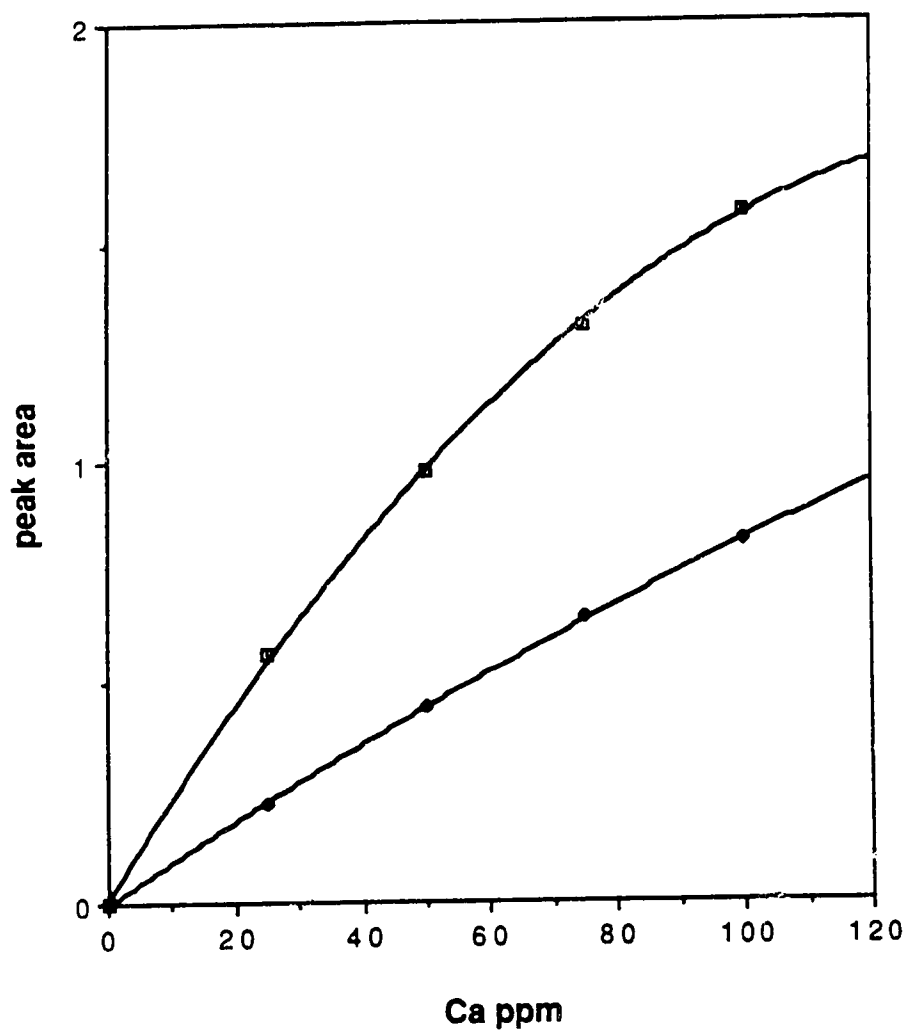


Figure 6.4: Calibration curves for standard  $\text{Ca}^{2+}$  solutions in;  $\square$ , 0.3M and  $\blacklozenge$ , 0.5M  $\text{KNO}_3$ .

electrolyte in solution. The result is a larger than expected peak area. Thus, perturbation of ion exchange equilibria during the initial stages of the wash cycle gives a positive systematic error. Note that the concentration of electrolyte and of  $\text{Ca}^{2+}$  are continuously changing at the interface, and so the resin will sorb a variably greater quantity of  $\text{Ca}^{2+}$  depending on a variety of factors such as initial concentrations of electrolyte and  $\text{Ca}^{2+}$ , tubing size and condition, pump rate, and so on.

Thus a change in the experimental procedure which could eliminate or minimize this perturbation of the ion exchange equilibrium during the wash cycle would be highly desirable. The criterion for selecting the best technique is the size of the peak area of the eluted  $\text{Ca}^{2+}$ . Since the error is a positive one, the best technique should be the one which gives the lowest peak area for a given free  $\text{Ca}^{2+}$  concentration.

When this kind of perturbation was observed with  $\text{Mg}^{2+}$ , the wash cycle was eliminated and the peak area obtained was corrected for the  $\text{Mg}^{2+}$  present in the solution in the dead volume of the flow system<sup>179</sup>. That procedure could not be applied to the present study because the  $\text{Ca}^{2+}$  levels analysed here were millimolar and so much higher than the  $\text{Mg}^{2+}$  levels used in that study. For very high concentrations of  $\text{Ca}^{2+}$  in solution and very small amounts of sorbed  $\text{Ca}^{2+}$ , as is the case in the present study, the difference between the peak area obtained by the no-wash method and that obtained due to the dead volume in



the tubing of the flow system can be smaller than the random fluctuations in the measurements. Therefore other alternatives were considered.

#### 6.4.1 Using an air purge cycle between the load cycle and the wash cycle

An air purge cycle was introduced between the load and wash cycles simply by introducing air into the system. This air gap prevented massive mixing of water and solution. The peak areas obtained were much smaller than those obtained with regular wash cycles. However, since the same tubing was used for the load, air and wash cycles, solution coated on the inner walls of the tubing was washed during the wash cycle to form a dilute solution.

Although this solution contained a much smaller amount of  $\text{Ca}^{2+}$  compared to that of the interface region in the regular wash cycle, it still increased the sorbed  $\text{Ca}^{2+}$  on the column to a measurable extent. The error caused by this process can be minimized by reducing the length of tubing from the sample inlet to the column. However even with incorporation of the minimum length of tubing, significant error was still noted.

#### 6.4.2 Removal of the column from the system between the air purge and wash cycles

In this case the procedure was similar to that in section 6.4.1 except that the column was removed after the air cycle and the rest of the system was run through a conventional wash cycle. Then the column was re-attached and the

system was carried through a second wash cycle. This procedure gave the lowest peak area of any. In this case the only change in sorbed  $\text{Ca}^{2+}$  occurs due to solution coated on the resin column walls and between resin particles. The amount of  $\text{Ca}^{2+}$  left in these places should be very small after the air cycle. Also, the quick flushing that occurs during the second wash cycle does not allow much time for the column to sorb  $\text{Ca}^{2+}$  from these sources. Therefore this is the best possible way to determine the true amount of  $\text{Ca}^{2+}$  sorbed by the resin during equilibration. However this is not a practical method of routinely determining free  $\text{Ca}^{2+}$  because of the inconvenience of detaching and reattaching of the column during each run. Therefore revisions to the design of the flow system were developed.

#### 6.4.3 Modification of flow system

Modifications were introduced to the flow system as follows. The waste and the column outlet tubing were swapped. An additional valve (valve C, figure 3.2) was incorporated into the flow system so that the wash and the elution cycles use tubing separate from that used during the load cycle. This flow system, flow system 2, and its advantages over the early systems are described in detail in chapter 3, and are not repeated here. Peak areas obtained with this flow system were identical to those obtained in section 6.4.2, demonstrating that this is the best possible practical way to obtain a reliable value for the sorbed  $\text{Ca}^{2+}$ .

To evaluate the performance of this improved technique using flow system 2, the selectivity of the method to free  $\text{Ca}^{2+}$  with flow system 1 is compared with that obtained with flow system 2. All  $\text{Ca}^{2+}$  solutions used in this experiment contained 0.35M  $\text{Na}^+$  and 0.15M  $\text{K}^+$ . Free  $\text{Ca}^{2+}$  values were measured for 100 ppm calcium solutions with 4 different levels of citrate using each of the two flow systems and the results compared with those obtained colorimetrically using the indicator TMMA as described in chapter 5, and the calculated free  $\text{Ca}^{2+}$  values (figure 6.5). This figure clearly shows the effect of the modified system on measured free  $\text{Ca}^{2+}$  concentrations. Flow system 1 values are much higher than the calculated values while those obtained using flow system 2 are very close to the calculated values. Also, the free  $\text{Ca}^{2+}$  levels obtained with flow system 2 are almost identical to those obtained with the indicator TMMA. Considering the uncertainties in the stability constants used in the calculations and the experimental errors in solution preparation, it is safe to state that with flow system 2 the method is more selective for free  $\text{Ca}^{2+}$ .

## 6.5 Conclusions

Studies done in chapters 5 and 6 show that alkyl ammonium ions are not suitable electrolytes for use in the sample pretreatment step of the column equilibration method. Therefore the alternative is to use metal ions for the purpose. With  $\text{Na}^+$  and  $\text{K}^+$  changing the degree of cross linking did not affect the linearity of the calibration curve. Therefore 8% cross-linked resin was used

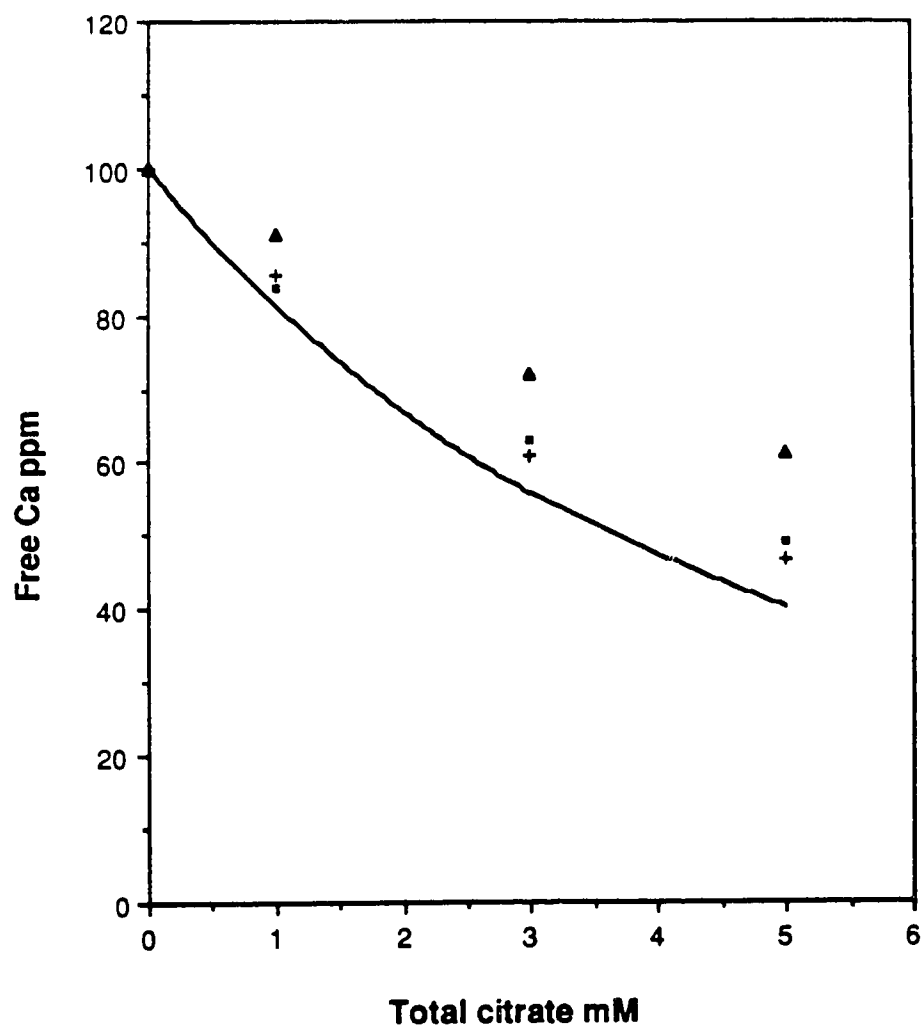


**Figure 6.5:** Variation of free  $\text{Ca}^{2+}$  concentration with total citrate in 0.35M  $\text{Na}_+$  and 0.15M  $\text{K}_+$ : obtained from ion exchange ( $\Delta$ , flow system 1 and  $+$ , flow system 2);  $\blacksquare$ , colorimetry; and by calculation (solid line)

for the rest of this study since it provides higher sensitivity.

It should be noted that the ion exchange column equilibration method is a very flexible technique with many parameters that can be manipulated to optimize the system for a particular application. These parameters include:

1. The nature of the electrolyte
2. The concentration of the electrolyte
3. The degree of resin cross linking
4. The amount of resin in the column.

The effect of each of these parameters is evident from the studies that are described in this chapter. This flexibility makes the method a powerful means of analysis for free metals.

No serious perturbation of the ion exchange equilibrium during the wash cycle was detected in the early free metal analysis done with ion exchange resins<sup>124-128</sup> including the work on chapter 4. The reason for this may have been the large amount of resin used in the columns in these studies. The amount of resin used in the present study was about 10 times less than the amounts used in earlier studies. Therefore the relative change in sorbed  $\text{Ca}^{2+}$  due to the equilibrium perturbation is much larger.

The improved technique for the ion exchange column equilibration method, flow system 2, produced good results for free  $\text{Ca}^{2+}$  determinations. Although not completely free of error, it should give very reliable values for sorbed  $\text{Ca}^{2+}$  because:

1. The determination of sorbed  $\text{Ca}^{2+}$  is based on a calibration curve. As long as samples and standards are treated in a similar manner, systematic errors can cancel out.
2. As seen in section 6.4.3, free  $\text{Ca}^{2+}$  values measured using flow system 2 agree well with those obtained using the indicator TMMA and with calculated values.

Therefore no further improvements to the system were introduced during the remainder of this study; all subsequent studies used flow system 2.

## CHAPTER 7

### MEASUREMENT OF FREE CALCIUM UNDER NON-TRACE CONDITIONS

#### 7.1 Introduction

As discussed in chapter 2, when an ion exchange column is equilibrated under trace conditions, the concentration of free  $\text{Ca}^{2+}$  sorbed on the resin becomes directly proportional to the amount in solution. Therefore, under trace conditions, a straight line relation between free  $\text{Ca}^{2+}$  concentration in solution and that sorbed on the resin column can be obtained. However, in order to satisfy trace column conditions for free  $\text{Ca}^{2+}$  concentrations up to 200 ppm, which corresponds to the range found in urine, a very high concentration of electrolyte is required in solution. As shown in chapter 4, the addition of a high concentration of electrolyte perturbs the  $\text{Ca}^{2+}$ -ligand equilibria in kinetically labile urine-like systems and changes the free  $\text{Ca}^{2+}$  concentration of the system. If the added electrolyte concentration can be kept small, changes in free  $\text{Ca}^{2+}$  concentrations can be minimized. Therefore the possibility of using organic cations (which have higher affinities for the ion exchange resin than  $\text{Na}^+$  or  $\text{K}^+$ ) and the possibility of using a lower percentage cross linked

resin (which has less selectivity for  $\text{Ca}^{2+}$ ) were investigated. In chapters 5 and 6 it was shown that these options either did not provide trace column conditions or did not give reliable free  $\text{Ca}^{2+}$  values. Therefore the best way to determine free  $\text{Ca}^{2+}$  was found to involve use of metal ions as the electrolyte and an 8% cross linked resin. But for millimolar levels of free  $\text{Ca}^{2+}$  high concentrations of sodium or potassium electrolyte salts required to obtain trace conditions perturb sample equilibria. Therefore the best way to obtain a reliable free  $\text{Ca}^{2+}$  value for urine is to operate the column under non-trace conditions.

As shown in section 6.3.3, even with very low concentrations of electrolyte, the calibration curves obtained up to 200 ppm were satisfactory, i.e. no saturation or plateau is reached. Moreover, with suitable computer software, an equation for the best fit can be obtained for a calibration curve almost as easily as for a linear plot. Considering the high sensitivity and the minimal perturbation achieved with low electrolyte concentrations, the use of non-trace conditions was expected to be the best alternative. This chapter investigates the level of sodium and potassium typically found in normal urine samples as counterions for free  $\text{Ca}^{2+}$  determination by the ion exchange column equilibration technique.



## 7.2 Experimental

Flow system 2 was used with a flow rate of 5 mL/min. An equilibration time of 30 seconds was found sufficient for all experiments. The columns were constructed as described in chapter 3. About 0.5 mg of 8% cross-linked resin was used for all measurements unless otherwise mentioned. The chemicals used were the same as in the early chapters.

## 7.3 Use of KNO<sub>3</sub> as electrolyte

As shown in chapter 6, 0.3M KNO<sub>3</sub> as electrolyte gives a calibration curve (figure 6.2) which is usable for the analysis of free Ca<sup>2+</sup> concentrations up to 200 ppm. The selectivity of the method for free over bound calcium using this electrolyte was tested as follows.

A solution of 100 ppm Ca<sup>2+</sup> was prepared in 5mM tri potassium citrate and 0.3M KNO<sub>3</sub>; the pH was adjusted to 6.6 using HNO<sub>3</sub>. Ca<sup>2+</sup> peak area for this solution was measured and the corresponding free Ca<sup>2+</sup> concentration was estimated using a calibration curve such as figure 6.2. The expected free Ca<sup>2+</sup> value for this solution was calculated by taking into account the complexation of both Ca<sup>2+</sup> and K<sup>+</sup> by citrate. Stability constant values used for the Ca<sup>2+</sup>-citrate complexes were the same as those reported earlier in this thesis. In addition, two additional stability constant values were included to take into account complexation between K<sup>+</sup> and citrate<sup>145</sup>. The stability constants used are given in table 7.1.

Table 7.1: Stability constants used in calculation of free calcium in the presence of citrate and  $\text{KNO}_3$ . (charges on species are not shown for convenience; triply charged citrate ion is written as L)

---

<u>equilibrium</u>	<u>log K (<math>\mu</math>, temp.°C)</u>
CaL <sub>3</sub> /Ca.L	4.68 (0, 25)
CaHL/Ca.HL	3.09 (0, 25)
CaH <sub>2</sub> L/Ca.H <sub>2</sub> L	1.10 (0, 25)
KL/K.L	0.56 (0.15, 37)
KHL/K.HL	-0.30 (0.15, 37)
HL/H.L	6.396 (0, 25)
H <sub>2</sub> L/H.HL	4.761 (0, 25)
H <sub>3</sub> L/H.H <sub>2</sub> L	3.128 (0, 25)

---

All stability constants were corrected for the solution ionic strength using the Davies equation before they were entered into the computer program COMICS for calculation of free  $\text{Ca}^{2+}$  concentrations. The results for free  $\text{Ca}^{2+}$  in the system described above were: calculated, 34 ppm; measured, 36 ppm with a standard deviation of 1 ppm.

The experimental values agree well with the calculated, showing that the selectivity of the method for free  $\text{Ca}^{2+}$  is satisfactory when 0.3M  $\text{KNO}_3$  is used as electrolyte.

The above calibration curve could be used to measure free  $\text{Ca}^{2+}$  in urine, if the level of  $\text{K}^+$  in the urine sample were 0.3M and the level of  $\text{Na}^+$  were sufficiently low not to affect the equilibria. Were  $\text{K}^+$  is the only electrolyte cation present in urine, for any  $\text{K}^+$  concentration is less than 0.3M it has to be raised to 0.3M by adding potassium nitrate. To get a rough idea of the perturbation of the free  $\text{Ca}^{2+}$  level caused by such an addition, the preceding calculation of free  $\text{Ca}^{2+}$  was carried out for zero concentration of  $\text{KNO}_3$ . The free  $\text{Ca}^{2+}$  value obtained was 24 ppm. This means a 30% increase in the free  $\text{Ca}^{2+}$  concentration was caused by the addition of 0.3M  $\text{K}^+$  to the sample. This increase is the result of a combination of  $\text{K}^+$  competition for citrate and ionic strength effects.

To obtain correct free  $\text{Ca}^{2+}$  values little or no electrolyte should be added to the sample. This means that the electrolyte concentration of the standards should be matched with the sample rather than vice versa.

#### 7.4 Use of Na<sup>+</sup> and K<sup>+</sup> salts as electrolytes

Na<sup>+</sup> and K<sup>+</sup> are the major cations present in urine. Based on the discussion in section 7.3, it is clear that for the greatest accuracy in free Ca<sup>2+</sup> concentrations standards should be matched with samples in terms of both potassium and sodium.

Since the free Ca<sup>2+</sup> value is changed by 30% upon addition of 0.3M KNO<sub>3</sub>, the addition of a smaller amount of K<sup>+</sup> must cause less than 30% error. Urine contains both sodium and potassium salts, so the amount to be added to match the standards may be lower than 0.3M depending on the electrolyte concentrations used in the standards. As a preliminary experiment, Ca<sup>2+</sup> standards were prepared containing upper normal levels of sodium and potassium. This allows preparation of a calibration plot for the analysis of any urine sample following addition of sodium and potassium to match the standards. The objective of the study was to test the selectivity of the method for free Ca<sup>2+</sup> in the presence of both Na<sup>+</sup> and K<sup>+</sup> at the high end of normal levels and to evaluate the effect on free Ca<sup>2+</sup> measurements of the addition of sufficient Na<sup>+</sup> and K<sup>+</sup> to match the standards.

According to reported values<sup>168,180</sup>, the highest normal concentrations of sodium and potassium in urine are 0.35M and 0.15M respectively. Standards were therefore prepared containing concentrations of Ca<sup>2+</sup> ranging from 0 to 200 ppm. The pH values of the solutions were found to be within the range 4

to 5. A calibration curve for free  $\text{Ca}^{2+}$ , constructed from peak areas measured for these solutions, is shown in figure 7.1.

Solutions containing 100 ppm  $\text{Ca}^{2+}$  and different concentrations of citrate were also prepared in 0.35M  $\text{NaNO}_3$  and 0.15M  $\text{KNO}_3$ . The pH values were adjusted using  $\text{HNO}_3$  to be within the range 6.6 to 6.9. Peak areas were measured and corresponding free  $\text{Ca}^{2+}$  values were estimated using the above calibration curve. Expected free  $\text{Ca}^{2+}$  values for each solution were calculated using the stability constants for complexations of  $\text{Ca}^{2+}$ ,  $\text{Na}^+$  and  $\text{K}^+$  citrate from tables 4.1 and 7.1. All stability constants were corrected for the solution ionic strength using the Davies equation before being entered as input to the

OMICS program. Free  $\text{Ca}^{2+}$  values for the same solutions were also measured colorimetrically using the indicator TMMA as described under 1(d) of section 5.4.7. No corrections were required for sodium interference since all solutions and standards contained the same concentration of sodium. The average free  $\text{Ca}^{2+}$  values obtained by these methods are compared in figure 7.2.

The results show that free  $\text{Ca}^{2+}$  values obtained by the ion exchange method are close to calculated values and almost identical to values obtained by the TMMA indicator. The differences in the calculated and experimental values may be due to uncertainties in stability constants and in estimation of stability constants for different ionic strengths, and also to experimental errors in solution preparation. However, overall agreement is satisfactory, suggesting

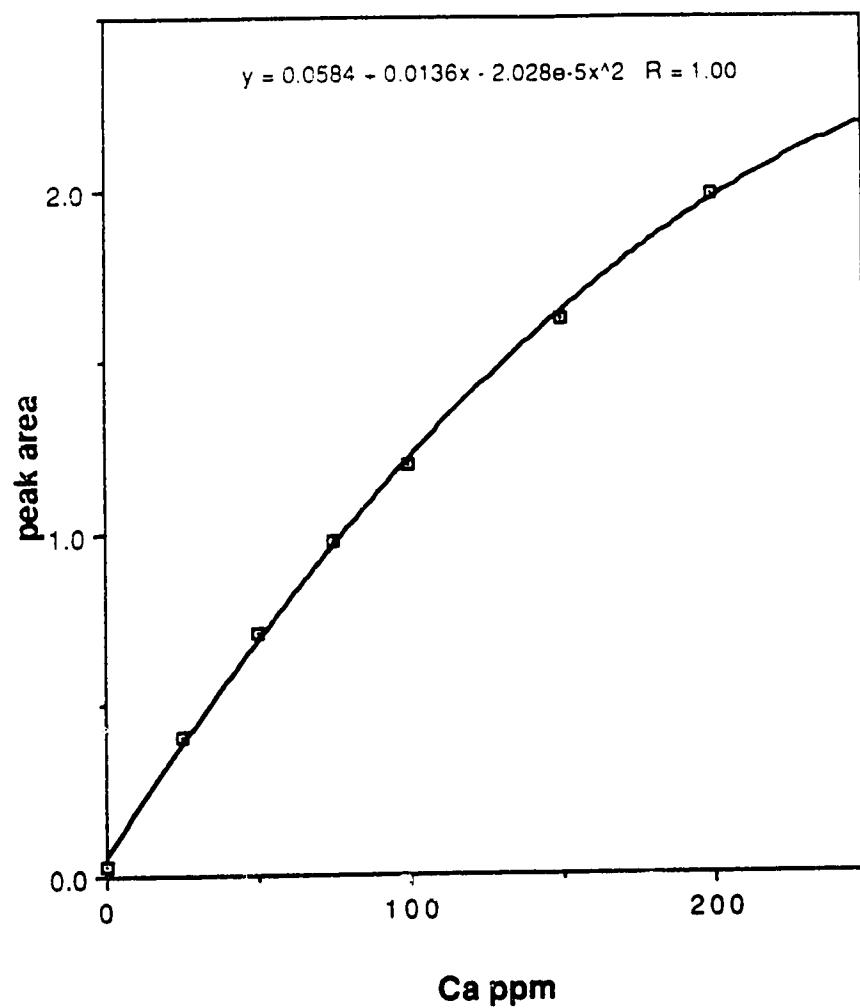
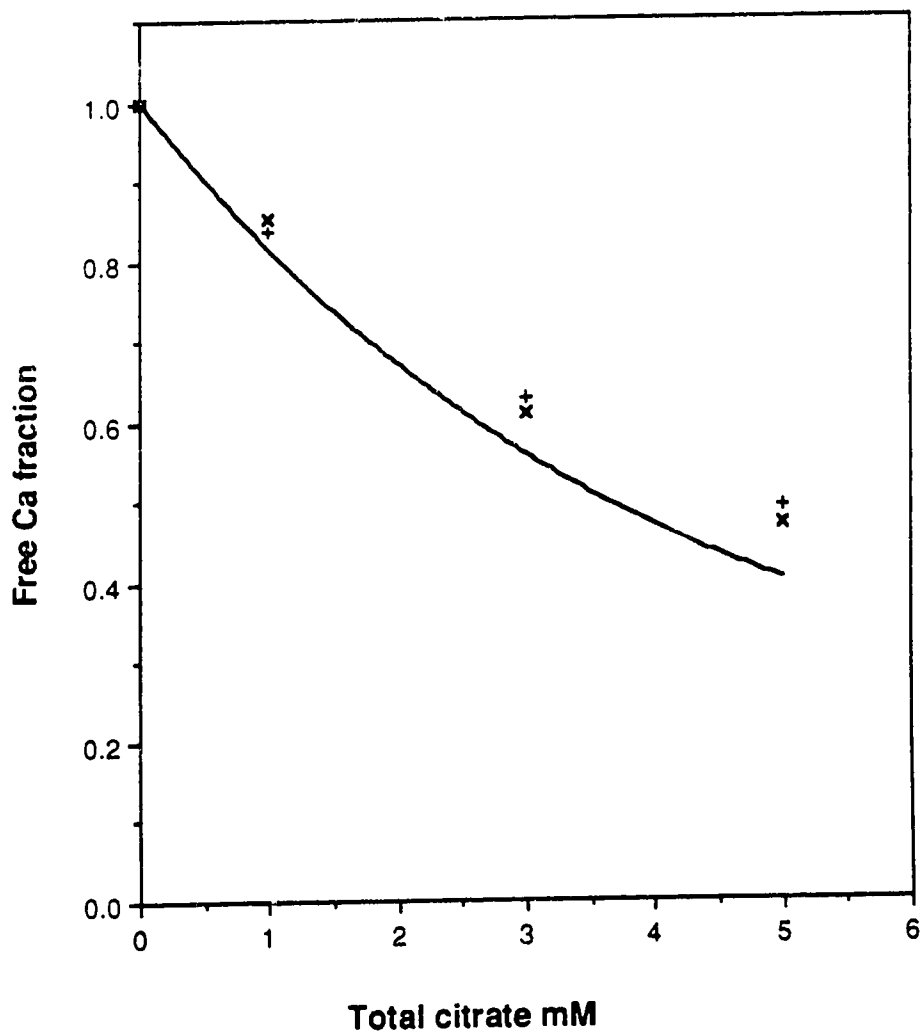


Figure 7.1: Calibration curve for standard  $\text{Ca}^{2+}$  solutions in 0.35M  $\text{NaNO}_3$  plus 0.15M  $\text{KNO}_3$ .



**Figure 7.2:** Variation in free  $\text{Ca}^{2+}$  concentration with total citrate level in  $0.35\text{M NaNO}_3$  and  $0.15\text{M KNO}_3$ , as measured by x, ion exchange and +, colorimetry. Solid line shows the calculated values.

that the method is adequately selective for free  $\text{Ca}^{2+}$  in the presence of sodium and potassium at the concentrations found in urine.

To estimate the extent of perturbation of sample equilibria due to the addition of sodium and potassium to bring their concentrations to 0.35M and 0.15M respectively, several calculations were carried out using the COMICS program as described below.

A typical free  $\text{Ca}^{2+}$  concentration of 100 ppm was chosen along with 5mM as a typical citrate level. Sodium and potassium levels were varied over the reported normal range for urine. Although the highest reported levels were 0.35M for sodium and 0.15M for potassium, a private communication with the University of Alberta hospital revealed that more typical values for the majority of patients are of the order of 0.1M for sodium and 0.05M for potassium. Therefore their levels were systematically varied only up to 0.2M and 0.1M. The highest reported values were also included for comparison. Ionic strengths were estimated for each solution and stability constants were adjusted for that ionic strength using the Davies equation. Calculations were done at pH 5 and 7 in order to represent the typical pH range of urine. The results (Table 7.2) show that, depending on pre-existing levels of sodium and potassium in the urine samples, the free  $\text{Ca}^{2+}$  concentration varies with sodium and potassium levels up to 0.35M and 0.15M respectively. The lower the initial sample electrolyte level, the larger will be the change in free  $\text{Ca}^{2+}$  in the sample due to the addition of sodium and potassium. Although reliable free



Table 7.2: Calculated free  $\text{Ca}^{2+}$  concentrations for a solution containing 100 ppm total calcium and 5mM total citrate.  $\text{Na}^+$  and  $\text{K}^+$  concentrations and pH were varied to represent typical variations in urine.

---

<u>[Na<sup>+</sup>]</u>	<u>[K<sup>+</sup>]</u>	<u>Free Ca<sup>2+</sup>, ppm</u>	
		<u>pH 5</u>	<u>pH 7</u>
0.05	0.05	42	17
0.10	0.05	48	23
0.10	0.10	51	28
0.15	0.05	51	28
0.15	0.10	56	34
0.20	0.05	56	34
0.20	0.10	56	34
0.35	0.15	59	40

---

$\text{Ca}^{2+}$  values can be obtained for samples with high electrolyte concentrations, free  $\text{Ca}^{2+}$  values for samples with low electrolyte concentrations will be biased.

### 7.5 Determination of minimum number of sets of standards required

According to table 7.2, if only one set of standards were to be used to determine free  $\text{Ca}^{2+}$  in any urine sample, the error in measured free  $\text{Ca}^{2+}$  would vary from moderate to severe. One way of overcoming this problem is to use several sets of standards containing varying amounts of  $\text{Na}^+$  and  $\text{K}^+$ .

In this section the minimum number of such sets of standards was estimated. The estimate is based on a maximum allowable error of about 5% in the free  $\text{Ca}^{2+}$  level caused by the addition of electrolytes to the sample. The results in table 7.2 were used in this estimation.

One interesting feature of the results shown in table 7.2 is that despite the differences in individual Na/K levels, at constant ionic strength (i.e.  $[\text{Na}^+] + [\text{K}^+]$ ) the free  $\text{Ca}^{2+}$  levels are similar. Also, the change in free  $\text{Ca}^{2+}$  values due to the addition of electrolytes is smaller at higher ionic strengths. Therefore the minimum number of sets of standards allowing a maximum error of about 5% is as follows:

1. 0.05M  $\text{Na}^+$  + 0.05M  $\text{K}^+$
2. 0.1M  $\text{Na}^+$  + 0.05M  $\text{K}^+$
3. 0.15M  $\text{Na}^+$  + 0.05M  $\text{K}^+$
4. 0.2M  $\text{Na}^+$  + 0.1M  $\text{K}^+$

A free  $\text{Ca}^{2+}$  determination can, then, be carried out using these standards as follows:

1. Measure the  $\text{Na}^+$  and  $\text{K}^+$  levels of the sample.
2. From the 4 sets above choose the one that most closely matches the amounts of  $\text{Na}^+$  and  $\text{K}^+$  present in the sample, but is larger.
3. Add sufficient  $\text{NaNO}_3$  and  $\text{KNO}_3$  to the sample to bring the concentration of  $\text{Na}^+$  and  $\text{K}^+$  to levels of the standards and carry out the measurement of the free  $\text{Ca}^{2+}$  peak area.
4. Using the appropriate calibration curve for the chosen set of standards, estimate the corresponding free  $\text{Ca}^{2+}$  concentration.

This procedure is based on the assumption that  $\text{Na}^+$  and  $\text{K}^+$  levels in urine are positively correlated. This may not be true. Furthermore, the calculations were done for only one typical level of total calcium and one level of citrate, and did not include other complexing ligands that may be present in urine. Therefore the above estimation is preliminary and provides only a rough estimate of the minimum number of standards required for the determination of satisfactory free  $\text{Ca}^{2+}$  concentrations in urine. It does however, give an idea of the variation in free  $\text{Ca}^{2+}$  with variations in sodium and potassium concentrations, and with ionic strength which can be useful in deciding the optimum  $\text{Na}^+$  and  $\text{K}^+$  concentration to be used in standards for the analysis of urine samples. For example, if the ionic strength of a set of samples is high, then even though individual levels of  $\text{Na}^+$  and  $\text{K}^+$  may be different, the

samples can be analysed for free  $\text{Ca}^{2+}$  using a single set of standards with no serious error. In general, the approach discussed above is useful in that it provides information about the effect on free  $\text{Ca}^{2+}$  concentrations resulting from addition of differing amounts of sodium and potassium electrolytes at various ionic strengths.

#### 7.6 Using one set of $\text{Na}^+/\text{K}^+$ concentrations in the $\text{Ca}^{2+}$ standards

Section 7.5 shows that at least 4 sets of standards are required to determine the free  $\text{Ca}^{2+}$  in urine if the error is to be held to the order of 5%. The higher the number of sets of standards, the better will be the accuracy of the measured free  $\text{Ca}^{2+}$  value. Therefore this method is still not a practical way of routinely analysing free  $\text{Ca}^{2+}$  in urine.

In the ion exchange column equilibration method,  $\text{Na}^+$  and  $\text{K}^+$  participate in two ways:

1. As the electrolyte, the addition of which causes changes in the free  $\text{Ca}^{2+}$  level of the sample through complex formation and through ionic strength effects on ion activities.
2. As counterions in the process of ion exchange.

Sections 7.4 and 7.5 show that the contributions of  $\text{Na}^+$  and  $\text{K}^+$  are similar in terms of altering free  $\text{Ca}^{2+}$  concentrations in samples. This may be due to the similarity of the stability constants for the formation of Na-citrate and K-citrate complexes.

With regard to the second point, in terms of the behavior of  $\text{Na}^+$  and  $\text{K}^+$  as counterions, we did not carry out detailed comparison studies. The difference in the affinity of  $\text{Na}^+$  and  $\text{K}^+$  for the resin depends upon their hydration radii. As seen in chapter 6, the affinities differ. However, if we assume that the behavior of  $\text{Na}^+$  and  $\text{K}^+$  as counterions are not very different within the required range of ionic strengths, then we can treat them as the same. Therefore, by this approach the free  $\text{Ca}^{2+}$  signal may be considered to be a function of the total solution ionic strength rather than of individual  $\text{Na}^+$  and  $\text{K}^+$  concentrations. If the above assumption is valid, the following procedure can be used to determine free  $\text{Ca}^{2+}$  in urine using only one set of standards.

1. Prepare several sets of  $\text{Ca}^{2+}$  standards ranging from 0 to 200 ppm, each set at a different ionic strength, ranging from 0 to about 0.4 (the range of normal urine ionic strengths)
2. Calculate the activity coefficient of  $\text{Ca}^{2+}$  for each ionic strength using the Davies equation.
3. Convert all  $\text{Ca}^{2+}$  concentrations to activities using appropriate activity coefficients.
4. Measure the  $\text{Ca}^{2+}$  peak area for each standard solution and plot them against the activity of  $\text{Ca}^{2+}$  ion in the solution.

5. Measure the sample sodium and potassium levels and estimate the ionic strength as the sum of the sodium and potassium concentrations. Calculate the activity coefficient of  $\text{Ca}^{2+}$  in the sample from the ionic strength.
6. Measure the  $\text{Ca}^{2+}$  peak area of the sample and estimate the  $\text{Ca}^{2+}$  ion activity from the calibration plot.
7. Using the value for activity and activity coefficient of  $\text{Ca}^{2+}$  in the sample obtained by steps 5 and 6, calculate the free  $\text{Ca}^{2+}$  concentration of the sample.

To study the relative effects of  $\text{Na}^+$  and  $\text{K}^+$  as counterions, the following experiment was performed. A set of solutions, each containing 100 ppm of  $\text{Ca}^{2+}$ , were prepared with various amounts of  $\text{Na}^+$  and  $\text{K}^+$  so as to fall within several different ranges of ionic strengths. The  $\text{Ca}^{2+}$  peak area for each of these solutions was measured. The column used in this experiment contained only about 0.2 mg of resin. This smaller than usual amount of resin was used because of the larger amounts of  $\text{Ca}^{2+}$  sorbed from the solutions containing low concentrations of counterions. Three measurements were made for each solution and the average values are shown in table 7.3. Since 3 measurements were made on each solution, ANOVA tests were carried out between different ionic strengths. This test gives the probability that two sets are drawn from the same population. Using these probabilities the following conclusions could be made:

Table 7.3: Variation in 100 ppm  $\text{Ca}^{2+}$  signal ( $n=3$ ) with ionic strength and  $\text{Na}^+/\text{K}^+$  ratio.  $\mu$  = Ionic strength, PA =  $\text{Ca}^{2+}$  peak area

$\mu$	$[\text{Na}^+]$	$[\text{K}^+]$	PA
0.1	0	0.1	2.513
0.1	0.05	0.05	2.819
0.15	0	0.15	2.072
0.15	0.05	0.1	2.035
0.15	0.1	0.05	2.257
0.2	0	0.2	1.653
0.2	0.1	0.1	1.689
0.2	0.15	0.05	1.841
0.3	0	0.3	1.197
0.3	0.2	0.1	1.188
0.3	0.25	0.05	1.218

1. At a constant ionic strength, the  $\text{Ca}^{2+}$  signal changes to a greater extent with changes in  $\text{K}^+$  compared to changes in  $\text{Na}^+$ , i.e. the  $\text{Ca}^{2+}$  signal is more sensitive to  $\text{K}^+$  than to  $\text{Na}^+$ .
2. As the ionic strength increases, the change in  $\text{Ca}^{2+}$  signal due to individual  $\text{Na}^+/\text{K}^+$  levels becomes smaller. For example, at ionic strengths above 0.2, there is no significant difference seen in the  $\text{Ca}^{2+}$  signal due to varying  $\text{Na}^+/\text{K}^+$  ratios at the 95% confidence level. This means that at high ionic strengths the behavior of  $\text{Na}^+$  and  $\text{K}^+$  as counterions is similar.

At ionic strengths greater than 0.2, therefore, the possibility exists that one set of standards is enough for the analysis of free  $\text{Ca}^{2+}$  in any urine sample as described earlier. However, 0.2 is at the higher end of the range of ionic strengths normally observed in urine, and few samples can be expected to fall in this range of ionic strengths. Therefore this method does not seem applicable to a wide variety of samples.

An estimation of a typical maximum error caused as a result of considering  $\text{Na}^+$  and  $\text{K}^+$  to behave as a single metal ion was done as described below.

Two sets of  $\text{Ca}^{2+}$  standards were prepared containing the range of 0 to 200 ppm  $\text{Ca}^{2+}$ , one set in 0.15M  $\text{KClO}_3$  and the other set in 0.1M  $\text{NaNO}_3$  plus 0.05M  $\text{KNO}_3$ . The latter set matches typical levels of these cations in urine.  $\text{Ca}^{2+}$  peak areas for each set of solutions were measured and two calibration curves were constructed (figure 7.3). For the point at which the two calibration



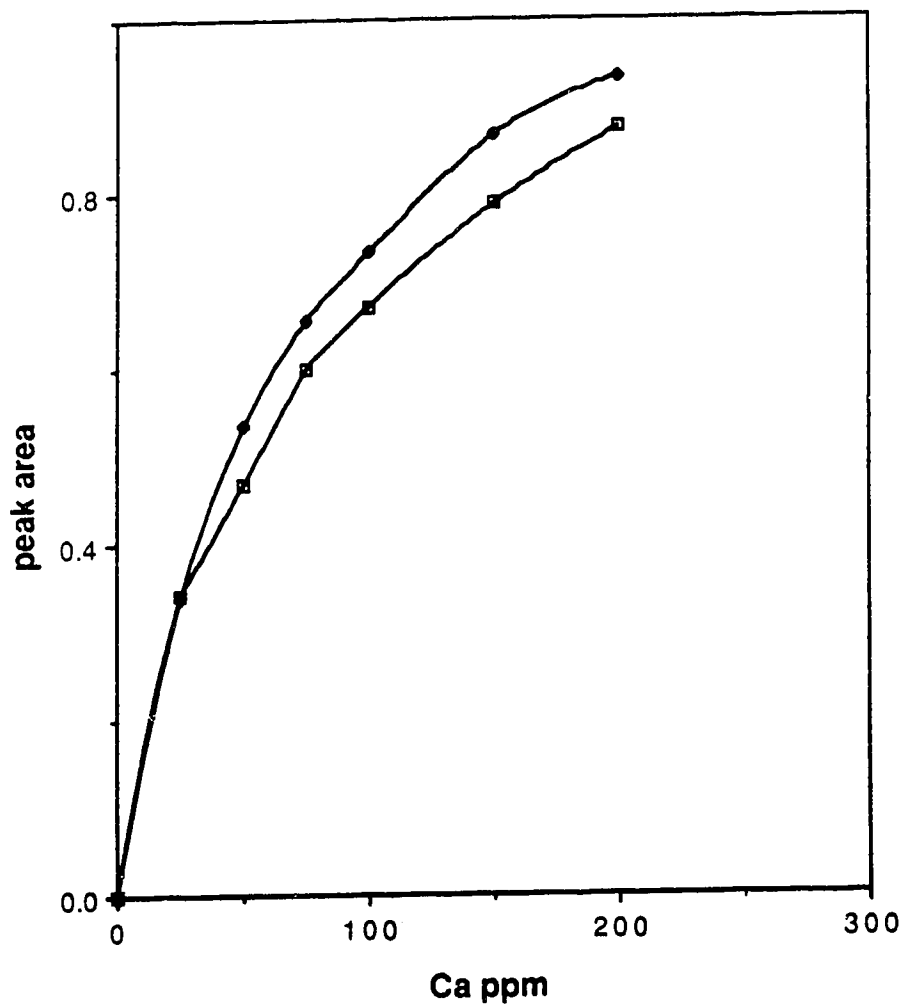


**Figure 7.3:** Calibration curves for standard  $\text{Ca}^{2+}$  solutions;  $\square$ , in 0.15M  $\text{KNO}_3$  and  $\blacklozenge$ , in 0.05M  $\text{KNO}_3$  plus 0.1M  $\text{NaNO}_3$ .

curves showed the largest difference, the concentration of  $\text{Ca}^{2+}$  was estimated from each curve. The difference between the two free  $\text{Ca}^{2+}$  concentrations obtained in this way was 30 ppm. This means that at typical sodium and potassium levels an error as high as 30 ppm can result if  $\text{Na}^+$  and  $\text{K}^+$  are considered as one metal ion. At ionic strengths typical of urine the behavior of  $\text{Na}^+$  and  $\text{K}^+$  as counterions clearly differs.

### 7.7 Conclusion

Free  $\text{Ca}^{2+}$  concentrations in urine can be accurately measured without the addition of electrolytes to the sample, when the column is operated under non-trace conditions. The accuracy of the measured free  $\text{Ca}^{2+}$  concentrations depends on how closely the standards are matched with the sample in terms of  $\text{Na}^+$  and  $\text{K}^+$ . Attempts were made to design a method such that each sample does not require a different set of standards. If several sets of standards are to be used to measure free  $\text{Ca}^{2+}$  concentrations with less than 5% error, more than 4 sets are required. Since  $\text{Na}^+$  and  $\text{K}^+$  do not function in a similar manner as counterions during the ion exchange process, they cannot be considered to behave interchangeably at typical urine ionic strengths. This makes it impossible to use a single calibration curve for the analysis of any urine sample. Therefore, at present, the best alternative to obtain a reliable free  $\text{Ca}^{2+}$  value for a urine sample is to make a unique set of standards with  $\text{Na}^+$  and  $\text{K}^+$  concentrations which are similar to those in the sample.

## CHAPTER 8

### DETERMINATION OF BOTH FREE CALCIUM AND FREE MAGNESIUM IN URINE

#### 8.1 Introduction

The effects of the major metal ions present in urine,  $\text{Na}^+$  and  $\text{K}^+$ , were extensively studied in early chapters. It was found that by matching the  $\text{Na}^+$  and  $\text{K}^+$  levels of standards with those of the sample, the free  $\text{Ca}^{2+}$  concentration can be accurately measured using the ion exchange column equilibration method.

Another metal ion which is also present in urine at significant levels, and is likely to participate during the ion exchange process to a significant extent is  $\text{Mg}^{2+}$ . Ion exchange equilibration studies done with 0.75M  $\text{Na}^+$  showed that  $\text{Mg}^{2+}$  does not interfere with the free  $\text{Ca}^{2+}$  signals<sup>128</sup>. However, in the present study, where electrolyte concentrations are much lower, the contribution of  $\text{Mg}^{2+}$  during the ion exchange process may not be as small as that with 0.75M  $\text{Na}^+$ . Although the concentration of  $\text{Mg}^{2+}$  in urine is similar to that of  $\text{Ca}^{2+}$ <sup>168</sup>, its affinity for the resin is somewhat lower than that of  $\text{Ca}^{2+}$ .

Therefore the  $\text{Ca}^{2+}$  signal should be prominent even though  $\text{Mg}^{2+}$  does interfere with it to some extent.

In this chapter the extent of  $\text{Mg}^{2+}$  interference on the  $\text{Ca}^{2+}$  signal is studied and ways in which the  $\text{Ca}^{2+}$  signal can be corrected for such interferences are discussed. A method is developed for the simultaneous analysis of free  $\text{Ca}^{2+}$  and free  $\text{Mg}^{2+}$ , and is tested on both synthetic and real urines.

The possibility of using the ion exchange column equilibration method for the analysis of free  $\text{Ca}^{2+}$  and free  $\text{Mg}^{2+}$  at trace levels is also explored.

## 8.2 Experimental

A Ca-Mg hollow cathode lamp was used for the atomic absorption measurements. The monochromator wavelength of the AAS was set at 422.7nm for the calcium measurements and 285.2nm for the magnesium measurements. To correct for any fluctuations in the signal from switching between the two wavelengths, and for drifts in the instrument for extended periods of time, the following procedure was used. An injector valve was connected between valve B and the AAS. A 10  $\mu\text{L}$  portion of a solution consisting of 150 ppm  $\text{Ca}^{2+}$  and 25 ppm  $\text{Mg}^{2+}$  was injected immediately after the elution of each peak and the signal was integrated for 15 seconds. This measurement is called the reference signal for that peak. The calcium and magnesium peaks were integrated for 40 seconds to obtain their respective

peak areas. These peak areas were then divided by the 15 second reference signals that followed them to obtain corrected peak areas free of detector drift. Since the injector valve was found to be precise within 1%<sup>†</sup>, any variation in the reference signal is due almost entirely to the detector, i.e. in the AAS. Flow system 2 (chapter 3) was used in this study with a 5 mL/min flow rate and various columns of 8% cross linked resin. The equilibration time was 30 seconds unless otherwise noted. The multiple regression option of the Macintosh program STATWORKS was used to find the best fit to the experimental data to prepare calibration curves. In this regression both  $\text{Ca}^{2+}$  and  $\text{Mg}^{2+}$  concentrations were independent variables, and were jointly used to predict the values of  $\text{Ca}^{2+}$  and  $\text{Mg}^{2+}$  peak areas. Peak areas were plotted against several different combinations of metal ion concentrations. The coefficients for each combination of the multiple regression equation were obtained for each trial. Goodness of fit was decided based on several different criteria, some of which were obtained as a part of STATWORKS output. These criteria are described below.

#### 1. t-statistics

The t-statistic gives the significance of the coefficient of each concentration term relative to a zero coefficient. In other words, it provides an

---

<sup>†</sup> Using the injector valve eight 10  $\mu\text{L}$  portions of a concentrated permanganate solution were injected into 10 mL volumetric flasks, diluted to the mark and the peak absorbance of the solutions were measured. The precision of absorbance values was within 1%.

idea about the significance of each concentration term. The higher the  $t$  value and the lower the probability of obtaining such a high value by mere random fluctuation ( $\text{Prob} > t$ ), the higher will be the significance of each concentration term. In this work only terms with  $\text{Prob} > t$  less than 5% were chosen as being significant.

## 2. F-test

The value of the F-statistic is the ratio of the variance due to the regression over the variance due to the scatter in points. Therefore a larger value of F represents a better fit of the regression model. STATWORKS also provides the probability that the value observed for the F statistics arises entirely due to random fluctuations under the null hypothesis ( $\text{Prob} > F$ ). In this work therefore the highest F and the lowest (less than 5%)  $\text{Prob} > F$  were the criteria used to select the best fit.

## 3. Correlation coefficient

The higher the value of the correlation coefficient, the better correlated will be the predicted and observed values for the dependent variable Y. The criterion for selecting the best fit in this case is therefore the largest value of the correlation coefficient.

## 4. Y residuals

STATWORKS gives the Y residual for each data point in a regression model. The smaller the residuals, the better the fit. Also, the presence of a systematic variation in the Y-residuals can give a clue to what the best fit could

be. For example, if a straight line model is used to fit a set of data which actually arise from a quadratic relation, the Y residuals will show initially positive values, then negative values followed again by positive values. This pattern suggests a curvilinear model would better represent the relationship in the data.

#### 6. Predictive validity test

The STATWORKS regression model was used to predict the concentrations for several standards which were not included in the preparation of the calibration line. These predicted values were then compared with the known concentrations of the standards, and the deviations compared to the Y-residuals from the calibration points. This provides an idea of the accuracy that can be expected when using this regression model to predict truly unknown concentrations.

To calculate the concentrations of free  $\text{Ca}^{2+}$  and free  $\text{Mg}^{2+}$  from the two regression equations, a set of simultaneous equations were solved using the MATHCAD program on an IBM PC. The correction of the stability constants, according to the Davies equation, for required ionic strengths was performed with a macro written in the program EXCEL on a Macintosh PC.

The chemicals used were the same as in early chapters, with the following exceptions and additions. A 1000 ppm  $\text{Mg}^{2+}$  solution was prepared by dissolving 1.000-g of cleaned Mg metal (Anachemia) in about 20 mL of concentrated nitric acid, followed by dilution to 1 L. A 0.5 ppm  $\text{Mg}^{2+}$  solution

was prepared from this solution by dilution and its AAS signal measured. This signal was compared with the AAS signal of a second 0.5 ppm  $Mg^{2+}$  solution, which was prepared from a 1000 ppm AAS  $Mg^{2+}$  standard solution (Aldrich). The two signals were identical. A stock solution of 0.25M citrate was prepared from trisodium citrate (J. T. Baker). A 0.5M phosphate stock solution was prepared from disodium phosphate (Mallinckrodt) and a 0.5M stock sulphate solution from sodium sulphate (Fisher). Norit A (Fisher) was used to decolorize urine samples for some experiments.

SRM 2670 (Toxic metals in freeze dried urine) was obtained from United States National Institute of Standards and Technology (NIST). This consisted of 4 vials of freeze dried urine, two bottles each at low and elevated levels of toxic metals. These samples can be reconstituted by the addition of 20 mL of water per bottle. Certified values of free metals were not available for these materials; a list of certified total metal concentrations is shown in table 8.1.

### 8.3 $Mg^{2+}$ interference with measurements of free $Ca^{2+}$

The total magnesium level in urine varies between 80 and 120 ppm<sup>168</sup>. Assuming about 50% of the total magnesium will typically be free (based on the fact that both  $Ca^{2+}$  and  $Mg^{2+}$  bind to urinary ligands to similar extents, and typical free  $Ca^{2+}$  fraction in urine is 50%), approximately half of the above total levels corresponds to the typical range of free  $Mg^{2+}$  which can interfere



Table 8.1: Certified values of constituent elements in SRM 2670 (freeze dried urine). The values in parentheses are not certified but are given for information only.

<u>Element</u>	<u>Conc. units</u>	<u>normal level</u>	<u>elevated level</u>
Al	$\mu\text{g/mL}$	(0.18)	(0.18)
As	$\mu\text{g/mL}$	(0.06)	$0.48 \pm 0.10$
Be	$\mu\text{g/mL}$	( $\leq 0.0005$ )	(0.033)
Cd	$\mu\text{g/mL}$	(0.00040)	$0.088 \pm 0.003$
Ca	$\text{mg/mL}$	$0.105 \pm 0.005$	$0.105 \pm 0.005$
Cr	$\mu\text{g/mL}$	(0.013)	$0.085 \pm 0.006$
Cu	$\mu\text{g/mL}$	$0.13 \pm 0.02$	$0.37 \pm 0.03$
Au	$\mu\text{g/mL}$	(0.000008)	(0.24)
Pb	$\mu\text{g/mL}$	(0.01)	$0.109 \pm 0.004$
Mg	$\text{mg/mL}$	$0.063 \pm 0.003$	$0.063 \pm 0.003$
Mn	$\mu\text{g/mL}$	(0.03)	(0.33)
Hg	$\mu\text{g/mL}$	(0.002)	$0.105 \pm 0.008$
Ni	$\mu\text{g/mL}$	(0.07)	(0.30)
Pt	$\mu\text{g/mL}$	(0.000008)	(0.12)
K	$\text{mg/mL}$	(1.5)	(1.5)
Se	$\mu\text{g/mL}$	$0.030 \pm 0.008$	$0.46 \pm 0.03$
Na	$\text{mg/mL}$	$2.62 \pm 0.14$	$2.62 \pm 0.14$

with uptake of free  $\text{Ca}^{2+}$  on the ion exchange resin. Typical free  $\text{Ca}^{2+}$  levels in urine range from 75 to 100 ppm. Therefore to test for interference by  $\text{Mg}^{2+}$  on free  $\text{Ca}^{2+}$  signals, 0 to 100 ppm  $\text{Mg}^{2+}$  were added as  $\text{Mg}(\text{NO}_3)_2$  to a 100 ppm  $\text{Ca}^{2+}$  solution, and  $\text{Ca}^{2+}$  peak areas measured using a column containing about 0.08 mg resin. The detector peak areas for  $\text{Ca}^{2+}$  were then plotted against the concentration of added  $\text{Mg}^{2+}$ . Since the ionic strength of urine typically varies between 0.1 and 0.3, the above experiment was carried out at two different ionic strengths. One set of solutions contained 0.05M  $\text{Na}^+$  and 0.05M  $\text{K}^+$  while the other set contained 0.2M  $\text{Na}^+$  and 0.1M  $\text{K}^+$ . The results obtained for the two sets of solutions are shown in figure 8.1.

According to this figure, unlike the case of 0.75M  $\text{Na}^{128}$ , interference from  $\text{Mg}^{2+}$  on the free  $\text{Ca}^{2+}$  signal is significant. The sensitivity of the signal to  $\text{Mg}^{2+}$ , as reflected in the slope of the plots, is more serious at low ionic strength. However, the slopes are also a function of the amount of sorbed  $\text{Ca}^{2+}$ , which in turn is dependant upon the weight of the resin in the column. Since more  $\text{Ca}^{2+}$  is sorbed on the resin from low ionic strength solutions, the slope is expected to be larger. Therefore a definite inference cannot be made about the dependance of  $\text{Mg}^{2+}$  interference on ionic strength.

The same experiment was therefore carried out again in a slightly different way. This time the low ionic strength solutions were run on the same column (0.08 mg resin), while the high ionic strength solutions were run on a column containing about 0.2 mg resin. With this modification the low ionic

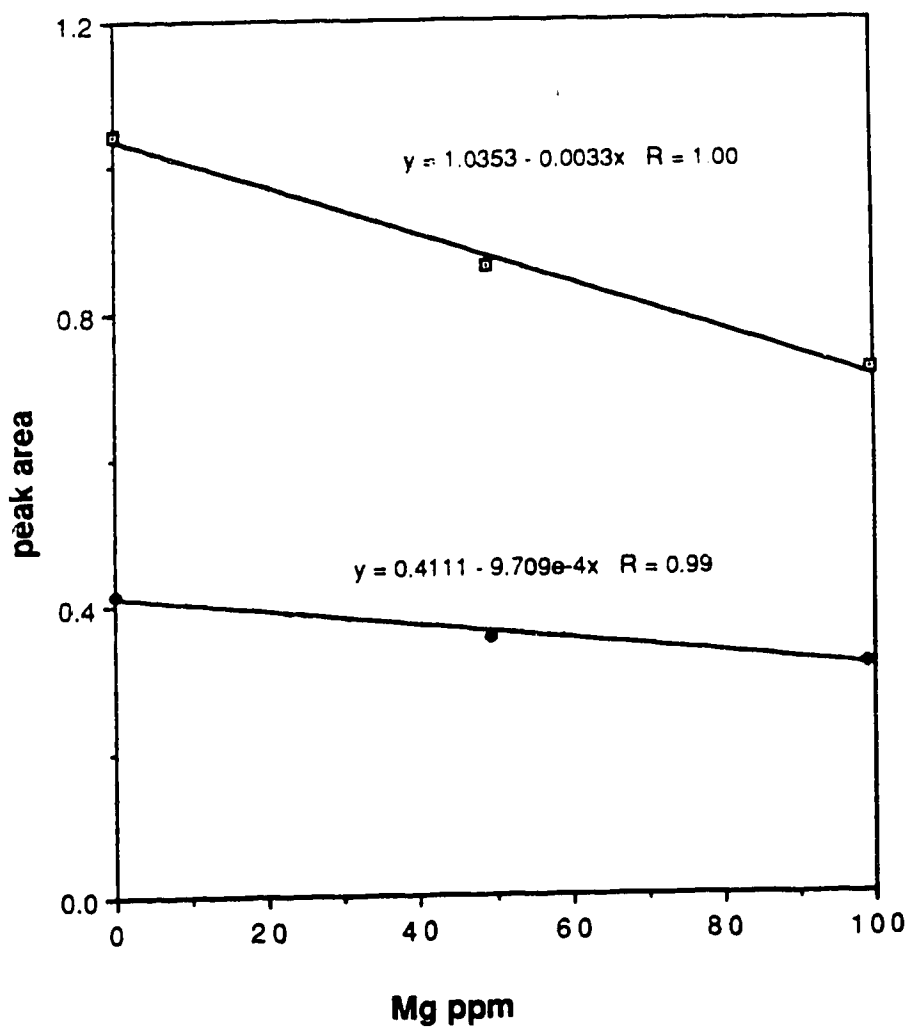


**Figure 8.1:** Peak area for a 100 ppm  $\text{Ca}^{2+}$  signal as a function of  $\text{Mg}^{2+}$  concentration at ionic strengths of  $\square$ , 0.1 and  $\blacklozenge$ , 0.3.

strength solutions should give larger peak areas. The results are shown in figure 8.2. As expected, the low ionic strength solutions gave larger peak areas, but smaller slopes, than the high ionic strength solutions. Therefore, if two columns were selected of relative size such that the peak areas for 0 ppm  $\text{Mg}^{2+}$  solutions in the two sets are similar, the slope obtained for the low ionic strength solutions will be larger than that obtained for the high ionic strength solutions. Clearly, the interference of  $\text{Mg}^{2+}$  on the free  $\text{Ca}^{2+}$  signal is more serious at low ionic strengths.

Even at the highest ionic strength studied here, 0.3, interference by  $\text{Mg}^{2+}$  on the free  $\text{Ca}^{2+}$  signal is large enough that it cannot be ignored. This finding is in contrast with that found in the earlier work at 0.75M  $\text{Na}^{128}$ . This means that over a range of ionic strengths, measured free  $\text{Ca}^{2+}$  concentrations are not free of interference from  $\text{Mg}^{2+}$ . Several different options were considered to correct the  $\text{Ca}^{2+}$  signal for this interference. Three of these are considered in the following sections.

### 1. Use of $\text{Mg}^{2+}$ blanks

A typical way of correcting a signal for interference is by subtracting an appropriate blank signal. For example, in spectrophotometric methods, if both analyte and interferent absorb or emit light at the same wavelength, the absorbance of a blank solution which contains only the interferent at the sample concentration is subtracted from the absorbance obtained for the sample. The corrected signal then represents only the analyte of interest. A

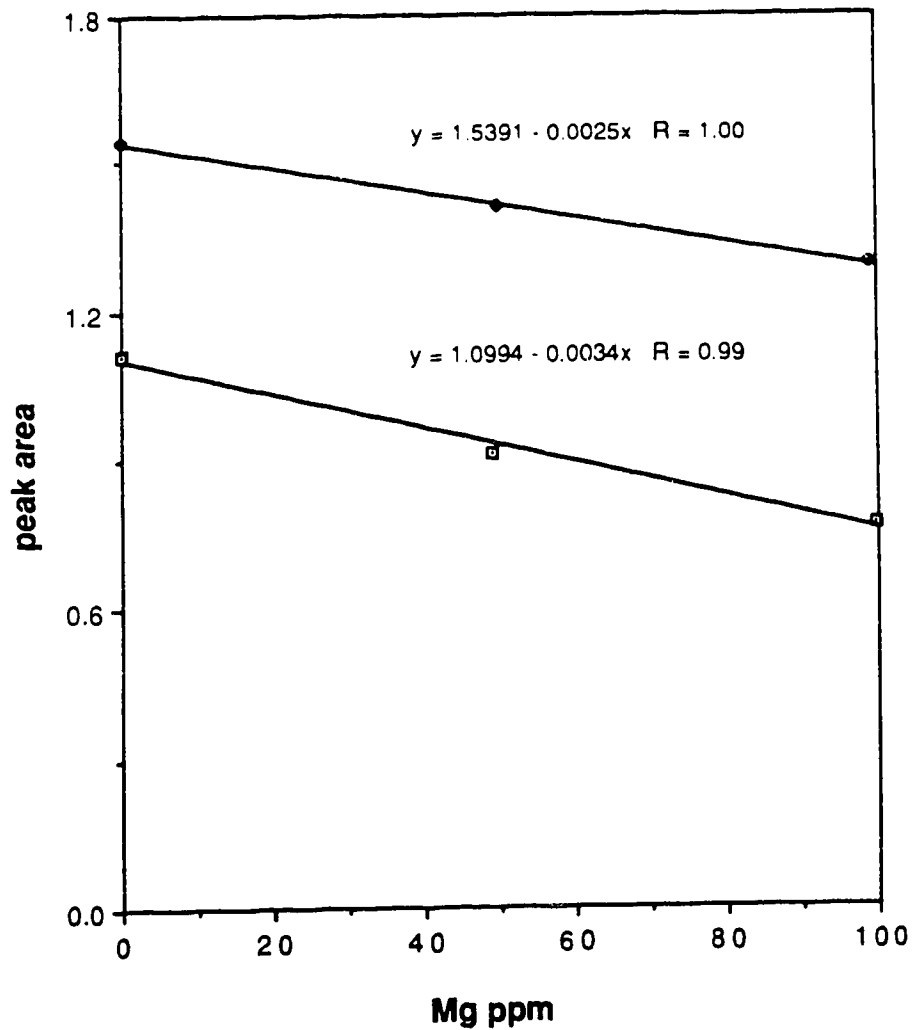


**Figure 8.2:** Peak area for a 100 ppm  $\text{Ca}^{2+}$  signal as a function of  $\text{Mg}^{2+}$  concentration;  $\square$ , at 0.1 ionic strength using a column containing 0.08 mg resin, and  $\blacklozenge$ , at 0.3 ionic strength using a column containing 0.2 mg resin.

parallel approach for our study would be to use a solution containing only  $\text{Mg}^{2+}$  at the sample concentration as the blank. Since the column has a fixed capacity, it can only sorb a certain number of ions from any solution. Unlike in spectrophotometry, in this case the signals from the analyte and from the interferent are not simply added up to produce the net signal, rather the net signal is the result of competition between the two ions for the fixed number of sites available in the column for sorption. Therefore, when the column is equilibrated with a solution containing only  $\text{Mg}^{2+}$  (i.e. the blank), all sites are available to sorb  $\text{Mg}^{2+}$  since there is no competition for the sites from other divalent ions. When the column is equilibrated with sample, the same sites may sorb either  $\text{Ca}^{2+}$  or  $\text{Mg}^{2+}$ . Therefore subtraction of a blank signal to obtain the  $\text{Ca}^{2+}$ -only signal in the ion exchange system described here is meaningless, unlike in the case of spectrophotometry.

## 2. Use of $\text{Mg}^{2+}$ in standards

If an interferent such as  $\text{Mg}^{2+}$  is present in all the  $\text{Ca}^{2+}$  standards at the same concentration as it is in the sample, the standards can be considered similar to the sample in terms of  $\text{Mg}^{2+}$  matrix. Therefore, both standards and sample are subjected to the interference. Since a calibration curve prepared with  $\text{Ca}^{2+}$  standards with matching  $\text{Mg}^{2+}$  matrix is used for the estimation of the  $\text{Ca}^{2+}$  concentrations, the measured sample free  $\text{Ca}^{2+}$  concentration is free of interference. This kind of correction can be applied not only in spectrophotometric analysis but also to ion exchange analysis.

For this method to be used in our study, the concentration of magnesium in the sample must be measured first. This can easily be done by atomic absorption spectroscopy. However, interference during the process of ion exchange equilibration is not caused by all magnesium species in solution, but is the result of  $Mg^{2+}$  ions, or free  $Mg^{2+}$ . As discussed in chapter 1, to date there are no experimental methods available for the determination of free  $Mg^{2+}$  in urine. Therefore, the first step of this correction procedure, the measurement of the interferent in the sample, is not possible.

### 3. Determination of the amount of sorbed $Mg^{2+}$ on the column

As mentioned earlier, the net signal obtained is the result of competition between the two ions for available exchange sites. Unlike other methods for the determination of free  $Ca^{2+}$ , such as  $Ca^{2+}$  ion selective electrode potentiometry, our method has additional selectivity because by atomic absorption spectroscopy sorbed  $Ca^{2+}$  and sorbed  $Mg^{2+}$  can be measured without interference from each other. Therefore, although it is not possible to correct the free  $Ca^{2+}$  signal for interference by  $Mg^{2+}$ , at least it is possible to estimate the extent of interference by measuring the sorbed interferent. This opens another interesting option, the simultaneous determination of free  $Ca^{2+}$  and free  $Mg^{2+}$  in the sample.

#### 8.4 Simultaneous determination of free $\text{Ca}^{2+}$ and free $\text{Mg}^{2+}$ in a single solution

The usual way of determining a species in a sample is to prepare standards containing different amounts of that species and to construct a calibration curve which then is used to estimate the species concentration in the sample. Similarly, two species in a sample can be determined by using a single set of standards containing different amounts of each species. If the signals for the two species are not independent of each other, as is the case with free  $\text{Ca}^{2+}$  and free  $\text{Mg}^{2+}$ , it is not possible to construct independent calibration curves to determine the two species. In this situation a calibration curve could be prepared with 3 axes, one each for the concentrations of the two species (independent variables) and one for the signal of one species (dependent variable). Since two species are present, two such plots would be required to determine the concentrations of both species. Multiple regression could be used to obtain a best fit equation for each of these calibration plots in terms of the signal and two species concentrations. In a normal 2-axis plot the concentration of a species in the sample is calculated using a regression equation involving the detector signal and the species concentration. In other words, when the signal for the sample is obtained, there is only one unknown in the regression equation to be solved to give the concentration of the species in the sample. The regression equations obtained for the two 3-axis calibration curves have 2 unknowns each. Since two such equations are available,



simultaneous solution of this set of equations will give the concentrations of each species.

The amount of sorbed  $\text{Ca}^{2+}$  and  $\text{Mg}^{2+}$  can be independently measured with no interference from each other by measuring their atomic absorbances at 422.7 nm and 285.2 nm respectively. The amount of  $\text{Mg}^{2+}$  sorbed by the resin used in this work is smaller than the amount of  $\text{Ca}^{2+}$  sorbed for a given solution concentration. Fortunately, this is not a problem in terms of instrumental detection limit, since the sensitivity of AAS for magnesium is about 8 times higher than that for calcium. The recommended AAS slit width to use for detecting magnesium was the same as for calcium, 7Å. The linear range for magnesium was tested and found to be at least 0 to 1 ppm. Therefore, with a column of about 0.08 mg resin it was possible to determine both free  $\text{Ca}^{2+}$  and free  $\text{Mg}^{2+}$  in a solution of any ionic strength in the range 0.1 to 0.3 ( which corresponds to the typical range of ionic strengths in urine), without exceeding instrumental linear range for either metal.

#### 8.4.1 Determination of free $\text{Mg}^{2+}$

So far in this study it has been shown that the ion exchange column equilibration method can be used for the determination of free  $\text{Ca}^{2+}$  at urine-like concentrations and that the method is selective for free over bound calcium. No studies had been done to this point, however, on the determination of free  $\text{Mg}^{2+}$  using the ion exchange column equilibration method. Therefore a set of experiments was done on this system.

Electrolyte levels of 0.1M NaNO<sub>3</sub> and 0.05M KNO<sub>3</sub> were chosen to represent typical values in urine. Standards were prepared over the range 0 to 50 ppm Mg<sup>2+</sup> in 0.1M NaNO<sub>3</sub> and 0.05M KNO<sub>3</sub>. The pH values of these solutions were within the range 3 to 4 and were not adjusted since the concentrations of all species in the solution were pH independent. A calibration curve was constructed (figure 8.3), based on sorbed amounts of Mg<sup>2+</sup>, plotted as peak areas, on a column containing about 0.08 mg of resin.

Two sets of 50 ppm Mg<sup>2+</sup> solutions were prepared in 0 to 5mM citrate and 0.1M NaNO<sub>3</sub> and 0.05M KNO<sub>3</sub>. The pH of one set was adjusted to be within 4.1 to 4.6, while the other set was adjusted to within 6.2 to 6.6 in order to represent typical pH variation in urine. Adjustment of pH was done by adding of HNO<sub>3</sub> or NaOH before final dilution. When NaOH was added, the amount of Na<sup>+</sup> added to the solution was estimated and was found to be negligible compared to the background level of 0.1M. After equilibrating the column with each solution and eluting as before, the peak area of each solution was measured and the corresponding free Mg<sup>2+</sup> concentration estimated using the above calibration curve.

The expected concentrations of free Mg<sup>2+</sup> for each solution were calculated using the COMICS program taking into account the complexes of Mg<sup>2+</sup>, Na<sup>+</sup> and K<sup>+</sup> with citrate. The stability constants used for the sodium and potassium complexes were listed in earlier chapters; the Mg<sup>2+</sup>-citrate stability constants are given in section 8.4.2. All of the stability constants were

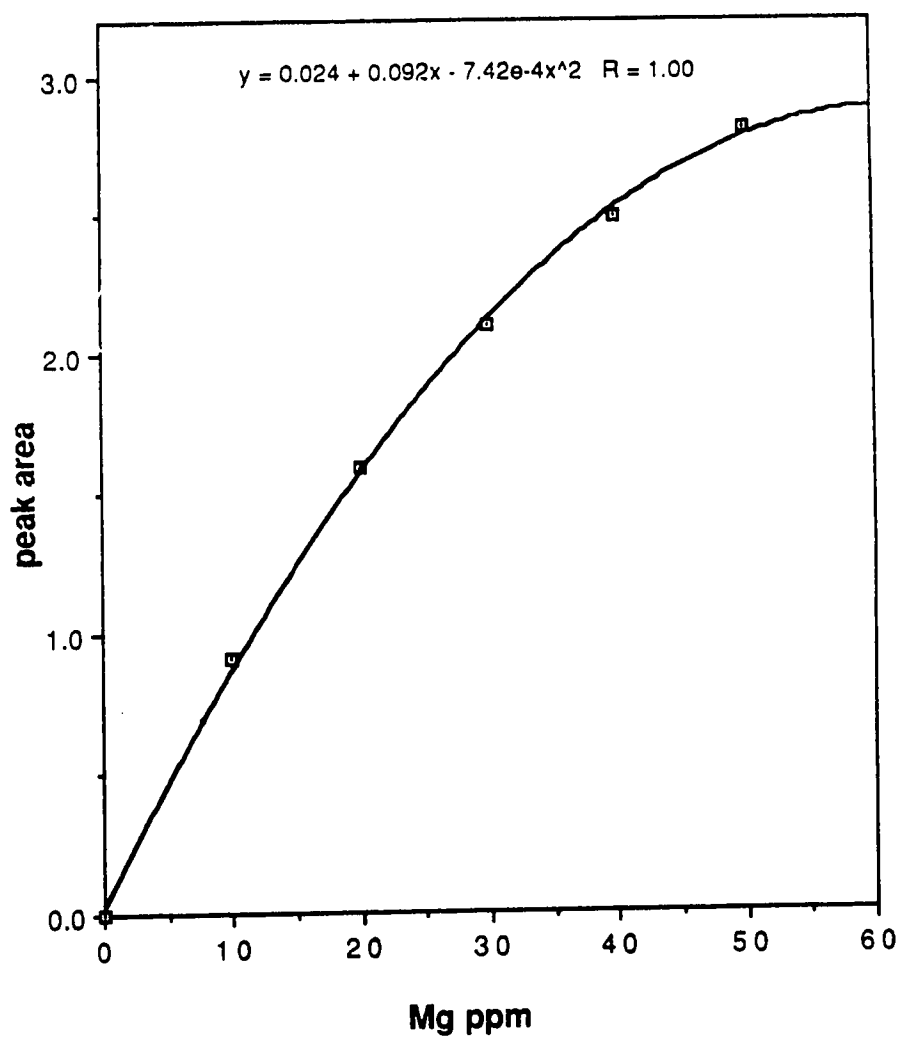


**Figure 8.3:** Calibration curve for set of standard  $Mg^{2+}$  solutions in 0.1M  $NaNO_3$  plus 0.05M  $KNO_3$ .

corrected for the ionic strengths of the solutions studied here using the Davies equation.

The calculated and experimental free  $Mg^{2+}$  values are plotted against the ligand concentration in figure 8.4. At both pH ranges, the experimental values agree well with the calculated values. This means that the ion exchange column equilibration method is selective for free  $Mg^{2+}$  at pH values and ionic strengths which are similar to those in urine. The results could not be compared with a different experimental method as was done for free  $Ca^{2+}$  owing to the lack of a reliable method for free  $Mg^{2+}$ . However, in light of the similarity between the calculated and multiple experimental values for  $Ca^{2+}$ , the good agreement observed between the two values found for  $Mg^{2+}$  lends support to the evidence that the method is selective for free  $Mg^{2+}$ .

#### 8.4.2 Determination of free $Ca^{2+}$ and free $Mg^{2+}$

The standards for this section of experiments were prepared to resemble SRM 2670, freeze dried urine. Since this is a combination of urine samples collected from a large number of normal subjects, it can be considered representative of a typical sample of urine. The certified concentrations of  $Na^+$  and  $K^+$  for SRM 2670 are listed as 0.114M and 0.038M respectively; the total calcium and total magnesium levels are 105 ppm and 63 ppm respectively. Since the extent of complexation of  $Ca^{2+}$  and  $Mg^{2+}$  by the major ligands in urine are similar<sup>136,137</sup>, the ratio of free  $Ca^{2+}$  to free  $Mg^{2+}$  in the sample can be postulated to be similar to the ratio of total calcium to total magnesium.

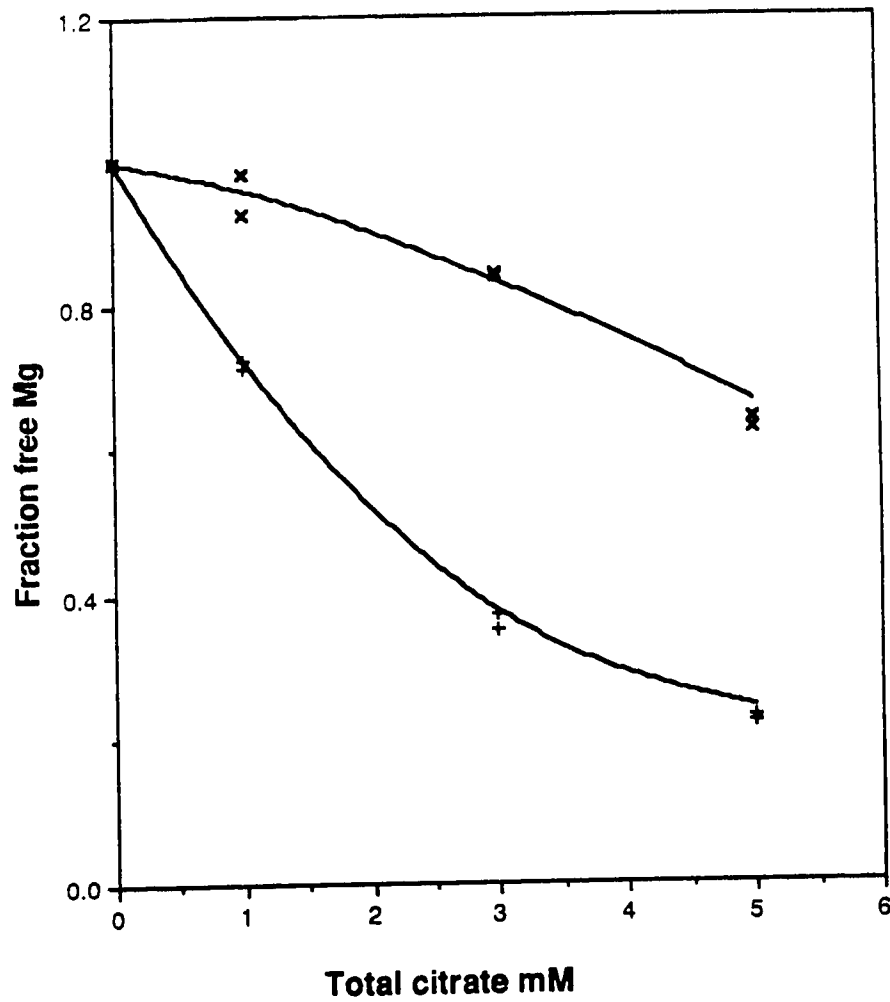


**Figure 8.4:** Variation of free  $Mg^{2+}$  fraction with total citrate level, in the pH range 4.1 to 4.6 (top) and 6.2 to 6.6 (bottom); x and +, as measured by ion exchange. Solid lines show the calculated values.

Therefore 12 standard solutions were prepared with differing amounts of  $\text{Ca}^{2+}$  and  $\text{Mg}^{2+}$  but with ratios similar to the ratio of total calcium to total magnesium in SRM 2670. The  $\text{Na}^+$  and  $\text{K}^+$  concentrations of all these solutions were prepared to be the same as those in SRM 2670. The pH levels of all of the standards were within the range 3 to 4. The ion exchange column used in these experiments contained about 0.08 mg of resin.

Four runs were performed for each standard, two to obtain  $\text{Ca}^{2+}$  peak areas and two to obtain  $\text{Mg}^{2+}$  peak areas. All peak areas were corrected for detector fluctuations as described in section 8.2, and the corrected average peak areas were plotted against the concentrations of  $\text{Ca}^{2+}$  and  $\text{Mg}^{2+}$  to yield two 3-axis calibration curves (figure 8.5). The vertical bars in the figures give the magnitude of the peak areas. The best fits were obtained when the following types of equations were used in the multiple regression.

$$\text{CaS}^2 = a C_{\text{Ca}} + b C_{\text{Ca}} C_{\text{Mg}} \quad (8.1)$$

$$\text{MgS}^2 = p C_{\text{Ca}} + q C_{\text{Mg}} + r C_{\text{Ca}}^2 + s C_{\text{Mg}}^2 + t C_{\text{Ca}} C_{\text{Mg}} \quad (8.2)$$

where a,b,p,q,r,s and t are coefficients obtained for each of the concentration terms, CaS and MgS are  $\text{Ca}^{2+}$  and  $\text{Mg}^{2+}$  peak areas respectively and  $C_{\text{Ca}}$  and  $C_{\text{Mg}}$  are concentrations of  $\text{Ca}^{2+}$  and  $\text{Mg}^{2+}$  in ppm.

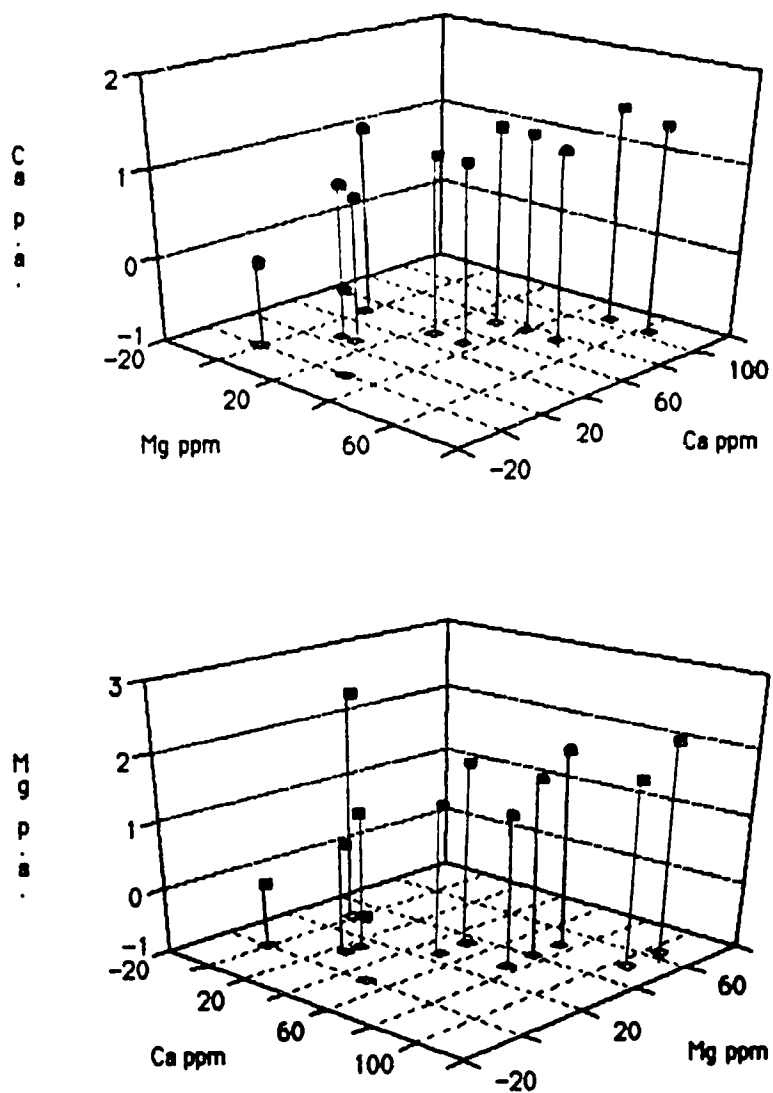


**Figure 8.5:** 3-axis calibration curves for standard Ca<sup>2+</sup> and Mg<sup>2+</sup> solutions in 0.114M NaNO<sub>3</sub> plus 0.038M KNO<sub>3</sub>. Vertical bars represent the magnitudes of Ca<sup>2+</sup> (top) and Mg<sup>2+</sup> (bottom) peak areas.

The coefficients in the above equations are given in tables 8.2 and 8.3. The t and F statistics for these regressions are also shown in these tables. Applying the criteria described in section 8.2, these tables show that the fits obtained using regression equations 8.1 and 8.2 are good. In addition to the Y residuals, the predictive validity test also shows that these regression equations are well suited to the estimation of unknown concentrations of free  $\text{Ca}^{2+}$  and free  $\text{Mg}^{2+}$ .

In order to assess the selectivity of this method for free  $\text{Ca}^{2+}$  and free  $\text{Mg}^{2+}$  in the presence of the major ligands found in urine, the following experiments were done.

Five sets of solutions were prepared with ligand levels similar to those in urine. All the solutions contained 105 ppm  $\text{Ca}^{2+}$ , 63 ppm  $\text{Mg}^{2+}$ , 0.114M total sodium and 0.038M total potassium to resemble SRM 2670. The pH of all the solutions were adjusted using  $\text{HNO}_3$  and negligibly small amounts of  $\text{NaOH}$ .

The compositions of the sets was as follows:

Set #1 - Total citrate levels ranging from 0 - 5 mM to represent urinary citrate levels as in earlier chapters. The pH of this set varied between 4.3 and 5.5.

Set #2 - Similar to set #1 except that the pH values were adjusted to fall within the range of 6 to 6.8.

Set #3 - Since urinary phosphate is reported to vary over the range of 0.01 to  $0.03^{168}$ , this set of solutions was prepared to contain 0 to 0.04M phosphate, with pH values ranging from 5.5 to 6.5.



**Table 8.2:** The F-test and t-test results for calibration curve given by equation 8.1 in terms of  $\text{Ca}^{2+}$  peak areas (Statworks printouts).

StatWorks™ Data Coefficients Thu, Mar 28, 1991 12:39 PM  
Data File: SRM calib.

Variable Name	Coefficient	Std. Err. Estimate	t Statistic	Prob > t
Ca ppm	0.02792018	0.00105611	26.43687630	0.000
Ca*Mg	-0.00015890	0.00002258	-7.03651953	0.000

StatWorks™ Data ANOVA Table Thu, Mar 28, 1991 12:40 PM  
Data File: SRM calib.

Source	Sum of Squares	Deg. of Freedom	Mean Squares	F-Ratio	Prob>F
Model	5.60169928	2	2.80084964	23.71424169	0.000
Error	0.05949209	9	0.00661023		
<b>Total</b>	<b>5.66119138</b>	<b>11</b>			

Coefficient of Determination 0.98949124  
Coefficient of Correlation 0.99473174  
Standard Error of Estimate 0.08130334  
Durbin-Watson Statistic 1.99263167

**Table 8.3:** The F-test and t-test results for calibration curve given by equation 8.2 in terms of  $Mg^{2+}$  peak areas (Statworks printouts).

StatWorks™ Data Coefficients Thu, Mar 28, 1991 12:42 PM

Data File: SRM calib.

Variable Name	Coefficient	Std. Err. Estimate	t Statistic	Prob > t
Ca ppm	-0.03839649	0.00298288	-12.87230301	0.000
Mg ppm	0.14809267	0.00529833	27.95084190	0.000
Ca2	0.00076422	0.00005085	15.02906704	0.000
Mg2	0.00205037	0.00016210	12.64890957	0.000
Ca*Mg	-0.00261557	0.00011332	-23.08101845	0.000

StatWorks™ Data ANOVA Table Thu, Mar 28, 1991 12:43 PM

Data File: SRM calib.

Source	Sum of Squares	Deg. of Freedom	Mean Squares	F-Ratio	Prob>F
Model	41.10069884	5	8.220139756	1302.4626	0.000
Error	0.07516928	6	0.01252821		
Total	41.17586812	11			

Coefficient of Determination 0.99817443  
 Coefficient of Correlation 0.99908680  
 Standard Error of Estimate 0.11192950  
 Durbin-Watson Statistic 2.41912868

Set #4 - Urinary sulphate falls normally in the range of 0.01 to 0.03M<sup>168</sup>.

Therefore this set contained 0 to 0.03M sulphate, with pH values falling within the range 6 to 6.4.

Set #5 - These solutions were prepared to simulate a normal urine. They contained 3mM citrate, 0.02M phosphate and 0.02M sulphate, all typical levels of these ligands in urine. The pH of these solutions were within the range 4.3 to 5.5.

All the above solutions were run in the same way as the standards and Ca<sup>2+</sup> and Mg<sup>2+</sup> peak areas were obtained for each. Then these peak areas were substituted into equations 8.1 and 8.2 and the two equations were solved simultaneously to obtain free Ca<sup>2+</sup> and free Mg<sup>2+</sup> values for each solution.

The free Ca<sup>2+</sup> concentration of each solution was also measured spectrophotometrically using the Ca<sup>2+</sup> indicator TMMA. The procedure was similar to that used in early chapters except that 3 mL of solution and 60  $\mu$ L of TMMA stock were used here to reduce the sample size.

Free Ca<sup>2+</sup> and free Mg<sup>2+</sup> concentrations of each solution were also calculated using COMICS. All stability constants were corrected for the ionic strength of each solution. The stability constants used for citrate, phosphate and sulphate solutions are shown in tables 8.4, 8.5 and 8.6 respectively. The calculations for set #5 included all the stability constants in tables 8.4, 8.5 and 8.6, and therefore involved 33 equilibria. This appears to be the best way of simulating the equilibria that occur in a sample of urine.

Table 8.4: A list of the stability constants used in the calculation of free  $\text{Ca}^{2+}$  and free  $\text{Mg}^{2+}$  concentrations in the presence of citrate. (charges of species are not shown for convenience; triply charged citrate ion is denoted as L)

---

<u>equilibrium</u>	<u>log K (<math>\mu</math>, temp.°C)</u>
CaL/Ca.L	4.68 (0, 25)
CaHL/Ca.HL	3.09 (0, 25)
CaH <sub>2</sub> L/Ca.H <sub>2</sub> L	1.10 (0, 25)
MgL/Mg.L	3.37 (0.1, 25)
MgHL/Mg.HL	1.92 (0.1, 25)
MgH <sub>2</sub> L/Mg.H <sub>2</sub> L	0.84 (0.1, 25)
KL/K.L	0.56 (0.15, 37)
KHL/K.HL	-0.30 (0.15, 37)
NaL/Na.L	0.70 (0.1, 25)
NaHL/Na.HL	0.10 (0.15, 37)
HL/H.L	6.396 (0, 25)
H <sub>2</sub> L/H.HL	4.761 (0, 25)
H <sub>3</sub> L/H.H <sub>2</sub> L	3.128 (0, 25)

---

**Table 8.5:** A list of the stability constants used in the calculation of free  $\text{Ca}^{2+}$  and free  $\text{Mg}^{2+}$  concentrations in the presence of phosphate. (charges of species are not shown for convenience; triply charged phosphate ion is denoted as L)

---

<u>equilibrium</u>	<u>log K (<math>\mu</math>, temp.°C)</u>
CaL/Ca.L	6.46 (0, 25)
CaHL/Ca.HL	2.68 (0, 25)
CaH <sub>2</sub> L/Ca.H <sub>2</sub> L	0.80 (0, 25)
MgL <sub>2</sub> /Mg.L	4.83 (0, 25)
MgHL/Mg.HL	2.75 (0, 25)
MgH <sub>2</sub> L/Mg.H <sub>2</sub> L	1.18 (0, 25)
NaL/Na.L	0.75 (0.15, 37)
NaHL/Na.HL	0.60 (0.2, 25)
NaH <sub>2</sub> L/Na.H <sub>2</sub> L	0.114 (0.3, 37)
KL/K.L	0.60 (0.15, 37)
KHL/K.HL	0.48 (0.15, 37)
KH <sub>2</sub> L/K.H <sub>2</sub> L	-0.20 (0.3, 37)
HL/H.L	12.35 (0, 25)
H <sub>2</sub> L/H.HL	7.199 (0, 25)
H <sub>3</sub> L/H.H <sub>2</sub> L	2.148 (0, 25)

---

Table 8.6: A list of the stability constants used in the calculation of free  $\text{Ca}^{2+}$  and free  $\text{Mg}^{2+}$  concentrations in the presence of sulphate. (charges of species are not shown for convenience; doubly charged sulphate ion is denoted as L)

---

<u>equilibrium</u>	<u>log K (<math>\mu</math>, temp.°C)</u>
CaL/Ca.L	2.33 (0, 25)
MgL/Mg.L	2.23 (0, 25)
KL/K.L	0.79 (0, 25)
NaL/Na.L	0.68 (0, 25)
HL/H.L	1.97 (0, 25)

---

The free metal concentrations obtained by the three methods were converted to free metal fractions by dividing each free metal concentration by the total metal concentration. They were then plotted against the ligand concentration or pH as shown in figures 8.6, 8.7, 8.8, 8.9 and 8.10.

The fraction of free metal ions decreases with increasing ligand concentrations. In the case of phosphate this trend is not very clear since the pH of solution set #3 is not constant. The decrease in free metal ion concentration at high concentration of phosphate is counteracted by the low pH values of the solution.

In general, all 3 methods agree fairly well for solution sets #1 to #4 which are systems with one ligand. Although a second method was not used for the analysis of free  $Mg^{2+}$ , comparisons with free  $Ca^{2+}$  plots support the selectivity of the ion exchange method for free  $Mg^{2+}$ . There are several factors that may contribute to the differences observed between the calculated and experimental free metal values.

1. Uncertainties in the values of the stability constants used in the calculations.
2. Errors involved in the theoretical estimation of stability constants (using the Davies equation) at ionic strengths other than measured.
3. Experimental errors in solution preparation and pH measurements.

In the case of solution set #5, simulated urine, the calculated values are about 15% lower than the measured values for  $Ca^{2+}$  and about 24% lower for

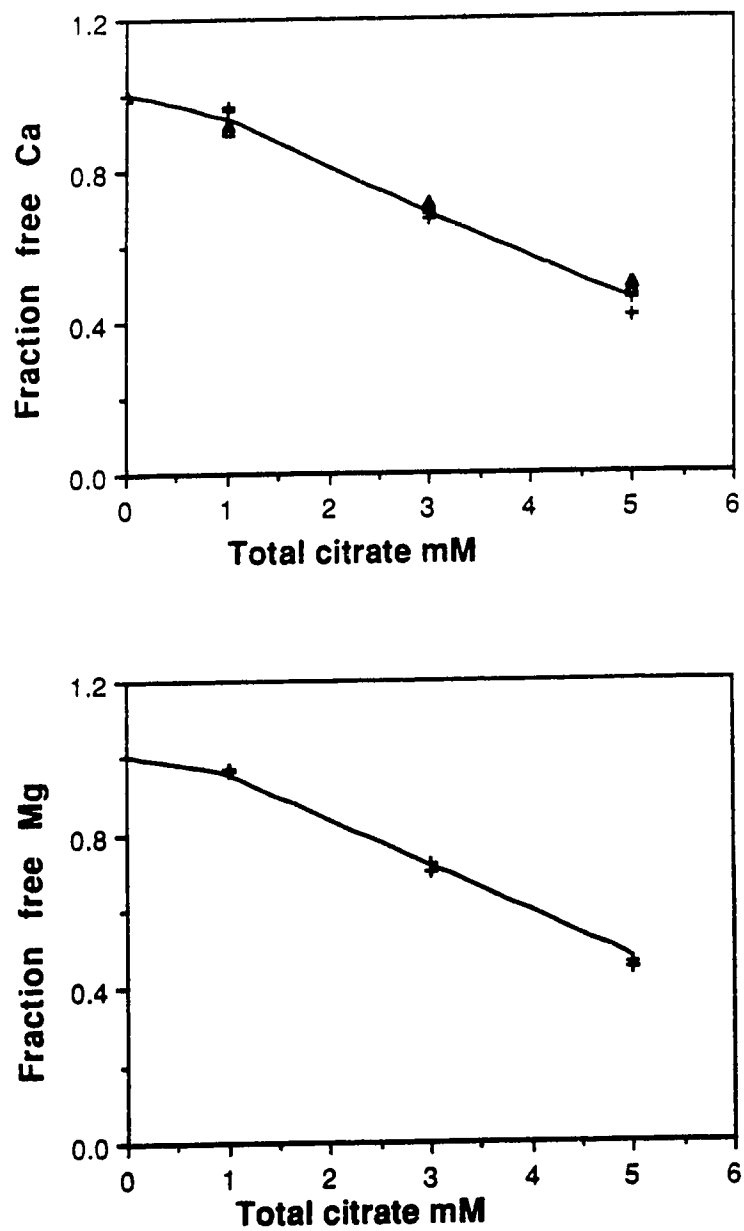


**Figure 8.6:** Variation of free  $\text{Ca}^{2+}$  (top) and free  $\text{Mg}^{2+}$  (bottom) fractions with total citrate, at pH range 4.3 to 5.5 (solution set #1), as measured by; +, ion exchange and  $\Delta$ , colorimetry. Solid lines show the calculated values.



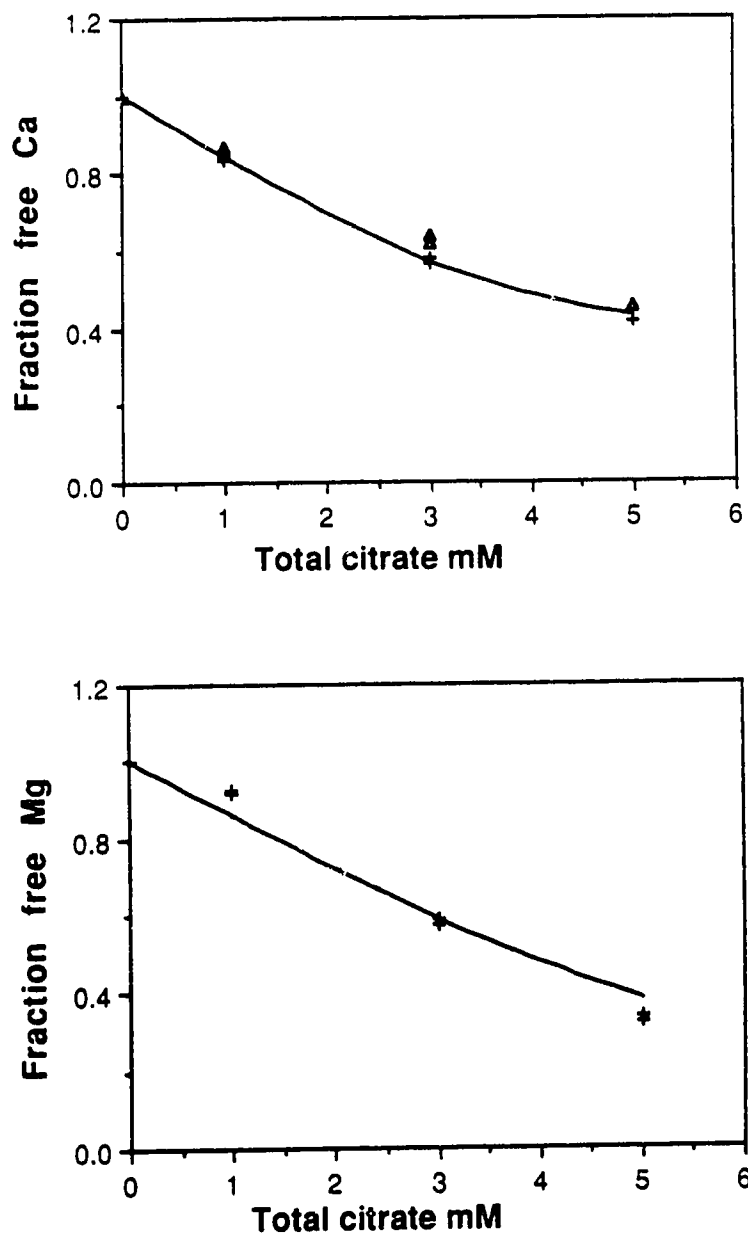


**Figure 8.7:** Variation of free  $\text{Ca}^{2+}$  (top) and free  $\text{Mg}^{2+}$  (bottom) fractions with total citrate, at pH range 6 to 6.8 (solution set #2), as measured by; +, ion exchange and  $\Delta$ , colorimetry. Solid lines show the calculated values.

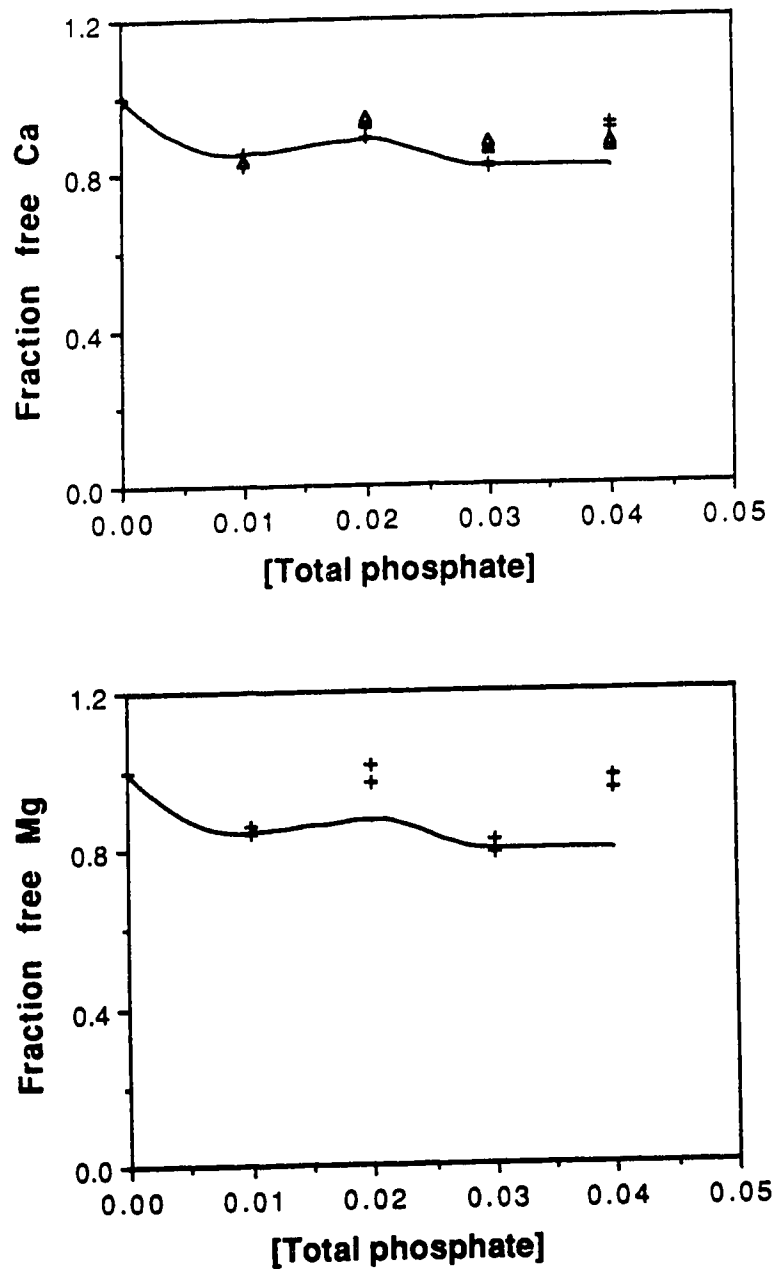


**Fig. 8.8:** Variation of free  $\text{Ca}^{2+}$  (top) and free  $\text{Mg}^{2+}$  (bottom) fractions with total phosphate, at pH range 5.5 to 6.5 (solution set #3), as measured by; +, ion exchange and  $\Delta$ , colorimetry. Solid lines show the calculated values.

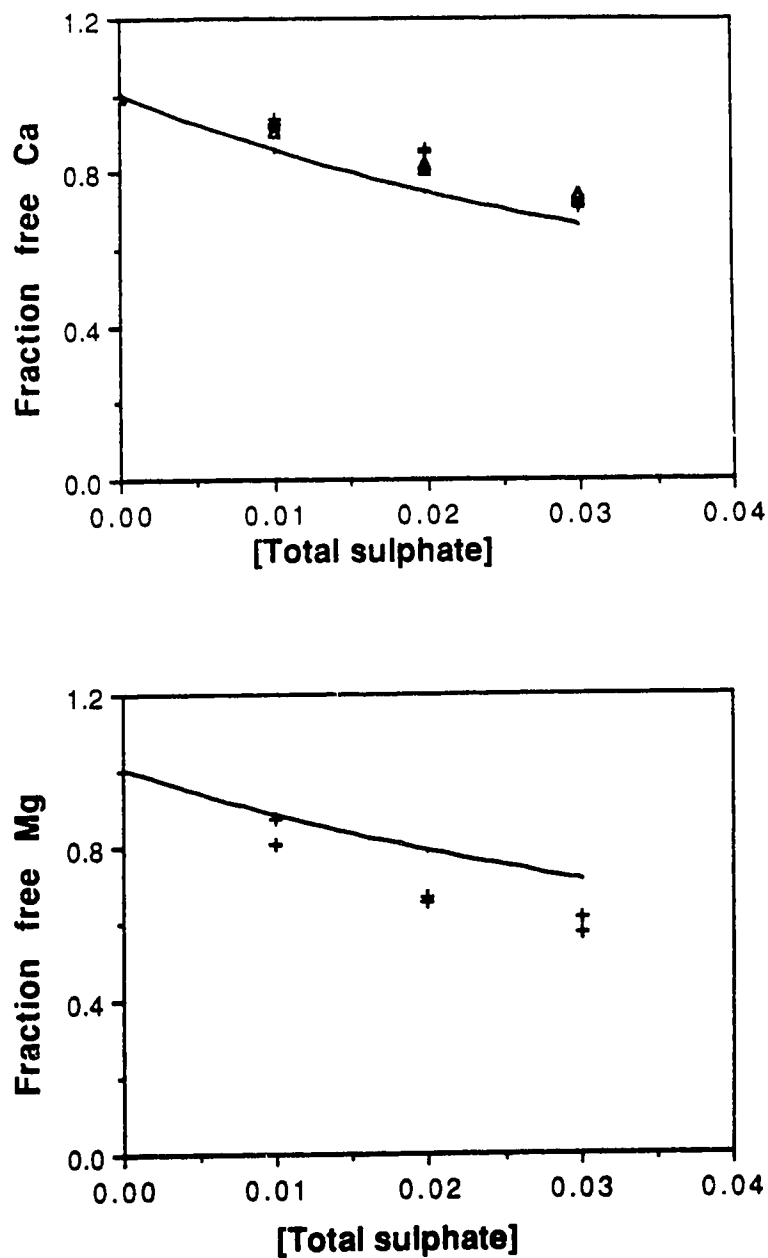


**Figure 8.9:** Variation of free  $\text{Ca}^{2+}$  (top) and free  $\text{Mg}^{2+}$  (bottom) fractions with total sulphate, at pH range 6 to 6.4 (solution set #4), as measured by; +, ion exchange and  $\Delta$ , colorimetry. Solid lines show the calculated values.

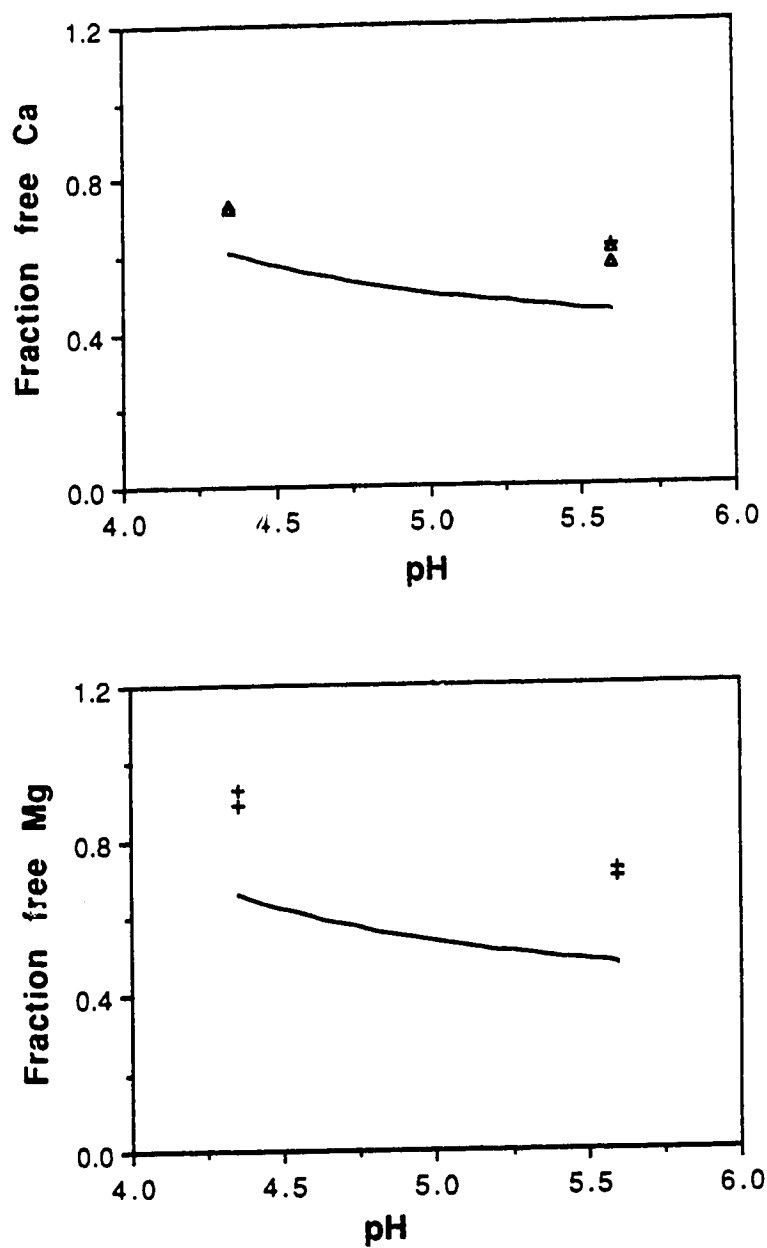


**Figure 8.10:** Variation of free  $\text{Ca}^{2+}$  and free  $\text{Mg}^{2+}$  fractions, in a solution of 3mM citrate, 0.02M phosphate and 0.02M sulphate (solution set #5), with pH as measured by; +, ion exchange and  $\Delta$ , colorimetry. solid lines show the calculated values.

$\text{Mg}^{2+}$ . In the case of  $\text{Ca}^{2+}$ , the two experimental (ion exchange and spectrophotometric) values agree very well.

Considering the large number of stability constants (33) used in these calculations, and their uncertainties, this kind of difference between experimental and calculated values is not surprising. The agreement between the values obtained with two experimental methods indicates the experimental results for free  $\text{Ca}^{2+}$  are more likely correct than the calculated values. Since similar differences between the experimental and calculated values were obtained for free  $\text{Mg}^{2+}$ , the selectivity of the method for free  $\text{Mg}^{2+}$  is likely as valid as it is for free  $\text{Ca}^{2+}$ . Thus in general, the ion exchange column equilibration method appear to show satisfactory selectivity for both free  $\text{Ca}^{2+}$  and free  $\text{Mg}^{2+}$  in a simulated urine sample.

Having determined the free  $\text{Ca}^{2+}$  and free  $\text{Mg}^{2+}$  in a simulated urine, the next step was to analyse a real sample. Since the standards used in the last set of experiments were prepared with the same  $\text{Na}^+$  and  $\text{K}^+$  concentrations as SRM 2670, the determination of free  $\text{Ca}^{2+}$  and free  $\text{Mg}^{2+}$  in SRM 2670 was carried out as described below.

The two samples of urine provided, one with normal and one with elevated levels of heavy metals, were reconstituted by the addition of 20 mL of pH 6.2 nano-pure water. The reconstituted samples had a pH of 4.5 to 4.6, and were analysed immediately after reconstitution so that refrigeration could be avoided. The determinations by ion exchange and the spectrophotometric

method were carried out the same way as for solution sets #1 to #5. A theoretical calculation of free  $\text{Ca}^{2+}$  and free  $\text{Mg}^{2+}$  concentrations was not possible because the concentrations of all ligands were not available for SRM 2670. The results obtained are given below:

1. Normal level sample:-

Fraction free  $\text{Ca}^{2+}$  by ion exchange method =  $0.49 \pm 0.03$

Fraction free  $\text{Ca}^{2+}$  by colorimetric method =  $0.69 \pm 0.04$

Fraction free  $\text{Mg}^{2+}$  by ion exchange method =  $0.49 \pm 0.02$

2. Elevated level sample:-

Fraction free  $\text{Ca}^{2+}$  by ion exchange method =  $0.44 \pm 0.01$

Fraction free  $\text{Ca}^{2+}$  by colorimetric method =  $0.71 \pm 0.04$

Fraction free  $\text{Mg}^{2+}$  by ion exchange method =  $0.44 \pm 0.01$

The ion exchange and spectrophotometric methods give different values for the free  $\text{Ca}^{2+}$  fractions. Since no alternative methods for free  $\text{Mg}^{2+}$  are available, no comparison is possible. The discrepancy between the free  $\text{Ca}^{2+}$  values appears to be due to a systematic error in one of the methods. In order to find out which method is correct, a third method for the analysis of free  $\text{Ca}^{2+}$  in SRM 2670 was sought. Ion selective electrode potentiometry is the only other method available for the determination of free  $\text{Ca}^{2+}$ . As discussed

in chapter 1, the  $\text{Ca}^{2+}$  ion selective electrode has been primarily used clinically for the determination of free  $\text{Ca}^{2+}$  in blood and is not reliable in urine. Also, according to one manufacturer, it can be affected by low pH and by the ammonia often present in urine (see chapter 1). Therefore the use of this technique as a third method was not possible.

Several possible reasons for the difference observed between the free  $\text{Ca}^{2+}$  values measured using the ion exchange and spectrophotometric methods were investigated. These are discussed below.

1. Interference by other metal ions in SRM 2670

From table 8.1, SRM 2670 contains a number of metal ions which are capable of interfering with the free  $\text{Ca}^{2+}$  signal. If the ion exchange and spectrophotometric methods are affected by these metals, especially if in opposite ways, measured free  $\text{Ca}^{2+}$  values could show a large discrepancy. Interference studies on some of these metals have been reported for the spectrophotometric method with TMMA<sup>74</sup>. It was found that  $\text{Al}^{3+}$  and  $\text{Hg}^{2+}$  do not interfere, while  $\text{Cd}^{2+}$ ,  $\text{Cu}^{2+}$ ,  $\text{Mn}^{2+}$  and  $\text{Ni}^{2+}$  can interfere but the degree of interference is low. On the other hand, any metal ion can interfere in the ion exchange method if its concentration and its affinity for the resin are both sufficiently high. However, as shown in table 8.1, the concentrations of most metals in SRM 2670 are so low that a serious interference would not be expected with either method. If a serious interference were to occur due to these metals, the free  $\text{Ca}^{2+}$  values measured for the normal level sample should

be different from the free  $\text{Ca}^{2+}$  values measured for the elevated level sample. Considering the differences in concentration of other heavy metals, the two measurements of free  $\text{Ca}^{2+}$  show very little difference. While the ion exchange and spectrophotometric methods indeed show opposite deviations in going from the normal to the elevated sample, the differences are not large. This means that the interference of other metals, even if present, is not likely to be the major cause of the difference in free  $\text{Ca}^{2+}$  values obtained with the two methods.

## 2. Improper matching of electrolytes in the sample and the standards

The concentration of  $\text{K}^+$  reported for SRM 2670 (table 8.1) is not a certified value. Since this value was used in the preparation of the standards, the standards may not have been matched with the samples in terms of  $\text{K}^+$ . Also, if any significant concentration of  $\text{NH}_4^+$  ions are present in the sample, their effect would not be accounted for. These deviations if present also mean that the standards and the samples would not be matched in terms of ionic strength. If the dependence of the free  $\text{Ca}^{2+}$  signal on ionic strength shows opposite trends with the two methods, inadequate matching of ionic strength could cause a difference in the measured free  $\text{Ca}^{2+}$  values. As shown in chapter 6, free  $\text{Ca}^{2+}$  signals obtained by the ion exchange method decrease with increasing ionic strength. In order to investigate the dependence of the colorimetric method on ionic strength, the following experiment was carried out.



Varying amounts of  $\text{KNO}_3$  were added to a 100 ppm  $\text{Ca}^{2+}$  solution and the colorimetric signal was measured using TMMA as in the earlier experiments.  $\text{KNO}_3$  was used to vary the ionic strength to avoid interference by  $\text{Na}^+$  with the colorimetric free  $\text{Ca}^{2+}$  signal. The results are shown in figure 8.11. In order to estimate the effect on measured concentrations of free  $\text{Ca}^{2+}$ , a calibration curve was prepared using 0.15M  $\text{KNO}_3$  as the electrolyte (i.e. using the average ionic strength of solutions in figure 8.11), and from this calibration curve the  $\text{Ca}^{2+}$  concentrations that correspond to each of the peak areas in figure 8.11 were estimated. Then these  $\text{Ca}^{2+}$  concentrations were plotted against the concentration of  $\text{K}^+$  or the ionic strength as shown in figure 8.12. The results shows that the measured free  $\text{Ca}^{2+}$  value is strongly dependent upon solution ionic strength. Therefore even with the colorimetric method, a single set of standards which contains average concentrations of electrolytes cannot be used for the determination of free  $\text{Ca}^{2+}$  in urine samples. The error in the measured free  $\text{Ca}^{2+}$  can be as high as 20% for a 0.1 difference in ionic strength between the sample and the standards.

Figures 8.11 and 8.12 show that the variation in the free  $\text{Ca}^{2+}$  signal with ionic strength in the spectrophotometric method is in the same direction as with the ion exchange method; both show a negative dependence. Therefore, if the sample and the standards are not matched in terms of ionic strength, the free  $\text{Ca}^{2+}$  concentration measured by either method will deviate from the actual concentration, and in the same direction. The discrepancy in free  $\text{Ca}^{2+}$

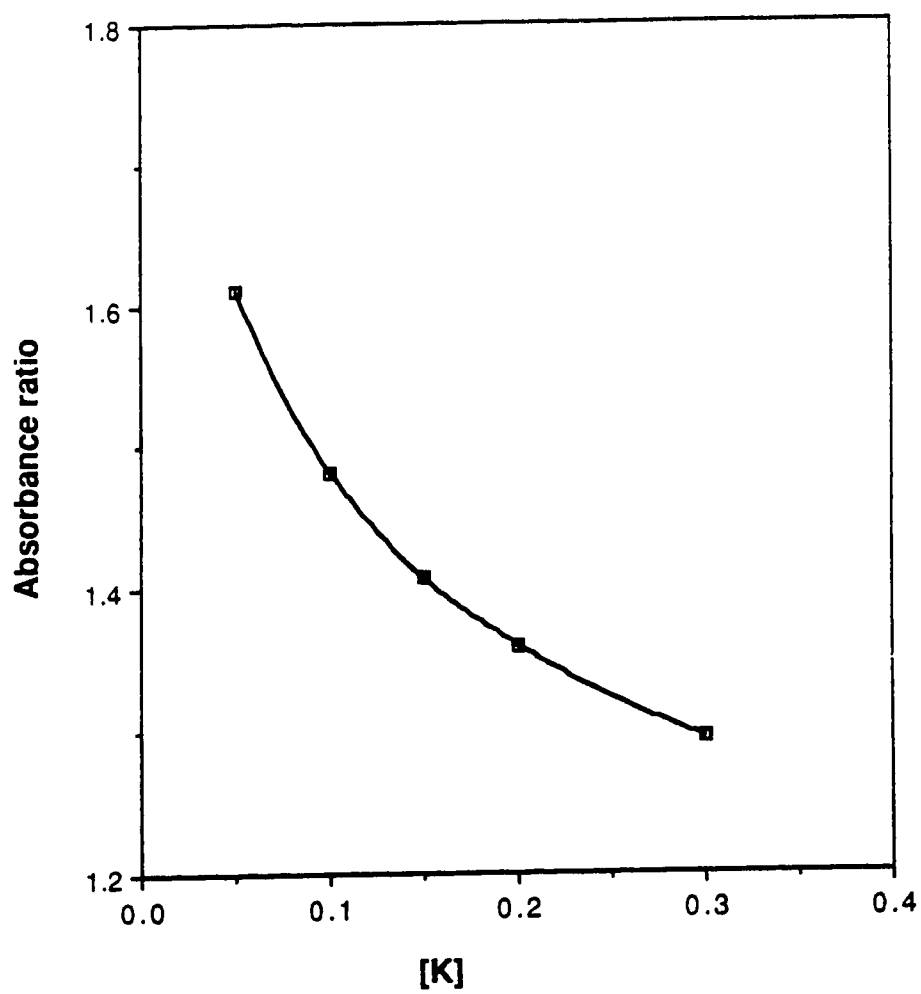


**Figure 8.11:** Variation of absorbance ratio (480 nm/550 nm) for 100 ppm Ca<sup>2+</sup> as a function of KNO<sub>3</sub> concentration.

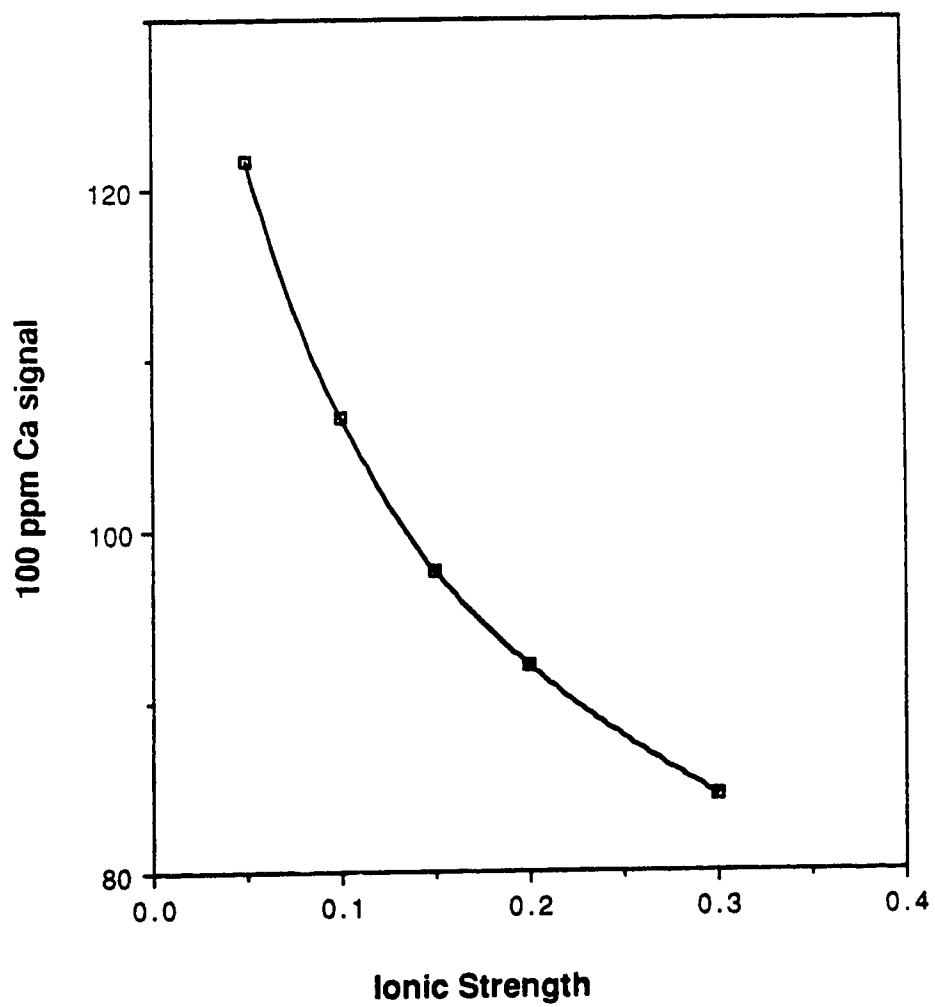


**Figure 8.12:** Estimated variation of spectrophotometrically determined free  $\text{Ca}^{2+}$  signal for a 100 ppm  $\text{Ca}^{2+}$  solution as a function of the ionic strength.

concentrations measured by the two methods due to mismatched ionic strength therefore is not likely to be very large.

### 3. Interference from organic substances

Urine contains high concentrations of urea, as well as a large number of other organic compounds at lower concentrations. The ion exchange studies done previously have shown that measurements of free  $\text{Ca}^{2+}$  are not affected by the presence of urea at concentrations similar to that in urine<sup>128</sup>. Studies of possible interference by urea with the spectrophotometric method with TMMA have not been reported. Also, as mentioned in chapter 1, since proteins interfere with the spectrophotometric method it has not been used for the analysis of free  $\text{Ca}^{2+}$  in blood. There is a possibility of interference from urea on the spectrophotometric method. The concentration of urea is not available for SRM 2670, so that comparison of the measured free  $\text{Ca}^{2+}$  values by the two methods cannot be done in terms of interference from urea.

### 4. Interference from background absorbance of urine with the spectrophotometric method

As shown earlier, measured free  $\text{Ca}^{2+}$  concentrations by the ion exchange and spectrophotometric methods showed very good agreement for all the synthetic samples studied. This was not however the case with urine. One major difference between the synthetic and real samples is the background color of urine, caused by several organic compounds that absorb at the wavelength of detection in the spectrophotometric method. The ion exchange

method is not affected by the colored organic compounds found in urine. The colorimetric method, when applied to urine, normally uses urine as a reference to compensate for the inherent sample background. However, in general colorimetric methods are not recommended for samples that absorb to a significant extent at the wavelength of analytical interest. This is in fact the case for the spectrophotometric method for determination of free  $\text{Ca}^{2+}$  in urine. A comparison of free  $\text{Ca}^{2+}$  concentrations measured by the spectrophotometric method using TMMA with other methods is not available except for the multiple equilibrium calculation method described in chapter 1. The method involves measurement of all the major metals and ligands, followed by the calculation of free  $\text{Ca}^{2+}$  in the system considering all possible metal-ligand complexations reactions and using reported stability constants. Considering the problem of numerical accuracy associated with calculated free  $\text{Ca}^{2+}$  values as discussed for figure 8.10 above, the experimental errors associated with the measurement of the metal and ligand concentrations and the unavailability of accurate stability constants for some of the possible metal-ligand complexes, the calculation method cannot be considered highly reliable. This means that the accuracy of spectrophotometrically determined free  $\text{Ca}^{2+}$  values in urine has not been confirmed by comparison with other methods.

One spectrophotometric study with TMMA<sup>79</sup> overcame the color problem by absorbing the colored components of urine on activated carbon, Norit. In this work it was assumed that the treatment with activated charcoal does not

affect the free  $\text{Ca}^{2+}$  concentration in urine. Therefore SRM 2670 was analyzed using Norit to check whether presence of colored compounds were contributing to the observed discrepancy between free  $\text{Ca}^{2+}$  values measured by ion exchange and by spectrophotometric method with TMMA. For this purpose the following experiment was performed.

A sample of urine was treated with Norit A following the procedure of reference 79, followed by a determination of the free  $\text{Ca}^{2+}$  on the treated as well as the untreated urine by the ion exchange method. The peak area obtained for the Norit-treated sample was about 10% lower than that obtained for the untreated sample. Moreover, when the total Ca signal was measured by direct AAS, it was found to be lower for the treated sample by about 6%. This indicates that both free and total calcium concentrations are affected by the Norit treatment and that the above assumption is not valid. Therefore it was decided that it would not be possible to estimate the error contributed by the colored compounds in urine in the colorimetric method for the determination of free  $\text{Ca}^{2+}$  in urine.

##### 5. Comparison of measured with expected fractions of free $\text{Ca}^{2+}$ and $\text{Mg}^{2+}$

According to literature, about 50% of the calcium in normal urine is in the free form<sup>35,57</sup>. As mentioned earlier, since  $\text{Ca}^{2+}$  and  $\text{Mg}^{2+}$  bind to the ligands found in urine to similar degrees, the fraction of free  $\text{Mg}^{2+}$  in urine can be expected to also be about 50%. Since the urine comprising SRM 2670 was collected from normal healthy individuals, the fractions of free  $\text{Ca}^{2+}$  and free

$Mg^{2+}$  in this sample may be postulated to also be around 50%. The fraction of free  $Ca^{2+}$  measured by the ion exchange method was found to be close to 50%, as was the fraction for free  $Mg^{2+}$ . The fraction of free  $Ca^{2+}$  measured using the colorimetric method was about 20% higher than expected.

The above discussion in general supports the results obtained by the ion exchange method; however, no firm conclusions can be drawn. Further, inference as to whether free  $Ca^{2+}$  concentrations measured using the ion exchange method are more reliable than those obtained using spectrophotometric method is not possible without further studies.

#### 8.5 Determination of free $Ca^{2+}$ and free $Mg^{2+}$ at low concentrations under trace conditions

All of the studies on the determination of free  $Ca^{2+}$  and free  $Mg^{2+}$  reported thus far were carried out at millimolar concentrations with the aim of measuring the levels of these species in body fluids such as urine and blood. The method should, however, also be applicable to the determination of these ions at concentrations at least a 100 times lower, around  $10^{-5}M$ . Accordingly a study was carried out using the concentration of electrolyte of 0.1M to provide trace conditions. This work more or less resembles earlier free metal studies using the ion exchange column equilibration method to determine free  $Cu^{2+}$  and free  $Ni^{2+}$  <sup>124-127</sup>.

To increase the sensitivity of the method so as to permit the measurement of low concentrations, a relatively large amount of resin (0.7 mg) was used in the column. The loading time required to establish complete equilibration between the resin and the solution was estimated for  $\text{Ca}^{2+}$  and  $\text{Mg}^{2+}$  solutions as described below, using  $2.5 \times 10^{-5} \text{M}$   $\text{Ca}^{2+}$  or  $\text{Mg}^{2+}$  in 0.1M  $\text{KNO}_3$ .

The column was loaded with the solution for different lengths of time and the peak areas of  $\text{Ca}^{2+}$  or  $\text{Mg}^{2+}$  was measured as usual. The peak areas were plotted against loading time as shown in figure 8.13. In addition, the effluent was monitored during loading and the time required for the signal to reach a plateau (complete breakthrough) was also measured. Both experiments showed that a period of about 3 minutes was sufficient for complete equilibration. A 3-minute equilibration time for  $\text{Mg}^{2+}$  and a 5-minute equilibration time for  $\text{Ca}^{2+}$  were used in all of the following experiments.

Both  $\text{Ca}^{2+}$  and  $\text{Mg}^{2+}$  standards were prepared over the concentration range 0 to  $5 \times 10^{-5} \text{M}$  in 0.1M  $\text{KNO}_3$  as electrolyte. The pH of all standards was within the range 5.2 to 5.3. Calibration curves were constructed for each metal using these standards, as shown in figure 8.14. As expected, the calibrations are straight line plots since trace conditions are satisfied for this range of  $\text{Ca}^{2+}$  and  $\text{Mg}^{2+}$  concentrations with 0.1M  $\text{K}^+$  as the electrolyte.



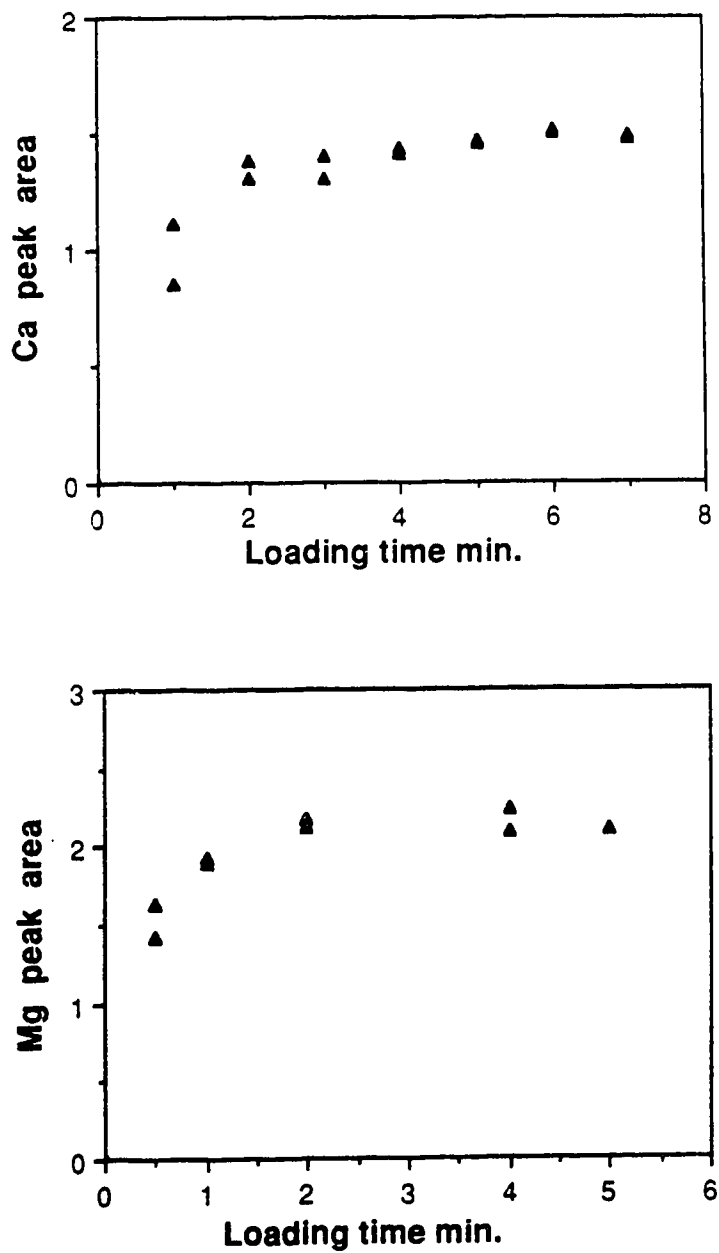


**Figure 8.13:** Loading curves for  $2.5 \times 10^{-5} \text{M}$   $\text{Ca}^{2+}$  (top) and  $\text{Mg}^{2+}$  (bottom) solutions in  $0.1 \text{M}$   $\text{KNO}_3$ .

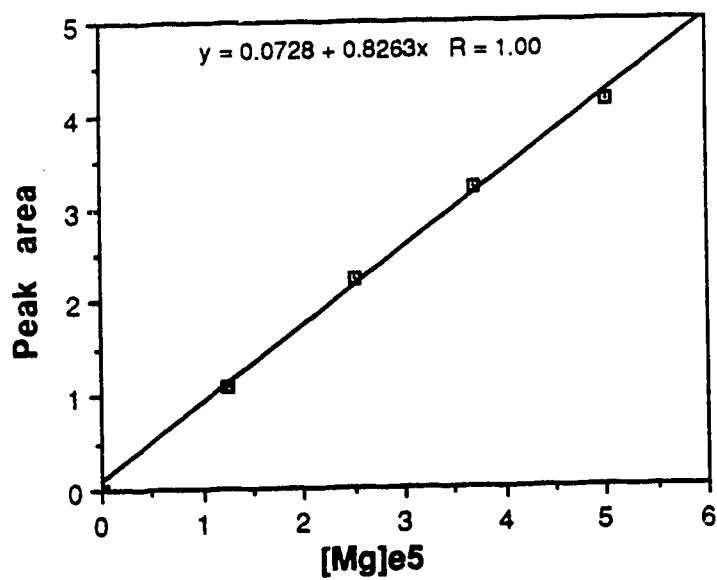
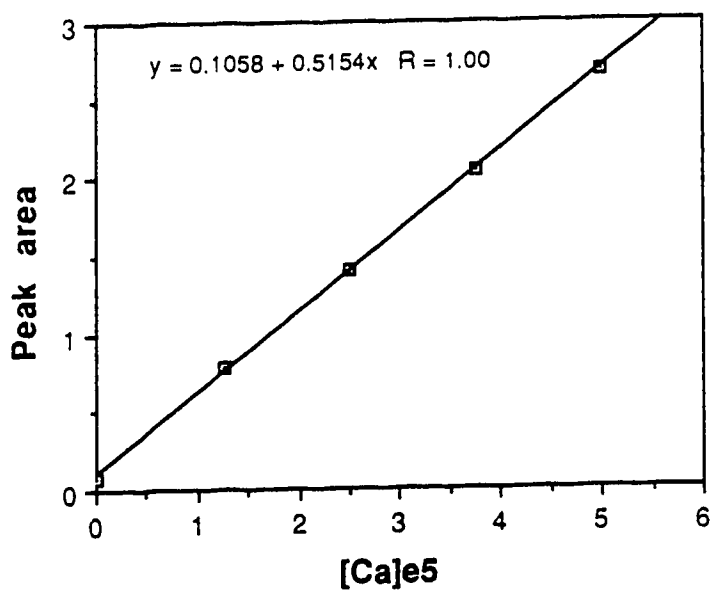


Figure 8.14: Calibration curves for standard  $\text{Ca}^{2+}$  (top) and  $\text{Mg}^{2+}$  (bottom) solutions in 0.1M  $\text{KNO}_3$ .

The selectivity of the method was evaluated in the presence of citrate and phosphate as follows. From 0 to 0.5 mM citrate was added to a solution containing a total calcium or magnesium concentration of  $5 \times 10^{-5} \text{M}$ . The pH values of these solutions were within the range of 6 to 7. Also, from 0 to 0.03M phosphate was added to solution containing a total calcium or magnesium concentration of  $5 \times 10^{-5} \text{M}$ ; the pH values of these solutions were about 7. In both cases the ligands were added as potassium salts but the total concentration of  $\text{K}^+$  in all the solutions was held at 0.1M.

Peak areas were measured and the corresponding free  $\text{Ca}^{2+}$  or free  $\text{Mg}^{2+}$  concentration in each solution was estimated using the calibration curves in figure 8.14. Predicted free  $\text{Ca}^{2+}$  and free  $\text{Mg}^{2+}$  concentrations were calculated by the COMICS program, taking into account complexes of  $\text{Ca}^{2+}$ ,  $\text{Mg}^{2+}$  and  $\text{K}^+$  with citrate and phosphate, and using stability constants from tables 8.4 and 8.5. All the stability constants used in the calculations were corrected to an ionic strength of 0.1 by the Davies equation.

An attempt was made to use the spectrophotometric method with TMMA as a second method for the determination of free  $\text{Ca}^{2+}$ , but the  $\text{Ca}^{2+}$ -TMMA signals obtained over the range of standards were similar. It was concluded that the spectrophotometric method is not sensitive enough to be useful for the low range of concentrations studied in this experiment. Therefore a neutral carrier type  $\text{Ca}^{2+}$  ion selective electrode (see chapter 5) was used to obtain a second set of free  $\text{Ca}^{2+}$  values for comparison.

The free  $\text{Ca}^{2+}$  and free  $\text{Mg}^{2+}$  values obtained by the above methods are summarized in figures 8.15 and 8.16. Agreement between the experimental and calculated values can be considered satisfactory. In view of possible experimental errors associated with preparation of solutions at low concentrations and the tightness of the concentration range used in this study, the ion exchange column equilibration method shows good selectivity and sensitivity for both free  $\text{Ca}^{2+}$  and free  $\text{Mg}^{2+}$  at the  $10^{-5}\text{M}$  level.

#### 8.6 Conclusions and suggestions for future work

The determination of only free  $\text{Ca}^{2+}$  in urine by the ion exchange column equilibration method using the procedure developed in this thesis was not possible due to the interference of  $\text{Mg}^{2+}$  at the concentrations and ionic strengths found in urine. Under these conditions, however, the ion exchange column equilibration method showed good selectivity for not only free  $\text{Ca}^{2+}$  but also for free  $\text{Mg}^{2+}$  in the presence of major urinary ligands. Therefore this method was modified for the simultaneous determination of both free  $\text{Ca}^{2+}$  and free  $\text{Mg}^{2+}$  in urine. The modified method was tested with simulated urine samples for selectivity to free  $\text{Ca}^{2+}$  and free  $\text{Mg}^{2+}$  and the results obtained were positive. However, free  $\text{Ca}^{2+}$  concentrations measured by the ion exchange method and those measured by the spectrophotometric method with TMMA did not agree when a real sample, SRM 2670, was analysed. Possible reasons for this discrepancy were discussed. Free  $\text{Mg}^{2+}$  in SRM 2670 was

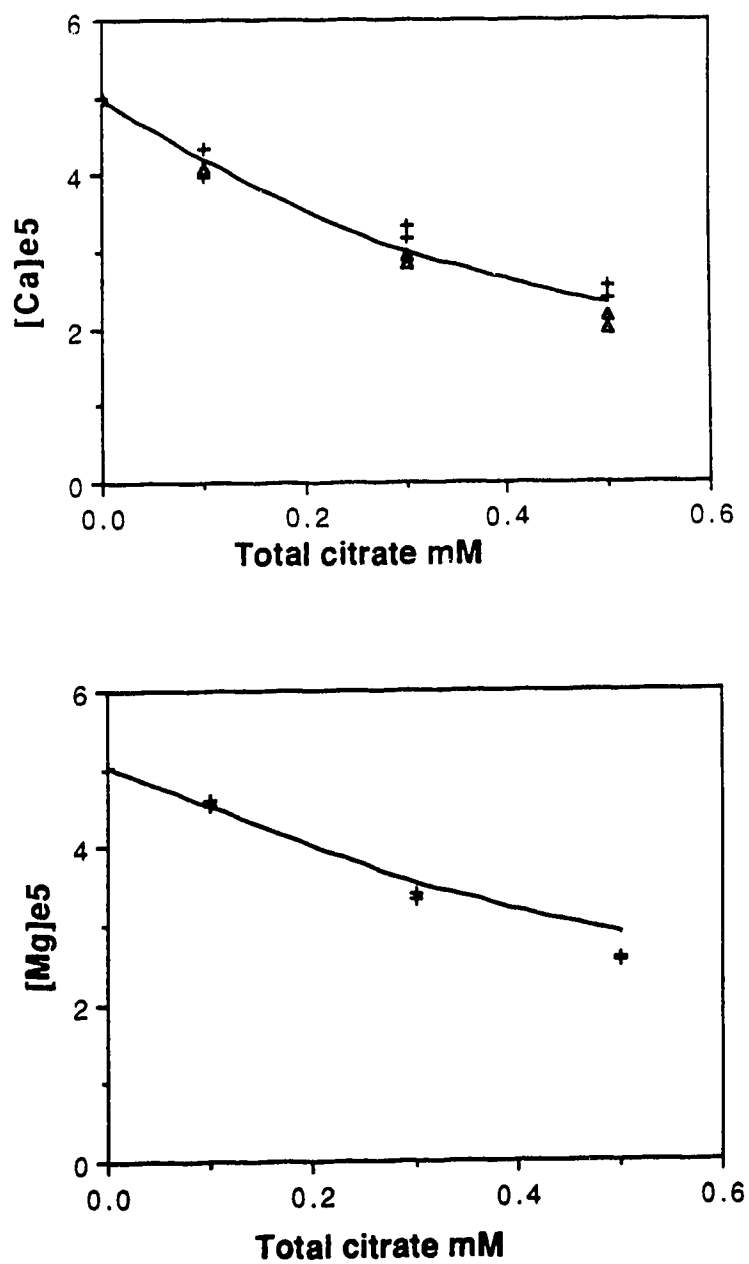


**Figure 8.15:** Variation of free  $\text{Ca}^{2+}$  (top) and free  $\text{Mg}^{2+}$  (bottom) concentrations with total citrate, at pH range 6 to 7, as measured by; +, ion exchange and  $\Delta$ , ISE potentiometry. Solid lines show the calculated values.

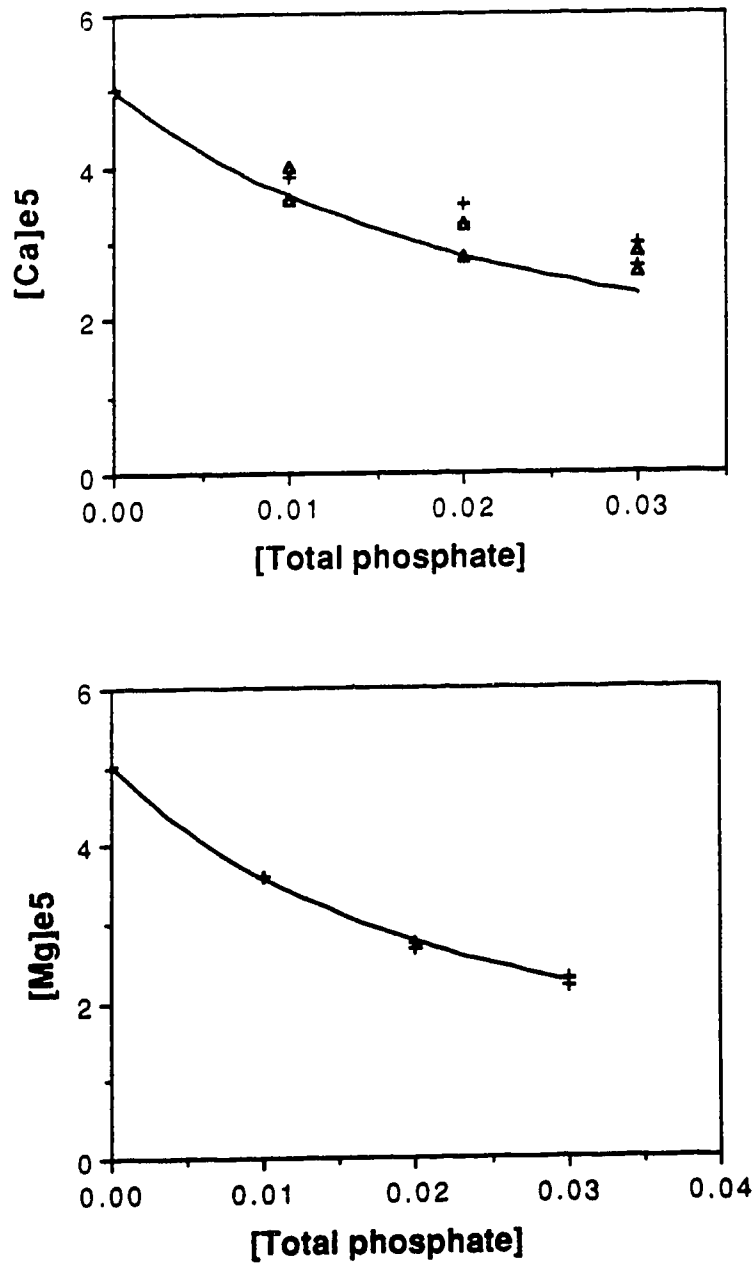


**Figure 8.16:** Variation of free  $Ca^{2+}$  (top) and free  $Mg^{2+}$  (bottom) concentrations with total phosphate at pH 7, as measured by; +, ion exchange and  $\Delta$ , ISE potentiometry. Solid lines show the calculated values.

measured only by the ion exchange method due to the lack of satisfactory alternative methods for comparison purposes.

The ion exchange method at the present stage of its development cannot be considered a candidate for routine use for the determination of free  $\text{Ca}^{2+}$  and free  $\text{Mg}^{2+}$  owing to the necessity of matching samples and standards in terms of  $\text{Na}^+$  and  $\text{K}^+$  concentrations. Since urine levels of  $\text{Na}^+$  and  $\text{K}^+$  vary from sample to sample and are not known in advance, preparation of standards prior to the analysis of samples is not possible. Also, urine samples cannot be stored for more than about 2 hours prior to analysis owing to decomposition (refrigeration causes precipitation that perturbs urinary equilibria as described in chapter 4), making the determination of free  $\text{Ca}^{2+}$  and free  $\text{Mg}^{2+}$  using standards prepared after obtaining the sample unfeasible for routine work. The other two methods for determining free  $\text{Ca}^{2+}$  described in this study, spectrophotometric method with TMMA and ion selective electrode potentiometry, are also subject to this limitation because of sample to sample variations in composition that are associated with urine. As described in chapter 1, the spectrophotometric method has been extensively studied for more than a decade in effort to overcome this problem by estimation of the effects of  $\text{Na}^+$  and  $\text{K}^+$ . And in spite of the tremendous amount of research done to date on  $\text{Ca}^{2+}$  ion selective electrodes, so far an electrode has not been developed that is accepted for the determination of free  $\text{Ca}^{2+}$  in urine.

Therefore, further studies of the ion exchange method described here are required in which the effects of  $\text{Na}^+$  and  $\text{K}^+$  on the  $\text{Ca}^{2+}$  and  $\text{Mg}^{2+}$  peak areas are quantified. In this way an estimate of the effects of the  $\text{Na}^+/\text{K}^+$  levels in the sample on the free  $\text{Ca}^{2+}$  and free  $\text{Mg}^{2+}$  signals can be made so that a single set of standards can be used for the routine analysis of these species in urine. Some preliminary studies on this idea were carried out during the course of the present study, as discussed in chapter 7.

Until such studies as described above are done, the ion exchange method at the present stage can only be used for samples like SRM 2670 whose  $\text{Na}^+$  and  $\text{K}^+$  levels are known in advance of reconstituting the sample. It may be possible to apply the method in its present form for the determination of free  $\text{Ca}^{2+}$  and free  $\text{Mg}^{2+}$  in blood or serum. Since sample to sample variation of  $\text{Na}^+$  and  $\text{K}^+$  concentrations is very small in these materials, a single set of standards could likely be prepared ahead of time. The selectivity of the method for free  $\text{Ca}^{2+}$  and free  $\text{Mg}^{2+}$  in the presence of proteins is yet to be determined, but theoretically the ion exchange method should not be affected by protein bound metals or by proteins at biological pH values. In general, the ion exchange column equilibration method shows promise for the determination of free  $\text{Ca}^{2+}$  and free  $\text{Mg}^{2+}$  in urine and possibly blood and serum.

As described in chapter 1, there are no methods available to date for the determination of free  $\text{Mg}^{2+}$  in any of the above biological fluids. The



colorimetric methods are limited to very narrow pH ranges and are affected by proteins, while the  $\text{Mg}^{2+}$  ion selective electrode suffers interference from  $\text{Ca}^{2+}$ . Although the ion exchange method also cannot discriminate between  $\text{Ca}^{2+}$  and  $\text{Mg}^{2+}$ , the additional selectivity supplied by the atomic absorption measurement makes it possible to obtain the contributions from each metal separately. The ability to determine sorbed  $\text{Ca}^{2+}$  and  $\text{Mg}^{2+}$  independently of each other makes the ion exchange column equilibration method very promising for the measurement of free  $\text{Ca}^{2+}$  and free  $\text{Mg}^{2+}$  in body fluids, where the two metals are often present in similar amounts.

The determination of low levels of free  $\text{Ca}^{2+}$  and free  $\text{Mg}^{2+}$  under trace conditions gave satisfactory results in terms of both sensitivity and selectivity. The spectrophotometric method for calcium with TMMA was not sensitive enough at these levels to be used for comparison purposes.

In general, the ion exchange column equilibration method, as modified during the course of this study, can be used to selectively determine free  $\text{Ca}^{2+}$  and free  $\text{Mg}^{2+}$  at millimolar to micromolar levels. When both metals occur in the same solution, the concentration of each can be determined without interference from the other. Unlike colorimetric methods, the ion exchange method can be used to analyse colored solutions.

The same instrumentation and procedure should be applicable to a wider variety of metals than ion selective electrode potentiometry, where for each metal a separate electrode is required. Such electrodes are not yet

available for many metals. The sensitivity of the ion exchange column equilibration method can be varied by changing the amount of resin in the column, by changing the resin itself, or by changing the means of detection. Therefore the ion exchange method allows tremendous flexibility. Moreover, the free metal probe in the ion exchange method, i.e. the column of resin, is very simple and inexpensive compared to probes such as ion selective electrodes. Also, compared to potentiometric and spectrophotometric methods, the ion exchange method is less prone to interferences from organic matter in complex matrices, and can be adapted to a number of metals for which ion selective electrodes or color forming chelates are not available. Additionally, as mentioned above, by changing the weight of resin in the column it is possible to analyse samples for very low levels of free metal ions.

**BIBLIOGRAPHY**

1. W. G. Sunda, D. W. Engel and R. M. Thuotte, *Environ. Sci. Tech.*, 12(4), 409 (1978).
2. W. G. Sunda and R. L. Guillard, *J. Mar. Res.*, 34, 511 (1976)
3. N. G. Zorkin, E. V. Grill and A. G. Lewis. *Anal. Chim. Acta*, 183, 163 (1986)
4. R. D. Guy and A. R. Kean, *Water Res.*, 14, 891 (1980)
5. H. E. Allen, R. H. Hall and T. D. Brisbin, *Environ. Sci. Tech.*, 14, 441 (1980)
6. P. T. S. Wong, Y. K. Chan and P. L. Luxon, *J. Fish. Res. Board Can.*, 35, 479 (1978)
7. R. Gachter, J. S. Davies and A. Nares, *Environ. Sci. Tech.*, 12, 1416 (1978)
8. R. W. Andrew, K. F. Biessinger and G. E. Glass, *Water Res.*, 11, 309 (1977)
9. V. M. Brown, T. L. Shaw and D. G. Shurben, *Water Res.*, 8, 797 (1974)
10. F. C. McLean and A. B. Hastings, *J. Biol. Chem.*, 107, 337 (1934)
11. F. C. McLean and A. B. Hastings, *J. Biol. Chem.*, 108, 285 (1935)
12. D. H. Copp, *J. Endocrinol.*, 43, 137 (1969)
13. H. Sigel, Ed., "Metal Ions in Biological Systems" Volume 17, Marcel Dekker, New York, 1984

14. B. E. C. Nordin, Ed., "Calcium, Phosphate and Magnesium Metabolism: Clinical Physiology and Diagnostic Procedures", Churchill Livingstone, Edinburgh, 1976
15. R. H. Wasserman, R. A. Corradina, E. Carafoli, R. H. Kretsinger, D. H. MacLennan and F. L. Siegel, Eds., "Calcium Binding Proteins and Calcium Functions", Elsevier North-Holland, New York, 1977.
16. E. Carafoli, F. Clementi, W. Drabikowski and A. Margeth, Eds., "Calcium Transport in Contraction and Secretion", North-Holland/ American Elsevier, Amsterdam, 1975
17. S. T. Ohnishi and M. Endo, Eds., "The Mechanism of Gated Calcium Transport Across Biological Membranes", Academic Press, New York, 1981
18. J. A. Lott, *CRC Crit. Rev. Anal. Chem.*, 3, 41 (1972)
19. C. O. Brostrom, F. L. Hankeler and E. G. Krebs, *J. Biol. Chem.*, 246, 1961 (1971)
20. R. Eckert and D. Tillotson, *Science*, 200, 437 (1978)
21. W. H. Seegers, L. McCoy, E. Marciniak, *Clin. Chem.*, 14, 97 (1968)
22. M. J. Geisow, *Nature*, 276, 211 (1978)
23. J. H. Ladenson, J. M. McDonald, J. Aguanno and M. Goren, *Clin. Chem.*, 25, 1821 (1979)
24. B. W. Renoe, J. M. McDonald and J. H. Ladenson, *Clin. Chem.*, 25, 1766 (1979)

25. B. W. Renoe, J. M. McDonald and J. H. Ladenson, *Clin. Chim. Acta*, 103, 91 (1980)
26. A. Hodgkinson and B. E. C. Nordin, Eds., "Proceedings of the Renal Stone Research Symposium", Churchill, London, 1968
27. G. N. Bowers, Jr., C. Brassard and S. F. Sena, *Clin. Chem.*, 32(8), 1437 (1986)
28. P. Urban, G. Buchmann and D. Scheidegger, *Clin. Chem.* 31, 264 (1985)
29. W. G. Robertson, B. E. C. Nordin, "Proceedings of the Renal Stone Symposium: A. Hodgkinson and B. E. C. Nordin Eds., Churchill, London, 1969.
30. K. O. Pedersen, *Scand. J. Clin. Lab. Invest.*, 30, 321 (1972)
31. R. W. Marshall, M. Cochran, W. G. Robertson, A. Hodgkinson and B. E. C. Nordin, *Clin. Sci.*, 43, 433 (1972)
32. T. A. Borden and E. S. Lyon, *Invest. Urol.*, 6, 412 (1969)
33. S. S. Gaur and G. H. Nancollas, *Kidney Int.*, 26, 767 (1984)
34. H. Ladenson, G. N. Bowers, *Clin. Chem.*, 19, 575 (1973)
35. W. G. Robertson and R. W. Marshall, *CRC Crit. Rev. Clin. Lab. Sci.*, 15, 85 (1981)
36. L. C. Herrig, *J. Urol.*, 88, 549 (1962)
37. M. Rubin and A. E. Martell, Chapter 4 in H. Sigel, Ed., "Metal Ions In Biological Systems", Vol. 16, Marcel Dekker, New York, 1983
38. Hans-Goran Tiselius, *Eur. Urol.*, 10, 191 (1984)

39. W. G. Robertson, *Clin. Chim. Acta*, 24, 149 (1969)
40. B. Finlayson and G. H. Miller, *Invest. Urol.*, 6, 428, (1969)
41. C. Y. C. Pak., *J. Clin. Invest.*, 48, 1914 (1969)
42. I. M. Barlow, S. P. Harrison and G. L. Hogg, *Clin. Chem.*, 34, 2340 (1988)
43. J. M. Baker, C. W. Gehrke and H. E. Affsprung, *J. Dairy Sci.*, 37 , 1409 (1954)
44. G. Christianson, R. Jenness and S. T. Coulter, *Anal. Chem.*, 26, 1923 (1954)
45. P. J. Muldoon and B. J. Liska, *J. Dairy Sci.*, 52, 460 (1969)
46. J. W. Ross, *Science*, 156, 1378 (1967)
47. J. R. Selwyn, J. Barkeley and H. F. Loken, *Clin. Chem.*, 30, 304 (1984)
48. H. Husdan, M. Leung, D. Oreopoulos and A. Ropoport, *Clin. Chem.*, 23, 1775 (1977)
49. S. E. Ryden, L. S. Kirkish and D. S. McCann, *Am. J. Clin. Path.*, 66, 634 (1976)
50. R. S. Hattner, J. W. Johnson, D.S. Bernstein, A. Wachman and J. Brackman, *Clin. Chim. Acta*, 28, 67 (1970)
51. H. Ladenson, G. N. Bowers, *Clin. Chem.*, 19, 565 (1973)
52. J. Thode, S. N. Holmegaard, J. Transbol, N. F. Anderson and O. S. Anderson, *Clin. Chem.*, 36, 541 (1990)
53. A. C. Hansen, K. Engel, P. Kildeberg and S. Wamberg, *Clin. Chim. Acta*, 79, 507 (1977)

54. J. Wandrup and J. Kvetny, *Clin. Chem.*, 31, 856 (1985)
55. R. Freaney, T. Egan, M. J. McKenna, M. C. Doolin and F. P. Muldowney, *Clin. Chim. Acta*, 158, 129 (1986)
56. N. E. L. Saris, *J. Clin. Chem. Clin. Biochem.*, 26, 101 (1988)
57. A. L. Jacobson, P. C. Singhal, H. Mandin and J. B. Hyne, *Biochem. Med.*, 22, 383 (1979)
58. A. L. Jacobson, P. C. Singhal, H. Mandin and J. B. Hyne, *Invest. Urol.*, 17, 218 (1979)
59. A. L. Jacobson, P. C. Singhal, H. Mandin and J. B. Hyne, *Clin. Biochem.*, 16, 79 (1983)
60. B. Finlayson, R. Roth and L. Dubois, *Invest. Urol.*, 10, 138 (1972)
61. S. F. Sena and G. N. Bowers, Jr., *Methods. Enzymol.*, 158, 320 (1988)
62. J. Thode, *Scand. J. Clin. Lab. Invest.*, 45, 327 (1985)
63. H. Yatzidis, *Clin. Nephrol.*, 23, 63 (1985)
64. W. B. Gratzler and G. H. Beaven, *Anal. Biochem.* 81, 118 (1977)
65. U. Pande and H. C. Pant, *Anal. Letters*, 18, 1289 (1985)
66. N. C. Kendrick, *Anal. Biochem.*, 76, 487 (1976)
67. K. T. Izutsu, S. P. Felton, I. A. Sigel, J. I. Nicholls, J. Crawford, J. McGough, W. T. Yoda, *Anal. Biochem.*, 58, 479 (1974)
68. O. Shimonura, F. H. Johnson and Y. Saiga, *Science*, 140, 1339 (1963)
69. J. R. Blinks, F. G. Prendergast and D. G. Allen, *Pharmacol. Rev.*, 28, 1 (1976)

70. K. T. Izutsu, S. P. Felton, *Clin. Chem.*, 18, 77 (1972)
71. J. Raaflaub, *Z. Physiol. Chem.*, 288, 228 (1951)
72. J. Ettore and S. M. Scoggan, *Arch. Biochem. Biophys.*, 78, 213 (1958)
73. B. E. C. Nordin, *The Lancet*, 1, 409 (1962)
74. K. O. Pedersen, *Scand. J. Clin. Lab. Invest.*, 25, 199 (1970)
75. J. Raaflaub, *Z. Physiol. Chem.*, 328, 198 (1962)
76. W. G. Robertson, M. Peacock and B. E. C. Nordin, *Clin. Sci.*, 34, 579 (1968)
77. B. E. C. Nordin and D. A. Smith, "Diagnostic Procedures in Disorders of Calcium Metabolism", p. 183, Churchill, London, 1965
78. L. D. Hunt and J. S. King Jr., *Invest. Urol.*, 1, 83 (1963)
79. B. E. Cham, *Clin. Chim. Acta*, 37, 5 (1972)
80. G. A. Rose, *Clin. Chim. Acta*, 37, 343 (1972)
81. W. G. Robertson, *Ann. Clin. Biochem.*, 13, 540 (1976)
82. T. J. French, B. E. Cham and R. B. Cross, *Lab Practice*, 21, 333 (1972)
83. S. T. Ohnishi, *Anal. Biochem.*, 85, 165 (1978)
84. C. E. Leme, R. Coslovsky and B. L. Wajchenberg, *Biomed.*, 19, 431 (1973)
85. J. K. Aikawa, "CRC Magnesium: Its Biological Significance", Chapter 14, CRC Press, BocaRaton, Florida, 1981
86. M. J. Halspern and J. Durlack, Eds., "Magnesium Deficiency: Physiopathology and Treatment Implications", Karger, New York, 1985



87. W. E. C. Wacker, "Magnesium and Man", Harvard University Press, Massachusetts, 1980
88. R. D. Berlin, *Anal. Biochem.*, 14, 135 (1966)
89. F. W. Heaton, *Clin. Chim. Acta*, 15, 139 (1967)
90. M. Rouilly, B. Rusterholz, U. E. Spichiger and W. Simon, *Clin. Chem.*, 36(3), 466 (1990)
91. M. Otto and J. D. R. Thomas, *Anal. Proc.(London)*, 21(10), 369 (1984)
92. J. S. Desmars and R. Tawashi, *Biochim. Biophys. Acta*, 313, 256 (1973)
93. P. O. Schwille, I. Schlenk, N. M. Samberger and C. Bornhof, *Urol. Res.*, 4, 33 (1976)
94. H-G. Tiselius, L. E. Almgard, L. Larsson and B. Sorbo, *Eur. Urol.*, 4, 241 (1978)
95. E. Takasaki, *Invest. Urol.*, 10, 147 (1972)
96. T. A. Borden and E. S. Lyon, *Invest. Urol.*, 6, 412 (1969)
97. M. S. Seelig, "Magnesium Deficiency in the Pathogenesis of Disease", Chapter 13, Plenum Press, New York, 1980
98. A. Jensen and E. Riber, "Metal Ions in Biological Systems", Volume 16, Chapter 8, Marcel Dekker, New York, 1983
99. R. P. Buck, J. C. Thompsen and O. R. Melroy, "Ion Selective Electrodes in Analytical Chemistry", H. Freiser Ed., Volume 2, Plenum Press, New York, 1980

100. F. Behm, D. Ammann, W. Simon, K. Brunfeldt and J. Halstrom, *Helv. Chim. Acta*, 68, 110 (1985)
101. M. V. Rouilly, M. Baldertscher, E. Pretsch, G. Suter and W. Simon, *Anal. Chem.*, 60, 2013 (1988)
102. M. Muller, M. Rouilly, B. Rusterholz, M. Maj-Zurawska, Z. Hu and W. Simon, *Mikrochim. Acta*, 111, 283 (1988)
103. A. C. H. Durham and J. M. Walton, *Cell Calcium*, 4, 47 (1983)
104. E. P. Diamadis and B. R. Hoffman, *Clin. Chem.*, 30, 1262 (1984)
105. M. Walser, *Anal. Chem.*, 32, 711 (1960)
106. A. Scarpa, *Biochem.*, 13, 2789 (1974)
107. D. G. McMinn and B. Kratochvil, *Can. J. Chem.*, 55, 3909 (1977)
108. L. A. Jelicks, J. Weaver, S. Pollack and R. K. Gupta, *Biochim. Biophys. Acta*, 1012, 261 (1989)
109. E. Murphy, C. Steenbergen, L. A. Levy and B. Raju, *J. Biol. Chem.*, 264, 5622 (1989)
110. K. J. Brooks and H. S. Bachelard, *J. Neurochem.*, 53, 331 (1989)
111. G. A. Smith, R. J. Hesketh, J. C. Metcalfe, J. O. Freeney and P. G. Morris, *Proc. Natl. Acad. Sci. U.S.A.*, 80, 7178 (1983)
112. L. A. Levy, E. Murphy, B. Raju and R. E. London, *Biochem.*, 27, 4041 (1988)
113. B. Raju, E. Murphy, L. A. Levy, R. D. Hall and R. E. London, *Am. J. Physiol.*, 256, C540 (1989)

114. E. Murphy, C. C. Freudenrich, L. A. Levy, R. E. London and M. Lieberman, Proc. Natl. Acad. Sci. U.S.A., 86, 2981 (1989)
115. A. H. Harman, A. L. Nieminen, J. J. Lemasters and B. Herman, Biochim. Biophys. Res. Commun., 170, 477 (1990)
116. G. A. Quamme and S. W. Rabkin, Biochim. Biophys. Res. Commun., 167, 1406 (1990)
117. M. S. Seelig, "Magnesium Deficiency in the Pathogenesis of Disease", Chapter 4, Plenum Press, New York, 1980
118. O. D. Bonner and V. Rhett, J. Phys. Chem., 57, 254 (1953)
119. O.D. Bonner and L. Livingston, J. Phys. Chem., 60, 530 (1956)
120. O. D. Bonner and L. L. Smith, J. Phys. Chem., 61, 326 (1957)
121. H. P. Gregor and J. I. Bregman, J. Colloid Sci., 6, 323 (1951)
122. O. D. Bonner and J. R. Overton, J. Phys. Chem., 65, 1599 (1961)
123. H. F. Walton, D. E. Jordan, S.R. Samedy and W. N. McKay, 65, 1478 (1961)
124. J. Treit, J. S. Nielsen, B. Kratochvil and F. F. Cantwell, Anal. Chem., 55, 1650 (1983)
125. F. F. Cantwell, J. S. Nielsen and S. E. Hruday, Anal. Chem., 54, 1498 (1982)
126. J. A. Sweileh, D. Lucyk, B. Kratochvil and F. F. Cantwell, Anal. Chem., 59, 586 (1987)
127. J. A. Sweileh, Ph. D. Thesis, Department of Chemistry, University of Alberta, Edmonton, Alberta, Canada, 1986.

128. V. P. Mutucumarana, M. Sc. Thesis, Department of Chemistry, University of Alberta, Edmonton, Alberta, Canada, 1988.
129. I. Tabani and B. Kratochvil, *Anal. Instrum.*, 14, 169 (1985)
130. F. Helfferich, "Ion Exchange" McGraw Hill, New York, 1962, Chapter 5
131. W. E. Harris and H. A. Laitinen, "Chemical Analysis" 2<sup>nd</sup> ed, McGraw - Hill, Toronto, 1975.
132. A. Ringbom, "Complexation in Analytical Chemistry", Interscience, New York, 1963
133. W. E. Harris and B. Kratochvil, "An Introduction to Chemical Analysis", Saunders College Publishing, Philadelphia, 1981
134. D. D. Perrin and I. G. Sayce, *Talanta*, 14, 833 (1967)
135. C. W. Davies, "Ion Association", Butterworth and Co., Toronto, Canada, 1962
136. A. E. Martell, R. M. Smith "Critical Stability Constants" vol.3: "Other Organic Ligands" Plenum Press, New York, 1977
137. A. E. Martell, R. M. Smith "Critical Stability Constants" vol.4: "Inorganic Complexes" Plenum Press, New York, 1976
138. P. Debye and E. Hückel, *Physik. Z.*, 24, 185 (1923)
139. E. Hückel, *Physik. Z.*, 26, 93 (1925)
140. R. H. Stokes and R. A. Robinson, *J. Am. Chem. Soc.*, 70, 1870 (1948)
141. J. Kielland, *J. Am. Chem. Soc.*, 59, 1675 (1937)
142. C. W. Davies, *J. Chem. Soc.*, 2093 (1938)

143. M. Walser, *J. Phys. Chem.*, 65, 159 (1961)
144. G. A. Rechnitz and S. B. Zamochnick, *Talanta*, 11, 1061 (1964)
145. V. Cucinotta, P. G. Daniele, C. Rigano and S. Sammartano, *Inorg. Chim. Acta*, 56, L45 (1981)
146. P. G. Daniele, C. Rigano and S. Sammartano, *Talanta*, 30, 81 (1983)
147. P. G. Daniele, M. Grasso, C. Rigano and S. Sammartano, *Annali Di Chim.*, 73, 495 (1983)
148. F. N. Ponnampereuma, E. M. Tianco and T. A. Loy, *Soil. Sci.*, 102, 408 (1966)
149. R. A. Griffin and J. J. Jurinak, *Soil. Sci.*, 116, 26 (1973)
150. L. C. Isaacson, *Invest. Urol.*, 5, 406 (1968)
151. A. E. Martell, R. M. Smith "Critical Stability Constants" vol.2: "Amines" Plenum Press, New York, 1975
152. Adrien Albert and E. P. Serjeant, "The Determination of Ionization Constants", T. A. Constable Ltd., Edinburgh, Great Britain, 1971
153. H. S. Dunsmore and D. Midgley, *J. Chem Soc. (A)*, 3238 (1971)
154. T. R. E. Kressman and J. A. Kitchener, *J. Chem. Soc.*, 1208 (1949)
155. R. S. Boikess and E. Edelson, "Chemical Principles", 3<sup>rd</sup> Edition, Harper and Row Publishers, New York, 1985, p.331
156. A. Schwarz and G. E. Boyd, *J. Phys. Chem.*, 69, 4268 (1965)
157. J. A. Marinsky and Y. Marcus Eds, "Ion Exchange and Solvent Extraction" vol. 9, Marcel Dekker, New York, 1985, Chapter 4

158. D. Reichenberg, K. W. Pepper and D. J. McCauley, *J. Chem. Soc.*, 493 (1951)
159. G. E. Boyd and Q. V. Larson, *J. Am. Chem. Soc.*, 89:24, 6038 (1967)
160. J. A. Marinsky and Y. Marcus Eds, "Ion Exchange and Solvent Extraction" vol. 7, Marcel Dekker, New York, 1977, Chapter 7
161. G. E. Boyd, *J. Phys. Chem.*, 78, 735 (1974)
162. G. Wiegner, *J. Soc. Chem. Ind.*, 50, 65T (1931)
163. B. L. Karger, L. R. Snyder and C. Horvath, "An Introduction to Separation Science", Wiley, New York, 1973, pp 55-57, 276
164. I. M. Kolthoff and P. J. Elving, Eds., "Treatise on Analytical Chemistry", Interscience Encyclopedia, New York, 1961, Part 1, Section C, Chapter 33
165. F. F. Cantwell, *Anal. Chem.*, 48, 1854 (1976)
166. B. E. Bidlingmeyer, S. N. Deming, W. P. Price, B. Sachok and M. Petrusek, *J. Chromatogr.*, 186, 419 (1979)
167. "Critical Micelle Concentrations of Aqueous Surfactant Systems", NSRDS, National Bureau of Standards, 36, 1971
168. R. D. Estham, "Biochemical Values in Clinical Medicine" 6<sup>th</sup> Edition, John Wright & Sons Ltd., Bristol, 1978.
169. Th. Briellmann, F. Hering, H. Seiler and G. Rutishauser, *Urol. Res.*, 13, 291 (1985)
170. N. E. Good, G. D. Winget, W. Winter, T. N. Connolly, S. Izawa and R. M. M. Singh, *Biochem.*, 5(2), 467 (1966)

171. Erik Högfeldt, IUPAC Chemical Data Series No.21 "Stability Constants of Metal-Ion Complexes", Part A, Inorganic Ligands, Pergamon Press, Oxford, 1982.
172. A. Craggs, G. J. Moody and J. D. R. Thomas, *J. Chem. Ed.*, 51, 541 (1974)
173. D. J. Harrison, L. L. Cunningham, X. Li, A. Teclemariam and D. Permann, *J. Electrochem. Soc.*, 135, 2473 (1988)
174. A. Millan, A. Conte, A. Garcia-Raso and F. Grases. *Clin. Chem.*, 33(7), 1259 (1987)
175. S. Top and D. Yucel, *Clin. Chem.* 34(8), 1658 (1988)
176. A. D. Kirk and A. K. Hewavitharana, *Anal. Chem.*, 60, 797 (1988)
177. N. E. Skelly, *Anal. Chem.*, 54, 712 (1982)
178. F. F. Cantwell, *J. Pharm. Biomed. Anal.*, 2(2), 153 (1984)
179. G. Persaud, Ph. D. Thesis, Department of Chemistry, University of Alberta, Edmonton, Alberta, Canada, 1990.
180. *CRC Hand Book of Clinical Laboratory Data*, Chemical Rubber Company, 2<sup>nd</sup> Edition, Ohio, 1968

## APPENDIX

### COMPUTER CALCULATION OF EQUILIBRIUM CONCENTRATION OF METAL IONS AND COMPLEXING SPECIES USING THE PROGRAM COMICS

COMICS is one of the commercially available programs designed for the calculation of equilibrium concentrations of species in solution. The procedure involved in this program is described in detail in the reference 134 and so will not be discussed here. However, a brief outline of the COMICS method is presented in figure A.1 which is based on the same reference, where  $T_x$  = total concentration of species x;  $[x]$  = equilibrium molar concentration of species x; M = metal ion; L = ligand. The general form of a complex species j, which contains a metal, a ligand and a proton or hydroxyl group, is given as  $M_{a_j}L_{b_j}H_{c_j}$  (a,b and c are stoichiometric coefficients for M,L and H respectively). Values of a and b can be positive or zero, while c can be either positive (for hydroxyl species) or negative (for protons).

#### A.1. Initial preparation

Prior to entering data and starting the computation, there are some calculations which should be performed manually.

1. The  $\beta$  values for simple metal-ligand species can be directly entered from tables or literature sources directly onto the input of COMICS. However, in



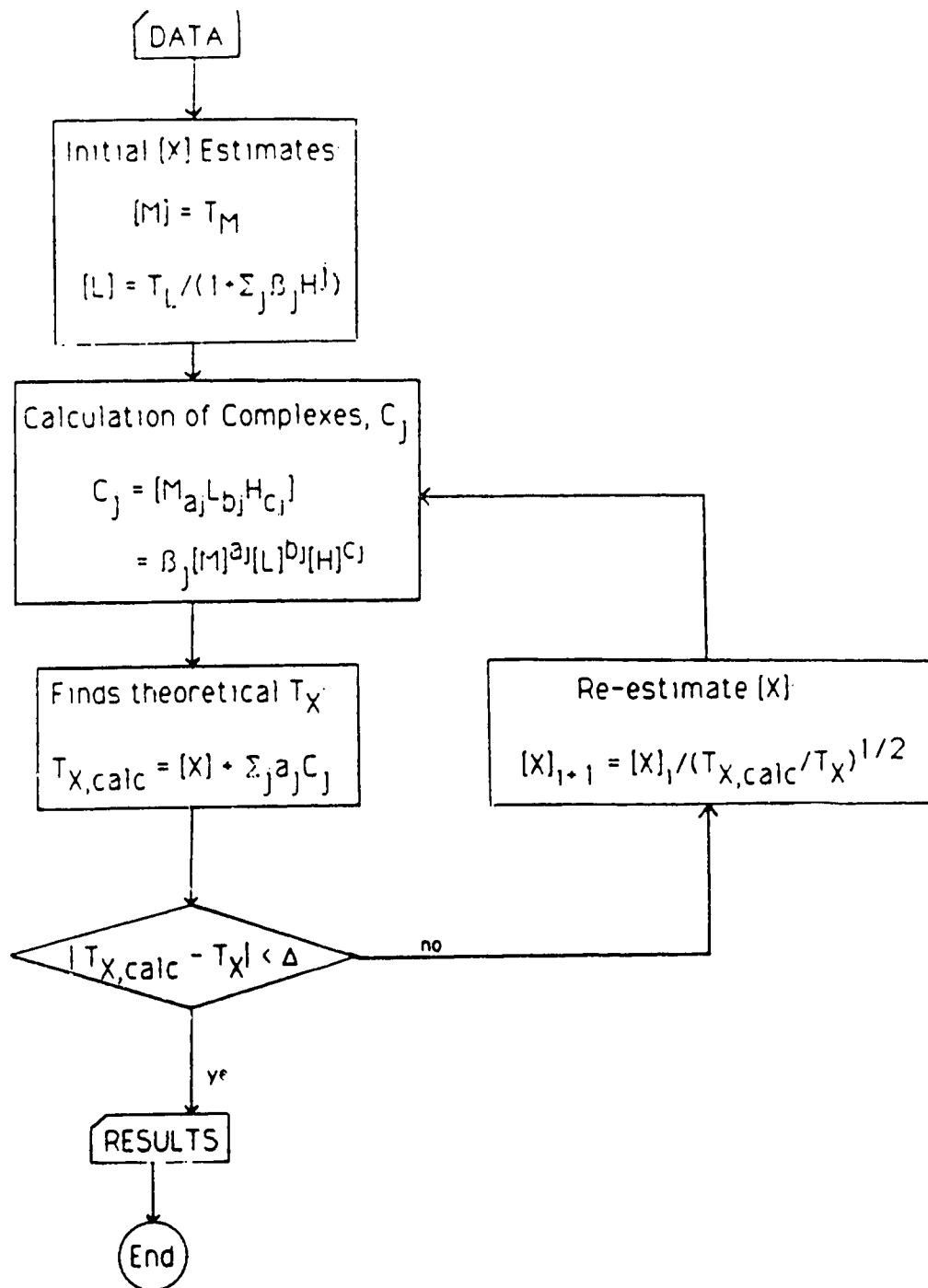


**Figure A.1:** Scheme of COMICS method.

the case of complex species which involve  $H^+$  or  $OH^-$ , the  $\beta$  values given in the literature sources require additional calculations before entry as COMICS input. The reason for this is that the program COMICS requires the  $\beta$  value for each complex or species to be the stability constant for the formation of the complex or species, starting from the smallest constituent ions. The two examples given below explain this requirement.

Example 1: Calculation of  $\beta$  for the species  $H_3PO_4$  -

$$C_j = [H_3PO_4] = \beta_j [H^+]^3 [PO_4^{3-}]$$

$\beta$  values given in the literature sources are:

$$H_3PO_4 / H^+ \cdot H_2PO_4^- \quad \log \beta_1 = 2.0000$$

$$H_2PO_4^- / H^+ \cdot HPO_4^{2-} \quad \log \beta_2 = 5.7213$$

$$HPO_4^{2-} / H^+ \cdot PO_4^{3-} \quad \log \beta_3 = 11.7399$$

Therefore  $\log \beta_j = \log \beta_1 + \log \beta_2 + \log \beta_3 = 19.4612$

i.e. COMICS input  $\beta$  for  $H_3PO_4$  should be 19.4612 rather than 2.0000.

Example 2: Calculation of  $\beta$  for the complex  $CaH_2PO_4^+$  -

$$C_j = [CaH_2PO_4^+] = \beta_j [Ca^{2+}] [H^+]^2 [PO_4^{3-}]$$

$\beta$  values given in the literature sources are:

$$CaH_2PO_4^+ / Ca^{2+} \cdot H_2PO_4^- \quad \log \beta_1 = 0.6434$$

$$H_2PO_4^- / 2H^+ \cdot PO_4^{3-} \quad \log \beta_2 = 17.4617$$

Therefore  $\log \beta_j = \log \beta_1 + \log \beta_2 = 18.1051$

i.e. COMICS input  $\beta$  for  $\text{CaH}_2\text{PO}_4^+$  should be 18.1051 rather than 0.6434.

## A.2. Data input procedure for University of Alberta MTS system

( <R> = press the Return key)

1. Sign on to the computer so that the MTS prompt, #, appears on the screen.
2. Create a data file (eg. AH18). i.e. Type #create AH18 <R>.
3. Get into edit mode by typing #edit <R>. Then type :visual 1 <R>, in order to get into visual mode of editing.

### Some useful commands during editing

- column numbers appear at the bottom of the screen. Start typing from number 1 after the tab.

- more lines can be inserted by moving the cursor to the line before the required line and pressing PF9.

- any line or a combination of lines can be deleted as follows:

Press the break key then type :Del line # <R>.

eg. Del 12 <R> - deletes line 12

Del 12 15 <R> - deletes lines 12 to 15

Once adding and deleting are done, the lines can be renumbered as follows:

Press the break key. Then type :Renum <R>.

4. Within the visual mode of editing, enter input as follows:

Listing of AMIB at 12 59 28 on FEB 19 1991 for CCASBPCH on UALTIMS

	Ca	Mg	P	K	Na	Species in urine	with citr	phosph	and sulph
1	1	0	0	0	0	0	0	0	0
2	4	33	0	0	0	0	0	0	3 2064
3	1	0	0	0	0	0	0	0	7 7668
4	1	0	0	0	0	0	0	0	10 5370
5	1	0	0	0	0	0	0	0	3 1864
6	1	0	0	0	0	0	0	0	7 4568
7	1	0	0	0	0	0	0	0	10 7070
8	1	0	0	0	0	0	0	0	0 5412
9	1	0	0	0	0	0	0	0	5 3467
10	1	0	0	0	0	0	0	0	0 6078
11	1	0	0	0	0	0	0	0	5 7667
12	1	0	0	0	0	0	0	0	5 6592
13	1	0	0	0	0	0	0	0	9 9280
14	1	0	0	0	0	0	0	0	12 8070
15	1	0	0	0	0	0	0	0	4 9864
16	1	0	0	0	0	0	0	0	13 3410
17	0	1	0	0	0	0	0	0	18 8300
18	0	1	0	0	0	0	0	0	3 3534
19	0	1	0	0	0	0	0	0	13 3810
20	0	1	0	0	0	0	0	0	19 0060
21	0	1	0	0	0	0	0	0	0 5732
22	0	1	0	0	0	0	0	0	12 0780
23	0	1	0	0	0	0	0	0	18 1450
24	0	1	0	0	0	0	0	0	0 7232
25	0	1	0	0	0	0	0	0	12 2460
26	0	1	0	0	0	0	0	0	18 4450
27	0	1	0	0	0	0	0	0	18 4450
28	0	1	0	0	0	0	0	0	11 6130
29	0	1	0	0	0	0	0	0	18 3210
30	0	1	0	0	0	0	0	0	20 2230
31	0	1	0	0	0	0	0	0	1 3476
32	0	1	0	0	0	0	0	0	1 2476
33	0	1	0	0	0	0	0	0	0 2888
34	0	1	0	0	0	0	0	0	0 1888
35	0	1	0	0	0	0	0	0	0 1888
36	0	1	0	0	0	0	0	0	1 4788
37	2	00E-032	00E-022	00E-02					
38	2	62E-032	58E-033	80E-021	14E-01				
39	5	50000							
40	5	50001							

Figure A.2: Data input for COMICS.

(Also refer to the input file AH18 shown in figure A.2. The stability constants used in this file were derived from tables 8.4, 8.5 and 8.6 and were corrected for an ionic strength of 0.168. Metals #1, #2, #3 and #4 are Ca, Mg, K and Na respectively. Ligands #1, #2 and #3 are citrate, phosphate and sulphate respectively.)

line 1: number of jobs to be done in columns 1 and 2.

line 2: title of the run.

line 3: number of ligands in columns 1 and 2, number of metals in column 3 and 4, and number of equilibria involved in columns 5,6,7.

lines 4 - x: columns are divided into 4 groups.

- I. Columns 2 - 20: for different ligands; column 2 for ligand #1, column 4 for ligand #2 etc.
- II. Columns 22 - 40: for different metals; column 22 for metal #1, column 24 for metal #2 etc.
- III. Columns 41 - 42: for  $H^+$  and  $OH^-$  in each complex. - enter the number of  $OH^-$  ions as positive integers and the number of  $H^+$  ions as negative integers.
- IV. Columns 51 - 58: for the  $\log \beta$  value of each species, calculated as explained in A.1.

(x depends on the number of equilibria involved in the calculation.)

- line (x + 1): Starting from column 1, input the ligand concentrations in the order ligand #1, #2, #3 etc, using 8 columns for each ligand, with no gaps between concentration values.
- line (x + 2): Starting from column 1, input metal concentrations in the same way as in line (x + 1).
- line (x + 3) to the end: Input on each line, one pH value starting from column 5 to column 10. In column 11, enter "0" if another pH value follows, or enter "1" for the last pH value.

#### An alternative way to input data

If there is access to the input file of program COMICS, created for a different solution, it will be easier to make changes to a copy of that file to create the required input file, as described below:

1. Create a file eg. XXX1.
2. Copy the existing input file to the created file. eg. #copy AH18 XXX1 <R>.
3. Edit XXX1 by typing edit XXX1 <R> and following the procedure described earlier in this section.

#### A.3. Running the program(also refer to output files AH18.OUT1 and AH18.OUT2, shown in figures A.3 and A.4 respectively.)

1. Once editing is complete, press the break key to go from visual mode to line edit mode. Then type :MTS <R>, which brings the MTS prompt.
2. Create 2 output files. i.e. #create file name <R>.



```

48 PH = 5.300
49 NUMBER OF ITERATIONS = 28
50 C1 C2 C3 C4 C5 C6 C7 C8 C9 C10
51 FREE METALS 1 205E-03 1 261E-03 3 634E-02 1 085E-01
52 FREE LIGANDS 3 883E-04 7 428E-10 1 552E-02
53 COMPLEX SPECIES
54 1- 10 7 718E-04 8 870E-05 1 852E-07 7 714E-04 4 548E-05 2 558E-07 5 033E-05 1 017E-05 1 751E-04 7 983E-05
55 11- 20 5 747E-04 3 375E-05 8 076E-08 8 672E-08 6 205E-05 7 616E-05 2 113E-09 7 120E-05 9 495E-05 1 010E-10
56 21- 30 1 021E-04 3 769E-04 4 259E-10 4 508E-04 2 244E-03 8 635E-04 1 555E-02 3 925E-06 4 162E-04 3 458E-04
57 31- 33 1 122E-03 2 888E-03 1 478E-06
58
59
60
61
62
63
64
65 PH = 6.500
66 NUMBER OF ITERATIONS = 38
67 C1 C2 C3 C4 C5 C6 C7 C8 C9 C10
68 FREE METALS 9 718E-04 8 840E-04 3 599E-02 1 072E-01
69 FREE LIGANDS 8 183E-04 4 311E-08 1 567E-02
70 COMPLEX SPECIES
71 1- 10 8 880E-04 1 112E-05 2 072E-09 9 456E-04 5 573E-06 3 135E-09 7 751E-05 1 566E-06 2 692E-04 1 227E-05
72 11- 20 8 938E-05 5 247E-07 1 256E-10 4 060E-06 2 905E-04 3 566E-05 9 689E-08 3 258E-04 4 345E-05 5 808E-09
73 21- 30 5 872E-04 2 167E-04 2 444E-08 2 588E-03 1 288E-03 5 592E-03 8 028E-03 2 218E-07 3 350E-04 2 754E-04
74 31- 33 1 122E-03 2 895E-03 1 482E-07
75
76
77

```

Figure A.3: COMICS output #1 contd.



```

1 LISTING OF ANTS OUT2 AT 12 41 11 ON FEB 19 1991 FOR CCIDEPKCH ON UALTAMTS
2
3
4
5 Co. MG. K & Na SPECIES IN URINE WITH CITR. PHOSPH AND SULPH
6
7 LIGAND CONC = 3.000E-03
8 METAL CONC = 2.620E-03
9
10 FREE
11 METAL C1 C2 C3 C4 C5 C6 C7 C8 C9
12 5.500 0.460 0.295 0.034 0.000 0.000 0.000 0.024 0.029 0.159
13 6.500 0.371 0.369 0.004 0.000 0.000 0.002 0.111 0.014 0.129

```

Figure A.4: COMICS output #2.

eg. AH18.OUT1 and AH18.OUT2

3. Run the program by typing the following command:

Run modcom.1 1=AH18 3=AH18.OUT1 4=AH18.OUT2 <R>.

4. Get a listing of the output files.

eg. List AH18.OUT1 <R>.

List AH18.OUT2 <R>.

5. Sign on to the printer and get a listing of the output files by typing List filename <R>.